A STUDY ON WOUND ROLL SLIPPAGE

By

NANDAKUMAR VAIDYANATHAN

Bachelor of Engineering (Honors)
Birla Institute of Technology and Science
Pilani, Rajasthan, India
1989

Master of Science
Oklahoma State University
Stillwater, Oklahoma
1991

Submitted to the Faculty of the
Graduate College of the
Oklahoma State University
in partial fulfillment of the
requirements for
the Degree of
DOCTOR OF PHILOSOPHY
July, 1996

A STUDY ON WOUND ROLL SLIPPAGE

Thesis Approved:

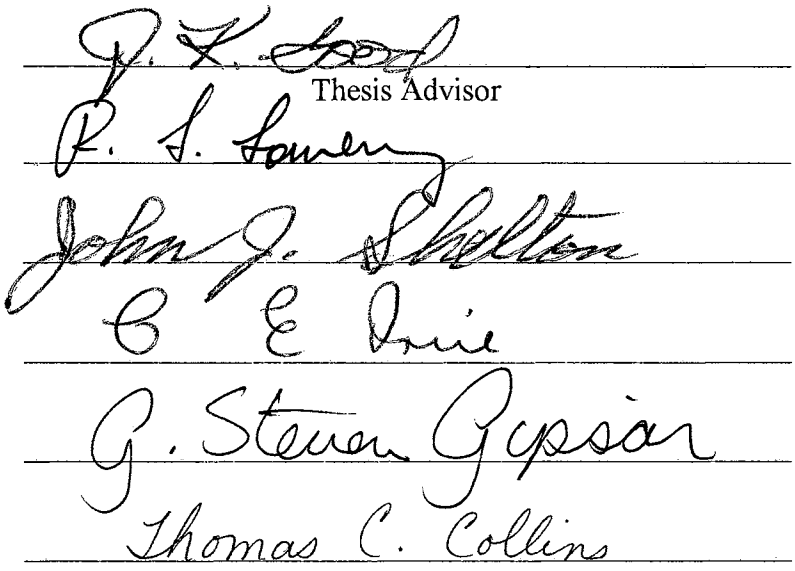

Thesis Advisor

Dean of the Graduate College

ACKNOWLEDGMENTS

I would like to extend my gratitude and heartfelt thanks to my Guru Dr. J. K. Good. The Sanskrit word Guru means "Remover of Ignorance". His infinite wisdom has never ceased to amaze me. My sincere thanks and appreciation also go to Dr. Lowery, Dr. Price, Dr. Steven Gipson and Dr. John Shelton for their helpful advice and comments. I am specially very grateful to Dr. J. K. Good for providing me with resources and freedom to take the webs "boldly - where no webs have gone before".
I am very grateful to Dr. J. J. Shelton and Mr. Bruce Feiertag for sharing with me their thoughts on web handling issues.

My sincere thanks to Ron Markum ("The - Chief - Research - Gizmologist") for his help. I would also like to thank Dr. Keith Ducotey for all his help and witty criticisms. My thanks to Dr. William Robert Qualls ("The Quintessential American") for sharing with me his spirit of hard work, and positive never - give-up-attitude. My sincere thanks also go to Jerry Dale for helping me with the machinery in the lab. I would also like to extend thanks to my parents and sister in India. Their encouragement and support have been tremendous. I am indebted to my other sister for her good wishes. My heartfelt thanks to my wife Anitha, for her constant support, love affection and positive attitude. I thank my Acharya for showing me the "way". Finally I thank God for blessing me with a sound mind and soul.

TABLE OF CONTENTS

LIST OF TABLES

LIST OF FIGURES

NOMENCLATURE

α	Angular Deceleration
α	Hysteresis Loss Factor
a	Half width of contact
d_0	Outer Diameter of the Wound Roll
d_i	Inner Diameter of the Wound Roll
Δl	Change in Length
$\delta\sigma_r$	Incremental change in the radial stress
ε	Strain
E_θ, E_t	Tangential Modulus
E_r	Radial Modulus
F_{normal}	Normal Force
F_{peak}	Peak Force
$Force_{Rolling-Resistance}$	Rolling Resistance Force
g	Acceleration due to gravity
h	Caliper of web
I	Mass Moment of Inertia of the wound roll
k_1	Curve Fit Parameter
k_2	Curve Fit Parameter
l	Length of the web
μ	Coefficient of Friction (Static)

μ_k	Kinetic Coefficient of Friction
μ_s	Static Coefficient of Friction
ν	Poisson's ratio
r	Radius
ρ	Density of the Web Material
$r_{nip\ roll}$	Radius of Nip Roll
$r_{wound\ roll}$	Radius of Wound Roll
R^*	Equivalent Radius of Contact
s	Radius of outer most layer
σ	Stress
$\sigma(r)$	Radial Stress (function of Radius)
σ_θ	Circumferential Stress
t	Thickness of web (caliper of web)
$T_{dynamic}$	Dynamic Torque
$T_{app\ -\ external}$	Applied External Torque
T_w	Web Tension
T_{cap}	Torque Capacity
$Torque_{Rolling\ -\ Resistance}$	Rolling Resistance Torque
w	Web Width
W	Nip Load
$W.O.\ T.$	Wound on Tension

CHAPTER I

INTRODUCTION

Background

Wound rolls of web material are often subjected to unwinding and rewinding before they are converted to a finished product. Commonly, paper, polymer films and metals such as aluminum and steel are processed in web form. Popular techniques for winding these web materials are center winding and surface winding. The quality of the wound roll is governed by the structural integrity of the roll. Good structural integrity of the roll is essential for the roll to sustain additional processing.

The most important parameter which can be controlled, which affects the quality of the wound roll, is the tension of the web prior to being laid on the roll as a wrap. Material properties such as the modulus of the stack of the web, the tangential modulus of the web, the caliper of the web, the surface roughness, the Poisson's ratio of the web material, the web width, the permeability of the web, the physical properties of the core and the dimensions of the core, also influence the quality of the roll being wound. However, from a winding perspective, these characteristics are dependent on the process by which

the web material is made, and the final product that the web will be converted to, and are not controlled by the winder. Additional interactions occur constantly between rollers and web material prior to the actual process of winding and unwinding.

Center Winding

In center winding, a torque is applied to the core of the roll being wound, see Figure 1a. This may sometimes be in the presence of a lay-on roll (nip roll) riding on the surface of the roll being wound, Figure 1b. For center winding without a nip roll, two important properties that can be controlled by the winder are the web tension, and the winding speed. In the case of center-winding with the nip roll, the loading on the nip is another critical parameter that can be controlled. Winding speed is of importance especially when winding webs of non-permeable material. Air entrainment during winding has been of great concern and often leads to poor quality of wound rolls. The concept of using a lay-on roll originated to reduce the air entrainment in center-winding, by nipping the roll being wound so as to exude or squeeze the air at the wound roll nip interface.

Many polymers, and metals such as steel and aluminum, are wound using the center-winding technique. While winding these web materials in a center-winding scheme with or without the nip roll, different tension profiles can be chosen. Typical profiles are constant tension, taper tension and constant torque, see Figure 2a. The taper tension profile shown is a non-linear taper, with a taper value of 50 %. In Figure 2b, the tension resulting from using a lay-on nip roll has been illustrated. The final wound on tension is

the superposition of the web tension and the additional tension induced by the nip. There is no clear reasoning available for choosing one particular form of tension variation over the other. The process of controlling the tension schemes is a separate area of study in itself and will not be considered here. The structural integrity of the roll being wound is determined primarily by the web tension.

In modern production facilities, center winders have the capacity to automatically cut the end of the web, paste it, and unload the fully wound roll when it has reached its final diameter. Winding continues on a new core without stopping the process. Generalizations regarding the dimensions of rolls wound using this scheme will be discussed later.

Surface Winding

In surface winding, the roll is wound in the presence of nip(s) and a torque is applied to the roll via the nip roll(s). A common configuration of the surface winding scheme is the two drum winder where there may be two nips in contact with the roll being wound, Figure 3. Paper is most commonly wound using surface winding, although exceptions exist. In certain cases there may be an additional nip roll riding on top of the wound roll, called the rider roll. The purpose of the rider roll is to provide a tight start to the web when the first layer of web is wrapped around the core. The core is positioned in the

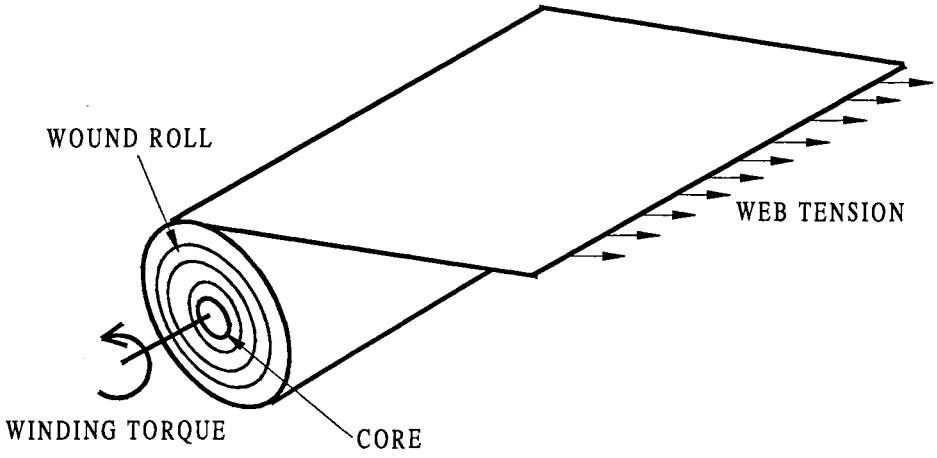

Figure 1a. Schematic of Center-Winding without Lay-On-Nip Roll

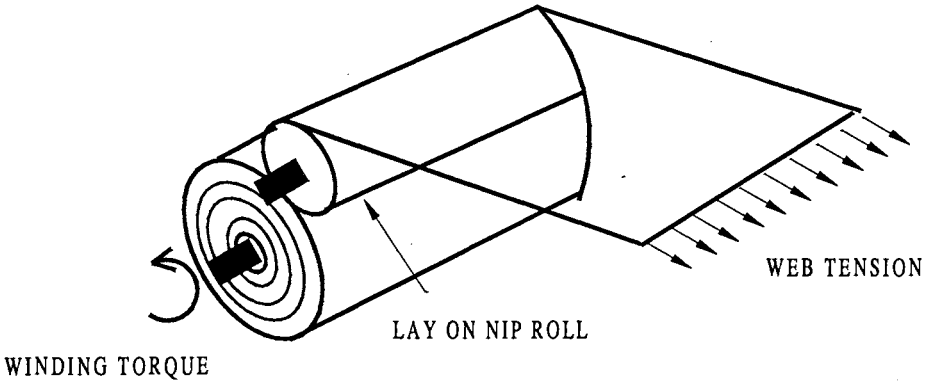

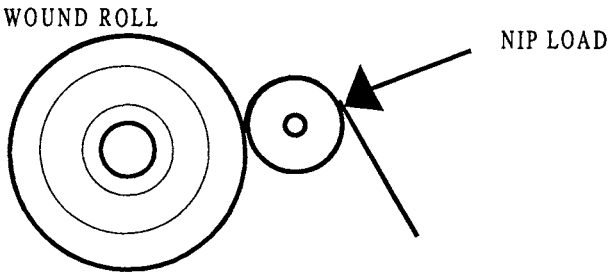

Figure 1b. Schematic of Center-Winding with Lay-On-Nip Roll

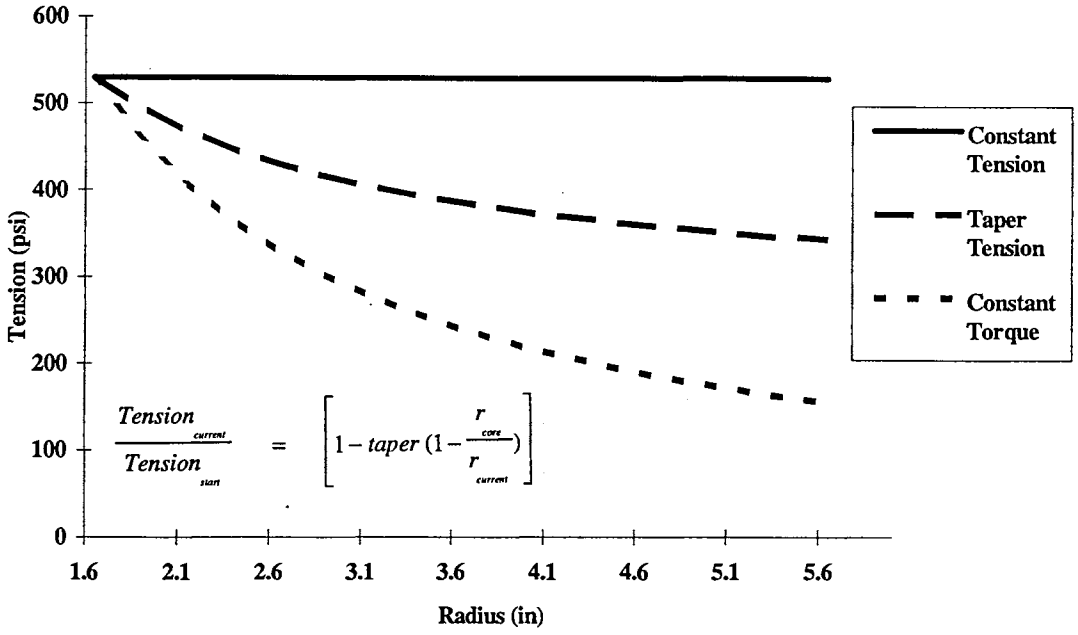

Figure 2a. Typical Tension Profiles

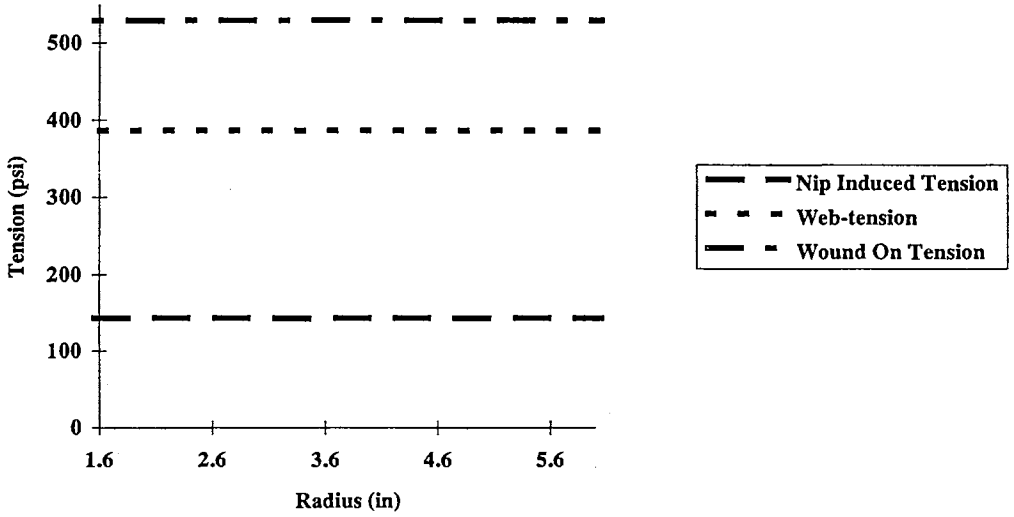

Figure 2b. Tension resulting from a Lay On Nip Roll

notch between the two drums. The web is threaded around one of the drums and started around the core. In Figure 3 the area enclosed by the inner rectangle can be considered as the surface winder. If there is a rider roll, then the rider roll provides the nipping necessary to hold the web firmly as winding proceeds.

The torque to wind the roll comes through the drums around which the web is threaded, or sometimes a torque differential is provided between the drums. In surface winding, the presence of a core shaft is optional, and in the absence of a core shaft there are shaftless core chucks which help in positioning the core and also assist in removing the wound rolls.

Loading, due to the nip, occurs in two drum winding due the increasing weight of the wound roll. As the roll builds up, the weight of the roll is supported by the winding drums. In the case of surface winding with a rider roll, there is an additional source of nip loading from the rider roll. Most modern surface winders have some way of controlling the nip loading from both the sources. There is capacity to maintain a constant nip-load on the roll being wound by relieving the rider load and by, also, automatically relieving the wound roll as it builds up in size.

Older two-drum winders which are in use, do not have the capacity to relieve the wound roll of excessive nip loads due to the self weight of the roll being wound. Only the nip load, provided by the rider roll, is usually relieved as the roll builds in size. This is to ensure that excessive tensions are not induced in the web in addition to the web-line

tension. As mentioned in center winding, different tension schemes can be implemented for controlling the tension of the web prior to entry within the nip zones in the roll being wound. But, surface winding has been a mysterious phenomenon since the tension of a particular layer, as it is being wrapped on the layer beneath it, has not been determined accurately. The nips have been suspected of producing inter-layer slippage within the wound rolls, which disturbs the structural integrity of the roll.

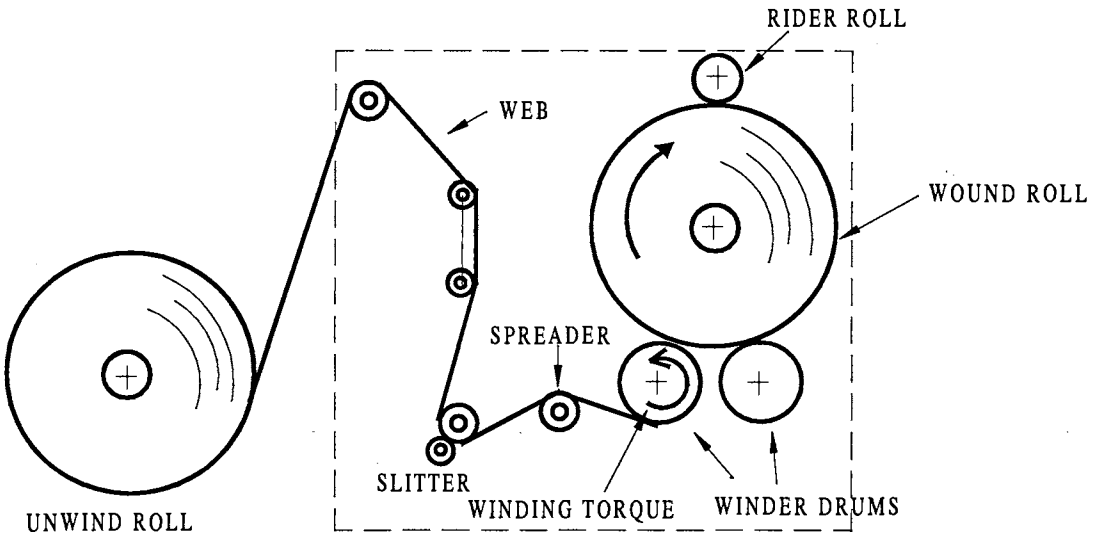

Figure 3. Schematic of a Two Drum Winder

There has been no clear understanding as to why a certain web material is wound by using a particular kind of winder. Shelton[1] has pointed out that the trend in the industry has been to adopt trial and error methods to determine a suitable winding technique for a particular web material. According to a broad trend identified by Shelton, most polymer films and metals are wound using center winding with or without a lay-on roll. Most grades of paper are wound using surface winding schemes. Exceptions are smooth grades of paper which are center wound. Sometimes polymer films are wound on a

combination winder, which is a hybrid between center-winding and surface winding. In combination winding there are two sources of torque to drive the roll being wound. One is provided at the core, as in center winding, and another is provided through the nip roll, as in surface winding. The broad generalization outlined above seems to point to the fact that impermeable webs are usually considered for center winding and permeable webs are considered for surface winding. However, exceptions to this broad categorization exist.

The roll size, which is determined by the width of the roll and the diameter of the roll, is another parameter that is decided through a variety of reasons. Shelton points out that as the value added to the roll increases the web material starts to get expensive and, rolls are smaller in diameter and are wound at lower speeds. In general, Feiertag[2] has pointed out that wound roll size is not a function of the web material. Feiertag considers the additional processing or converting, and the end use of the web to be important factors that determine roll sizes. However, there may be occasions when the wound rolls sizes are arbitrarily chosen.

In center winding, the size of the winding motor (drive), limits the size of the roll being wound. The torque requirements on the motor driving the winder are based on the web tension required, the speed at which the roll is to be wound and the dimensions of the wound roll. Feiertag has pointed out that the width of the web is an important factor as it is more efficient to pack more web material in a wound roll format, thereby increasing productivity. According to Feiertag, width manipulation is easier to accomplish from the

perspective of modifying the winder, than changing the diameter of the wound roll to achieve the same packing efficiency.

In providing a general range of dimensions, Feiertag reveals that during converting processes, polymer films and metals are around 200 to 300 inches wide, and paper products are about 400 inches wide. Again, exceptions exist, and are probably dictated by the end use or the converting process. The thickness of the web is also another factor that is driven by the cost of the web material and the end use. On a wide spectrum, webs range in thickness from 0.0005 inches (1/2 mil) to 0.25 inches (carpets). Wound roll diameters, which are implicitly dictated by the width and the thickness of the web material can range between 30 - 40 inches for polymer films and metals during converting, and 70 - 100 inches for paper during converting processes. Another point to be borne in mind is that as the ratio of width to the diameter of the roll gets smaller, roll stability problems arise. The dimensions mentioned above are rough estimates to develop a feel for the magnitudes involved, but, exceptions exist in all the cases discussed.

CHAPTER II

STATEMENT OF THE PROBLEM

Wound Roll Defects

While winding and unwinding, or during converting operations, wound rolls are susceptible to the formation of defects. Defects degrade the quality of the roll and in certain cases render the rolls useless leading to economic trauma. Consequently, it is imperative to produce rolls with a minimum of defects. In this study, attention will be given to wound roll defects called crepe wrinkles, that have been known to occur in smooth and thin newsprint grades, due to inter-layer slippage that occurs in the wound rolls, Figure 4. While investigating crepe wrinkles another defect that surfaced was starring, Figure 5. Starring was never associated with inter-layer slippage in the past.

Crepe Wrinkles

A crepe wrinkle is an accordion like collection of web material that runs across the width of the web material. It occurs suddenly in wound rolls of newsprint and other slick and thin grades of paper.

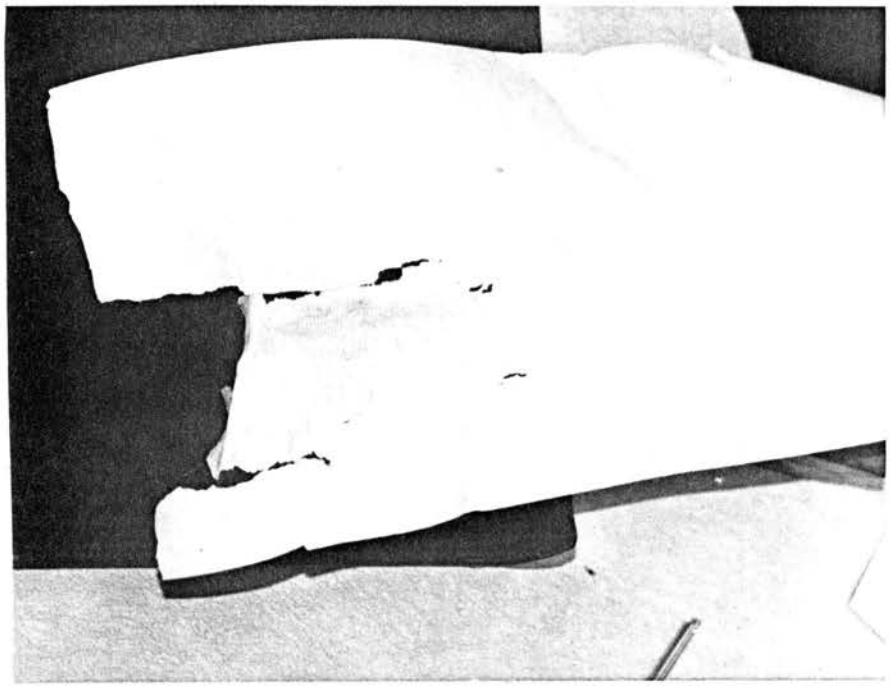

Figure 4. Crepe Wrinkle In A Web Of Newsprint.

Figure 5. Photograph Of A Starred Roll.

Crepe wrinkles have also been observed while winding polymer films at the WHRC. Crepes may involve one layer or a few layers of material which have locally collapsed in a circumferential direction at different points along the radius of the roll. Crepes have been described in some cases as the ingestion of loosely wound material through a nip, Lemke et al[3], Lucas[4]. This defect affects how well a roll performs during printing or additional processing of the roll, as well as locally degrading the web quality.

When rolls in which crepe wrinkles are present are unwound, the web, which was accumulated as a crepe, extends at low tension when the roll has unwound to the radius at which a crepe was present. While the creped web is extending it is common for the angular velocity of the unwinding roll to slow, as a result of the tension control attempting to return the tension in the unwind zone to the set point value. When the creped material has fully extended, it is common for the web to burst, as the web must withstand the steady state tension plus the dynamic tension due to the peripheral speed of the unwinding roll being less than the web line velocity. Thus, the rolls which contain crepe wrinkles pose problems to the end user of the wound roll and reflect on the quality of the roll.

Another difficulty, is the inability to observe the defect prior to its formation. The detection of this defect in wound rolls is by using J-Lines, Lucas[4]. The J-Lines will be discussed later in the chapter on slippage. The J-Lines are carefully scrutinized for minute discontinuities in an otherwise smooth curve on the edge of the wound roll.

Historically, "quick fixes" to remove crepe wrinkles were attempted and this may have contained the problem temporarily.

Based on the open literature, crepe wrinkles have been documented from the late sixties to the present. Modernization in the paper industry has led to the development of winding machinery capable of operating at high speeds, and capable of winding large rolls of paper. This development has been partly due to demands placed on the paper roll manufacturers by the printing industry which prefers to use larger rolls, as it involves fewer changes between rolls and more continuous production. In addition, there has been an increased demand for low cost, thin and smooth grades of paper, such as newsprint and light weight glossy coated magazine grades. However, with changes in material properties of the web, the problem of crepe wrinkles has re-surfaced and there is a need to study the mechanics of the problem from a fundamental perspective.

Starring

Starring, or Spoking, is another defect that occurs in wound rolls. The nomenclature of this defect varies across the industry. The defect visibly appears like a star (spokes) of buckled material. Sometimes the buckles radiate from the core and proceed outward along the radius of a wound roll. At other times the spokes of buckled material appear uniformly around the periphery of the core. A single spoke may also appear somewhere in the middle of the wound roll along a radius. Starring permanently deforms the wound

roll and often times the roll tears or bursts at the point of the most severe distortion, Figure 5. Starring has been documented in rolls wound of both film and paper webs. In the next few sections the objectives of the study and the organization of this report will be laid out and certain preliminaries for visualizing and monitoring both slippage in wound rolls and the different kinds of slippage will be outlined.

Objective of the Study and General Organization of the Report

The general objective of this study is to quantify slippage and identify the different parameters contributing to wound roll slippage. Specifically, attention will be focused on the wound roll defects of crepe wrinkles and starring. This study will concentrate on developing a simple quantifiable model for predicting slippage in a wound roll, based on some of the parameters documented in the literature, such as angular deceleration, tension loss due to splices, and slippage induced due to torque driven nips.

This study is arranged in the following manner. First a review of the available open literature is presented. Although this study addresses slippage in general, most of the available open literature addresses issues concerning slippage as a part of slippage related wound roll defects, and points to different parameters that are responsible for causing the defects. The summary presented at the end of the literature review will show the main cause for the formation of crepe wrinkles to be slippage. So, to understand defects, such as crepe wrinkles, it is important to understand slippage.

Based on the identification of slippage as the most fundamental parameter leading to the formation of crepe wrinkles, a model for slippage in a center wound roll is presented. This slippage model utilizes the torque capacity to quantify slippage in a center wound roll. Additionally, the parameters that govern the torque capacity are presented.

An experimental verification of the torque capacity model for center-winding is presented focusing on how the torque capacity of a wound roll governs the formation of defects, namely crepe wrinkles and starring. Also, presented are methods to alleviate the formation of the defects. Most of the experimental verification has been carried out on rolls that have been center wound, as center winding has been well understood and experimentally verified models simulating center winding are available.

The nip rolls have been pointed out in the literature as a source that produces slippage in wound rolls. The rolling resistance encountered by a torque driven nip will be quantified, and, shown to be responsible for slippage in the wound roll. An attempt will be made, based on the torque capacity model developed earlier, to predict the onset of slippage.

Some Experimental Tools to Monitor and Qualitatively understand Slippage

The object of this study is to understand why crepe wrinkles occur in wound rolls. From a review of the available literature, it is clear that slippage is responsible for the formation of the defect. In what follows, the existing literature on crepe wrinkles will be presented and an attempt will be made to understand the causes for the formation of crepe wrinkles.

Prior to presenting the literature, the different kinds of slippage that occur in a wound roll, and the tools that are used to visualize slippage will be introduced.

In this section no attempt will be made to study the mechanisms that are responsible for promoting slippage, instead, focus will be directed on classification and identification of slippage. This is important because the trade literature is littered with jargon that needs to be collectively organized such that the common features can be characterized. Although the different kinds of slippage that exist in wound rolls are clear to experts, there is no literature that exists which addresses this issue. The nature of slippage that occurs is different depending upon the way in which a roll is wound and the nature of the external torque that causes slippage. This section is organized such that the tools to visualize or monitor slippage will be presented first and then a general qualitative description of the slippage that occurs in different kinds of winding/unwinding scenarios will be identified.

Tools To Visualize/Monitor Slippage Radial Lines, Figure 6.

This refers to lines that are scribed on the edge of a roll as it is being wound. This may be done while winding or by stopping the roll during the winding process and scribing a line. Winding continues and, depending on the slippage that occurs after drawing the radial line, the radial line distorts into curves. In the paper industry, it has been a familiar practice to use a chalk line to snap a radial marking on the edge of the roll. Different devices to accomplish this have been devised, the most common being the chalk string stretched across a bow. There are not many references in the literature from the polymer film industry dealing with radial lines to observe slippage. However, if a visible radial

line can be scribed on the edge of the roll and if the roll body undergoes slippage it is possible to observe it using these radial lines. Depending on the winder, it may or may not be possible to stop the winder to draw these lines. It is, also, possible to spray a jet of ink without stopping the winder such that the ink forms a straight radial line on the edge of the roll.

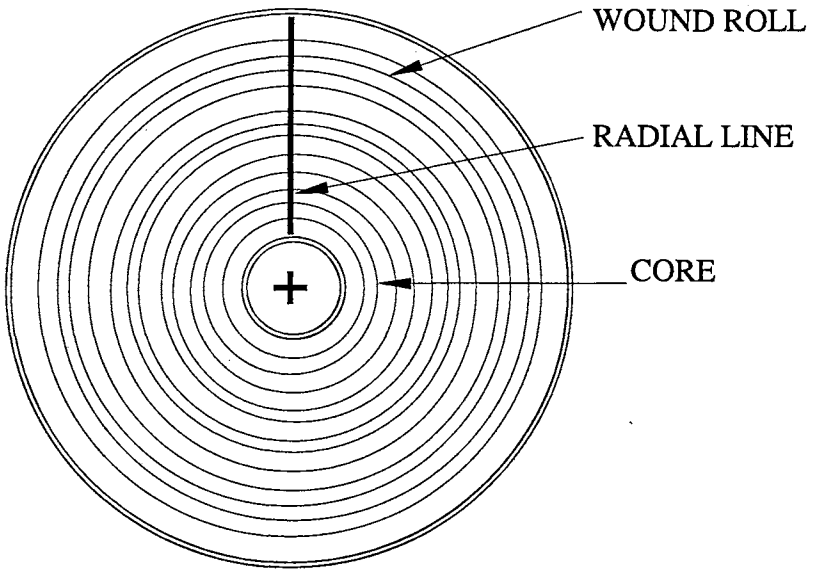

Figure 6. Radial Line on a Wound Roll.

Instantaneous J-Line Printer (I.J.L.P), Figure 7.

This is a device designed at the WHRC to observe the slippage that occurs in a roll as every lap is wound on. The main difference between the I.J.L.P and the radial lines, described earlier, is that the I.J.L.P markings reveal all slippage that occurs in a roll from the start of the winding to the end of the winding. The marking from I.J.L.P. consists of a small jet of ink which comes from the cartridge of an ink-jet printer.

The I.J.L.P. consists of a stand and a spring loaded bearing fixture which is capable of positioning the ink jet cartridge at the top of the outer most layer of web material. In addition, there is a pair of terminals which supply the cartridge with a signal to spray ink. The stand is positioned such that the cartridge is directed at a fixed point above the core. As layers of web material are added, a height tracking wheel guides the ink-jet to a new position above the new layer. This is accomplished quite unobtrusively, such that the winding itself is not disturbed in any way. The signal to spray the jet of ink comes as a zero pulse from an encoder mounted at the back of the core shaft. The encoder zero pulse is designed to spray a jet of ink on the layer once every rotation of the core shaft. Thus, at the end of the winding process, if there is no slippage, the marks from the ink jet align perfectly in a radial fashion. If there is slippage then the radial line is not straight and there is curvature indicating the occurrence of slippage. The author has conducted tests at the WHRC using the I.J.L.P. successfully to monitor slippage that occurs in wound rolls.

Velocity Differential Measurement Between Winding Drums And Wound Roll In Surface Winding

This method does not provide visual clues as the previous two techniques do. It has been used for monitoring slippage while winding paper. By means of high resolution encoders it is possible to determine velocity differences that exist between the roll being wound at its periphery and the tangential velocity of either of the drums driving the wound roll. The velocity differential is an indicator of slippage that occurs in the wound roll.

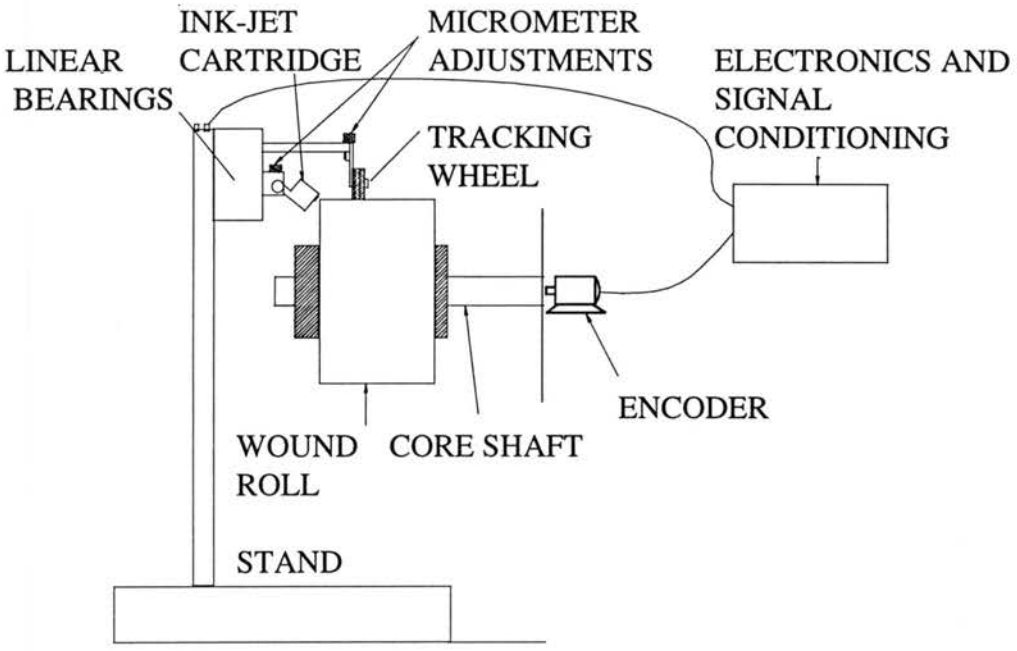

Figure 7. Schematic of the I.J.L.P.

Different Kinds Of Slippage

Slippage In Center Winding, Figure 8

As described earlier, in center winding, the torque to drive the roll comes through the core of the roll being wound. When slippage occurs during center winding, there is a tendency for the roll to slip in the core region. The slippage that occurs is of the "cinching" type. This means web material in the core region will tend to tighten towards the core and if the slippage is uniform and excessive then the slippage proceeds all the way to the outermost wrap, and there will be an overall reduction in the diameter of the roll. Consequently, a radial line marked on the edge of the roll will tend to curve in the direction in which the torque is applied to the core. Depending on the severity of the cinching effect some of the layers above the cinched portion may be completely devoid of any radial stress.

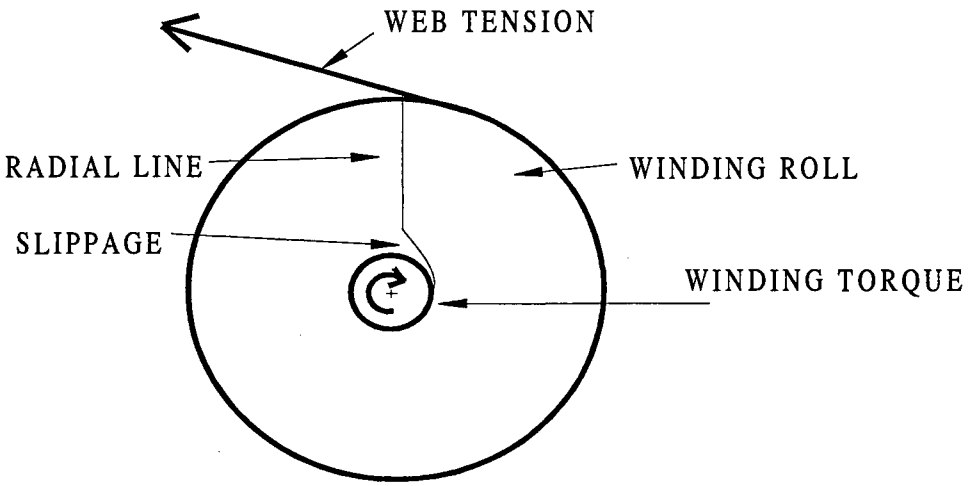

Figure 8. Slippage during Center-Winding.

Slippage In Center Winding In The Presence Of A Lay-On Nip Roll

In this kind of winding, the torque to wind the roll still comes from the core. So, a radial line scribed on the edge of the roll, will still have a tendency to "cinch" in the direction of the applied torque on the roll being wound. Thus, the slippage that occurs in center winding in the presence of a lay-on nip will be similar to the case of the roll being center wound without a nip.

Slippage During Unwinding, Figure 9

Slippage is similar to the case of center winding. The "cinching" of the unwinding roll occurs in the direction of the braking torque. The web material near the core region tends to get cinched in the direction of the braking torque and, consequently, the radial line distorts in the direction of the braking torque. The comments pertaining to the severity of the cinching, made with respect to center winding, hold good for the unwinding case.

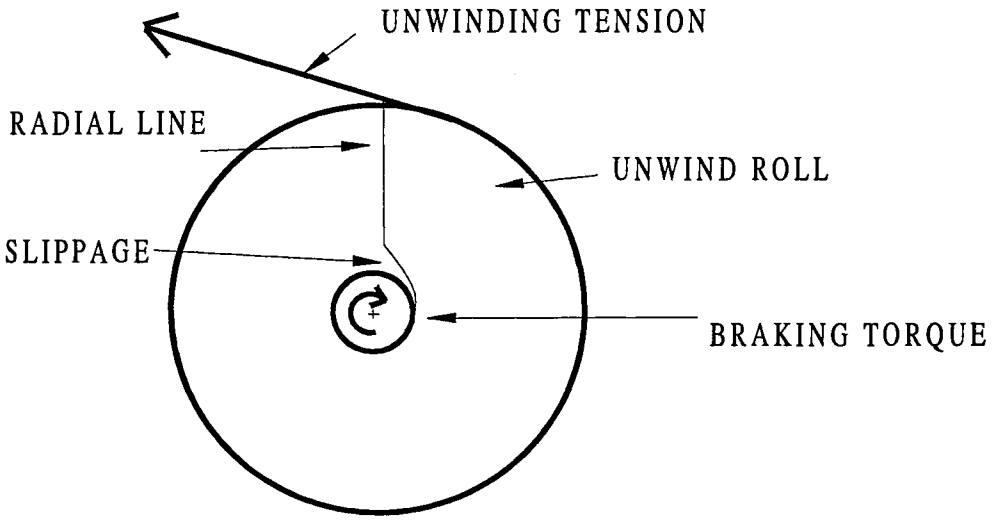

Figure 9. Slippage during Unwinding.

Slippage In Surface Winding

In surface winding, the torque to wind the roll comes from the nips in contact with the roll. This situation is different from the center-winding case. Interestingly, the slippage in surface winding is of the "loosening" kind, as opposed to the cinching effect that occurs in center winding. Most of the slippage, also, occurs in the vicinity of the location of the nips. Consequently, a radial line scribed on the edge of the roll will later curve in the direction of the loosening of the wind if there is slippage, giving the radial line the familiar hook or curving popularly known as "J-Line", Figure 10. The straight portion of the J-Line lies towards the core region, the curved portion of the J-Line is towards the periphery of the roll and the curve of the J-Line points toward a loosening direction of the wind. In general, as paper is wound on surface winders, whenever slippage occurs in wound rolls of paper, the trade literature refers to the slippage by J-Lines. The general tendency has been to identfiy all slippage related radial line curving as "J-Lining", regardless of whether it is a cinching type effect or a loosening slippage. Sometimes, there is tightening of the layers towards the core in addition to the loosening type slippage occurring near the periphery of the roll in surface-winding cases. In such cases the J-Line will curve in a cinching direction towards the core region, Figure 11. In other words, the straight portion of the J-Line will also curve to reflect the tightening of the layers near the core region.

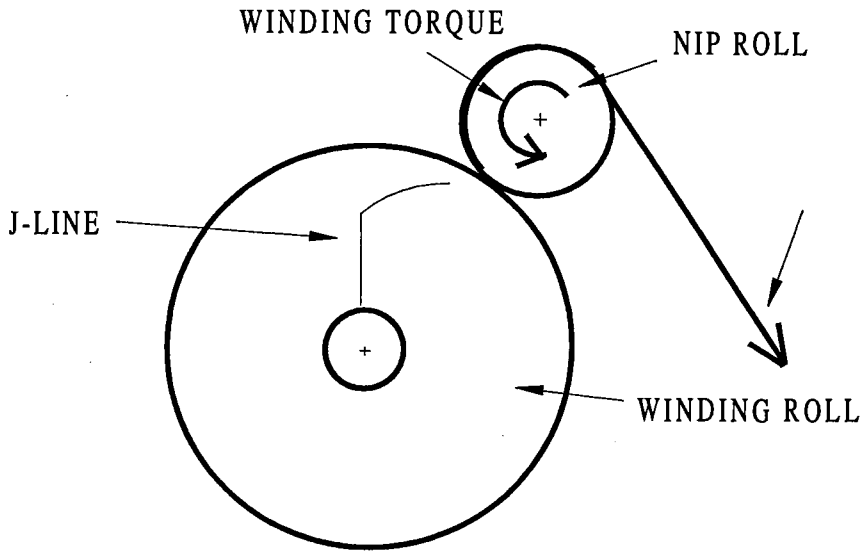

Figure 10. Slippage during Surface Winding showing the J-Lining.

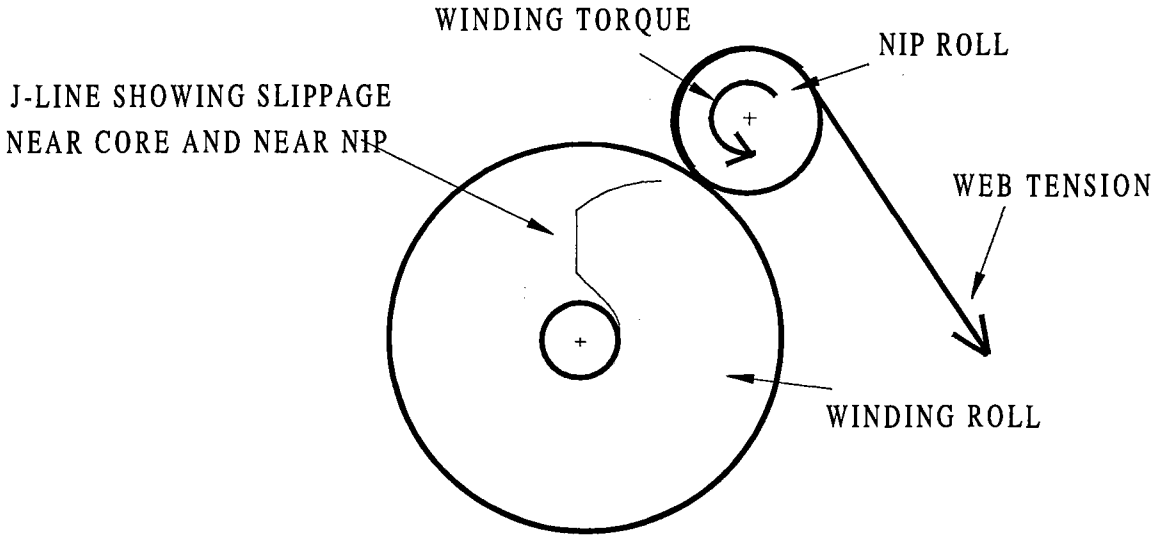

Figure 11. Slippage during Surface Winding showing the J-Lining and 'cinching' in the core region.

CHAPTER III

LITERATURE REVIEW

In the previous chapter, certain fundamentals of slippage were introduced as a prelude to understanding the literature on crepe wrinkles. In this chapter, a critical review of the literature that exists on crepe wrinkles and slippage related defects in general will be presented. Most of the literature is qualitative, however interesting details are sometimes brought out, which will serve as a spring-board to conduct quantitative and experimental excursions to understand the problem of slippage related wound roll defects in general.

A review of the literature reveals the continuing lack of clarity in understanding the problem of quantifying and predicting slippage related wound roll defects. In general the literature has been reviewed to glean parameters that can be used to understand slippage. The literature has been presented to reflect the views presented by the authors and additional comments have been made to highlight the lack of relevant information in some cases.

In an early study by Laumer[5] on minimizing defects that occur during winding, interesting information pertaining to J-Lines and slippage is available.

Based on the descriptions provided, it appears that all the information pertains to surface winding (probably 2 drum winder) with paper. No clear information on what kind of paper was used is available. Some observations include:

1. J-Lines are due to inter-layer slippage. It appears that earlier theories related J-Lines to density of wound rolls. Since density and inter layer pressure are dependent upon one another this is not surprising. Laumer, also, identifies, the extent of slippage as being related to compressive forces provided by the nip and the coefficient of friction that exists between the layers
2. The curved end of a J-Line is in a loosening direction and, so, the slippage is related to the nip
3. A large (diameter) nip roll produces a smaller curving in the J-Line. Laumer associates this with nip penetration being more distributed than for the case of a smaller diameter nip.

Laumer suggests an interesting hypothesis concerning slippage that occurs in a surface wound roll. The loosening curve of the J-Line in the vicinity of the nip has been attributed to differential draw of the outer layers of a wound roll. If the inner layers of the wound roll could be considered as a compliant nip, and the surface could be considered as a rigid roll, then the layers of web at the interface would be subjected to a differential draw based on the amount of circumferential travel of the hard nip. In an effort to validate this hypothesis, Laumer conducted an experiment in which 8 webs were passed through a nip region composed of a steel roll of diameter 20 inches and a soft rubber nip (of unknown diameter and hardness). Based on the illustration (Figure 12) describing the

experiments, it appears that the web was 0.004 inches thick. It is not clear what the actual experiment consisted of but it is apparent that the steel drum was rotated one complete revolution and the movement of the free edges of the webs were measured. The 2nd web layer (in proximity to the steel drum), moved a distance of 0.027 inches with respect to the first web layer. Now, Laumer compares this to values that he theoretically derives based on the sheet length difference per revolution of the steel drum.

According to Laumer:

$$\text{Sheet length difference} = 2 * \pi * \text{thickness of web}$$

$$\text{Sheet length difference} = 0.025 \text{ inches.}$$

Interesting as the results may seem, it is not possible to extend the above technique to actually model the slippage as none of the physical parameters of either the web material or the hypothetical compliant nip are involved and the relationship is purely geometrical. However, slippage in an actual roll involves friction, nip loads and other parameters of the web material which are unknown at this point.

When documenting crepe wrinkles, Laumer has pointed to the location near the core of surface wound rolls. The defect was assumed to be related to slippage. Ideas such as "softening" of web material that was tight to begin with, due to compressive stresses from layers above it, have been considered. A suggestion, to alleviate the defect, has been to implement web tensions that are initially high at the start of the wind, but tapering down with increase in roll diameter. No specific quantification of parameters has been attempted and no physical winder parameters or web properties have been mentioned.

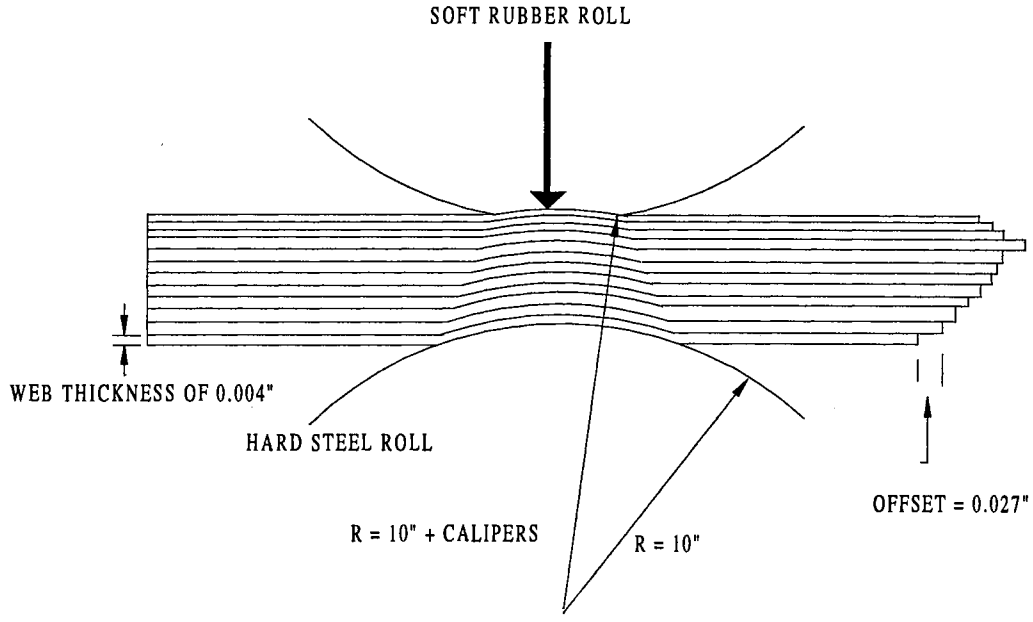

Figure 12. Illustration describing Differential Draw, from Laumer[5].

Daly[6], in a study addressing defects that occur on a two drum winder, has classified crepe wrinkles as a roll structure related defect. According to Daly, crepe wrinkles occur due to an uneven shearing of a layer in a wound roll. The shearing occurs due to axial and circumferential variations in the radial pressure. A locking up of points and free motion of other areas in a particular layer might lead to 'bunching' of the layer. Inter-layer slippage in conjunction with lubrication due to entrained air in the layers are considered by Daly to be additional factors aiding in the formation of crepe wrinkles. As this study was an attempt to consolidate wound roll defects based on the characteristics of

the defect, no quantitative data pertaining to winding conditions or physical properties of the web material are available.

Lucas[7], in a study on roll body slippage, has attempted to discuss wound roll models for rolls wound on a two drum winder. The assumptions behind the development of the model are unclear. An analogy known as "internal gearing" has been used to describe the slippage that occurs in a wound roll. The "internal gearing" analogy considers a loosely wound roll as a collection of circular hoops of stiff material nested concentrically within each other, Figure 13. When such a hypothetical wound roll can be lifted by its core and rotated, the stiff concentric hoops rotate (slip?) within each other with different speeds just as an internal gear would rotate within a planet gear. How the speeds of the different layers relate to the slippage is not clear, but as Lucas explains, the analogy serves to visualize the slippage qualitatively.

Lucas describes an experiment where he scribes a radial line on a roll that has been wound (winding method unknown). The roll is then mounted on an unwind stand, and simply rotated. When the roll is rotated, there is slippage that occurs near the core as evidenced by the curve in the J-Line. Lucas describes this behavior as analogous to slippage due to internal gearing. Based on accompanying illustrations, Figure 14, it appears a torque was applied through the core to the wound roll which caused a cinching of the material in the region of the core. Lucas, also, qualitatively proposes that if the

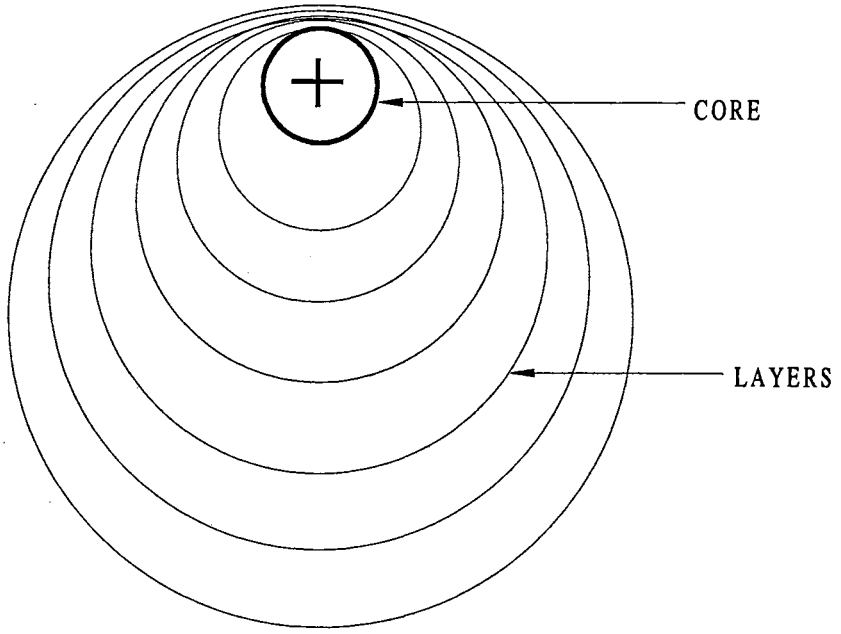

Figure 13. Illustration of "Internal-Gearing" Analogy from Lucas[7].

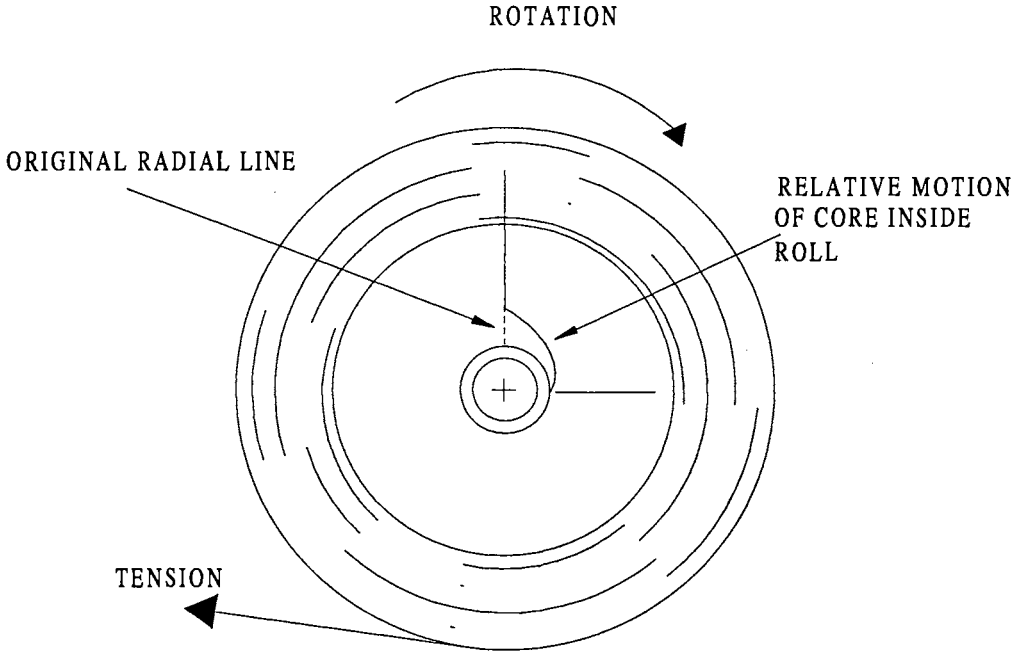

Figure 14. Illustration of Slippage due to "Internal-Gearing", from Lucas[7].

web tension leaving the unwind had been increased (while rotating the roll ?) then it might have been possible to reverse the direction of slippage. Lucas observes that in some cases if the web tension was increased considerably there would be slippage in the vicinity of the core, but, the direction of slippage would be reversed. This description points out that the slippage occurs due to an interaction of the applied torque and the capacity of the roll to sustain the torque.

Lucas also alludes to the possibility of telescoping and roll dishing being related to slippage. In addition, Lucas points to time dependent factors such as hygroscopic effects that might cause a core to dry out thus reducing its diameter, in turn leading to a loose core after the roll has been wound. A suggested cure is to wind rolls with an increase in the web tension, so the rolls have tighter starts. However, without any quantitative parameters on the web material and the winding techniques, no additional inferences can be made as to why the cure suggested alleviates the formation of slippage related wound roll defects.

Roll weight, core diameter, web to web coefficient of friction, and paper compressiblity have been identified as factors which facilitate "internal gearing". It is not clear what layer to layer compressibility means, however the simplest interpretation would be the radial modulus of the web material. Lucas observes that rolls wound on a two drum winder without a core shaft may not exhibit "internal gearing" as there are no forces that generate this mechanism. This is unclear, as he uses terms such as slippage and "internal gearing" interchangeably. Apparently Lucas uses the term "internal gearing" for a

cinching type slippage occurring in the core region, which is different from the J-Line slippage appearing in the wound roll due to a loosening effect from the nips.

Although the paper by Lucas was qualitative, descriptions of post slippage behavior have been made very well. Lucas describes a decrease in radial pressure following the onset of slippage. This radial pressure, proceeds outward from the core, decreasing the diameters of the internal layers, creating opportunity for "internal gearing". Studies made at the WHRC by Zhang[8], investigating post slippage behavior, have provided quantitative information on this behavior, and have demonstrated the existence of a wave of low radial stress that proceeds outward from the core region in the case of a center wound roll.

Generalizations such as increasing the web tension while winding, increasing the rider roll nip load, increasing the drum torque, reducing drum diameters, and threading webs with a back drum wrap, and increasing the core diameter of the rolls, have been proposed to reduce slippage in rolls. Intuitively, the parameters mentioned, except the last one, serve to increase the wound on tension, thereby leading to the winding of a hard roll. Lucas has, also, suggested center-winding to obtain a high start up wound on tension in certain cases.

In closing, a major drawback of this study, is that it provides no quantitative evidence to develop a predictive mechanism that can identify what is the exact cause of slippage in wound rolls. There is no mention of winding parameters or physical properties of web materials, therefore re-interpreting the results is difficult. The qualitative descriptions do

give insights into parameters which might be responsible for the formation of slippage related defects.

In another study on winder crepe wrinkles and methods to avoid the defects, Lucas[4] has identified inter-layer slippage as a key factor for the formation of crepe wrinkles. Lucas has also observed that the propensity of layers to slip increases with increasing surface smoothness and compressibility of layers. However, no bounds on the magnitudes of these factors have been given. Grades of paper prone to crepe wrinkle formation have been identified and include newsprint, catalog, telephone directory, and some lightweight coated super calendered publication grades. This is perhaps the only list of the different grades of paper identified in the literature.

Lucas remarks that crepe wrinkles have the propensity to occur anywhere in the wound roll and not necessarily in the vicinity of the nips. In trying to quantitatively establish methods to predict crepe wrinkles, Lucas relates the amount of motion occurring during slippage in a surface wound roll by measuring the amount of curvature in J-Lines. But the quantification is not clear or rigorous. Another point brought out is that as the nip loads increase, via the rider roll, so does the slippage.

Lucas identifies bow waves preceding the rider roll in a two drum winder, as being responsible for the formation of crepe wrinkles. This bow wave has been related to a drop in tension on the outermost web layer before entering the rider roll. No causes for this drop in tension or a connection between slippage and loss of tension have been

identified. Another mechanism that Lucas proposes is a circumferentially varying inter-layer slippage producing a "local log jam" of slipped web material that collects as a crepe wrinkle. Lucas suggests winding tighter rolls to reduce crepe wrinkles. However, the mechanism for increasing the tension, as pointed out by Lucas, is to control the torque applied to the drum rather than increasing the nip load via the rider roll. Surprisingly, Lucas observes, that increasing the nip load has a disastrous effect in that slippage increases in the roll being wound. Although further investigation into this phenomenon was not made, it points to the nip roll (rider roll) to be a contributing factor for the formation of crepe wrinkles.

Lucas, also, suggests reducing or removing the rider nip load profile such that a wound roll is not subjected to nip cycles immediately following an emergency stop, (causing a loosening of the layers?). This is the first time crepe wrinkles have been linked to decelerations that wound rolls undergo in the event of an emergency stop. A brief description of crepe wrinkle occurrence following rapid deceleration of the wound roll has been made using J-Lines, but no predictive means to identify the onset of slippage were recognized. Another point that is not clear is whether the crepe wrinkles were due to the deceleration of the wound rolls or due to the kneading of the wound roll by the rider roll.

In a summary provided by Lucas, to reduce crepe wrinkles while winding on a two drum winder, the following have been suggested:

(i) Increasing the incoming web tension (wound on tension ?)

(ii) Decreasing rider roll nip load as soon as a good start has been achieved

(iii) Increasing the front drum torque

(iv) Increasing deceleration rates (?)

(v) Spiral grooving the back drum

Upon closer scrutiny of the factors provided by Lucas, (i) and (iii) serve to increase the wound on tension. The second factor identified seems to indicate that the rider roll has a part to play in inducing slippage, and thereby crepe wrinkles although no investigation based on the geometry of the nip or the effect of the nip load in inducing slippage has been made. It is not clear whether Lucas is referring to the actual amount of deceleration or the time derivative of the deceleration. No experimental evidence of increasing deceleration rates leading to increased formation of crepe wrinkles was presented in the study, however this appears to be an important clue to the formation of crepe wrinkles. The last factor as identified by Lucas suggests that air entrainment is in some way connected to crepe wrinkle formation. A recent study by Tuomisto et al[9] has identified air entrainment as a factor leading to the formation of crepe wrinkles.

Welp et al[10] provided radial stress profiles for a roll wound on a two drum winder. This study is perhaps one of the few which provide such a quantification. No attempt at modeling has been made, as the study appears to be empirical. The radial stresses have also been called "roll hardness". The study was conducted to extend the limits set on wound roll sizes by conventional two drum winders, as it had been difficult to wind large rolls that were free of defects such as crepe wrinkles, bursts, out of roundness, non-uniform roll hardness and tears resulting from over stretched layers. No mention of the

limits were made. The authors consider a plateau region in the wound roll's radial stress profile as an optimal condition for an ideal roll. The authors have also emphasized the existence of maximum radial stresses near the core. There is no explicit reason mentioned for such a consideration.

Based on the empirical radial stress measures provided by Welp et al , it appears that for a roll wound on a conventional two drum winder, there is a tendency for the radial stresses to increase deviating from a plateau, as the roll size increases. In addition, in the region of the periphery of the wound roll, the radial stresses reach a peak. The authors indicate that the major parameters that are involved in producing an optimal wound roll are the web tension and the nip load.

As the conventional two drum winder depends on the self loading of the wound roll against the drums to produce the nip load, there is a tendency for the nip load to increase considerably if the winder does not have the ability to control the nip load. In addition, the rider nip load has been observed to produce a loosening type slippage that is detrimental to the wound roll quality. Based on the two observations made above, the authors have developed a new two drum winder with one of the drums being larger than the other, and arranged in a slanting plane, Figure 15. The idea is to distribute the increasing nip load to a larger diameter drum, and in addition to control the slippage that occurs in the outer layers of the wound roll by controlling the difference in the surface velocities of the two drums. The modified winder had the capacity to relieve the nip load via the rider roll.

In attempting to control the radial stresses produced on the wound roll, the authors relate the slippage that occurs when the two drums have a speed difference to the wound roll hardness. A simple study was conducted by Welp et al based on observations of the J-Lines on the rolls that were wound on the modified two drum winders. Many radial lines were scribed and the terminal points of all the J-Lines were connected to form an envelope curve, Figure 16. An interesting feature of the envelope curve is a tightening of the layers in the immediate vicinity of the nip, in addition to the loosening beneath the nip. The authors relate the envelope curve to the difference in speed between the two drums on which the wound roll rests.

The study compares the radial stresses of the rolls wound on a conventional two drum winder with the modified two drum winder. The comparisons made are based on the geometry of the winder, peripheral speed differences between the driver and the driven drums, web tensions and the rider nip loads. The conclusive points addressed by this comparative study are that the modified two drum winder produces rolls of "optimal hardness", optimality being described by the existence of a plateau in the radial stress profiles of the wound rolls. According to Welp et al, the hardness profile is related to the over speed between the drums, although the relation is not explicit or even clear. The modified two drum winder relies less on the rider nip load to provide the tension in the wound roll.

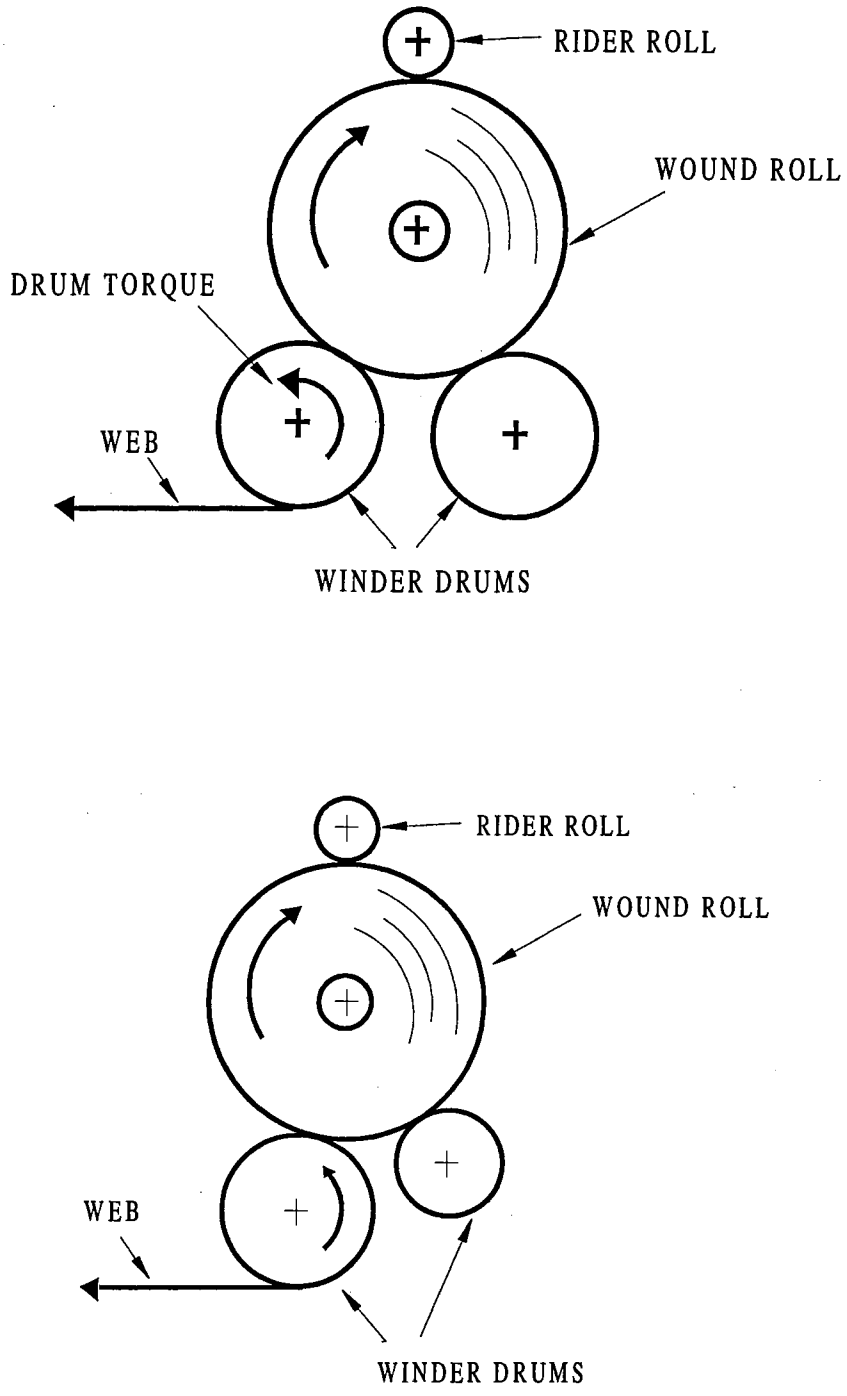

Figure 15. Illustration of the Two Drum Winder and the Modified Two Drum Winder from Welp et al[10].

The conventional winder derives most of the start-up tensions from the rider roll, which as the roll builds up starts to produce slippage that is detrimental if there is no proper control or relief provided to the rider roll. Thus, the authors point out that the modified two drum winder has the capacity to wind rolls that are not subjected to the detrimental influences of the rider nip load in inducing slippage that leads to crepe wrinkles. However no quantitative proof of reduction in crepe wrinkles due to the modification is available.

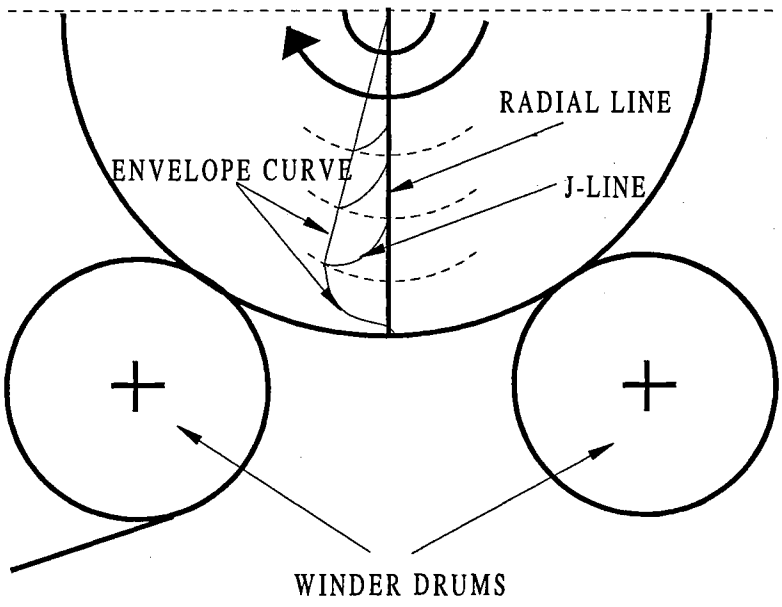

Figure 16. Illustration of Envelope Curves from Welp et al[10].

With respect to the web tension, the authors point out that an increase in tension leads to an increase in the hardness profiles of the wound rolls. However it is not clear whether the modification in the two drum winder is responsible for increased wound on tension in the roll. In light of the issues addressed above, there is experimental evidence provided, comparing rolls wound on the modified and the unmodified winder in the form of wound roll radial stress profiles. However, all the physical parameters of the web materials and the winder parameters including the geometric information are not included. The points of interest in this study are the attempts to relate the over speed between the winder drums to the slippage, and the "J-Lines" and quantifications of radial stresses of the surface wound rolls.

Frye[11] has provided a new definition of roll quality based on the printability and runnability characteristics of the wound roll. Frye has also grouped the parameters contributing to the roll quality into the following categories:

(i) Winder related, such as web tension, torque provided via the drums, and the nip loads, speed, drum wrap, drum diameters, drum surfaces, drum arrangement, rider roll diameter and drive type

(ii) Wound roll parameters, such as the roll diameter, core diameter, core shaft glides, core types and wound roll width

(iii) Web physical properties, such as basis weight, grade, tensile strength and tensile modulus and radial modulus of the stack of web material, coefficient of friction and web caliper profile.

Frye points out that non uniform nip loads are responsible for the formation of crepe wrinkles. Another interesting aspect of the study is the identification of tension as an important parameter dictating the structural integrity of the wound roll. It is not clear whether Frye refers to the wound on tension or the web tension prior to the nips. An empirical attempt to quantify the tension induced by a single nip and multiple nips has been made. No relationships between the nip loads or web tensions have been identified. Another suggestion made by Frye to reduce crepe wrinkles is to use carbide coated drums when surface winding. The carbide coating apparently facilitates gripping of the web to the drum, in comparison to the case where there is no carbide coating on the drum. The carbide coating, thus, leads to a tighter wrap around the core, resulting in higher wound on tension and higher radial pressures and thereby greater capacity to resist slippage. Frye points out that the carbide coating has led to a decrease in the formation of crepe wrinkles in rolls wound of light weight coated paper.

In a parametric study to quantify the parameters which affect the density of a wound roll, Odel l et al[12] have studied the effects of parameters such as rider roll relief force, drum torque differential, speed variations of the winder, web tension, drum diameters, paper grade, roll diameter time between paper making and winding and set location from parent reel. This is the only study where quantitative information has been provided. This study also pertains to rolls wound on a two drum winder with a rider roll. The study has been carried out on newsprint with basis weights of 36 g/m^2 and 49 g/m^2.

The roll quality has been characterized using the density of the wound roll. Information with respect to crepe wrinkles is addressed with respect to rider roll relief force and the drum diameters. With respect to the rider roll relief provided, Odell et al have observed the need for a high value of rider roll nip load at the start of the wind-up, to provide a tight start as there is no other way by which a tight start can be achieved in a roll being wound on a two drum winder. Odell et al have also observed the need to gradually reduce the nip load with increase in roll diameter. In an accompanying illustration, Figure 17, Odell et al have related the formation of crepe wrinkles to the maximum rider roll load and basis weight of the web material. The graph identifies limits on rider roll load that can be used to wind rolls for a particular basis weight of newsprint, without any crepe wrinkles occurring on the rolls. The graph also shows a linear increase in the rider roll load with increase in basis weight of the web material. The basis weights varied from 30 to 55 g/m^2. The rider nip loads vary from 10 to 30 N/cm. The graph indicates that a good cross machine direction caliper aids in increasing the rider roll load that can be provided to achieve a tight start. This is the first empirical attempt to quantify the occurrence of crepe wrinkles. But, the study lacks a capacity to predict crepe wrinkle prior to the occurrence of the defect. This is an indication of the inability to isolate the parameters that are responsible for the formation of the crepe wrinkle.

Crepe wrinkles have been described as a localized overloading of the drum nip, which upsets the uniform slippage that occurs beneath the nip. This indicates that crepe wrinkles develop beneath the nip and are related to slippage caused by the nip. Another variable addressed is the drum diameter. Odell et al suggest that larger diameter drums

lead to a reduction in crepe wrinkle formation. No empirical evidence has been provided as to what dimensions are considered large or small.

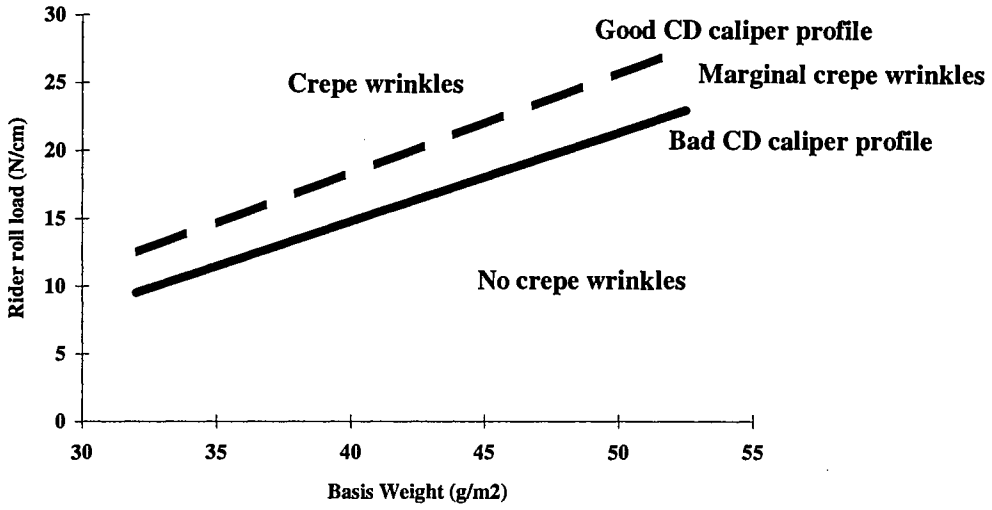

Figure 17. Illustration of the Variation of Rider Roll Nip Load and Crepe Wrinkle formation, from Odell et al[12].

In another study on core bursts and crepe wrinkles, Frye[13] defines core bursts as a tear that occurs in web material that has creped. In documenting the locations of the crepe wrinkles, Frye points out that most of the core bursts occurred within 2 inches of the core. Frye has documented the occurrence of crepe wrinkles over core notches. In the illustration accompanying the description of bursts, it appears that there has been a core collapse resulting in a star-like buckle with intermediate locations where there are bursts in the web. In isolating causes responsible for the formation of the defect, Frye considers the changes in the winder parameters and the physical properties of the web material. The only physical property pertaining to the web material that is mentioned is the basis

weight of the light weight papers. Most crepe wrinkle problems and core bursts occurred in categories with basis weights 0.0106, 0.01133, 0.0133 lb/ft^2. As documented by Frye, the major changes that occurred while winding these grades of web material were

(i) Torques applied to the winder drums

(ii) Reduction in web tension (less than 1.8 Pli)

(iii) Reduction in tensile strength of web

(iv) Increase in coating weight

Frye believes that an improperly located spreader roll might cause wrinkles while accelerating to a set speed. It is unclear whether wrinkles that originated at the spreader were wound in as crepe wrinkles. In addition, tension variation and speed changes to the winder are additional causes that Frye speculates to have led to the problem of crepe wrinkles. Frye also points to slippery front drums and short unwind core chucks as responsible for the formation of crepe wrinkles.

Frye observes that the asymmetry in geometric location between the rider roll and the front and the back drums is a potential cause for the formation of crepe wrinkles. In the special case of a two drum winder which Frye observed, the center line of the rider roll was closer to the center line of the back drum than to the center-line of the front drum. Frye points out that in the rolls that were wound on this winder, there was a reduction in start up tension and, consequently, a degradation in the roll structure. Although this study is qualitative, information pertaining to the location of occurrence of the defect is interesting. No clear identification of the cause of the crepe wrinkles or core bursts can

be made, as many factors have been pointed out to have an effect on the formation of crepe wrinkles.

In a statistical study, Paananen et al[14] point out that the propensity to form crepe wrinkles increases in rolls of paper that are wound from the middle and the inner (around the core) regions of the parent roll. The cause for this has been attributed to the redistribution of density of web material from the parent roll into the rolls that are wound from it. Paanannen et al consider that the presence of filler material, used in the process of making glossier grades of paper, provides a detrimental effect by modifying the coefficient of friction, and disrupting the uniformity of slippage. The crepe wrinkles documented were in the periphery of the wound rolls. Clues to the limits on the wound roll sizes are available. Paananen et al point out that it is difficult to wind rolls of newsprint with a density below 40 g/m^2 with diameters larger than 115 to 120 cm. It is apparent that these rolls were wound on a two drum winder, but what is unclear is whether a rider roll was involved.

In tracing the formation of crepe wrinkles Lemke et al[3] identify the need to control the entire process of papermaking for attaining uniformity of fiber orientation in the web along the machine direction. This observation is based on the presence of wrinkles in webs of newsprint during the winding stage, when the webs that did not possess a uniform fiber orientation across the width of the web were wound into rolls. However, whether the wrinkles were due to slippage is questionable as this information is not available.

Lemke et al point out that the kind of fiber used and the filler materials that are added to improve the smoothness and opacity of the newsprint actually decrease the coefficient of friction and the permeability of the web, thereby increasing the propensity of the web to slip and form crepe wrinkles. Other factors mentioned include the reduction in grammage and the reduction in caliper of the web. In an observation pertaining to the rolls that had crepe wrinkles in them, Lemke et al observe that rolls which were wound from the periphery of the parent rolls were more prone to crepe wrinkles than the rolls wound from the inner areas of the parent roll. While identifying the parameters of the winder that were responsible for the formation of crepe wrinkles, attention has been brought to low web tension and a high nip load, presumably from the rider roll. No magnitudes have been mentioned.

An interesting mechanism has been proposed to explain the formation of crepe wrinkles on two drum winders. The description involves a local drop in tension a few layers beneath the nip, and air entrainment between the loose layers in the periphery of the wound roll, Figure 18, stage 1. As the pressure of the entrained air increases, due to the increase in mass of the wound roll above, the air pocket attains the capacity to support the roll. Then, there is a sudden dispersion of this air pocket when it comes under a nip, and the authors feel that this air lubricates the layers, Figure 18, stage 2. At this stage, there is the presence of a loosening torque which tends to promote slippage in the layers beneath the nip. The origins of this loosening torque are not clear, however, this torque in combination with slippage has been attributed to the formation of crepe wrinkles, Figure

18, stage 3. Lemke et al propose that the loosening torque is higher when the roll is soft or when there is a high nip deformation. The reason for the drop in tension is unclear and so is the reason for the slippage. The qualitative description of the mechanism has focused attention on three aspects, namely:

(i) the slippage occurs at the periphery of wound rolls

(ii) the location of the defect and the presence of the nips in the vicinity of the slippage

(iii) the softness of the roll leading to higher nip indentation and the slippage induced due to the nips.

Other qualitative pointers, given by Lemke et al, include the need to have the drums in the two drum winder of the right size, and a roll structure control feature such that rolls with a "high hardness" can be produced with a "decreasing slope" from the core to the periphery of the roll. The need to minimize any spikes in the hardness profile has also been stressed.

Schoenmeier[15], in a separate study, has compared the efficiency of using a single drum surface winding scheme versus a two drum surface winding scheme to wind rolls of newsprint and other light weight coated paper rolls. Parameters such as

(i) nip loading

(ii) web tension

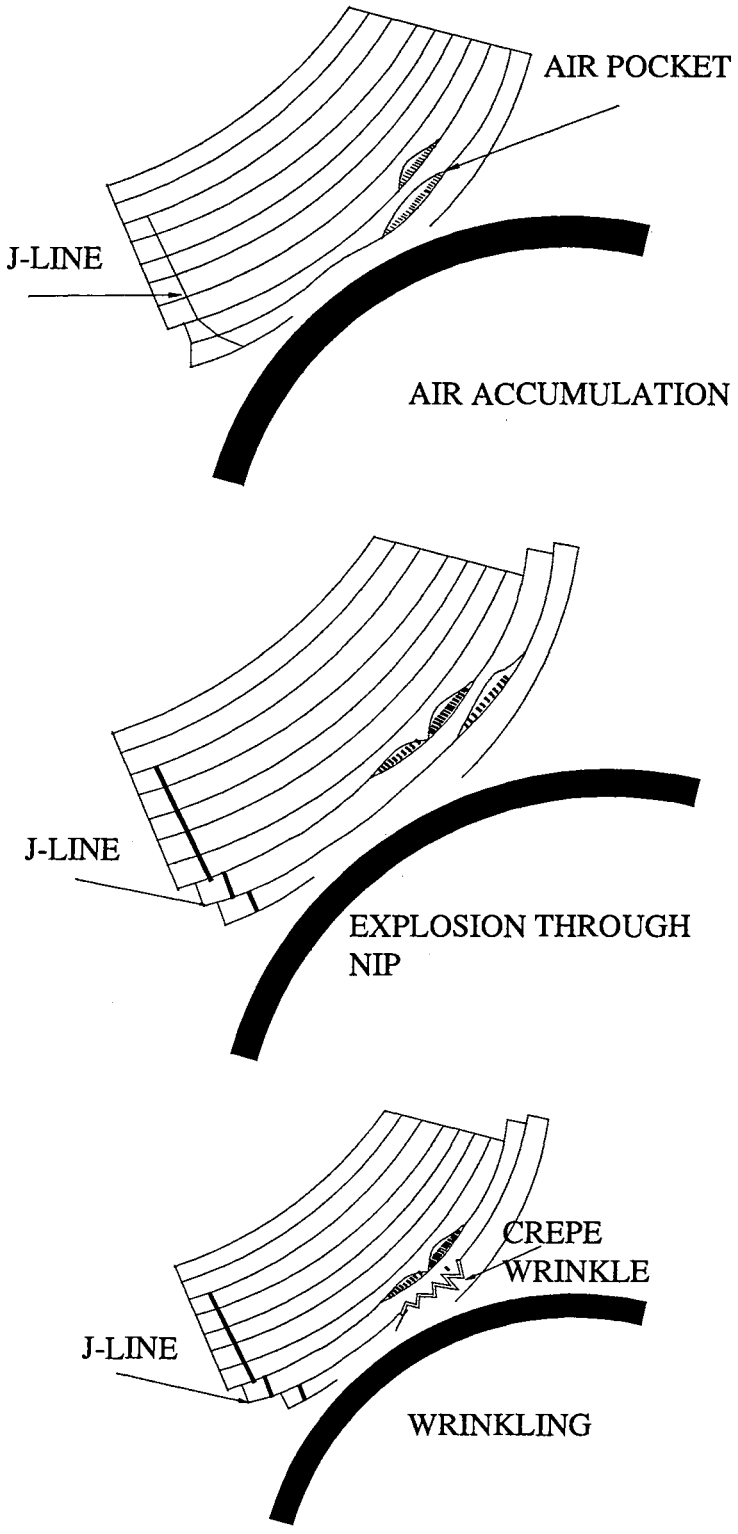

Figure 18. Illustration of Stages 1, 2 And 3 showing Crepe Wrinkle Formation, from Lemke et al[3].

(iii) coefficient of friction ("surface roughness")

(iv) compressibility of the paper

have been identified as important in controlling crepe wrinkles.

With respect to the location at which crepe wrinkles occur, Schoenmeier has identified two locations. In two drum winders, crepe wrinkles have been observed to occur in the periphery of the roll. The other location identified is the immediate vicinity of a splice (within 15 mm). The reason for the formation of the crepe wrinkle near the location of the splice is unclear. Schoenmeier identifies the nip cycles that the roll undergoes to be a primary reason for the formation of crepe wrinkles. However, the decelerations of the wound rolls have also been identified as a cause for the formation of these defects. It is unclear as to whether the crepes occurred after the roll was completely wound or if they occurred immediately following the web break.

In terms of the formation of crepe wrinkles on two drum winders and the ability to reduce the occurrence of the defect, Schoenmeier points to the inability to control nip loading, due to the self weight of the wound roll, as a key factor. Figure 19 shows the variation of nip load to be proportional to the square of the wound roll diameter in the case of the two drum winder after the roll reaches a certain diameter. It is not clear whether the data are from actual measurements or theoretical computation. However the key points stressed are the increase in nip load and the inability to control the nip load in a two drum winder without nip relieving.

Another important factor considered is the web tension. Schoenmeier considers this to be limited by the physical properties of the web. Most of the newsprint and light weight coated webs are considered incapable of sustaining a "high web tension" without tearing. Thus, Schoenmeier identifies a limited scope in controlling the formation of crepe wrinkles via the web tension. In addition, other material parameters, such as the coefficient of friction and the "compressibility", are also not controllable from the perspective of the winder. However, Schoenmeier points out that the "hardness profile" of the roll wound on a two drum winder has an effect on the formation of crepe wrinkles. Here, again, the key factor controlling the "hardness profile" has been the nip load from the self weight of the wound roll.

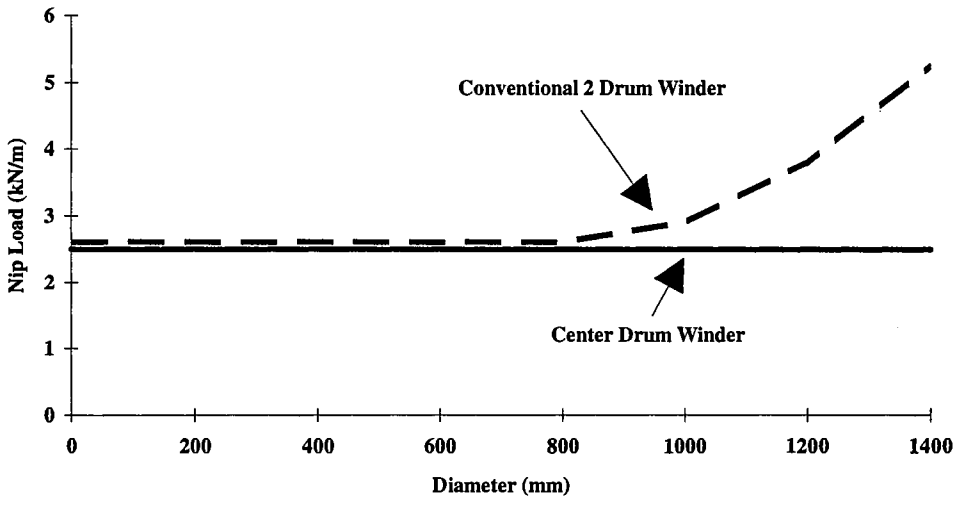

Figure 19. Illustration of variation of Nip Load with drum diameter, from Schoenmeier[15]

In an internal report generated at Beloit Corporation, Roisum[16] has statistically analyzed the effects of core notches, roll width, roll diameter and roll weight on the formation of crepe wrinkles. This statistical study does not reveal mechanisms responsible for the formation of the defect, but identifies trends. The study was based on reject rates of rotogravure paper rolls during a regular production run. The study is based on crepe wrinkles occurring in the rolls above the location of core notches by filling the core notches. The statistical study revealed the following trends:

(i) Rolls with larger widths had crepe wrinkles in them. The widths of the rolls ranged from 60 to 100 inches.

(ii) Rolls with larger diameter had no crepe wrinkles in them. The roll diameters ranged from 40 to 52 inches.

(iii) Heavier rolls had less crepe wrinkles in them. The roll weights ranged from 4200 to 5600 lb.

It is not clear what parameters were held constant in the statistics indicated above. In (iii) above, it is not clear whether the statement is made for rolls with equivalent diameters.

In a related study on stresses existing in rolls of paper during winding, Roisum[17] emphasizes the importance of using wound roll stresses as a means to quantify the quality of the roll. Roisum identifies:

(i) High radial stresses and high coefficients of friction lead to an increased resistance of the roll body to slippage.

(ii) High compressive circumferential stresses existing in a wound roll could lead to buckling related defects such as starring or creping. Roisum points out that the

regions of the wound roll which have negative circumferential stresses are locations where wound roll defects such as starring and creping are likely to occur.

(iii) Wound roll slippage, and slippage related defects such as telescoping and creping occur whenever the radial stresses are low.

(iv) The effect of centrifugal stresses disturbing the radial stresses while the roll is rotating at high speeds. Thus, there is a reduction in the radial stresses at high speeds which increases the tendency of the roll to telescope or slip on itself.

Although this study presents information pertaining to crepe wrinkles, there is no clear link between the different parameters discussed and slippage, and consequently slippage related defects. Thus the capacity to predict defect formation is non-existent.

In a third related study addressing the mechanics of slippage, Roisum[18] attempts to answer the question of "how slippage must have occurred" in a wound roll based on the geometry of the J-Lines. The limitation of this study with respect to answering the question of "Why slippage occurs" has been acknowledged. The study focuses on modeling the slippage from the geometry of the J-Line and attempts to show the progress of slippage, assuming uniform slippage.

In relating discontinuous roll body slippage and crepe wrinkle formation, Roisum has outlined characteristics that promote the defect formation. These are:

(i) The propensity to form crepe wrinkles increase when the "average paper/paper friction" decreases in value.

(ii) The possibility of crepe wrinkle formation increases with increased winding cycles. It is not clear whether slippage induced by the nips are responsible or whether physical changes that occur in the web material such as change in density of the web due to nip loading or a combination of both.

(iii) The variation of friction between layers promotes the possibility of occurrence of crepe wrinkles.

In an independent study on slippage related defects, such as crepe wrinkles and tears occurring during winding and unwinding of rotogravure paper rolls, Welp[19] points out that rolls undergo cyclical stressing and overloading in the region of the core, more specifically in the region of the core chucks and radially into the roll location, a region which is referred as the "reel center". According to Welp, the key parameters associated with the roll structure are web tension, nip loads, the torques provided at the cores and the torques provided at the winding drums. Welp states that it is possible to construct rolls with "good" structural integrity, with widths of 2.5 m. and diameters around 120 cm. and roll weights of about 4 tons. But, when these limits are extended, the rolls break down during processing due to slippage related problems such as crepe wrinkles and paper bursts. Welp has analyzed the problem of crepe wrinkles from a winding and an unwinding perspective. The winders considered belong to the single drum winder category (center drum winder) see Figure 20, a variation of surface winding.

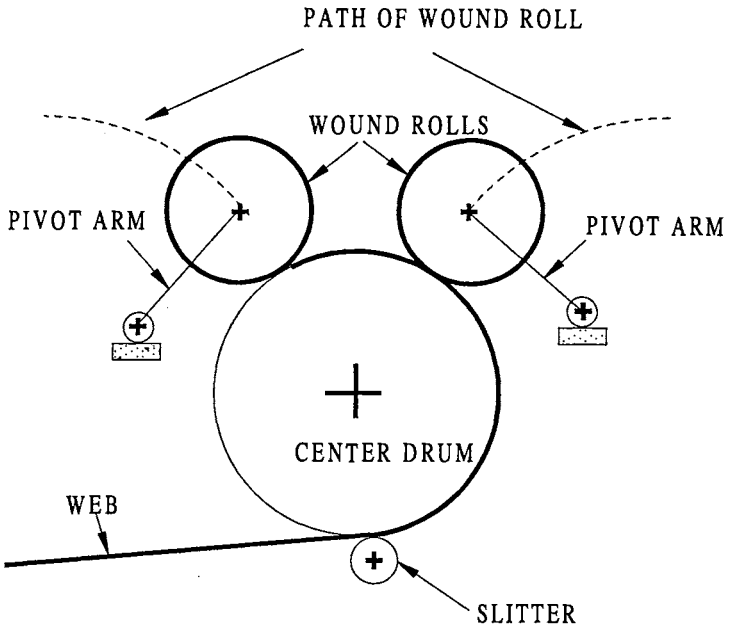

Figure 20. Illustration of a Center Drum Winder, from Welp[19]

The remedial action suggested includes increasing the diameter of the core, higher stiffness, higher tensile strength and a smaller mass of the core. Welp emphasizes that crepe wrinkles occur during winding when certain diameters have been exceeded, and during unwinding at the start of the process when the roll diameter is still large. No quantitative feel for the magnitudes is available.

In analysing crepe wrinkles, Welp states that core loading due to the self weight of the roll induces high shearing in the region of the core chucks and bending moments across the roll widths, which cause eccentricity of the core with respect to the axis of the roll. Welp believes the eccentricity of the core, with respect to the axis of the roll, to be responsible for the slippage. The maximum effects of these shearing forces and bending moments are in the region close to the roll edges. Welp attempts to relate cyclically

varying radial stresses and tangential stresses that exist across the width of the roll and, in addition, an "axial-stress" to cause stressing of the layers in the vicinity of the core chucks which promote tearing of the web. No criterion for the onset of slippage is available. Welp demonstrates the existence of slippage in the region of the core, using tests to simulate the existence of radial stresses in the roll and a differential torque that promotes slippage between the core and the rest of the layers. However, this study was qualitative in nature and does not create any links between the different characteristics outlined and the onset of slippage.

The study by Welp has brought out clues pertaining to crepe wrinkles:

(i) Crepe Wrinkles occur during rewinding with sudden layer slippage involving one or a few layers

(ii) Paper properties such as specific density, compressibility, smoothness and caliper variation influence the formation of crepe wrinkles

(iii) Core properties such as geometry, stiffness and strength influence the formation of crepe wrinkles.

Summary of the Literature Review and Catalog of Process Parameters Identified

The most common cause for the formation of crepe wrinkles, as identified in the literature, is inter-layer slippage. There is unanimous agreement on the the nip roll as a cause for slippage during surface winding, although the mechanism unclear. Consequently, all nip related parameters have been identified as potential causes for wound roll slippage.

In general, the literature can be divided in two categories. In the first category, quanfication of wound roll structure is based on wound roll density, for example studies by Laumer, Daly, Lucas, Frye, Odell et al, Paananen et al. In the second category, the quantification of wound roll structure is based on inter-layer radial stresses, for example, Roisum, Welp, Schoenmeier. The quantification of wound roll structure using inter-layer stresses is better than the wound roll density quantification, as it is possible to relate slippage via the torque capacity of the wound roll. This study will show that the torque capacity of a wound roll is a means of quantifying slippage, and the dependence of torque capacity is on the inter-layer radial stresses.

The literature lacks quantitative evidence to justify hypotheses outlined, for eample, studies by Laumer (differential draw), and Lucas (internal gearing). The lack of evidence, may be partly due to the fact that most of observations were made on production winders, and, so production considerations override experimental considerations.

In most of the studies, the trend towards resolving slippage related problems are based on increasing or decreasing process parameter values, such as nip loads, wound on tensions, nip diameters, nip torques, changing surface roughness of nip rolls. This situation leads to difficulty in identifying the most important parameters, for example, studies by Lucas, Welp, Frye, Odell et al, Schoenmeier, Lemke et al and Roisum.

In some of the studies, statistical approaches for identifying parameters causing slippage related defects have been carried out, for example, Paananen et al and Roisum. These studies, however, lack the ability to point out process parameters that are directly related to slippage. The geometry of the J-Lines has been used to look at the problem of the mechanism of slippage during surface winding, for example Lucas and Roisum. These studies however, address the question of how slippage must have occurred, rather than what causes wound roll slippage.

TABLE 1 shows a catalog of the parameters gleaned from the literature addressing slippage related wound roll defects.

Table[1] Catalog of factors identified from the literature.

Paper Reviewed	Location Of Crepe Wrinkles	Primary Parameter Suggested / Other Parameters Mentioned	Quantitative Modeling/ Data Interpretation
Laumer	Near core (2 drum winder)	Slippage,Basis weight Roll width, Tensile strength, Roll hardness.	Geometric modeling attempted
Daly	Not mentioned (2 drum winder)	Slippage, Tensile compressive stress strain behavior, Drum diameter, Nip load, Unwind stand tension, Torque transmitted via nip, Inter-layer shear resistance, Radial stress variation in rolls.	None attempted
Lucas	Near core, near nips (2 drum winder)	Slippage, Rider roll nip load, Front drum torque, Deceleration rates, Inter layer pressurem, Roll weight Core diameter, Coefficient of friction between layers, Paper compressibility, Unwind tension, Ingestion of bubble.	"J-line number" Internal gearing theory
Welp et al	Near core (2 drum winder)	Slippage, Rider roll nip load, Speed, Bending stresses in core area, Self weight of roll.	"J-line" studies and Speed differences between drums

Contd...

Paper Reviewed	Location Of Crepe Wrinkles	Primary Parameter Suggested / Other Parameters Mentioned	Quantitative Modeling/ Data Interpretation
Frye	Near core, near nips (2 drum winder)	Slippage, Self load of roll, Drum diameter, Web Tension, Torque, Speed, Drum wrap, Tensile modulus, Basis weight, Radial modulus, Inter-layer coefficient of friction.	
Odell et al	Near nip (2 drum winder)	Slippage, Rider roll relief, Caliper web, Basis weight of web, Wound roll diameter, Differential Drum torque, Web tension, Drum diameters, Time interval between paper making and winding.	Nip load - basis weight quantification
Paananen et al	Near nip, near core (2 drum winder)	Slippage, Web Grammage Caliper, Coefficient of friction.	
Lemke et al	Near nips (2 drum winder)	Slippage, Non uniform caliper, Air entrainment, Nip loads, web tension.	
Schoenmeier	Near nips, near splice location (2 drum winder)	Slippage, Nip load, Web tension, Interlayer coefficient of friction, Radial modulus.	
Roisum	Near core	Slippage, friction, Radial and, Circumferential stresses	"J-line" models

CHAPTER IV

TORQUE CAPACITY

The Importance of Torque Capacity in Predicting Slippage in Wound Rolls

The literature review revealed slippage as the most important factor responsible for the formation of crepe wrinkles. So, to understand crepe wrinkles, it is imperative to understand slippage. To be able to predict crepe wrinkle formation, the occurrence of slippage must be predicted. To predict slippage, it is important to identify the factors responsible for slippage and the interaction of the different parameters.

The capacity of a wound roll to resist slippage can be quantified via the torque capacity. Good[20] documented the importance of torque capacity as a tool to predict slippage, with wound roll models and experimental data. The torque capacity reflects a wound roll's ability to resist slippage when an external torque is applied to the roll. The torque capacity (T_{cap}) is a derived quantity and can be generated from the radial stress variation that exists in a wound roll. The radial stress variation is a measure of the structural integrity of the wound roll. Thus, to quantify slippage in a wound roll, it is imperative to understand the torque capacity of the wound roll, and to understand torque capacity, the radial stress variation existing in the roll must be quantified. In the following, the

relevance of the torque capacity of a wound roll is outlined, and then, means to quantify radial stresses that exist in wound rolls are explained.

In simulating the radial stresses which exist in wound rolls of web material, wound roll models to date accrete layers of web as concentric hoops of material in an iterative process. The ability to resist slippage between the hoops depends upon the radial stresses, the cylindrical area of the hoop at a given radius, the coefficient of friction between the web layers, and the radius of the hoop. The importance of torque capacity as a tool to predict slippage was realized early in the magnetic film industry and perhaps in the paper industry and the film industry too, but wound roll models had not been developed to a stage where they could be used with confidence to predict wound roll pressures.

If the radial stress profile of the roll can be expressed as $\sigma(r)$ (psi), the coefficient of friction as 'μ', the width of the web as 'w' (in) and the radius 'r' (in) then

$$T_{cap}(r) = \sigma(r)\left[2\pi r w\right]\left[r\mu\right] \text{ (lb-in)} \qquad (1)$$

There are many sources from which an externally applied torque (T_{app}), can be imposed on a wound roll, depending on the winding scheme chosen. For example, in center-winding without a lay-on nip, the winding torque, which is the product of the web tension and the instantaneous radius, is an applied external torque. During unwinding, the braking torque, which is the product of the wound off tension and the instantaneous

radius of the wound roll, is an external applied torque. There may, also, be external torques imposed due to dynamic effects such as rapid deceleration following an emergency stop, or rapid acceleration of an unwinding roll. In a wound roll, slippage occurs whenever the applied external torque ($T_{app\text{-}external}$) becomes greater than the torque capacity or:

$$(T_{app\text{-}external}) > (T_{cap}) \tag{2}$$

So, even before winding a roll, it is possible to predict the onset and the location of the occurrence of slippage if the torque capacity profile of the roll is known. Hence, the torque capacity is the most important quantitative parameter to characterize slippage in wound rolls of web material.

Wound Roll Models

The relevance of torque capacity has been outlined above. The radial stress variation, $\sigma(r)$ determines the torque capacity. The radial stress variation is a quantification of the structural integrity of a wound roll. Wound roll models reveal the variation of radial stress as a function of the radius. These models have been in existence for the last thirty years and have gradually evolved to incorporate realistic material properties. A compendium of wound roll models and the evolution of those models to the current state of the art has been established by Good[20]. The most widely used model, developed and experimentally verified for center winding by Hakiel[21], considers non-linear material

properties. An extension of this model to incorporate lay-on nip rolls was developed by Good et al[22] and has been experimentally verified. The development of wound roll models for surface winding is still in its infancy.

The model developed by Hakiel[21] for center-winding, without a lay on nip, has become a standard means of characterizing the structural integrity of the wound roll. This model considers the variation of the modulus of the web in the radial direction with the radial pressure. Some idealizations in the model include:

(i) A condition of plane stress in the wound roll.

(ii) The wound roll is a geometrically perfect cylinder, which implies uniformity in thickness along the width of the web.

(iii) Winding is considered as an accretion of pre-tensioned concentric hoops and not as an accretion of a continuous spiral.

(iv) The wound roll is considered to be an orthotropic elastic cylinder. It is linearly elastic in the tangential or circumferential direction and non-linearly elastic in the radial direction. The non-linear variation of the (material property) modulus with respect to the pressure is considered here.

(v) The radial stresses that exist in the wound roll are dependent on the radial location, but are independent of the circumferential location and axial location.

Hakiel's model has been derived considering the equilibrium equations for plane stress in the absence of shear, linear orthotropic constitutive equations in the radial and tangential directions and enforcing strain energy constraints and strain compatibility conditions as

$$r^2\frac{d^2\sigma_r}{dr^2}+3r\frac{d\sigma_r}{dr}-\left[\frac{E_\theta}{E_r}\right]\sigma_r=0 \tag{3}$$

In the equation (3), σ_r is the radial stress that exists in a pre-stressed sector of web material and is the unknown variable. E_θ (also known as E_t - or Circumferential Modulus) and E_r are the tangential modulus of the web material and the radial modulus of the web, respectively, and r is the radius of the hoop.

As winding progresses, more pre-tensioned hoops are added, in which case the differential equation can be adapted in a slightly different form as:

$$r^2\frac{d^2[\delta\sigma_r]}{dr^2}+3r\frac{d[\delta\sigma_r]}{dr}-\left[\frac{E_\theta}{E_r}\right][\delta\sigma_r]=0 \tag{4}$$

to reflect increments of radial pressure. In the modified equation (4), the unknown variable $\delta\sigma_r$ is the incremental compressive pressure in a the roll due to the addition of a layer. This is a second order non-linear ordinary differential equation and cannot be solved to yield a closed form solution, as the ratio $\frac{E_\theta}{E_r}$ cannot be evaluated without a prior knowledge of $\delta\sigma_r$. However, the differential equation can be solved numerically in a piece-wise linear solution (discretized), using central differences to replace the differential terms and a knowledge of two boundary conditions. The boundary conditions can be generated based on the continuity of deformation at the core and pre-tensioned

hoop interface and from the fact that incremental inter-layer pressure, due to the addition of a lap, can be generated by using the hoop stress equation.

$$\frac{d[\delta\sigma_r]}{dr}_{r=1} = \left[\frac{E_\theta}{E_r} - 1 + \upsilon\right][\delta\sigma_r]_{|r=1} \tag{5}$$

$$\delta\sigma_r|_{r=s} = \left[T_{w|r=s}\right]\frac{h}{s} \tag{6}$$

The extension of the modified differential equation, and the two boundary conditions, to quantify the radial stresses that exist in the wound roll can be accomplished by the discretization process which reduces the boundary value problem to a set of linearized algebraic equations:

$$A_i\ \delta\sigma_{i+1} + B_i\,\delta\sigma_i + C_i\,\delta\sigma_{i-1} = 0 \quad (i = 2,\ldots n) \tag{7}$$

where

$$A_i = 1 + 3\frac{h}{2r_i}$$

$$B_i = \frac{h^2}{r_i^2}\left(1 - \frac{E_\theta}{E_r}\right) - 2$$

and $C_i = 1 - \dfrac{3h}{2r_i}$

and the boundary conditions can be discretized in a similar fashion to yield

$$\delta\sigma_{i+1} = T_{w,(i+1)} \frac{h}{r_{i+1}} \tag{8}$$

and

$$\frac{\delta\sigma_2 - \delta\sigma_1}{h} = \left[\frac{E_\theta}{E_c} - 1 + \nu\right]\delta\sigma_1 \tag{9}$$

As every layer is added, these linearized algebraic equations are set up into a compact system of tri-diagonal matrix equations. The system of equations can be solved using matrix algorithms to yield discrete values of the incremental radial pressures. This process is repeated until all the layers are added. The incremental pressures at every lap due to the addition of laps above it are finally summed to yield the radial pressure at that point.

A secondary quantification of the structural integrity of the wound roll, which is available from the radial stress, is the variation of the circumferential stress as a function of the radius, as the circumferential stresses (tangential stresses) are related to the radial stresses via the equilibrium equation

$$\frac{rd\sigma_r}{dr} + \sigma_r - \sigma_\theta = 0 \tag{10}$$

The process of solving the differential equation numerically, can be programmed into a computer, and, given a set of input conditions, the differential equation can be solved. The solutions of the differential equation are discrete values of the radial stresses that exist in a center wound roll.

WINDER[1] is one such program and the inputs to this program are:

T_w Tension

E_t Tangential Modulus of the web material

E_r Radial Modulus of the stack of web material

E_c Core Modulus

h Web caliper

r_c, s The inner and the outer radii of the wound roll

r_{co},r_{ci} The inner and outer radii of the core

ν Poison's ratio of the web material

The numerical solution of the equations developed from the wound roll model can be visualized easily in the form of a graph. To obtain a realistic measure of the radial stresses and circumferential stresses which exist in a wound roll, it is important to provide realistic inputs to the model. Consequently E_t and E_r are usually measured experimentally and provided as inputs. The tests will be described explicitly in the next section.

[1] WINDER is a proprietary implementation of Hakiel's algorithm developed at the WHRC, Stillwater, OK

Measurement of the Physical Properties of the Web material

To model the radial stresses which exist in the wound roll, it is imperative to measure material properties accurately. In this chapter, tests to establish material properties which will be used to model the structural integrity of the wound roll will be described. Included are the "radial modulus test", popularly known as the stack test or E_r test , the "tangential modulus test" or the E_t test, and the test to determine the coefficient of friction between the layers. The coefficient of friction is not used to determine the radial stresses but is necessary to characterize the resistance of the roll to slippage, which will be discussed later. The experimental methods described are the same irrespective of the web material.

Radial Modulus Test

Pfeiffer[23] described this test in detail in an early paper during the 60's. A detailed description of the test was given by Swanson[24] in a later unpublished internal report. The radial modulus testing is done to determine the stress - strain behavior of web material when stacked in layers. This data correspond to the instantaneous stress - strain behavior in a stack of web. This test requires a material testing machine, such that loads can be applied on the material and the deformation on the material be monitored continuously along with the load.

At the WHRC an INSTRON 8502[2] is used for obtaining the stress strain relationships in a stack of web material. The INSTRON 8502 can be operated in three modes, namely load control, position control, and strain control. The loading frame is hydraulically controlled. The continuous load deformation history can be automatically acquired through a data acquisition system which can be connected to the INSTRON.

The material used in this study was mostly newsprint; however, the material preparation is identical for any other web material. Stacks of newsprint larger than the size of the platens are cut. The platens on the INSTRON 8502 are circular and 6 inches in diameter. So, square stacks of newsprint 6.5 inches on a side were cut. A stack of 1 inch thickness is used in all the measurements so that strains in the specimen are simply equal to the deformations (as strain $\varepsilon = \frac{\Delta l}{l}$, and $l = 1$ in).

The stack of material is placed between the platens of the INSTRON and the machine is set in the load control mode. A schematic of the material testing system is shown in Figure 21a. A specific value of the load corresponding to the required stress is entered into the console of INSTRON's interface. The rate at which this load is applied to the specimen can be input through the console. A data acquisition system connected to the interface acquires the load deformation history. The loading rate can be manipulated based on the sampling rate of the data acquisition system. The load deformation history can be converted to stress strain data by dividing the load by the area of the platens and by

[2] INSTRON is a Material Testing System manufactured by INSTRON CORPORATION

dividing the deformation by the original sample thickness (1 inch for all the tests used in this study). Figure 21b shows the actual stress-strain behavior in a stack of newsprint tested at the WHRC. The radial modulus is the slope of the stress strain curve. Thus, the radial modulus of the stack of web is given by

$$E_r = \frac{d\sigma}{dr} \tag{11}$$

As the stress-strain values are discrete, numerical methods are employed to determine the slope of the data. The stack of web material exhibits a non-linear relationship between the stress and strain, so the radial modulus is also a function of the stresses in the web material. Physically, this means that the modulus of the stack is dependent on the pressure that exists on the stack and varies non-linearly with respect to the pressure in the stack. Polynomial curve fits can be used to quantify the variation of radial modulus with the stack pressures. Exponential forms are a compact means of representing this variation, as has been demonstrated by Pfeiffer [23]. Care should be exercised in using any particular form to quantify the material behavior, as certain forms fit the experimental data better than the other forms. Care should be taken to insure that the curve fits are not used outside the domain in pressure over which stack data were collected.

All materials exhibit hysteresis or a loss of energy when taken in a cyclical fashion into loading and unloading. When the stress-strain behavior of such material is observed, during up-loading and down-loading, the curves do not take the same path. When a stack of web material is subjected to the E_r tests there is a difference in the material behavior.

The trend by most researchers is to use the up-load history to model the material property. Pfeiffer suggests using the down-load curve to model the material property. The choice is left to the individual researcher to determine a particular quantification. It is prudent to have both the up-load and down-load data if it is possible, as the hysteresis information can be of value when evaluating other factors, such as rolling resistance.

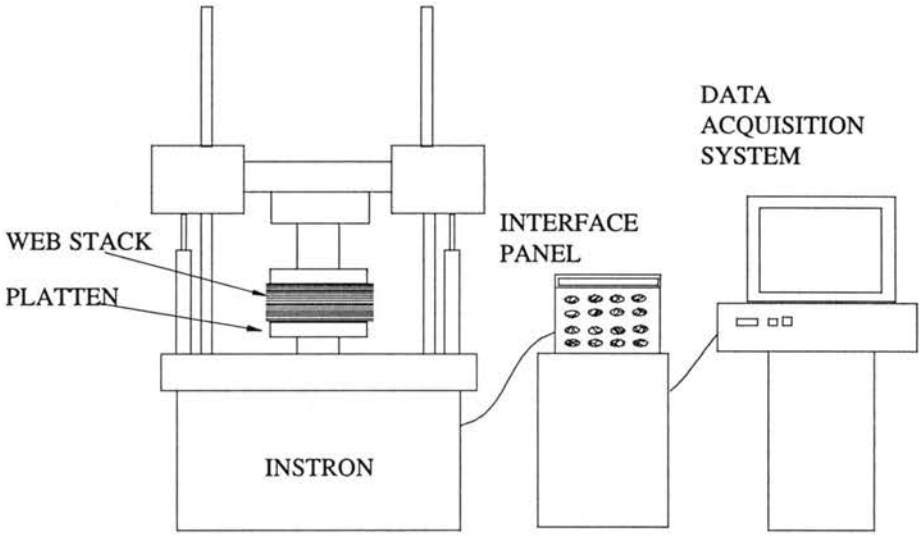

Figure 21a. Schematic of the Material Testing System for Measuring E_r.

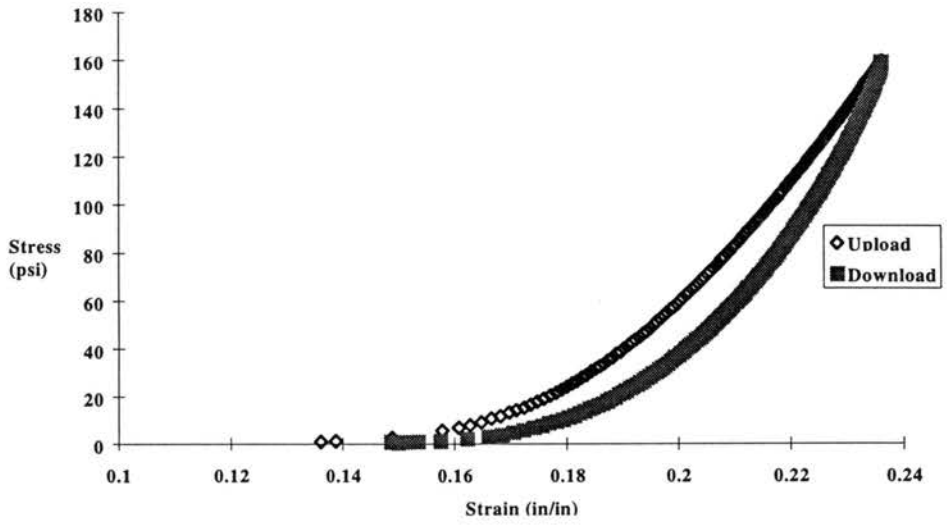

Figure 21b. Sample Stress-Strain Data for a stack of Newsprint.

Tangential Modulus Test

In this test, the modulus of the web material in the machine direction is measured by subjecting a strip of the web material to a gradually increasing uniaxial load and monitoring the deformation. Within the elastic limit, the stress in the specimen is proportional to the strain produced and the modulus of the material in the machine direction is the slope of the stress-strain curve.

At the WHRC E_t testing is carried out using the INSTRON 4202, a smaller version of the 8500 in which all testing is performed in stroke control. A load cell which is capable of measuring loads in the range of 0 to 30 lb is important, as the INSTRON was originally equipped with a 2000 lb load cell. When testing web material like newsprint, which has a low tearing strength, load cells which can measure small forces accurately are essential. The loading frame in the 4202 is driven by an electric motor, using power screws. The loading and the deformation of the specimen can be monitored using a data acquisition system which can be connected to an interface on the console of the INSTRON. Although the material used in most of the tests during this study was newsprint, the material preparation is identical for other web materials.

The web material is cut into thin strips of about 13 inches in length and 1 inch in width. A gage length of 10 inches is chosen in the middle and the inch and a half of web material on either side of the gage length is wrapped with a rough tape so that when this portion is attached to the grippers in the material testing machine there is enough roughness to clamp the web specimen in the grips of the material testing system. The specimen is

gripped firmly between the two grippers, one attached to the loading frame and the other attached to the base of the machine, Figure 22a . Care must be taken to align the web specimen straight between the grips. Any kinks in the web material will lead to the web tearing prematurely, due to uneven loading across the width of the web. The loading frame is set up to move at a low speed of 0.02 in/sec and the load deformation data is continuously acquired until the web tears. The load deformation data can be converted to stress-strain data, see Figure 22b, and the slope of the stress strain curve gives the modulus in the machine direction. As the data acquired is discrete, numerical techniques can be used to generate a slope. The slope, which represents the modulus of the web material in the machine direction, E_t, is linear within the elastic limit.

Paper webs tear, but other material such as plastics and non wovens do not tear, instead yield considerably and there is necking of the specimen. However, the modulus of the particular web material in the machine direction is the slope of the linear portion of the stress strain curve.

Coefficient of Friction

The coefficient of friction that exists in web materials is not a constant. The values of the coefficient of friction differ. Consequently, the friction test is repeated a few times and an average value is used from these tests. The apparatus to measure the coefficient of friction at the WHRC was constructed in accordance with ASTM standards.

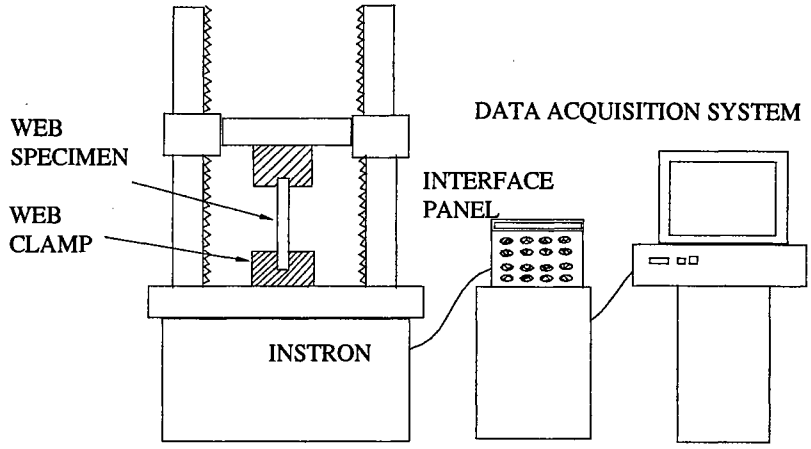

Figure 22a. Schematic of the Material Testing System for Measuring E_t.

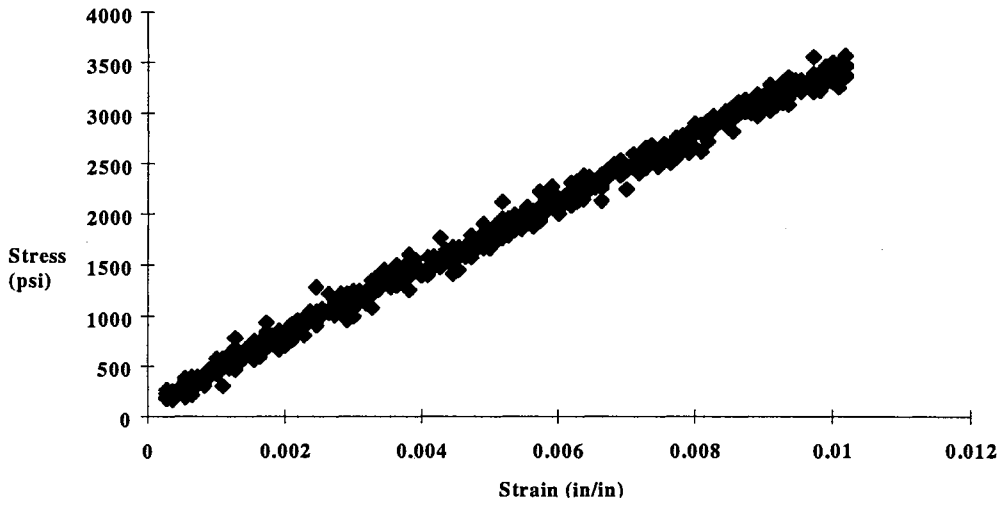

Figure 22b. Sample Stress-Strain Data for Newsprint.

The testing table consists of a sled, a plane and a force measuring device, Figure 22c. The web material is glued to the upper surface of the plane and the lower surface of the sled. In this fashion, the static coefficient of friction between the two web materials glued to the surfaces can be measured. The plane is the surface which moves on smooth linear shafts and is powered by a small DC motor driving a lead screw. The DC motor is

controlled via a computer, and the velocity with which the motor drives the shaft is measured by a small encoder attached to the motor. The sled is made of aluminum and is a small block measuring 2.5 in. X 2.5 in. and 0.25 in. thick. The plane which moves on the linear shaft is made of aluminum and has a layer of smooth plexiglass on top of it. The dimensions of the plane are 6 in. X 12 in. The force measurement is carried out using a load cell which can measure a maximum of 10 pounds. The sled is connected via a thin copper wire to the load cell, and at the start of the run the sled is positioned such that there is no slack in the wire. The test consists of gluing the necessary specimens to the bottom surface of the sled and the upper surface of the plane, then moving the plane at a low speed and monitoring the force on the load cell. The speed at which the plane is moved is 0.5 feet per minute with a tolerance of 0.1 feet per minute. The load cell output can be automatically acquired by a computer.

At the instant the plane is set in motion, the frictional force resisting the motion of the sled increases and peaks, after which there is motion. The peak value represents the static frictional force. The static coefficient of friction μ_s is given by

$$\mu_s = \frac{F_{peak}}{F_{normal}} \tag{12}$$

where F_{peak} and F_{normal} represent the peak frictional force and the normal load respectively due to the sled on the interface between the two specimens, Ducotey[25].

After the onset of relative motion, the frictional force drops and becomes fairly constant. This is the region where the kinetic coefficient of friction comes into play. In this region,

there may be an oscillatory behavior displayed by the force which has been characterized as the stick-slip behavior of the interface between the surfaces, Figure 22d. An average value of the frictional force is computed to yield the kinetic coefficient of friction given by μ_k. Thus:

$$\mu_k = \frac{1}{F_{normal}}\left[\sum_{i=1}^{n}\frac{(F_{frictional})_i}{n}\right] \tag{13}$$

where $F_{frictional}$ represents the force acquired by the load cell, and n is the number of samples. Both the static and kinetic coefficient of friction can be determined using the formulae outlined above. Usually, the static coefficient of friction is used to characterize the ability of a wound roll to resist slippage.

The material properties that are used to model the radial stresses resident in the wound roll have been described and methods to evaluate them have been outlined. The accuracy of the models are limited by the assumptions which have been used to derive them and also by the accuracy of the material properties provided as the input. Using the methods outlined above, characterization of the radial stresses existing in wound rolls has been carried out successfully.

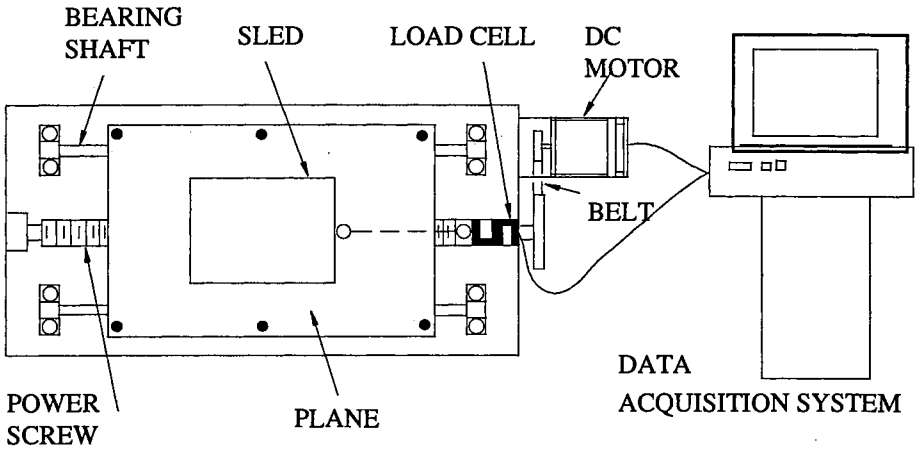

Figure 22c. Schematic of the Friction Testing Machine.

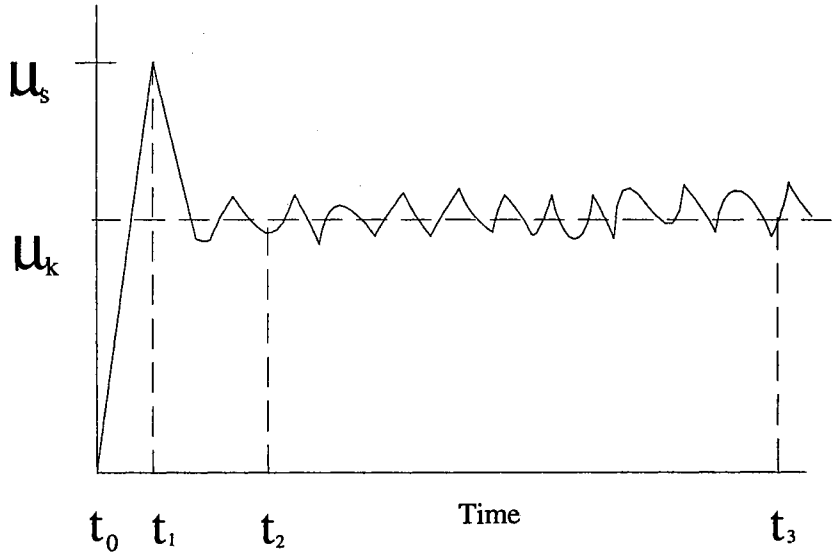

Figure 22d. Stick Slip Behavior.

Radial Stress And Torque Capacity Simulations

As an example, a winding model was implemented on a paper web whose properties are listed in TABLE 2 shown below.

TABLE 2. Input properties for the winding model.

Web Tension	130 Psi
E_r	$134.9 + 38.8\,\sigma - 0.075\,\sigma^2 + 0.00005\,\sigma^3$
E_t (Average)	240000 Psi
Web Caliper	0.0028 in (2.8 mils)
Coefficient of friction (μ) paper/paper	0.2
Width of web	6 in
Poisson's ratio	0.01
Wound roll dimensions	1.65 in. Inner Radius, 5.65 in. Outer Radius
Core	Steel, 1.5 in. Inner Radius and 1.65 in. Outer Radius

Note that this is a case of a constant tension winding. In constant tension winding, the torque to which the roll is subjected, increases linearly as the outer radius of the wound roll builds. The radial stresses, the torque capacity which resulted from the model, and the maximum applied torque, are shown in Figure 23. The applied torque is shown as a function of the radius, but at any instant the applied torque is a constant throughout the roll and is simply the product of the current winding tension of the roll and the instantaneous tension of the roll being wound. This is typical for a constant tension wind in that $T_{cap} > T_{app}$ for the entire radial domain, which indicates that no slippage should

occur in this roll. However, had this roll been wound to a larger radius, slippage would have begun at some point.

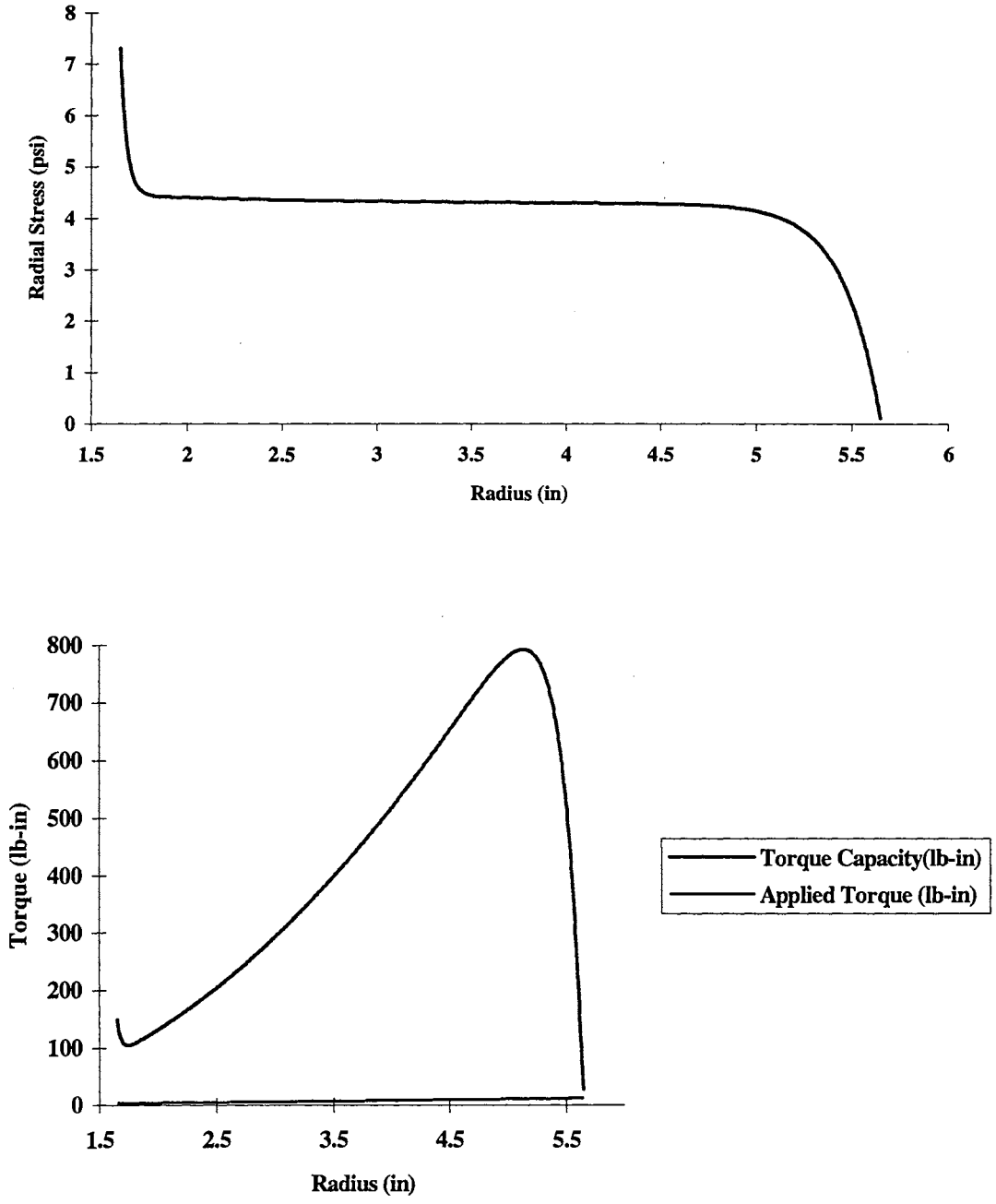

Figure 23. Radial Stress, Torque Capacity, and Applied Torque from the wound roll model.

Materials, like paper, commonly exhibit a plateau in radial stresses for constant tension winding, which is due to the ratio of $E_t/E_r(\sigma(r))$ being a large number, [21]. The effect of winding a larger roll in these circumstances does not alter the radial stresses at radii where a plateau in radial pressure has been achieved. To demonstrate the point, simulation runs were made with the material properties and input parameters outlined in TABLE 3, shown below.

TABLE 3. Input properties for the winding model.

Web Tension	100 Psi
E_r	$150 + 50\,\sigma - 0.08\,\sigma^2 + 0.00005\,\sigma^3$
E_t (Average)	200000 Psi
Web Caliper	0.003 in (3 mils)
Coefficient of friction (μ) paper/paper	0.3
Width of web	6 in
Poisson's ratio	0.01
Wound roll dimensions	1.00 in. Inner Radius, 40 in. Outer Radius
Core	Steel, 0.5 in. Inner Radius and 1.00 in. Outer Radius

Figure 24 shows snapshots of the torque capacity of the roll at different instants, when the outer radius of the roll is at 5, 10, 25, and 47 inches. Note that the lowest torque capacity is at a radius of 1.06 inches near the core, and has a value of 56.2 lb-in. Thus, the torque capacity in this radial zone remains unchanged while the applied torque increases linearly as a function of the outside radius of the wound roll, and at some point slippage will begin. If the value of the lowest torque capacity $T_{cap,\,min}$ and the radius at which it exists r_{min}, then when the wound roll's outer radius is r_{max} slippage occurs when:

$$T_w \cdot r_{max} > T_{cap,\,min} \tag{14}$$

from which r_{max} can be computed as

$$r_{max} = \frac{T_{cap,min}}{(T_w\, w\, t)} \tag{15}$$

where 'T_w' is web stress (psi), 'w' is width of the web (in), and 't' is caliper of web (in). For the case shown in Figure 24, slippage will originate when the radius of the roll is around 31 inches.

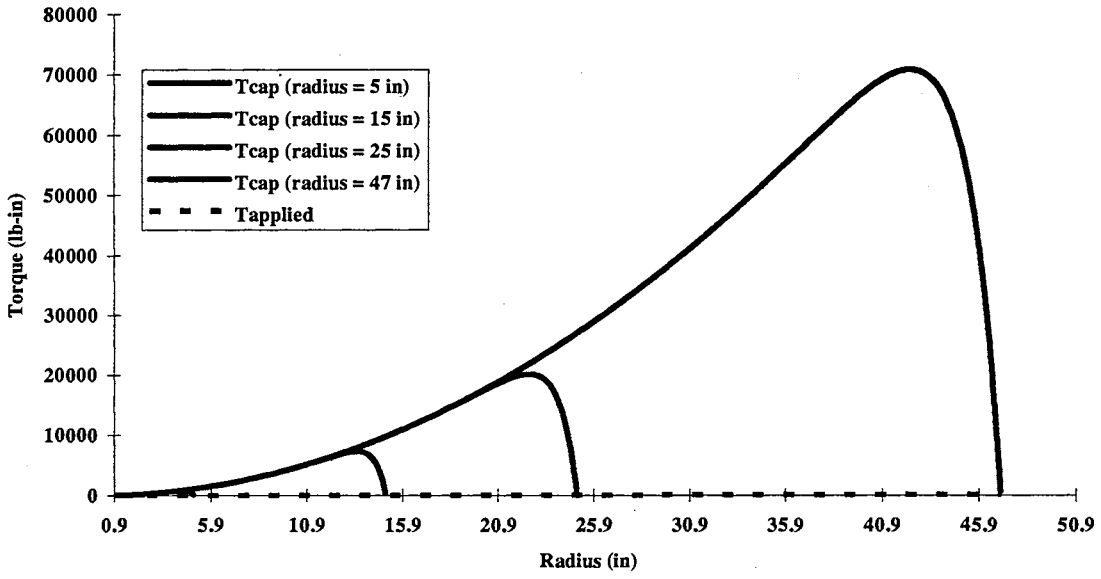

Figure 24. Snapshots of Torque Capacity at different instants during Winding.

Circumstances which promote slippage in a center wound roll are now outlined. The first involves a decrease in wound-on-tension, which might be due to a splicing operation.

This will be further discussed in the section on experimental work. The second involves slippage beneath the outer layer in a winding roll. The pressure beneath the outer layer in a winding roll is:

$$\sigma_r = \frac{W.O.T}{s} \qquad \text{(psi)} \qquad (16)$$

The W.O.T(Wound on Tension) is equal to the web line stress multiplied by the web thickness in center winding so:

$$\sigma_{r,s} = \frac{T_w h}{s} \qquad \text{(psi)} \qquad (17)$$

where 'h' is the caliper of the web (in) and 's' is the outer radius of the roll (in).

The torque capacity beneath the outer layer is:

$$T_{cap,s} = \frac{T_w h}{s}\left(2\pi s w \mu s\right) \qquad \text{(lb-in)} \qquad (18)$$

The applied torque is:

$$T_{app,s} = T_w h w s \qquad \text{(lb-in)} \qquad (19)$$

Slippage occurs whenever equation (2) is satisfied.

Substituting equations (17) and (18) into equation (19) show that slippage occurs whenever:

$$\mu \leq \frac{1}{(2\pi)} \tag{20}$$

This is interesting, as it shows why it is impossible to center-wind low coefficient of friction materials such as silicon coated release papers (μ=0.11). This type of material generally requires a surface assist to reduce the torque of center winding.

A Parametric Study of Torque Capacity

As outlined in the previous section, the material properties which determine the radial stresses determine the torque capacity of a wound roll. The winding scheme chosen to wind a particular material is also responsible for determining the torque capacity. The torque capacity can be broadly categorized as a function of the winding scheme and the material properties of the web. Using wound roll models, such as Hakiel's which was described earlier, it is possible to investigate the effect of variation of different input parameters which determine the torque capacity.

In this chapter we will examine the effect of different winding schemes such as

(i) Constant tension center winding

(ii) Constant tension center winding with lay-on nip roll

(iii) Constant torque center winding

(iv) Taper tension center winding

and the effect of variability of:

(i) Wound on tension (Web Tension)

(ii) E_t

(iii) E_r

(iv) Coefficient of friction μ

(v) Web caliper

on the torque capacity of a wound roll.

Although the effect of the web tension on the torque capacity has been considered, the effect of the variability of the web tension has not been clearly brought out.

In the simulation results presented, realistic material properties, corresponding to paper (newsprint) webs have been used. Figure 25a shows the torque capacities from the wound roll model for the different winding schemes chosen from the first category outlined. Figure 25b shows the low torque capacity zone near the core region for the different winding schemes, chosen at a higher magnification. The material properties used in the simulation are shown in the TABLE 4.

TABLE 4. Physical properties of the web material

Web Tension	Variable (see Figure for details) Standard Case 530 Psi
E_r	$134.9 + 38.8\sigma - 0.075\sigma^2 + 0.00005\sigma^3$
E_t	240000 Psi
Web Caliper	0.0028 in (2.8 mils)
Coefficient of friction (μ) paper/paper	0.2
Width of web	6 in
Poisson's Ratio	0.01
Wound Roll Dimensions	1.65 in Inner Radius, 5.65 in Outer Radius
Core	Steel, 1.5 in Inner Radius, 1.65 in Outer Radius

Figures 25a&b show that, depending on the winding scheme chosen, the torque capacity varies. In the immediate vicinity of the core, the torque capacities are low and vary between 500 and 900 lb-in. The lowest torque capacity will determine the maximum external applied torque before slippage originates in this region. So, with a judicious choice of winding scheme, it is possible to engineer the torque capacity such that the roll can withstand greater applied torques. The relevance of this is that larger rolls can be built such that the applied torques are well within the lowest torque capacity and the roll can withstand greater external torques. The constant torque case and the constant taper case were chosen such that at the start of the wind, the wound on tensions were the same as in the case of the roll wound with a lay on roll.

For the variation of the properties chosen from the second category, the physical properties of the web material are the same as shown in TABLE 4, earlier. But, for each of the parameters that are varied, the variations are outlined in TABLE 5. Constant tension center winding has been used in all the cases.

TABLE 5. Parametric Study of factors affecting Torque Capacity

Parameter varied	**Variations**	**Torque Capacity Trends and Reasons**
Wound on Tension (Constant Tension Center Winding)	250 Psi 400 Psi 530 Psi (All other properties are held constant and are outlined in Table [4])	As wound on tension increases, torque capacity increases. This is because as the wound on tension increases the radial stress $\sigma(r)$ increases, which increases the $T_{cap.}$ See Figure 26.
E_t	100000 Psi 241610 Psi 350000 Psi (All other properties are held constant and are outlined in Table [4])	As E_t increases, torque capacity decreases. This is because a larger ratio of E_t/E_r leads to a lower value of $\sigma(r)$, which decreases the $T_{cap.}$ See Figure 27.
E_r Profile # 1 Profile # 2 Profile # 3	 $27.46 + 74.01\sigma - 0.53\sigma^2 + 0.002\,\sigma^3$ $92.48 + 35.9\sigma - 0.24\sigma^2 + 0.0008\,\sigma^3$ $134.9 + 38.8\sigma - 0.08\sigma^2 + 0.00005\,\sigma^3$ (All other properties are held constant and are outlined in Table [4])	Harder the web stack, higher the torque capacity. This is because for a fixed E_t higher E_r leads to a lower E_t/E_r which leads to a higher value of $\sigma(r)$. Thus T_{cap} increases as $\sigma(r)$ increases. See Figures 28a&b.

Contd...

Parameter varied	**Variations**	**Torque Capacity Trends and Reasons**
Coefficient of Friction μ	0.1 0.2 0.5 1.0 (All other properties are held constant and are outlined in Table [4])	Smoother the web, lower the torque capacity. This is because T_{cap} increases as μ increases, Equation [1]. See Figure 29.
Caliper of Web	0.0014 in (1.4 mils) 0.0028 in (2.8 mils) 0.0056 in (5.6 mils) (All other properties are held constant and are outlined in Table [4])	Thicker the web, higher the torque capacity. This is because a higher value of web caliper leads to a larger value of $\sigma(r)$ beneath the outer layer which leads to a higher $\sigma(r)$ throughout the roll. Thus the increase in $\sigma(r)$ leads to an increase in $T_{cap.}$ See Figures 30a&b.
Width of Web		Higher the width, higher the torque capacity. This is because T_{cap} increases as width increases, Equation [1].

The width is an important factor affecting the torque capacity. As the width of the web is more controllable than the other parameters considered, no simulation results are presented. However, it is easy to see that with all other properties held constant, the torque capacity of the web increases with increase in the width of the web.

In this study, other factors such as air entrainment during winding, visco-elastic effects, non-linear core moduli and tension loss have not been considered. This was done to keep the study simple. Surface winding has not been considered, as wound roll models that simulate surface winding are still in the early stages of development. But, the variation in the torque capacity due to variations with the different parameters will be similar to that of center winding. There may be additional sources of external torque during surface winding from the nip rolls, perhaps inducing slippage in the wound rolls.

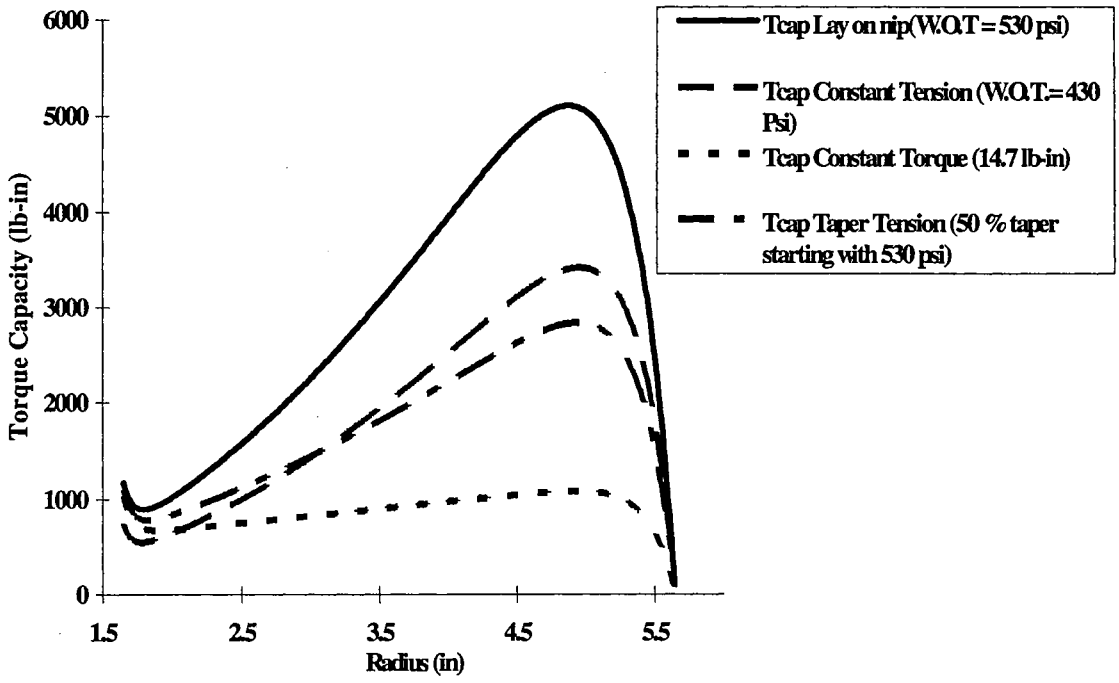

Figure 25a. Variation of Torque Capacity with different Winding Schemes.

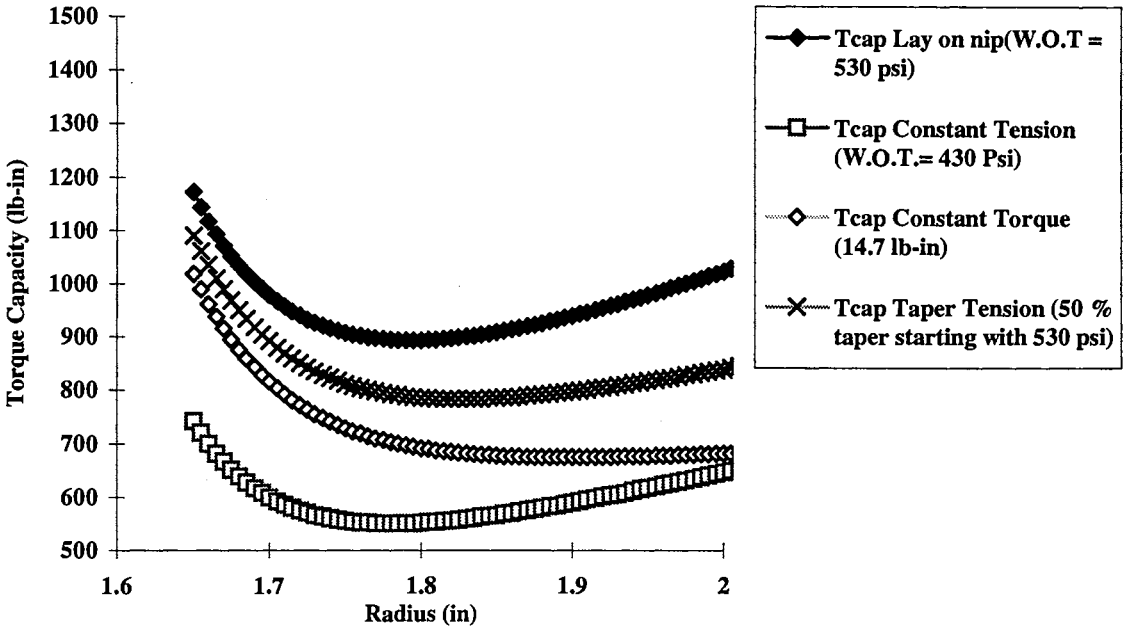

Figure 25b. Low Torque Capacity Zones near the Core.

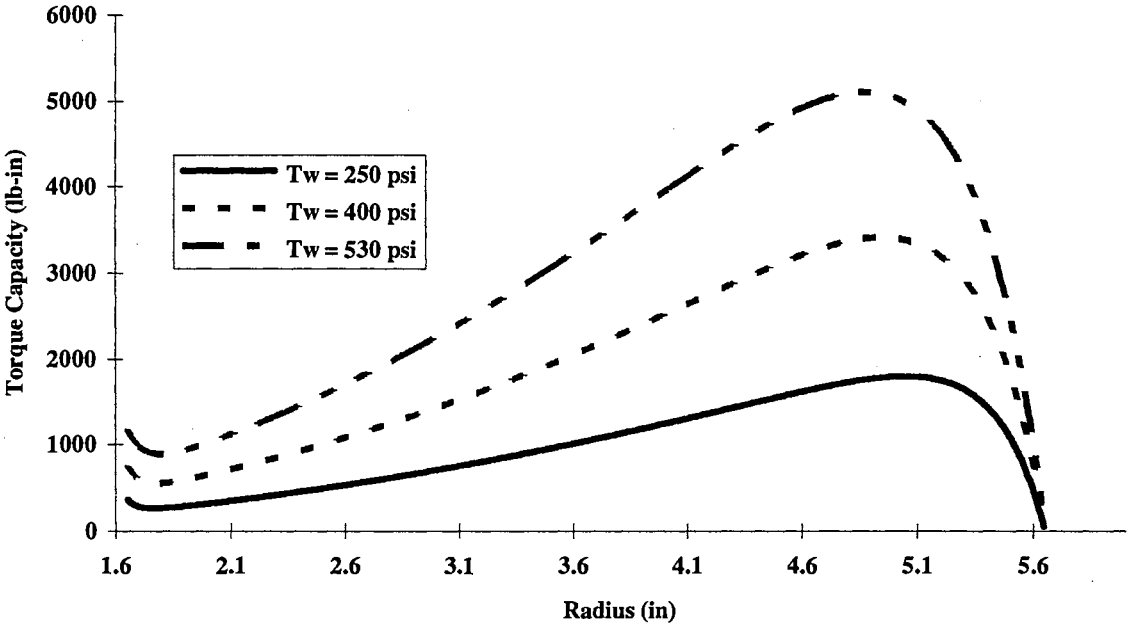

Figure 26. Variation of Torque Capacities with differing Web Tensions.

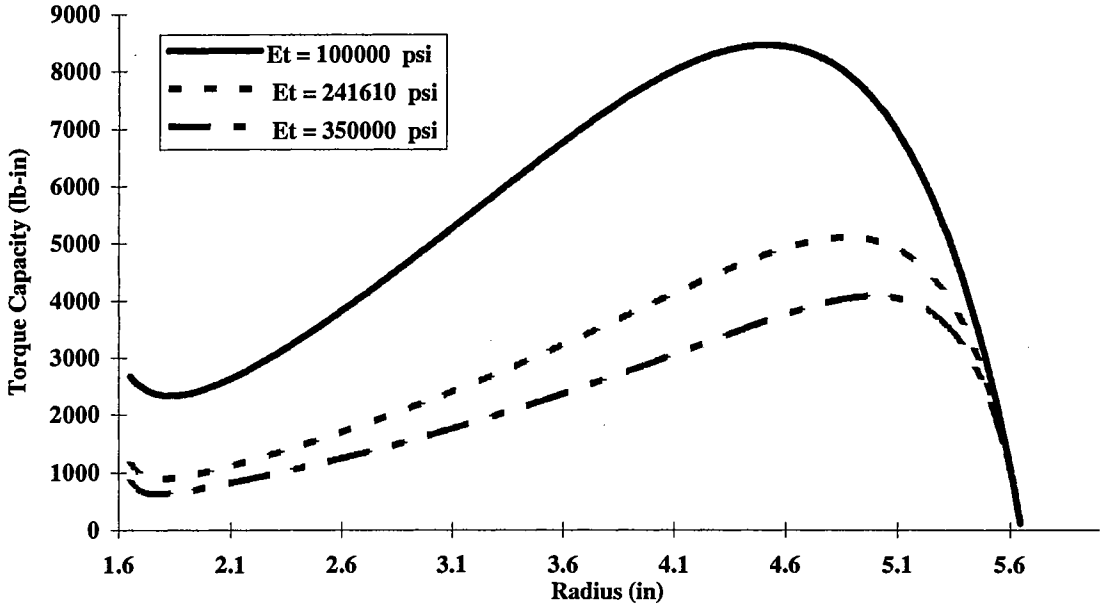

Figure 27. Variations of Torque Capacities with differing E_t.

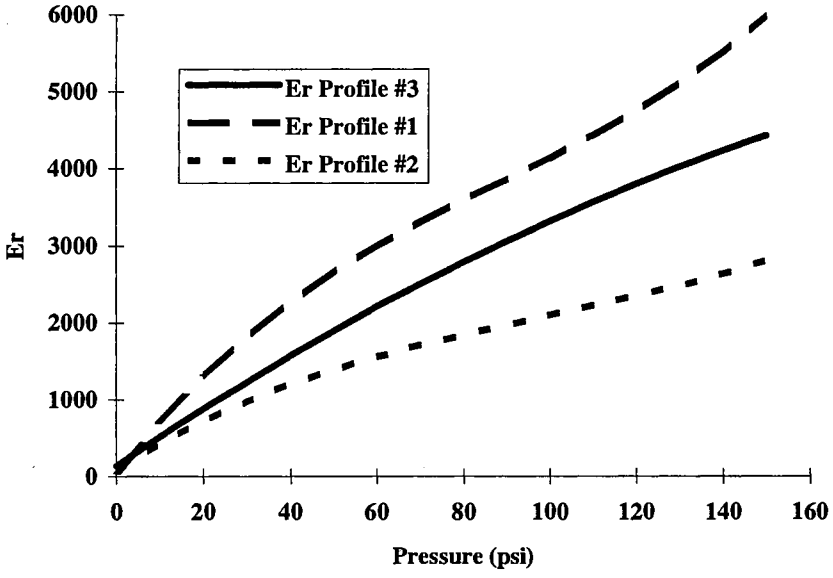

Figure 28a. Pressure Profiles.

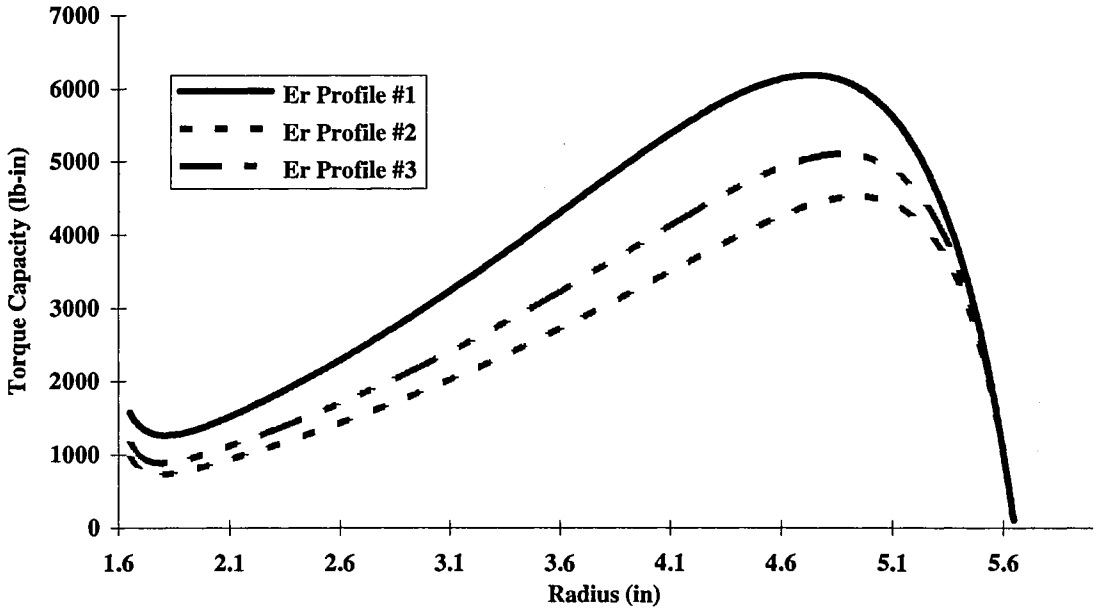

Figure 28b. Variation of Torque Capacities with Differing E_r.

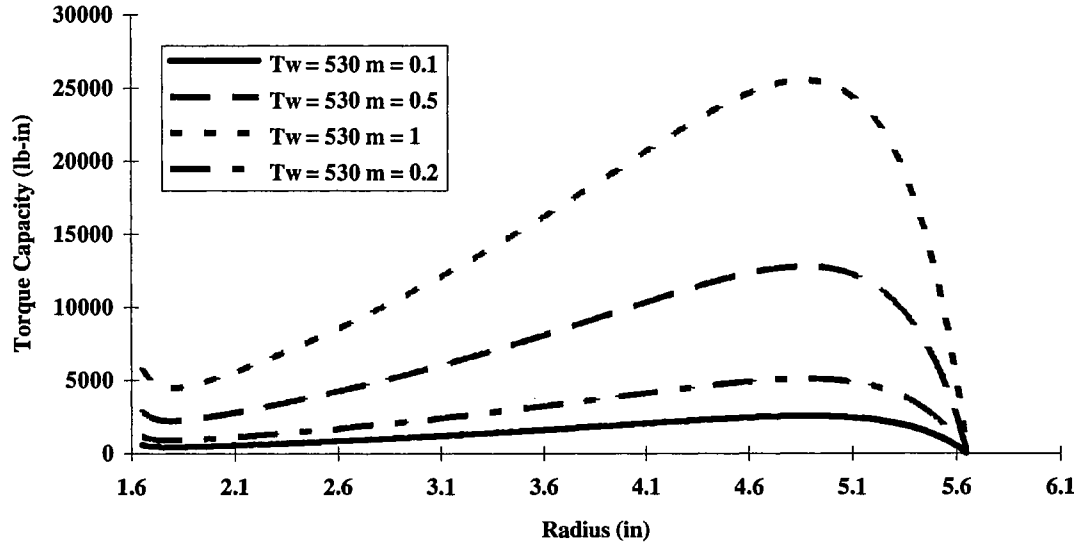

Figure 29. Variation of Torque Capacities with differing Coefficients of Friction (μ).

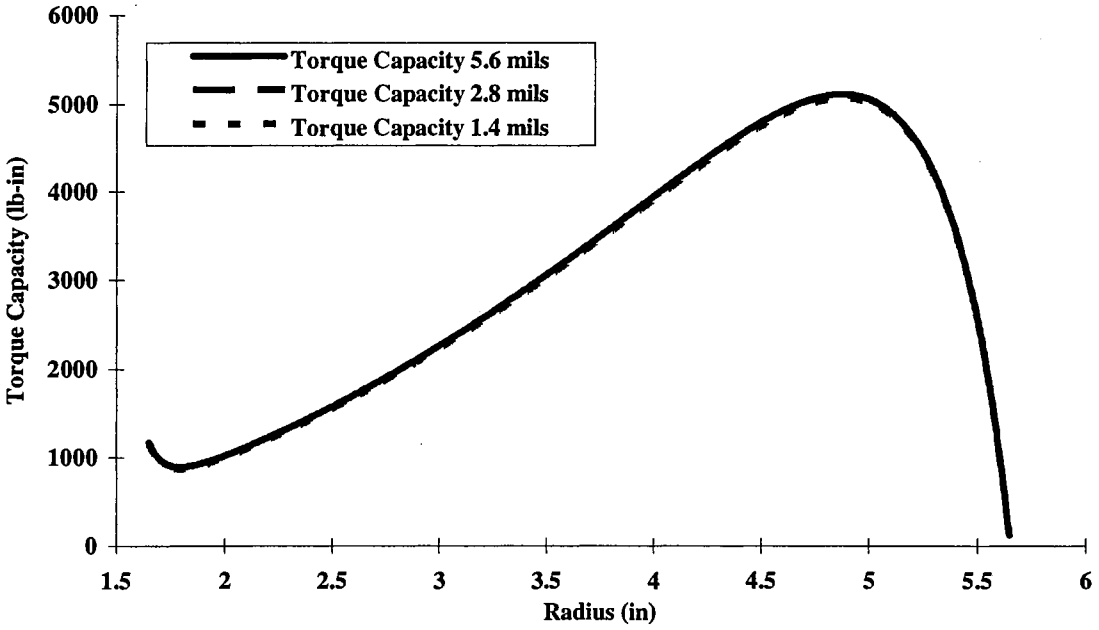

Figure 30a. Variation of Torque Capacities with Thickness.

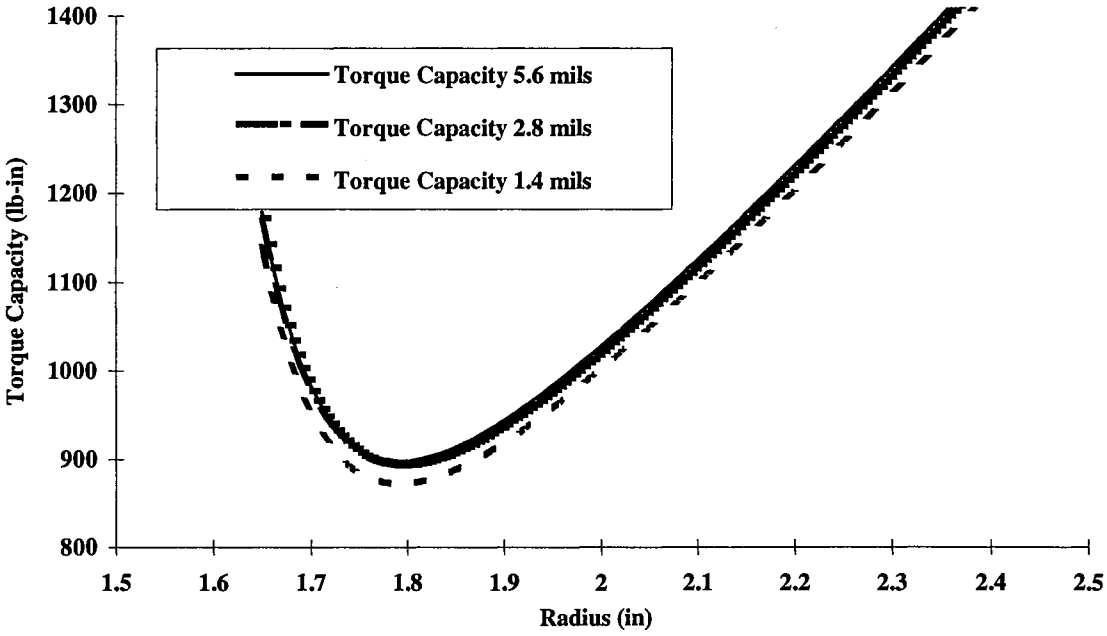

Figure 30b. Low Torque Capacity zones near the Core.

CHAPTER V

EXPERIMENTAL VERIFICATION OF THE TORQUE CAPACITY MODEL

Scope

Most of the parameters identified in the literature contributing to crepe wrinkles can be correlated via the wound roll model to the torque capacity, and thus to the slippage that occurs in a wound roll. In surface winding, the other major winder related parameters which remains are the torque applied to the wound roll through the nip, and the nip load. In this chapter an attempt will be made to verify that slippage occurs in a center wound roll whenever the torque capacity of the roll is exceeded by an external torque.

Deceleration Tests (Experimental)

Recall from the literature, Schoenmeier [15] documented crepe wrinkles in the immediate vicinity of a splice in rolls that decelerated to a stop following a web break. Two important parameters identified are the deceleration of the wound rolls, and the splice. During splicing operations, there is a substantial drop in the web tension, and there is a possibility of a localized drop in the torque capacity in the vicinity of the splice. Inertial effects associated with large decelerating rolls are considerable. Thus, there is the possibility of an external dynamic torque, which is the product of the mass moment of inertia of the wound roll and the deceleration which the wound roll undergoes.

Simulating a splice in the laboratory is relatively simple as tension is the only variable that needs to be manipulated. The mass moment of inertia of the wound roll can be quantified by the following:

$$I = \frac{m(d_0^2 + d_i^2)}{8} \text{ (lb-sec}^2\text{-in)} \tag{21}$$

where

$$m = \pi l \rho \left[\frac{d_0^2 - d_i^2}{4g}\right] \text{ (lb-sec}^2\text{/in)} \tag{22}$$

and,

'd_o' outer diameter of the wound roll (in)

'd_i' inner diameter of the wound roll (in)

'l' width of the web (in)

'ρ' density of the web material (lb/in^3)

'g' acceleration due to gravity (in/sec^2)

Note that the mass moment of inertia of the wound roll is really a function of the radius of the wound roll.

The dynamic torque is given by:

$$T_{dynamic} = I^*\alpha \text{ (lb-in)} \tag{23}$$

where I is given by equation (21) and α is the angular decleration of the wound roll.

The objective of this series of experiments is to study of the propensity of a wound roll to form crepe wrinkles in response to an imposed deceleration. This helps to isolate the effects of deceleration from other winder related parameters, such as nip load and torque applied to the wound roll via the nips during surface winding. Quantifying the dynamic torque, observing crepe wrinkle formation (defect formation) and quantifying slippage are additional outcomes of these experiments. Although most of the crepe wrinkles observed on paper, as mentioned in the literature, were with respect to surface winding, there are no models to simulate surface winding accurately. Consequently, it is difficult to characterize the roll structure and the capacity of the roll to resist slippage. Center-winding, on the other hand, has been well understood and accurate models have been developed which help characterize the roll structure and the slippage resistance capability. All the experiments conducted at the WHRC were on rolls of newsprint that were center wound.

Machinery Modification and Wound Roll Parameters

The 3M splicer winder was modified by mounting a disk brake and an encoder on the core shaft, Figure 31. A mounting bracket was fabricated to mount pneumatically operated brake calipers, such that the disk attached to the core shaft could be stopped when a button was pushed. The output from the encoder was sent directly to a data acquisition system so the angular velocity of the shaft could be acquired automatically.

Two basic variations of web tension were used in preparing the center-wound rolls which were subjected to the tests. In one case the entire roll was center wound with a constant tension of 130 psi. TABLE 6 gives the physical properties of the web.

TABLE 6. Physical properties of the web

Web Tension	130 psi
E_r	$134.9 + 38.8\,\sigma - 0.075\,\sigma^2 + 0.00005\,\sigma^3$
E_t (Average)	240000 Pi
Web Caliper	0.0028 in (2.8 mils)
Coefficient of friction (μ) paper/paper	0.2
Width of web	6 in
Poisson's ratio	0.01
Wound roll dimensions	1.65 in. Inner Radius, 5.65 in. Outer Radius
Core	Steel, 1.5 in. Inner Radius and 1.65 in. Outer Radius

The radial stresses, the torque capacity and the applied torque, and the circumferential stresses for the wound roll are shown in Figures 32a, b&c Care was taken to wind the rolls at a low speed such that air entrainment effects were negligible.

In the second variation, the rolls were center wound with a tension profile that changed, see TABLE 7.

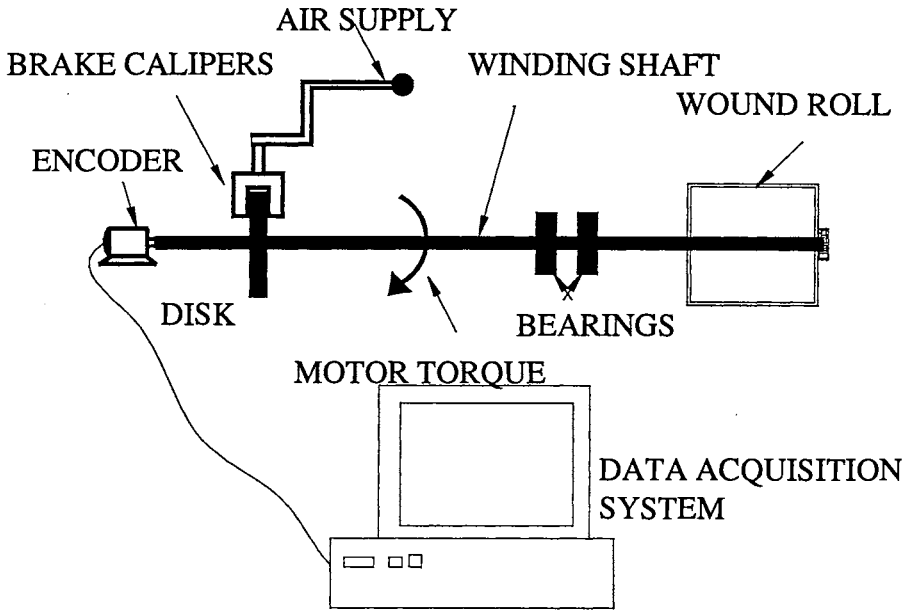

Figure 31. Schematic of the Modifications made on the Winder.

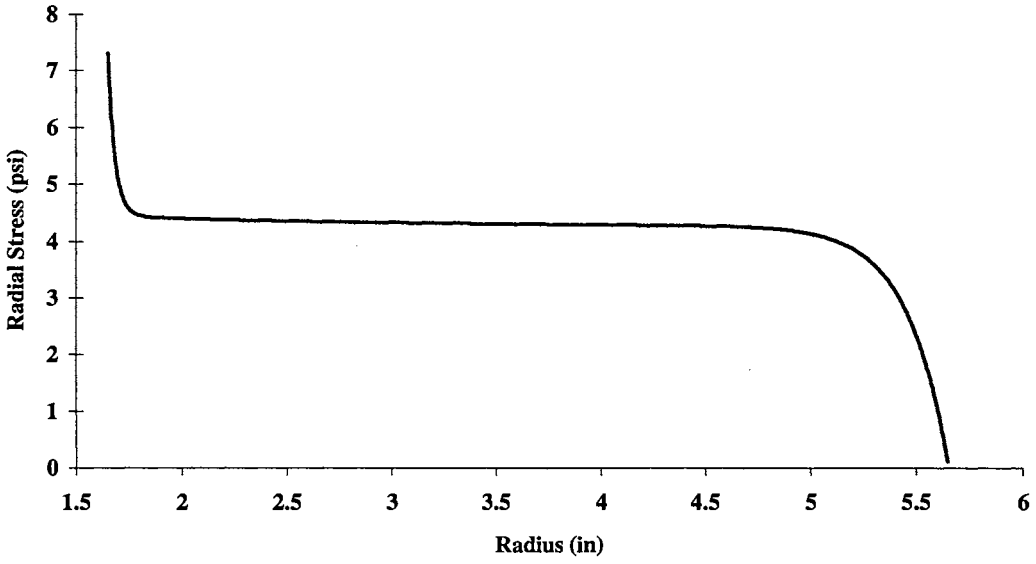

Figure 32a. Radial Stresses in the Wound Roll.

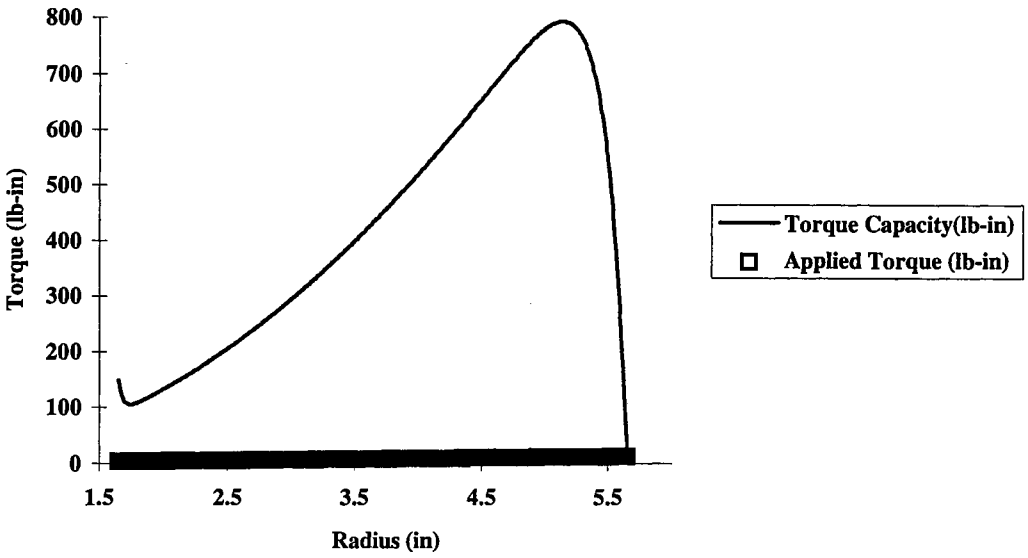

Figure 32b. Torque Capacity and Applied Torque in the Wound Roll.

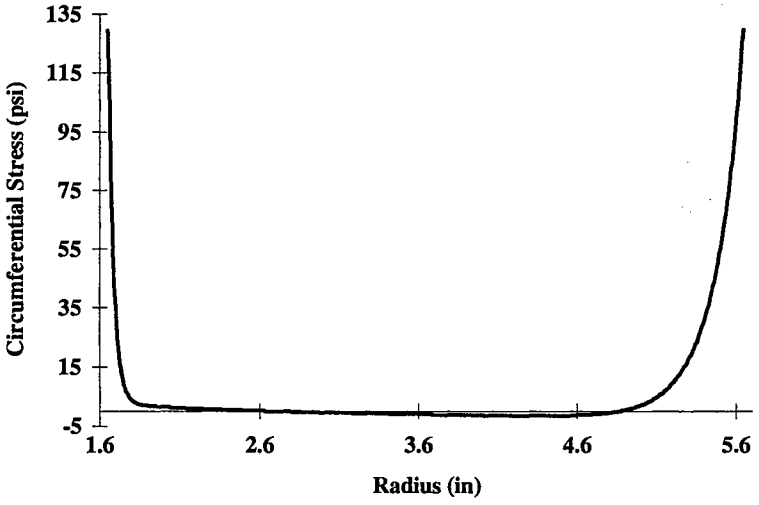

Figure 32c. Circumferential Stress in the Wound Roll.

TABLE 7. Physical properties of the web.

Web Tension	530 psi from radii 1.65 - 3.65 in 59 psi from radii 3.65 - 4.65 in 530 psi from radii 4.65 - 5.65 in
E_r	$134.9 + 38.8\,\sigma - 0.075\,\sigma^2 + 0.00005\,\sigma^3$
E_t (Average)	240000 psi
Web Caliper	0.0028 in (2.8 mils)
Coefficient of friction (μ) paper/paper	0.2
Width of web	6 in
Poisson's ratio	0.01
Wound roll dimensions	1.65 in. Inner Radius, 5.65 in. Outer Radius
Core	Steel, 1.5 in. Inner Radius and 1.65 in. Outer Radius

The roll was started with a tensile stress of 530 psi from the core to a radius of 3.65 in, then the stress was reduced and maintained constant at 59 psi to a radius of 4.65 in then, finally, the tension in the roll was brought back up to the initial value and held constant until the entire roll was wound. This variation was attempted to generate a roll that was soft in a selected radial portion. These conditions are characteristic of wound rolls with a splice in them. The intended web tension profile, the torque capacity for such a wound roll, and the circumferential stresses are shown in Figures 33a, b&c.

While winding the rolls with a variable web tension, care was taken to avoid slippage while bringing the tension back to the initial value. As described earlier, there is wound

roll slippage if the torque capacity is exceeded by the product of the web tension and the instantaneous radius of the roll. If the tension is gradually increased to a higher value, avoiding any instantaneous tension impulses, slippage can be minimized. This was ascertained by scribing radial lines in the wound roll as the roll was building up, and observing and ascertaining that there was not any appreciable curvature in the radial lines when the web tension was brought back to the initial value. The analysis of this situation will be described later in the chapter.

Before the rolls were mounted on the winder, radial lines were drawn on the edges of the roll so that internal slippage within the roll would be visible. The experiments consisted of mounting the center wound rolls, wound with the two different tension profiles, on the core shaft, bringing the shaft to a selected speed and applying the brakes so that the rolls were subjected to a deceleration. The data acquisition system automatically measures the angular velocity of the core shaft from the start of the test to the end of the test. The angular velocity data obtained from the encoder are shown in Figures 34a to i. The angular deceleration is obtained by differentiating a curve fit of the angular velocity data and is also shown in Figures 34a to i.

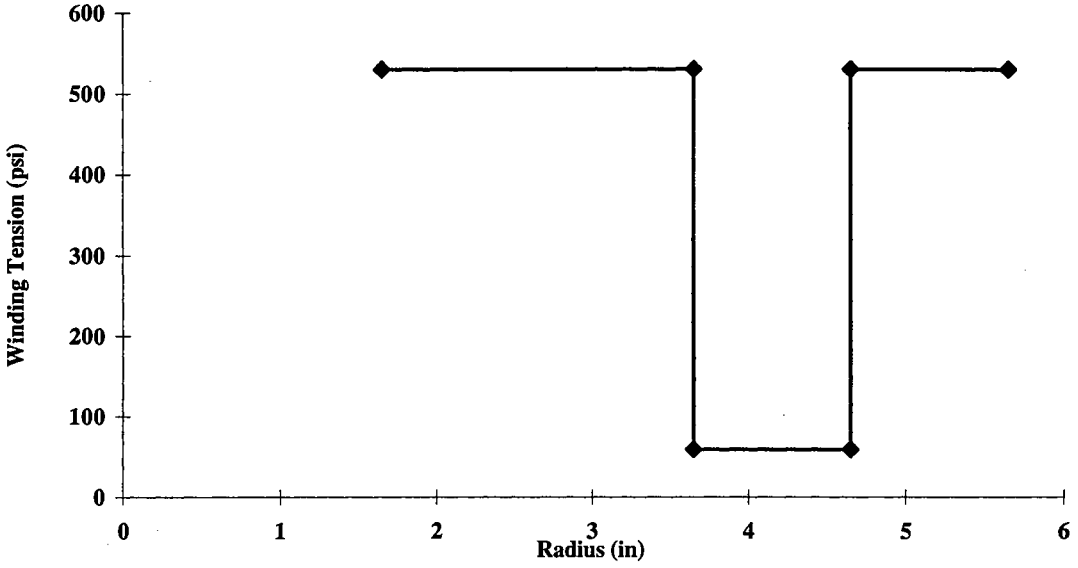

Figure 33a. Impulse Tension Profile.

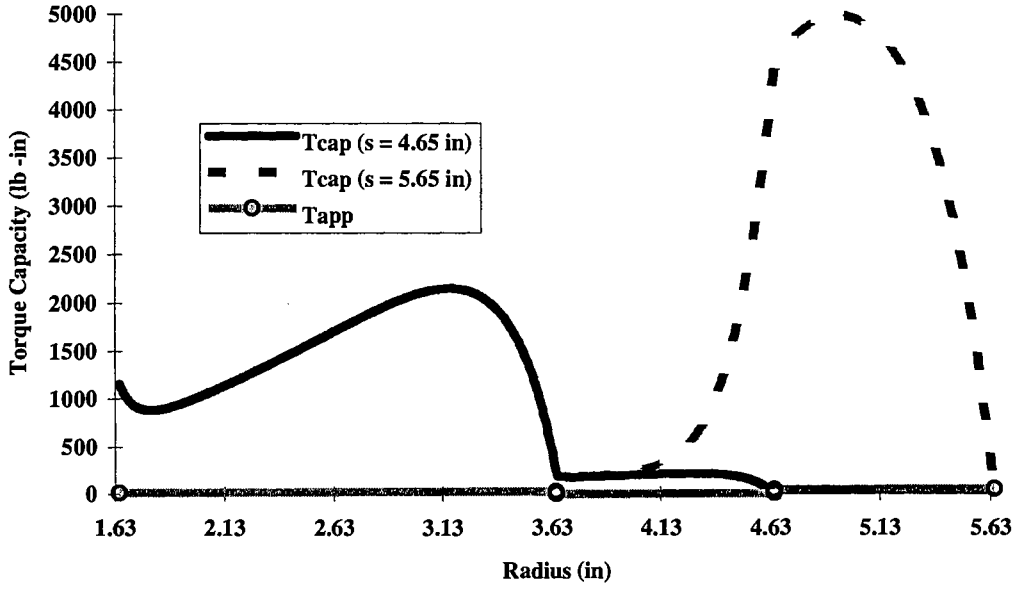

Figure 33b. Torque Capacity and Applied Torque in the Wound Roll.

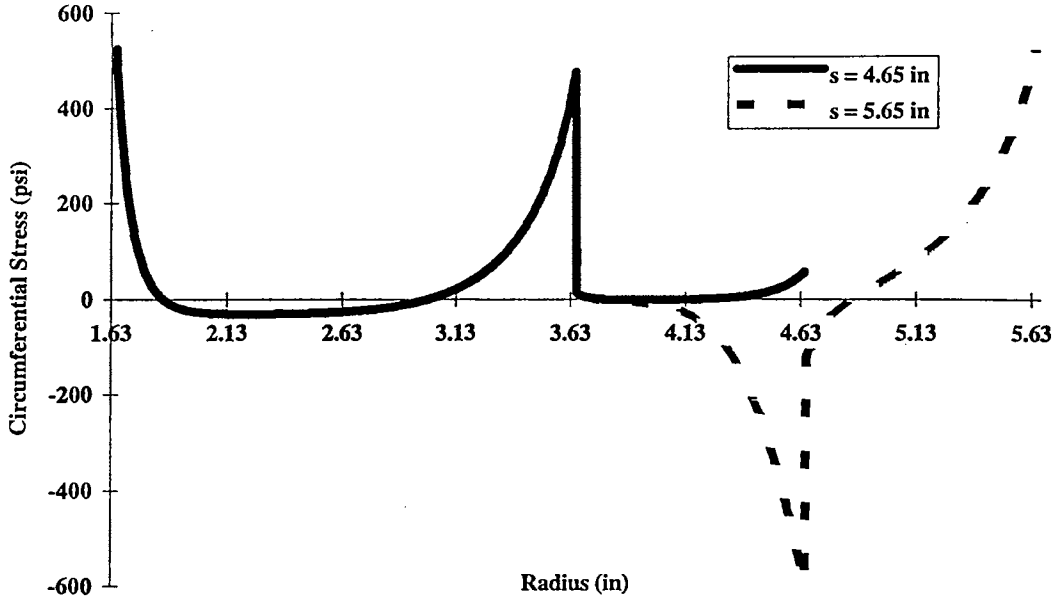

Figure 33c. Circumferential Stress in the Wound Roll.

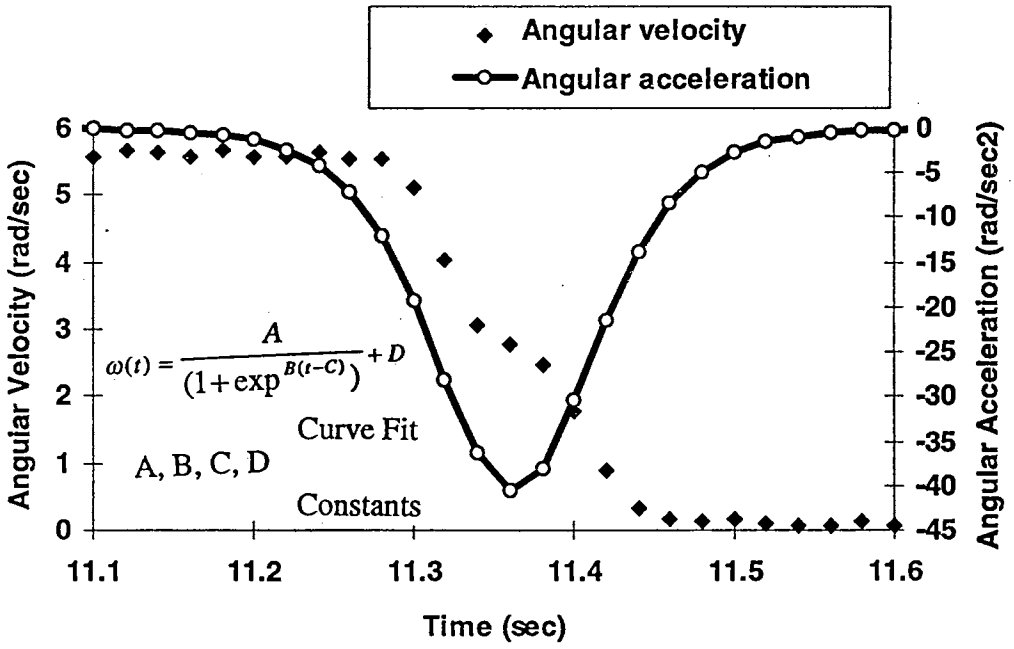

Figure 34a. Angular Velocity and Acceleration profiles from the Deceleration Tests (Maximum Deceleration = 40 rad/sec^2).

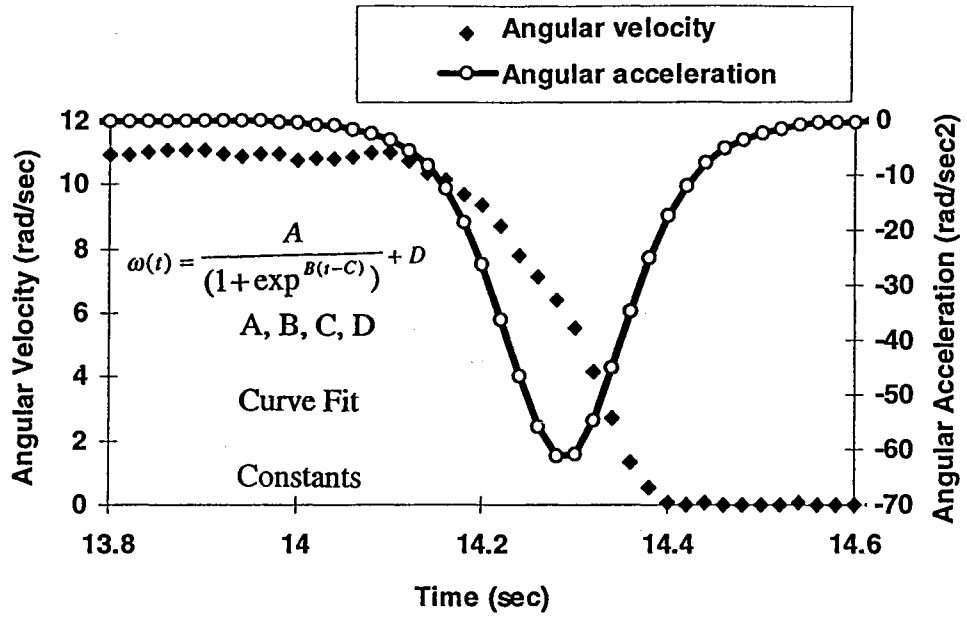

Figure 34b. Angular Velocity and Acceleration profiles from the Deceleration Tests (Maximum Deceleration = 61 rad/sec^2).

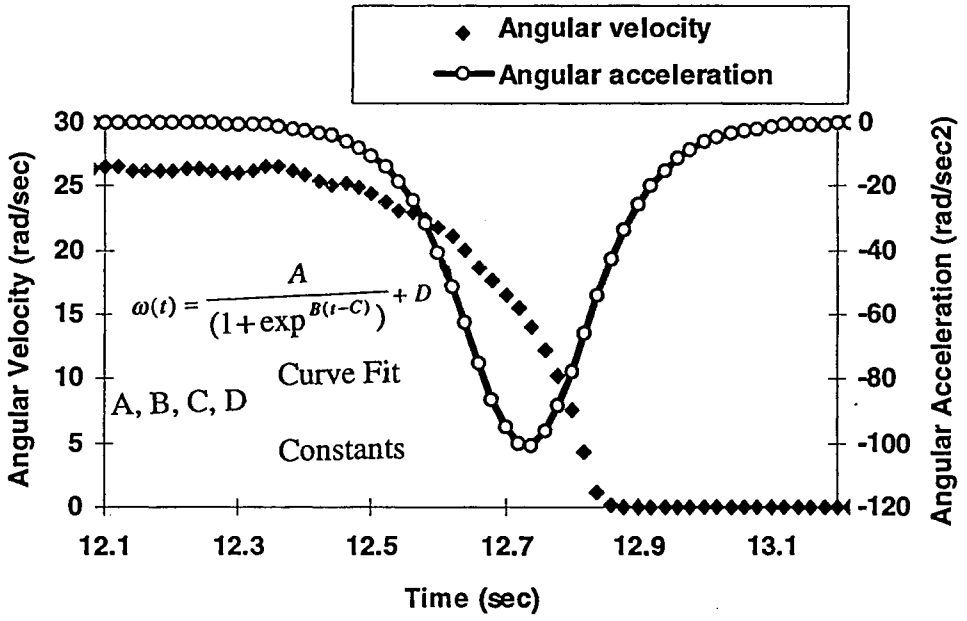

Figure 34c. Angular Velocity and Acceleration profiles from the Deceleration Tests (Maximum Deceleration = 100 rad/sec^2).

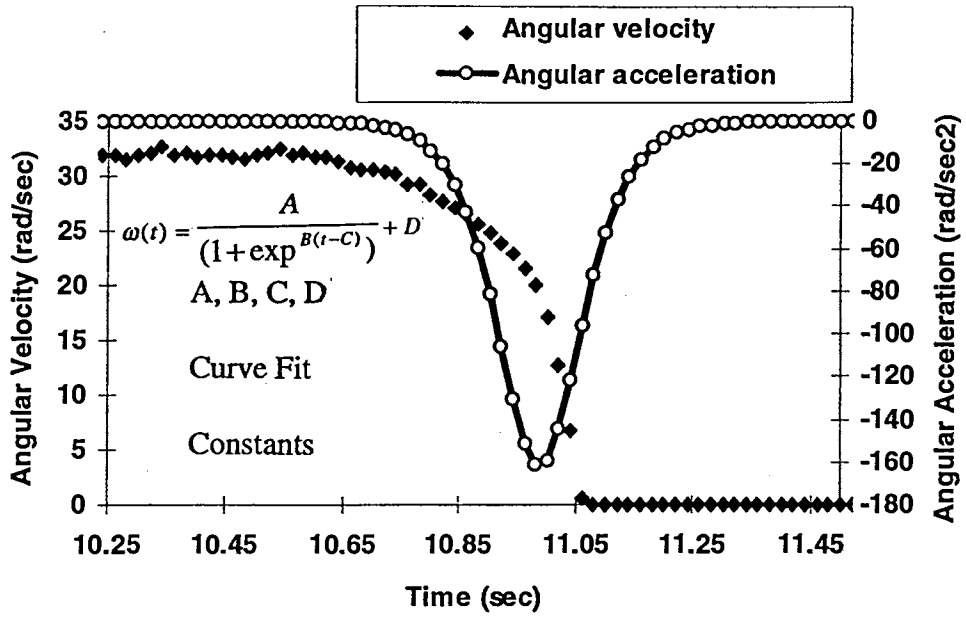

Figure 34d. Angular Velocity and Acceleration profiles from the Deceleration Tests (Maximum Deceleration = 161 rad/sec^2).

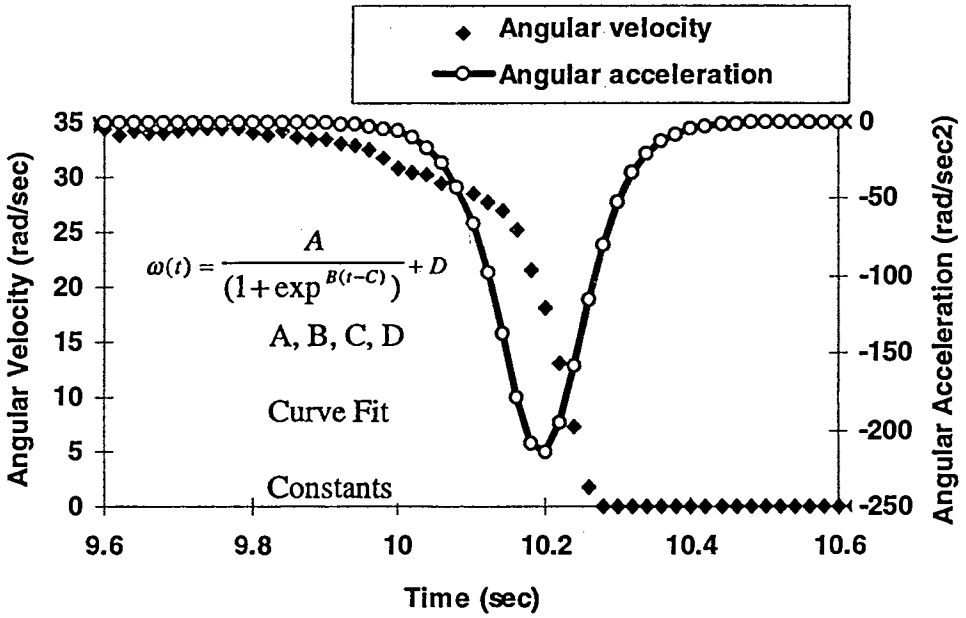

Figure 34e. Angular Velocity and Acceleration profiles from the Deceleration Tests (Maximum Deceleration = 214 rad/sec^2).

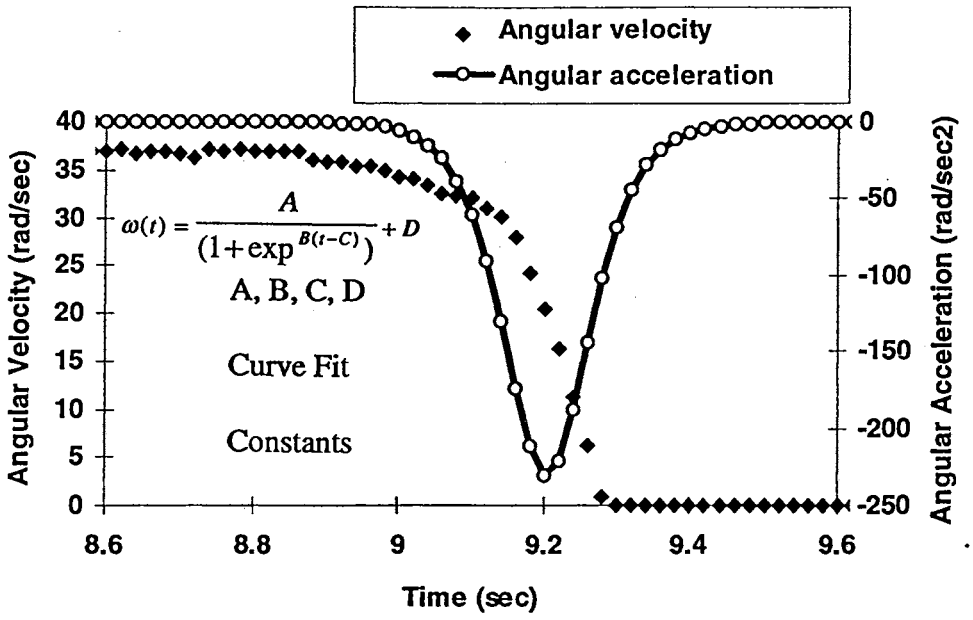

Figure 34f. Angular Velocity and Acceleration profiles from the Deceleration Tests (Maximum Deceleration = 230 rad/sec^2).

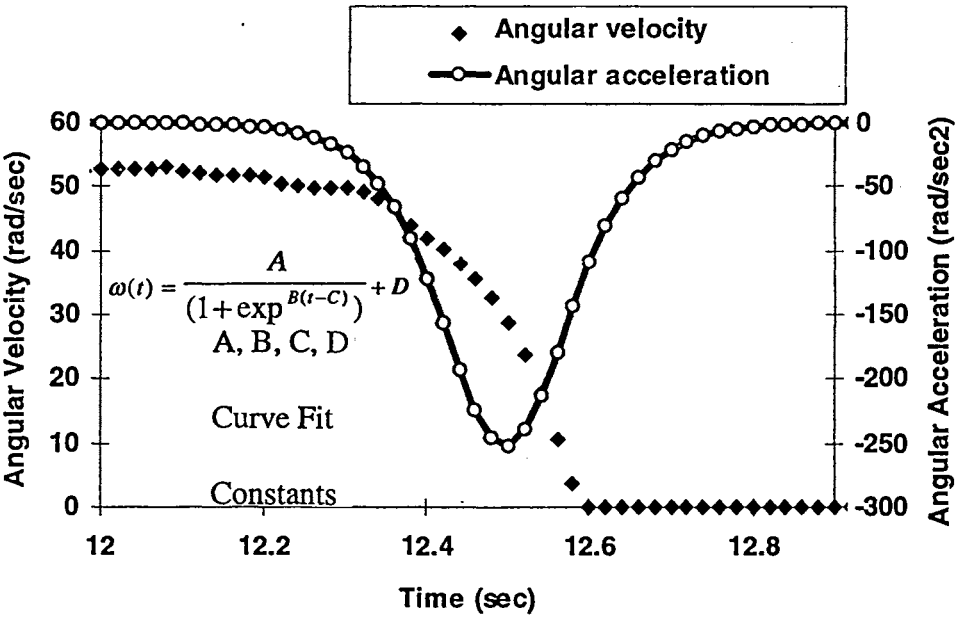

Figure 34g. Angular Velocity and Acceleration profiles from the Deceleration Tests (Maximum Deceleration = 251 rad/sec^2).

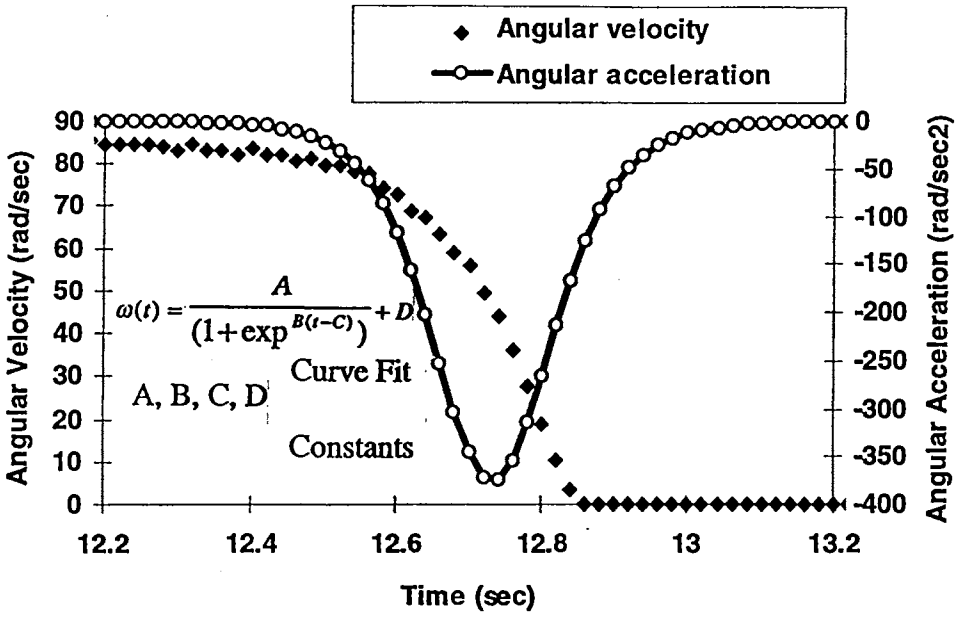

Figure 34h. Angular Velocity and Acceleration profiles from the Deceleration Tests (Maximum Deceleration = 374 rad/sec^2).

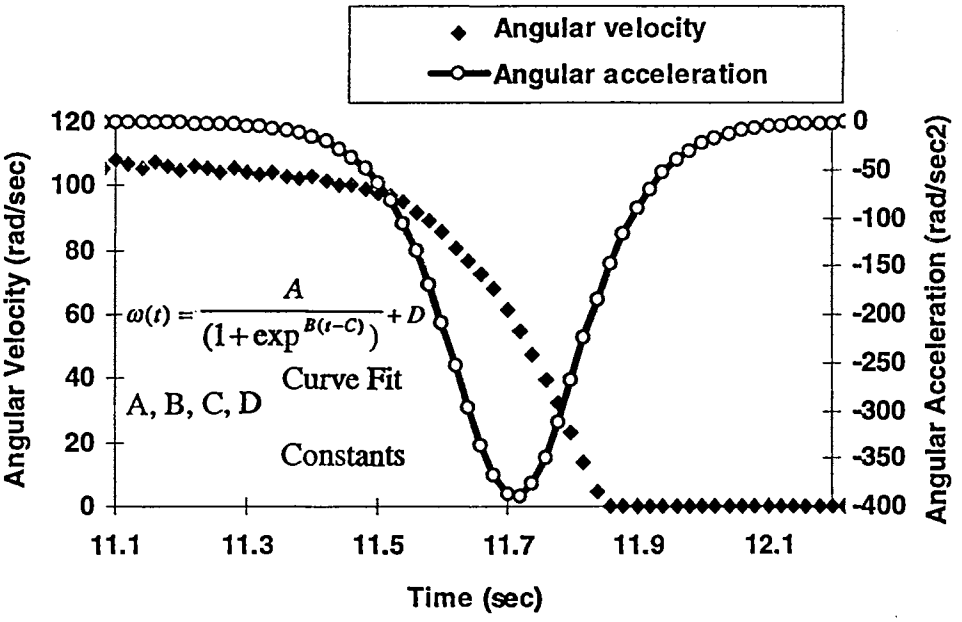

Figure 34i. Angular Velocity and Acceleration profiles from the Deceleration Tests (Maximum Deceleration = 389 rad/sec^2).

Analysis of the Results

A summary of the experimental outcomes for the case of the rolls wound with the constant tension is reported in the TABLE 8 below.

TABLE 8. Results of the Deceleration Tests

I (lb-in/sec^2)	$\lvert\alpha\rvert_{max}$ (rad/sec^2)	I*α (lb-in) Dynamic Torque	T_{cap} min (lb-in)	Nature of Defect
0.642	389	249.7	102.6	CREPE/SLIP
0.642	374	240.1	102.6	CREPE/SLIP
0.642	251	161.1	102.6	CREPE/SLIP
0.642	230	147.7	102.6	CREPE/SLIP
0.642	214	137.4	102.6	CREPE/SLIP
0.642	161	103.4	102.6	SLIP
0.642	100	64.2	102.6	SLIP
0.642	61	39.2	102.6	NO SLIP
0.642	40	25.7	102.6	NO SLIP

A conservative estimate of the moment of inertia I for the wound roll was used by considering the entire wound roll. No slippage occurred when the dynamic torque was lower than the torque capacity of the wound roll. Crepe wrinkles occurred when the deceleration torque exceeded the torque capacity by at least 1.3 times for the case of the constant web tension profile.

Thus, crepe wrinkles occurred when:

$$T_{applied} \Rightarrow I_{max}\alpha_{max} \geq 1.3\left(T_{capacity-min}\right) \tag{24}$$

The crepe wrinkles also occur in the core region, where the torque capacity is the least for the case of the rolls wound with constant tension. TABLE 8 also demarcates two distinct kinds of outcomes that resulted from the tests: One set of wound rolls without slippage and the second set of rolls with slippage and crepe wrinkles. In the second set of wound rolls, there were rolls with just slippage and no crepe wrinkles and others with considerable slippage and crepe wrinkles visible even from the edge of the wound rolls. In Figures 35a, b&c photographs of rolls which exhibited no slip, rolls which exhibited slip, and rolls which exhibited slip and crepe wrinkles are shown.

For the rolls wound with the variable tension case, crepes occurred where the torque capacity was the least, near the middle of the roll, and all the slippage was confined to the region corresponding to the low torque capacity zone as evidenced by the curvature in the radial lines, Figure 35d.

The torque capacity is axisymmetric prior to the occurrence of slippage. This means, that along the circumference of the roll, the torque capacity is constant for any given radius. Once slippage originates, this axisymmetry is disturbed. The absence of nips, was another factor that preserved the axisymmetry of the torque capacity. The presence of nips would disturb the axisymmetry of the torque capacity, even prior to slippage, and makes it difficult to differentiate between inertia related crepe wrinkles, and crepe wrinkles induced by nip effects.

The results of these experiments may be summarized as follows:

(i) Slippage occurred when the torque capacity was exceeded by the dynamic torque

(ii) Applied torques in excess of the torque capacity are required to generate crepe wrinkles

(iii) No nips were involved during the formation of these crepe wrinkles

(iv) The location at which the crepe wrinkles occurred was the location of the lowest torque capacity in the roll.

The torque capacity proved to be an invaluable aid in understanding the formation of crepe wrinkles in rolls which undergo deceleration. The angular deceleration which a roll undergoes during sudden stopping is responsible for the formation of crepe wrinkles under those circumstances. Thus, with a knowledge of the torque capacity of the wound roll, the angular deceleration, and the mass moment of inertia of the wound roll, it is possible to predict the onset of slippage and consequently any slippage related defects.

Tension Loss at Splices (Experimental)

As mentioned earlier, while discussing crepe wrinkles in locations neighboring splices, a simulation was undertaken in the laboratory where rolls with a stepped profile in web tension were wound. While winding these rolls, there were certain surprising and unexpected results. It proved to be difficult to wind good rolls with this profile in tension.

If the web-tension change occurred as an impulse, during a transition from the low to the higher web tension, slippage began and once the slippage proceeded to a certain extent

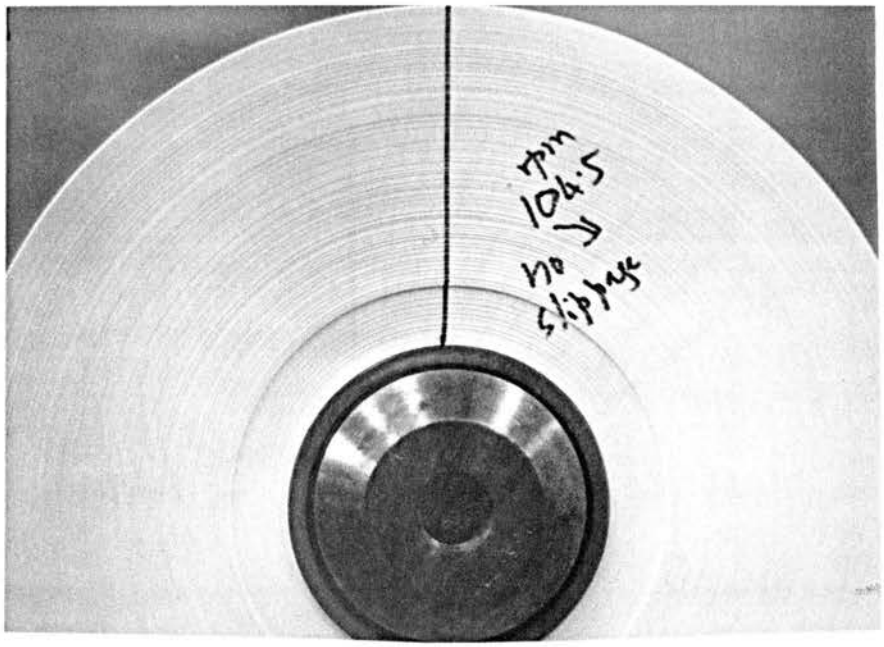

Figure 35a. Wound Roll - Post Deceleration: No Slippage Case.

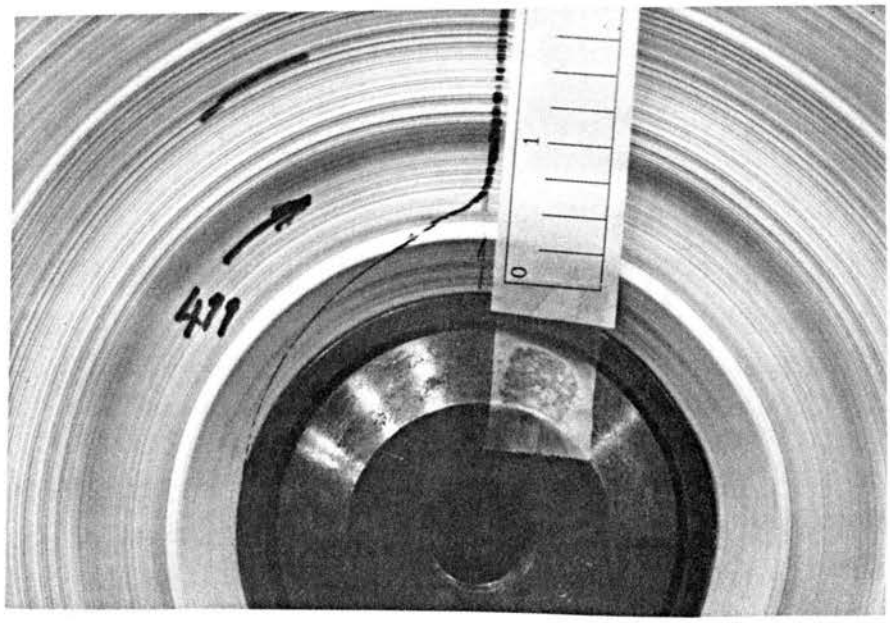

Figure 35b. Wound Roll - Post Deceleration: Showing Slippage.

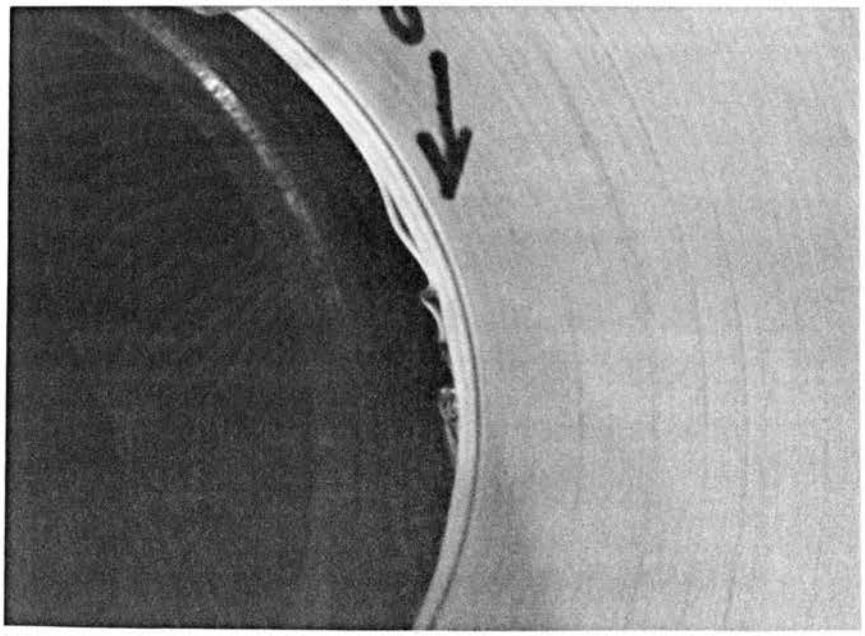

Figure 35c. Wound Roll - Post Deceleration: Showing Slippage and Crepe Wrinkles.

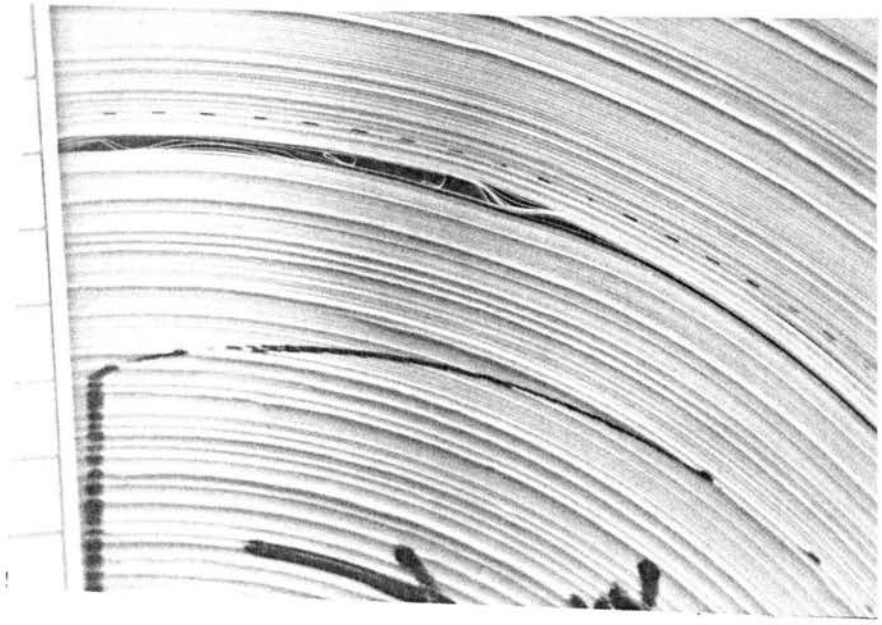

Figure 35d. Wound Roll - Post Deceleration: Showing Slippage and Crepe Wrinkles (Variable Tension Case).

there was a star which formed, accompanied by a snapping sound in the wound roll, Figure 36. This mode of formation of the starring defect, where slippage precedes star formation, or for that matter is associated with the star defect formation, has not been reported in the open literature.

The location of the star is in the region of the wound roll where there is low torque capacity, Figure 33b. To successfully wind these rolls without starring, the winding tension profile must be slightly altered. Instead of instantaneously increasing the winding stress from 59 psi to 530 psi at a winding radius of 4.65 in, the winding stress was increased from 59 psi at 4.65 in to 530 psi at 4.88 in and then held constant until the final winding radius of 5.65 in had been achieved, Figure 37. Both slippage and starring were absent from these rolls, which were next submitted to deceleration tests. Crepes and stars occurred in these rolls when they were subjected to deceleration. The location of the crepes was in the region of the lowest torque capacity. The slippage in the roll was also confined to this region of low torque capacity, Figure 35d. In Figure 33b, the torque capacity and applied torque are shown for the case in which the winding stress was instantaneously stepped from 59 psi to 530 psi, at a winding radius of 4.65 in. Note that the torque capacity is continually changing in the wound roll throughout the period of the wind, as long as the radial pressures are changing .

In Figure 33b, note that the torque capacity is shown at two instants in time, one in which the roll had completed winding to 4.65 in outside radius and a second instant when the roll

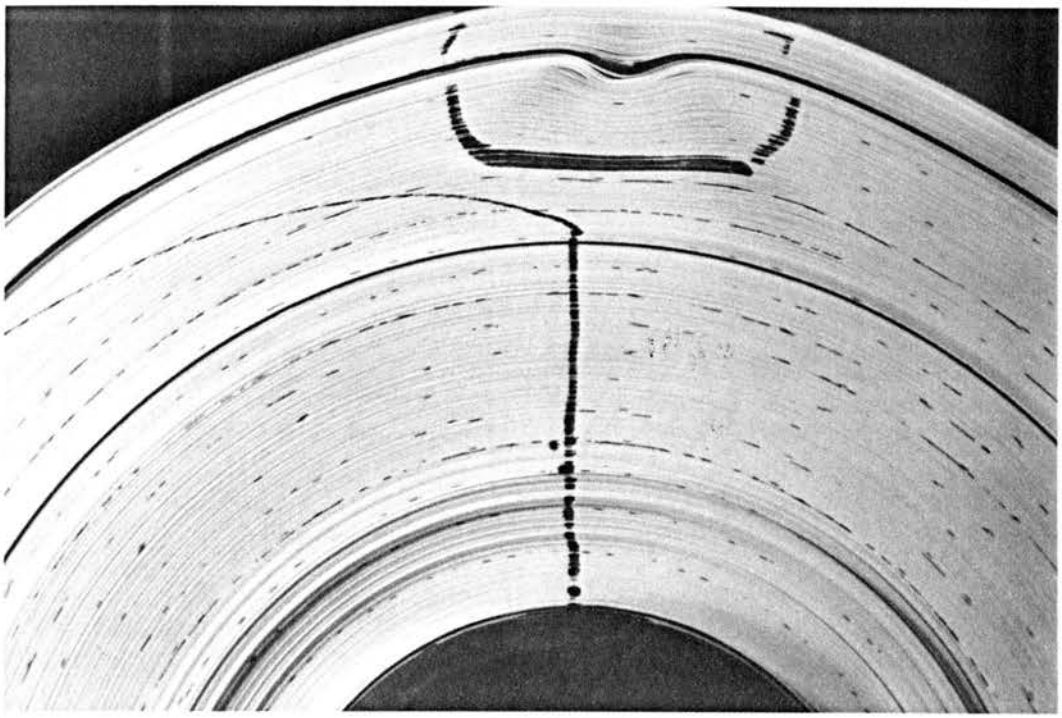

Figure 36. Wound Roll with Star Defect and Slippage.

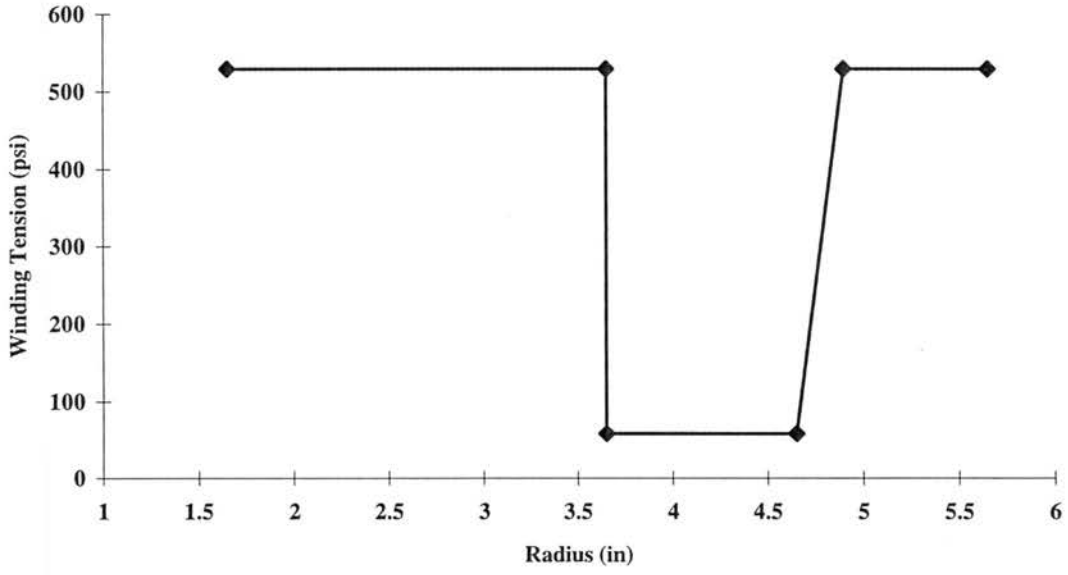

Figure 37. Ramp Tension Profile.

had completed winding at 5.65 in. The applied torque is shown as a function of radius, but at any instant the applied torque is constant throughout the roll and is simply the product of the current winding tension and outside radius of the wound roll, s. An expansion of the low torque capacity region of Figure 33b is shown in Figure 38. Note that at 4.65 in, as the winding stress is returned to 530 psi, the applied torque is several times the torque capacity, indicating that slippage should occur in the outside of the winding roll at that instant, (i.e. s = 4.65 in). The circumferential stresses after the roll completed winding to 4.65 in, and at 5.65 in are shown in Figure 33c. The result of the increase in winding tension is that the circumferential stresses, which were low but tensile in the 4.65 in region, were driven to high compressive values.

In Figure 39, the torque capacity and applied torque are shown for the case in which the winding stress was ramped from 59 psi to 530 psi, as shown in Figure 37. The torque capacity is shown at three instants during the wind. The first curve shows the torque capacity after winding the low winding stress segment at 59 psi has been completed, (i.e at s = 4.65), the second curve shows the torque capacity after the ramp up in winding stress to 530 psi has been completed, (i.e. s = 4.88 in) and the third curve shows the torque capacity after the roll has been completely wound (i.e. at s = 5.65 in). The applied torque is shown, again, as a function of radius and at any instant the applied torque is constant throughout the roll, and is simply the product of the current winding tension and outside radius of the wound roll, s. An expansion of the low torque capacity region of Figure 39

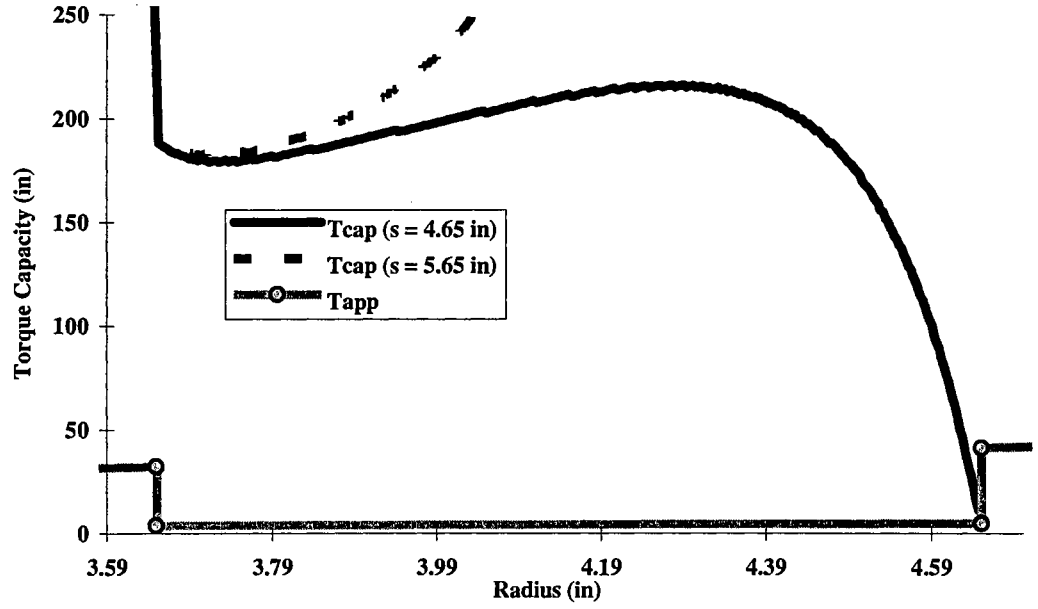

Figure 38. Detail of Low Torque Capacity Zone of Figure 33 b.

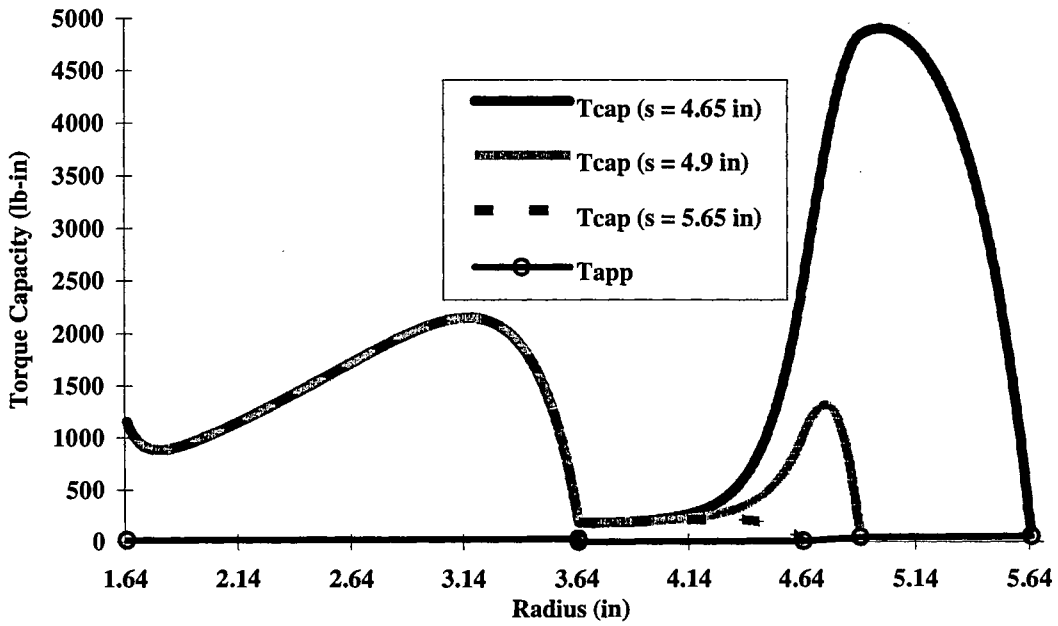

Figure 39. Torque Capacity and Applied Torque for the Ramp Tension Case.

is shown in Figure 40. Note that at 4.65 in. and at 4.88 in., the applied torque is less than the torque capacity, indicating that slippage should not occur in the winding roll. The circumferential stresses after the roll completed winding to 4.65, 4.88, and 5.65 in are shown in Figure 41. It is again apparent that the increase in winding stress has resulted in compressive circumferential stresses, but note that the ramp in winding stress has dramatically decreased the level of compressive stress.

The results of the constant tension winding tests, and the variable winding tension tests with a ramped increase in winding tension, all bear witness to the validity of using torque capacity as a measure of the quantification of the propensity of the roll to form crepe wrinkles and star defect. In each case, a torque capacity profile could be developed based upon the output of a wound roll model and compared to the applied torque, such as the dynamic torque due to decelerations or to the applied torque arising from the winding tension, to ascertain whether slippage will occur and thereby crepe wrinkles or star defect formation. Decelerations, of a magnitude which would generate dynamic torques in excess of the torque capacity, were required to generate crepe wrinkles.

The rolls, which were wound with the stepped profile in winding tension, proved that a combination of slippage and compressive circumferential stress was required to generate the starred roll defect. Additional proof was given by the rolls which were wound with a ramp in winding stress from 59 psi to 530 psi. These rolls were successfully wound without defects but had compressive circumferential stresses wound within the rolls.

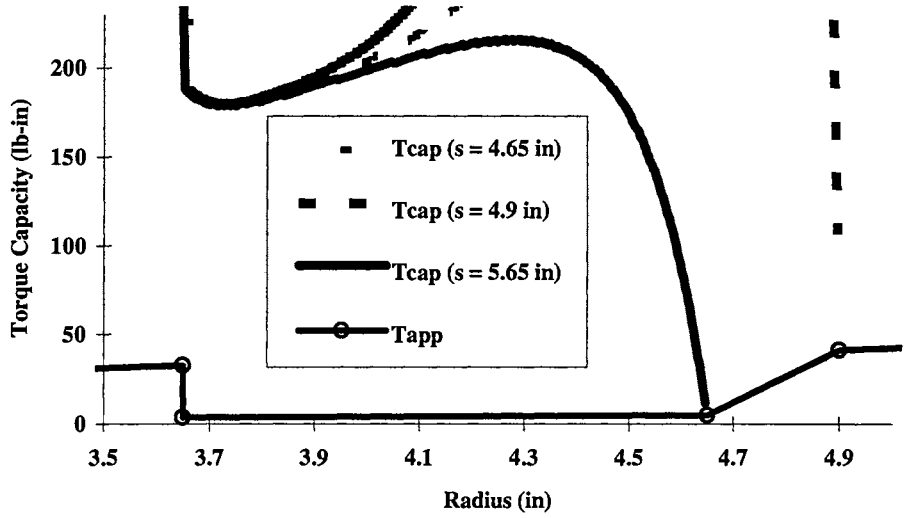

Figure 40. Detail of Low Torque Capacity Zone of Figure 39.

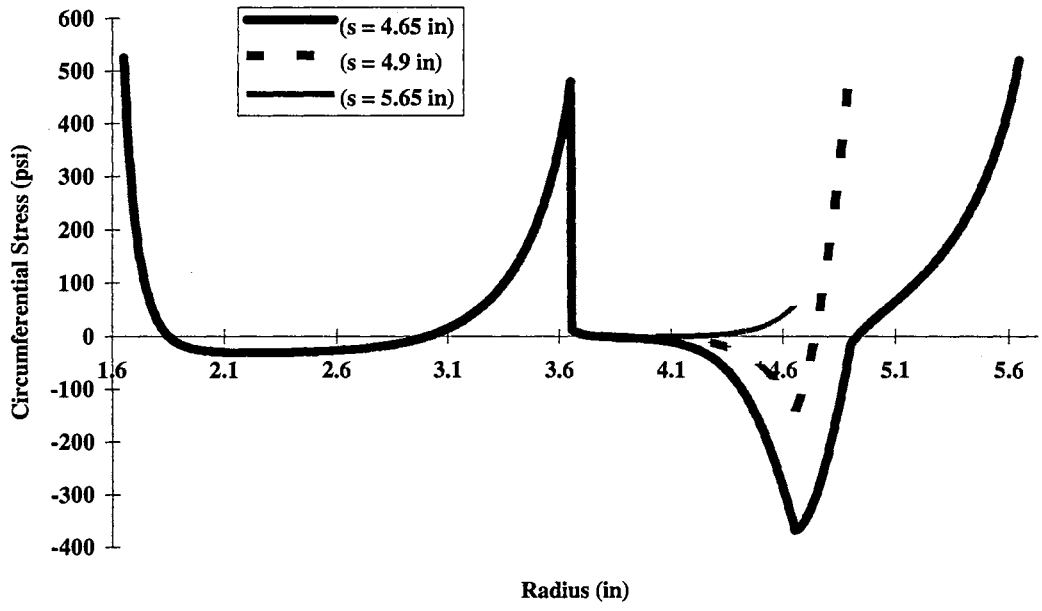

Figure 41. Circumferential Stress for the Ramp Tension Case.

Both stars and crepes resulted after slippage was induced by deceleration. Thus, the basic concept of avoiding the formation of crepe wrinkles and starring is by never applying torques greater than the lowest torque capacity in a wound roll.

Starring (Experimental)

Earlier, an analysis was presented to explain starring which occurred due to slippage, something which was not previously documented in the open literature. In this section, the literature pertaining to starring will be reviewed and quantitative methods to predict starring will be scrutinized to see if starring due to slippage can be predicted by conventional means. The idea advanced in this section is that starring occurs due to two different mechanisms. One due to slippage, and the other one due to a disturbance to the circumferential stresses which exist in the wound roll.

Star defect formation has been broached rather qualitatively, similar to the literature on crepe wrinkles. Quantitative generalizations based on the circumferential stresses which exist in the wound roll are available. The most quantitative method to date predicting starring in wound rolls was developed by Lee[26] at the WHRC.

Pfeiffer[23] identified star formation with a lateral buckling of layers of the wound roll due to "excessive" compressive circumferential stresses existing along radial locations in conjunction with a sudden disturbance to the wound roll. This disturbance may be due to

impact loading from improper handling of the wound roll, such as dropping during transportation.

Lee considers sectors of wound roll, Figure 42 where negative circumferential stresses exist, and models the selected areas of the wound roll as a beam on an elastic foundation subjected to axial loads. Based on theory developed for beams on an elastic foundation, buckling stresses and modes that would cause the beam to buckle are computed. Lee's algorithm, to predict the buckling stresses in wound rolls uses Hakiel's wound roll model to generate radial stress and circumferential stress information for a wound roll of web material.

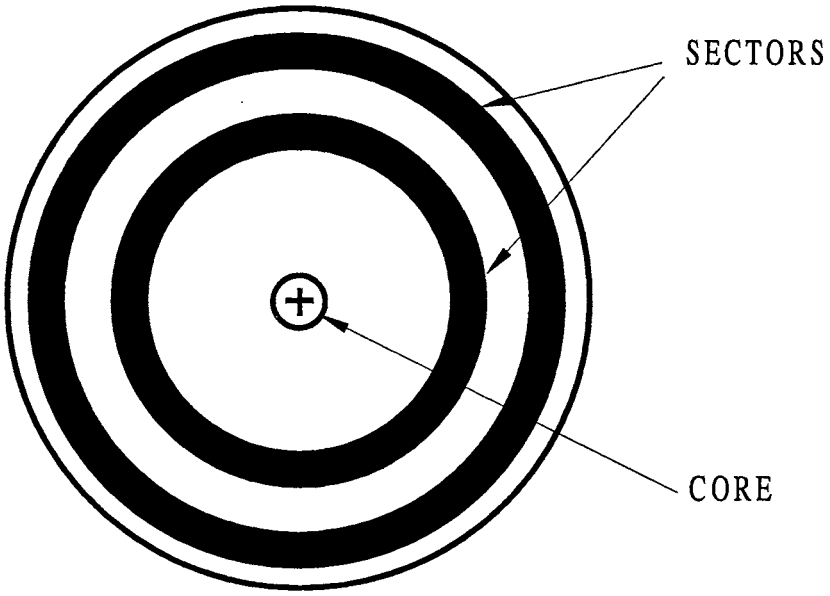

Figure 42. Sectors of Negative Circumferential Stresses in a wound roll, used in Lee's[26] algorithm to predict potential Starring Locations.

Lee's study models the stiffness of the elastic foundation as a function of the radial stresses which exist in the wound roll. The length of the modeled beam is a function of the radial extent of negative circumferential stresses which exist in the wound roll. Lee developed a quantification called "margin of safety", which measures the propensity of a wound roll to form starring defects.

The margin of safety reflects the difference between the maximum circumferential stress which exists and the stress required to cause buckling of layers in the wound roll. The margin of safety depends on the percentage of the maximum circumferential stresses in the wound roll for choosing the length of the beam to be modeled. The information needed to predict star defect formation using Lee's algorithm includes identification of the region in which starring defect would occur, based on a choice of the percentage of the maximum circumferential stresses in the wound roll, and the coefficient of friction between the layers of the web material.

According to Lee, the margin of safety is a failure criterion which determines whether a roll will buckle and form a star. Based on the description given by Lee, a schematic has been developed which shows the "safe" and "dangerous" regions based on the margin of safety, Figure 43. The exact location of the demarcations between the different zones cannot be determined based on the qualitative descriptions given by Lee. The figure shows only the relative positions of the different zones that exist in a wound roll, with respect to the margin of safety being positive or negative.

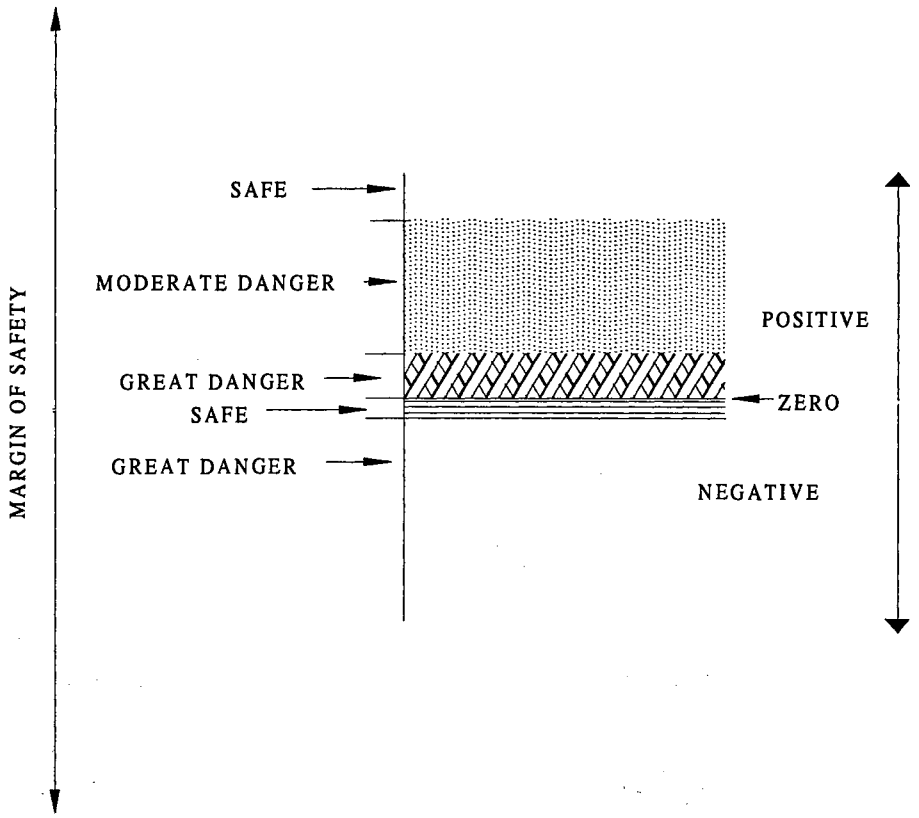

Figure 43. Illustration showing potential Starring zones in a wound roll, based on the qualitative description given by Lee[26]. Note that, the figure only identifies the relative position of the different zones with respect to the margin of safety.

Experiments and simulations were conducted at the WHRC to observe if Lee's algorithm was capable of predicting starring in rolls which had slippage as a precursor to the defect formation. Two rolls were wound of ICI 377 polyester film of 92 gage thickness. The relevant physical properties of the web material and the rolls are listed in TABLE 9. As TABLE 9 shows, the webs were subjected to a tension impulse while winding. The

TABLE 9. Wound roll physical properties

Web Tension (Variable Tension Case with slippage)	100 psi from radii 2 - 2.4 in 1992 psi from radii 2.4 - 4.1 in
Web Tension (Variable Tension Case without slippage)	362.3 psi from radii 1.7 - 4.1 in 1449.3 psi from radii 2.6 - 4.4 in
E_r	$56.157\sigma - 1.17\sigma^2 + 0.023\sigma^3$
E_t (AVERAGE)	653400 psi
Caliper of web	0.00092 in (0.92 mils)
μ, Coefficient of friction (web/web)	0.3
Width of web	6 in
Poison's ratio	0.01
Wound Roll Dimensions (Roll with slippage)	2 in - 4.1 in (Inner Radius and Outer Radius)
Wound Roll Dimensions (Roll without slippage)	1.7 in - 4.4 in (Inner Radius and Outer Radius)
Core Dimensions (Roll with slippage)	Steel 1.5 in Inner Radius, 0.5 in, Thickness
Core Dimensions (Roll without slippage)	Steel 1.5 in Inner Radius, 0.2 in, Thickness

differences between the wound rolls are only in their dimensions and the sizes of the core. In both the rolls, radial lines were drawn by stopping the roll when the rolls were built to the radius where the tension was varied from a lower to a higher value.

When the tensions were increased to the final values, there was slippage in the roll with a thick core, and immediately following there was a star. In the other roll there, was no

slippage as the radial line was still straight,and within the addition of a few laps of web material at high tension, starring occurred.

The results from the simulations are shown in Figures 44a&b and 45a&b. These are plots which show the propensity of the rolls to star defect formation. The margin of safety, which reflects the propensity of the rolls to develop a star, can be compared between the two rolls. Figure 44b shows that within 5% of the maximum circumferential stresses, the roll which slipped preceding star formation has a lesser propensity to form the starred roll defect using Lee's algorithm, than the roll which did not slip. The margins of safety all fall within 5%. The margins of safety for the roll which did not slip are slightly higher, indicating a greater propensity to form a star defect. Between 10 and 30% the roll which starred without slipping falls in a safer zone than the roll which slipped and had a star. Between 30 and 50% both rolls fall into the danger zone. The effect of variability of the coefficient of friction is also shown in the same plots. The coefficients of friction considered were 0.2, 0.3 and 0.4.

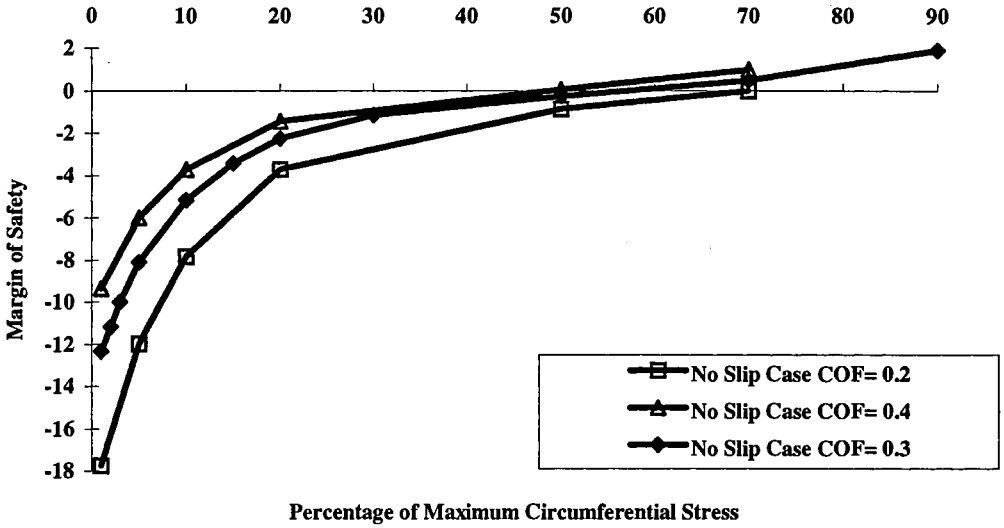

Figure 44a. Variations of the Margin of Safety for the Roll which did not Slip. (3 different cases with varying coefficients of friction are shown to demonstrate the varibility of the margin of safety).

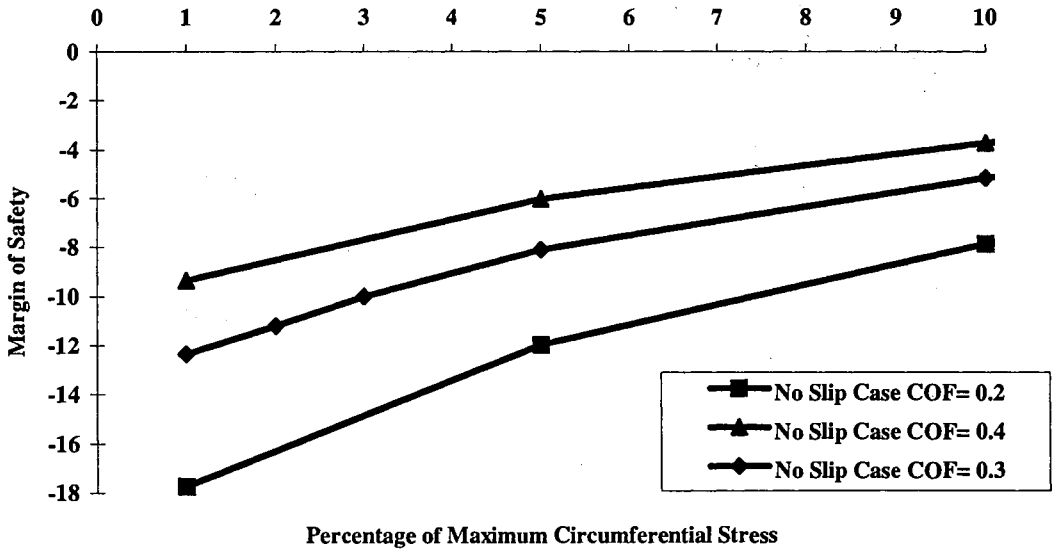

Figure 44b. Detail of Figure 44a, showing upto 10 % of the Maximum Circumferential Stress.

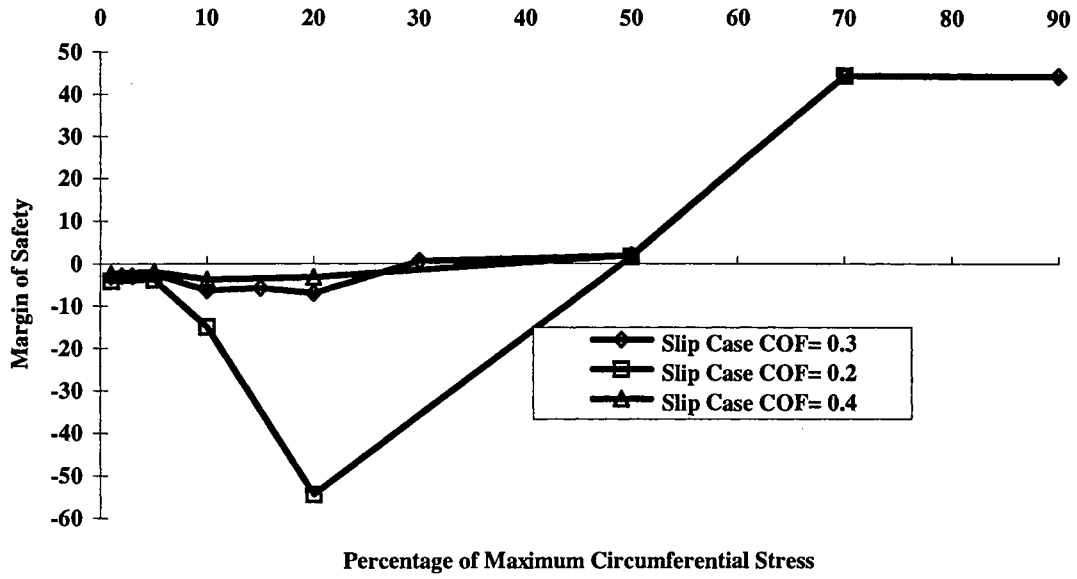

Figure 45a. Variations of Margin of Safety for the Roll which Slipped prior to Starring. (3 different cases with varying coefficients of friction are shown to demonstrate the varibility of the margin of safety).

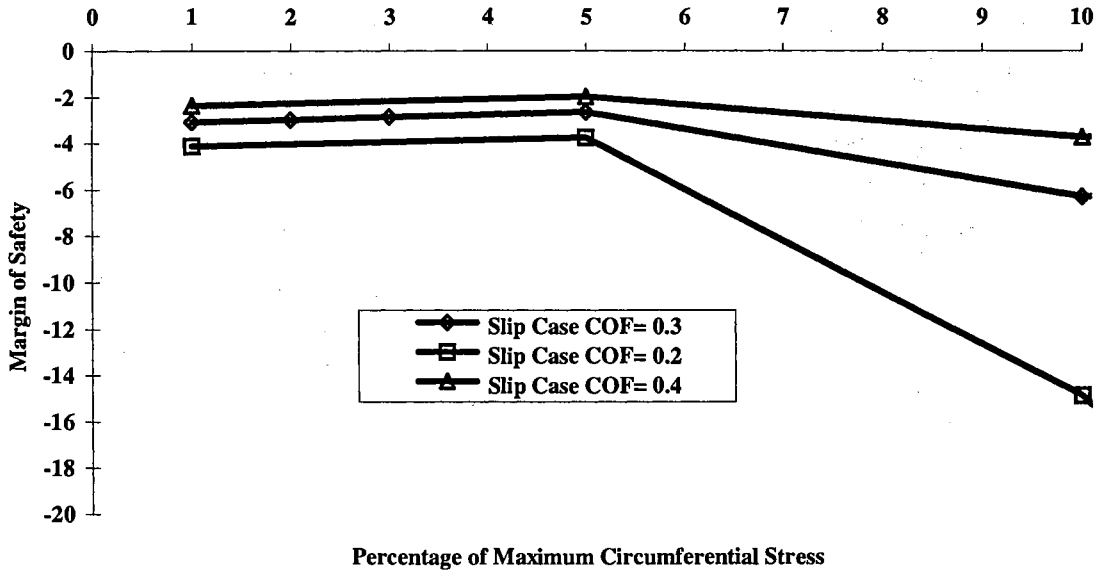

Figure 45b. Detail of Figure 45a showing upto 10 % of the Maximum Circumferential Stress.

Thus, Lee's algorithm may be insufficient in considering star defect formation preceded by slippage, as starring occurs due a completely different mechanism. The existence of compressive circumferential stresses within the wound roll is an inadequate means of generating star defects within wound rolls. Stable rolls were wound at constant tension with compressive circumferential stresses with newsprint, as discussed in the previous sections.

Conclusions

(i) At this point, it is clear that slippage occurs, in the absence of nips, whenever:

$$T_{\text{applied external}} > T_{\text{cap minimum}} \quad (25)$$

(ii) A source of dynamic torque resulting from angular decelerations of the rolls has been quantified and the effect of this dynamic torque in producing crepe wrinkles has been observed and quantified using wound roll models for center winding. Crepe wrinkles occur during deceleration when:

$$T_{\text{applied external, dynamic}} >> T_{\text{cap minimum}} \quad (26)$$

(iii) Starring is a phenomenon, that was never before associated with slippage, and previously thought to be only a function of negative circumferential stresses. This study has shown that starring occurs under certain circumstances due to slippage. A means of predicting the location of slippage related star defect, and avoiding the defect has been identified. So, Starring may occur in rolls whenever:

$$T_{\text{app external}} > T_{\text{cap minimum}}$$

CHAPTER VI

NIP INDUCED SLIPPAGE

Rolling Resistance

As demonstrated in the last chapter, wound rolls, subjected to angular decelerations or tension drops due to splices, suffer from inter-layer slippage and slippage related defects such as crepe wrinkles and starring. The defects occur at the location of the lowest torque capacity in the wound rolls. A perusal of the literature reveals the vicinity of the nips as the other location at which crepe wrinkles occur frequently in a (surface) wound roll, Lucas[7], Frye[11,13], Odell et al[12], Paananen et al[14], Lemke et al[3], and Schoenmeier[15]. However, the literature is unclear about the mechanism which is responsible for the formation of crepe wrinkles in the vicinity of the nips. It is quite possible that the rolling resistance to the nip rolls produces a loosening slippage in the wound roll during surface winding.

Good[27] has identified rolling resistance as a factor capable of providing a loosening torque. Rolling resistance is a steady state phenomenon which can produce a loosening of the roll structure. There is a need to develop means to quantify rolling resistance so that slippage induced by it can be understood.

Lucas[28] suggested that the easiest way to produce crepe wrinkles was to surface wind rolls that were initially soft, and then suddenly increase the hardness on the rolls by increasing the nip load. Upon reflection, as rolls are wound on a two drum winder where the nip load due to the self weight of the roll cannot be relieved, the nip loads due to the self weight of the rolls reach a very high value as the roll continues to build up. This increase in nip load has been said to lead to crepe wrinkle formation in rolls wound on a two drum winder. There is a good possibility that similar mechanisms are at work in producing the crepe wrinkles, whenever the nip loads increase beyond a certain value when winding a soft roll with a sudden increase in hardness.

Newsprint, with the properties outlined in TABLE 10 was used to surface wind rolls four rolls. For all the cases, the rolls were wound soft, such that there was at least 1 inch of soft material beneath the nip. The diameter of the nip roll was 8 inches, and a web line tension of 0.17 pli (pounds per linear inch) was used. The soft portion in all the rolls was wound with a nip load of 3.3 pli. After the soft portion of the rolls was wound, the rolls were stopped and a radial line scribed on it. The nip loads were then increased on each of the rolls to a higher value. For the first roll the nip load was increased to 20 pli, for the second roll the nip load was increased to 26.7 pli, for the third roll to a value of 33.3 pli and for the fourth roll to a value of 43.3 pli. Following the increase in nip loads, all the rolls showed slippage in a *loosening direction* as evidenced by the characteristic J-Line profile. The results of this experiment with observations are shown in TABLE 11.

TABLE 10. Physical properties of the web material.

Web Tension	60 psi
E_r	$134.9 + 38.8\,\sigma - 0.075\,\sigma^2 + 0.00005\,\sigma^3$
E_t (Average)	240000 psi
Web Caliper	0.0028 in (2.8 mils)
Coefficient of friction (μ) paper/paper	0.2
Width of web	6 in
Poisson's ratio	0.01
Core	Steel, 1.5 in. Inner Radius and 1.65 in. Outer Radius

TABLE 11. Results of the change in Nip Load for the qualitative experiments.

Final Nip Load (pli)	**Figure Number**	**Comments**
20 pli	46 a	Only slippage no defects.
26.7 pli	46 b	Slippage and star defect.
33.3 pli	46 c	Slippage and star defect.
43.3 pli	46 d	Slippage, star defect, and tightening near core.

The experimental evidence of slippage induced by the nips, reveal the existence of a loosening torque. Although the layers which had the radial line scribed on them are loosening, the new layers which are being wound have a greater wound on tension since the nip load has increased. So, layers with very little radial pressure are being compressed by the new outer layers.

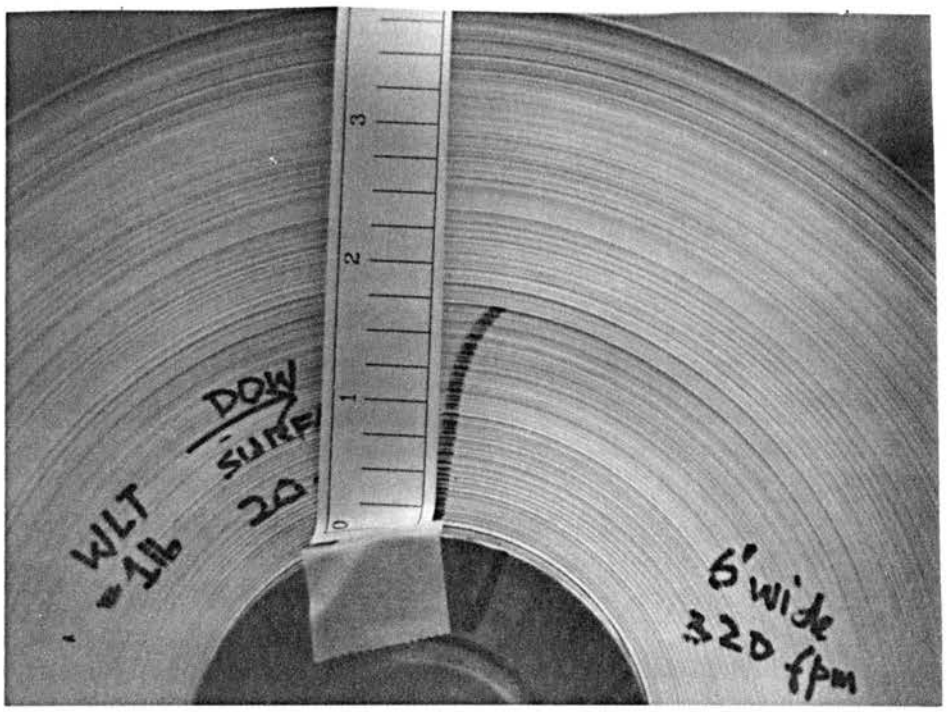

Figure 46a. Surface Wound Roll showing Slippage following an increase in Nip load from 3.3 to 20 pli. (The web line tension was 0.2 pli).

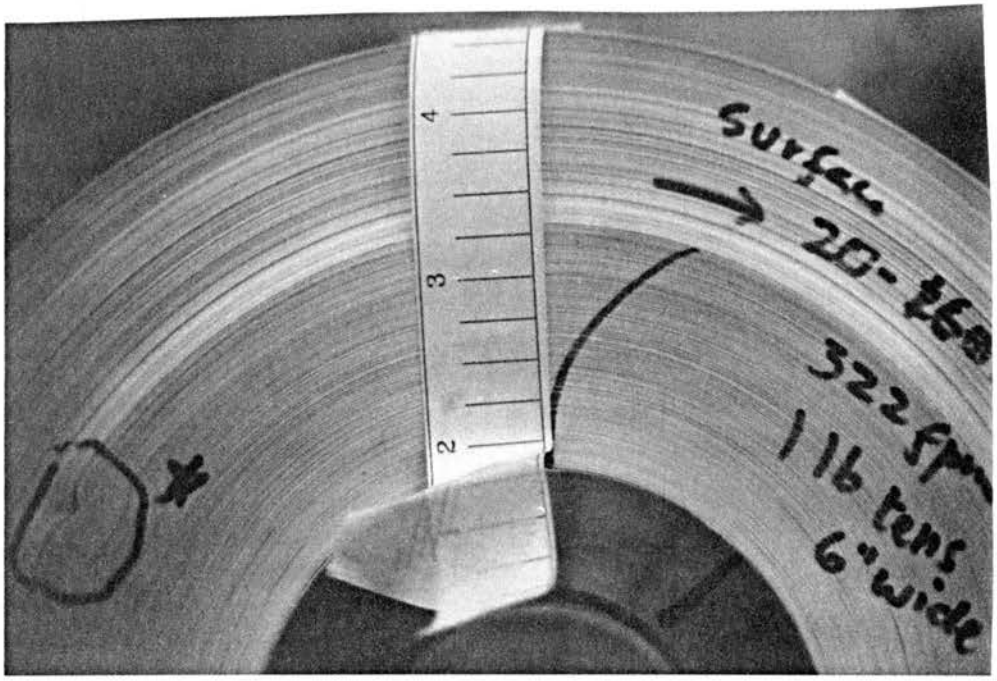

Figure 46b. Surface Wound Roll showing Slippage and Star defect formation following an increase in Nip Load from 0.2 pli to 26.7 pli. (The web line tension was 0.2 pli).

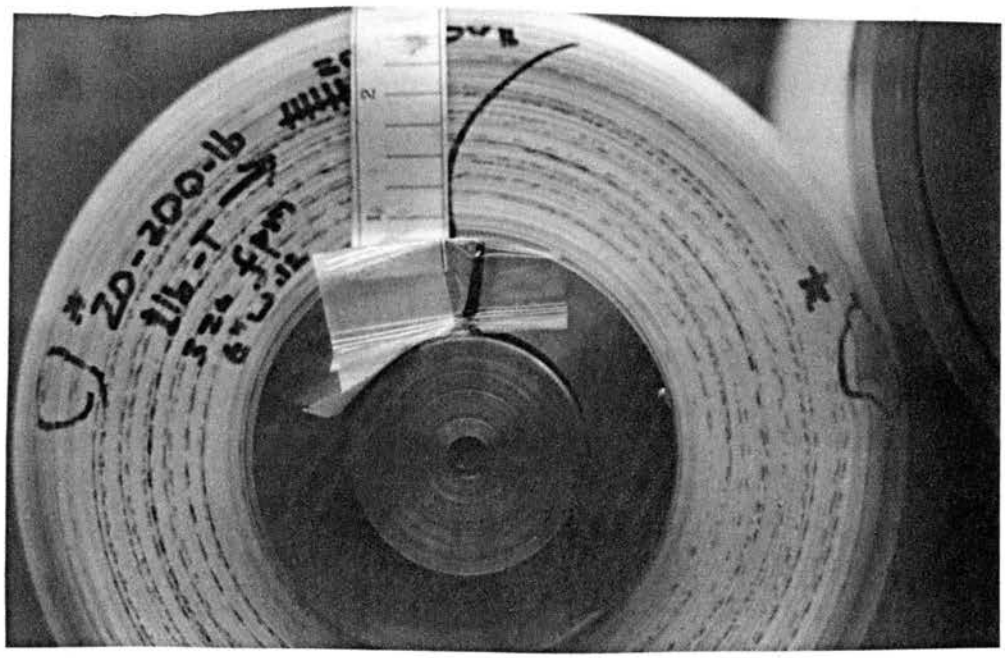

Figure 46c. Surface Wound Roll showing Slippage and Star defect formation following an increase in Nip Load from 0.2 pli to 33.3 pli. (The web line tension was 0.2 pli).

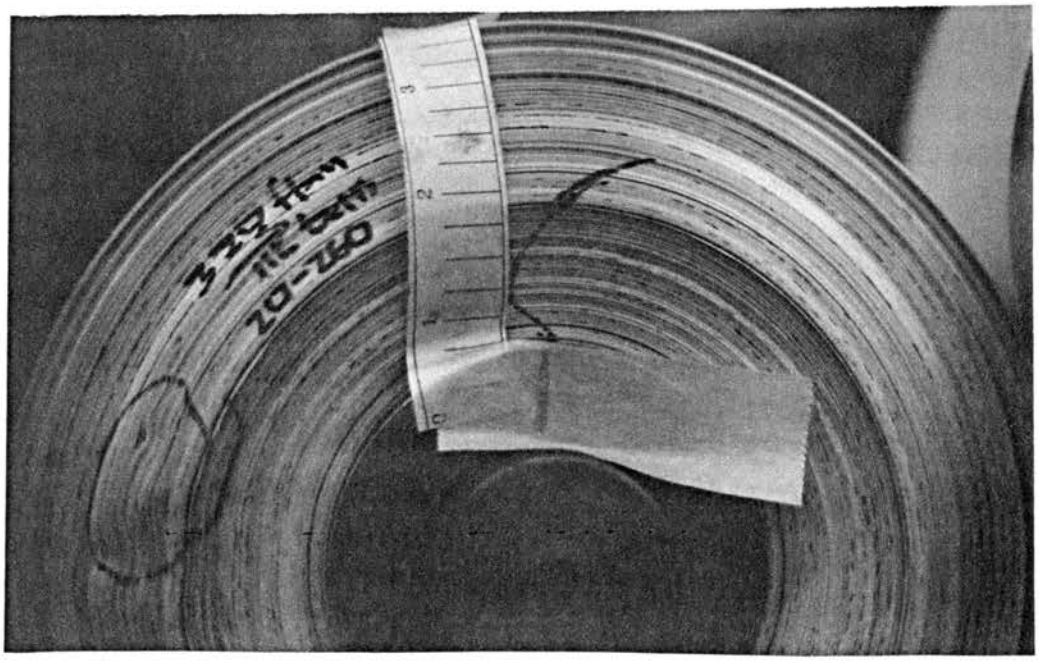

Figure 46d. Surface Wound Roll showing Slippage and Star defect formation following an increase in Nip Load from 0.2 pli to 43.3 pli. (The web line tension was 0.2 pli).

With this background, the literature pertaining to rolling resistance was reviewed to better understand rolling resistance. The literature pertaining to rolling resistance is in two broad categories. These are:

(i) Rolling resistance due to elastic time independent hysteresis of the material

(ii) Rolling resistance due to time dependent viscoelastic behavior of the material

For both the cases outlined above, rolling resistance is quantified by considering a rigid body rolling over a half space of the material which either displays time independent hysteresis losses or viscoelastic behavior. The simplest cases, of rigid bodies considered, are cylinders and spheres. A study by Greenwood et al[29] quantifying the problem of rolling resistance, when a rigid cylinder rolls over an elastic half space, will be considered in detail.

Quantifying rolling resistance, when a rigid cylinder rolls over a visco-elastic half space, has been made by May et al[30], Hunter[31], Morland[32] and Lynch[33]. The automotive tire industry is another source where much empirical work has been done to quantify the rolling resistance of an automotive tire. A handbook on the mechanics of pneumatic tires edited by Schuring[34] and a conference proceedings edited by Snyder[35], on tire rolling resistance, are two sources which provide insight for the work done in quantifying rolling resistance in the automotive industry. In this study, focus will be directed towards the work done by Greenwood et al as it closer in its approach to the problem at hand.

The study by Greenwood et al is based on the energy loss that occurs per unit rolling distance when a rigid cylinder rolls over an elastic half space. In this study, an expression for rolling resistance was developed and is given by:

$$F_{Rolling-Resistance} = \frac{2}{3\pi}\alpha\left[\frac{Wa}{r}\right] \text{(lb/in)} \tag{27}$$

where

'α' is the fraction of energy lost when an elastic material is taken through an upload download cycle

'W' is the nip load (lb/in)

'r' is the radius of the rigid cylinder (in)

'a' is the half width of contact between the rigid cylinder and the elastic medium (in)

Note that the rolling resistance is a force per unit width. The numerical coefficient $2/(3*\pi)$ is equal to 0.21.

The major assumptions in this derivation are:

(i) Elastic contact between the cylinder and the hysteretic material beneath (Hertzian theory for half width of contact)

(ii) The hysteresis loss factor is a constant

(iii) The material in contact with the cylinder is perfectly elastic and provides a finite, time independent hysteresis loss.

Greenwood et al remark that this expression predicts correctly the dependence of rolling resistance on the load, the cylinder diameter and the elastic constants of the material, but, this expression is inadequate in predicting the rolling resistance when a rigid cylinder rolls over a block of rubber. For the case of a rigid cylinder rolling over a block of rubber, the theoretical expression given by equation (27) was modified to incorporate a multiplicative factor. This factor takes into account a complex stress cycle which each element of the rubber material beneath the roller is subjected to, due to shearing that exists at different depths.

The modified expression given by Greenwood et al for the case of a rigid cylinder rolling over rubber is:

$$F_{Rolling-Resistance} = \frac{2(3.5)}{3\pi} \alpha \left[\frac{Wa}{r}\right] \tag{28}$$

which can be rewritten as:

$$F_{Rolling-Resistance} = 0.74\, \alpha \left[\frac{Wa}{r}\right] \tag{29}$$

Greenwood et al found equation (29) correlated well with measurements of rolling resistance for the specific rubber material used. However, what needs to remembered is

that this relationship was established for rubber with a Poisson's ratio of 0.5. In considering a similar situation for Perspex (poly methyl methacrylate), with a Poisson's ratio of 0.35, Wannop et al[36] have derived a different multiplicative factor.

Equation (27) is simple, and is based on a Hertzian contact which has a validity over a wide range of elastic materials. Note that the value of α should lie between 0 and 1, zero being no loss and one being complete loss, which means there will be no recovery of the material behind the roller.

Rolling Resistance During Winding

Earlier, rolling resistance was introduced, as described in the literature, without providing a feel for the phenomenon. Rolling resistance can be physically interpreted by considering the hysteresis losses which occur in a material when taken through a loading-unloading cycle. Consider the case of a cylinder indenting a perfectly elastic medium beneath it, Figure 47a. 'W' is the resultant of the vertical load on the cylinder. The pressure distribution beneath the cylinder is symmetric and is governed by Hertzian contact. As the cylinder starts to roll the elastic material beneath is subjected to a state of upload ahead of the roller. Simultaneously, the material just behind the roller, is being unloaded or downloaded. The exaggerated view shows the material behind the nip unable to reach the original level line due to hysteresis. Thus, the material ahead of the nip resists the continued motion of the cylinder, Figure 47b. The asymmetry of the pressure causes a horizontal resistive component of force, opposing the motion of the

roller. This resistive component of force is the rolling resistance encountered by the cylinder.

Now, consider the case of a nip in contact with a roll being wound, as would occur in surface winding, Figure 48. Using the concept of relative motion, if the wound roll is stopped and the roller continues to move around it, the nip encounters a resistance to its motion around the periphery of the roll being wound, due to the hysteresis phenomenon explained earlier. This force is responsible for providing a loosening torque in the vicinity of the nip. There is the possibility for slippage to occur in the vicinity of the nip when the torque capacity of the roll is exceeded by the loosening torque due to rolling resistance. The rest of this section describes experiments conducted at the WHRC to obtain a realistic measure of the rolling resistance when a nip rolls over a stack of web material.

Rolling Resistance Studies on the Flat Nip Mechanics Bed

The experiments performed to measure rolling resistance were carried out on the Flat Nip Mechanics Test Bed, Figure 49a. The flat nip mechanics test bed consists of a flat bed of aluminum about (1.75 inches) in thickness 12 feet in length and 12 inches in width, mounted on a frame. The bed can be aligned to be horizontal by means of set screws on the frame. There are two steel bearing shafts on either side of the edge of the bed. On

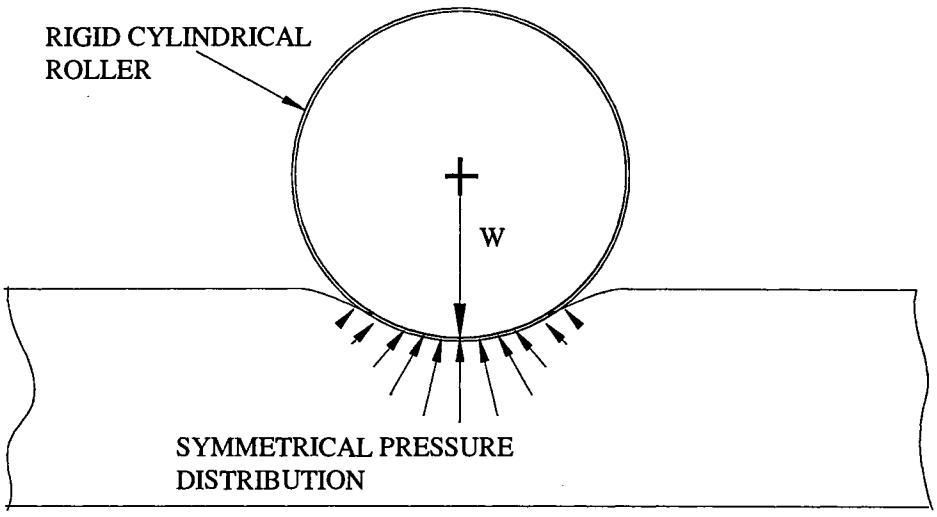

Figure 47a. Static Indentation of a Rigid Cylinder on an Elastic Medium.

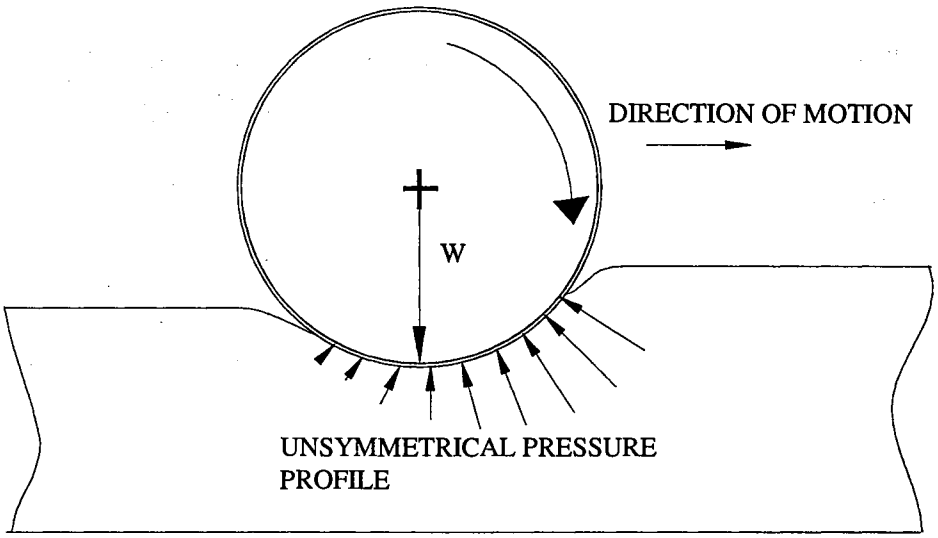

Figure 47b. Rolling Resistance due to Asymmetry in Pressure Profile.

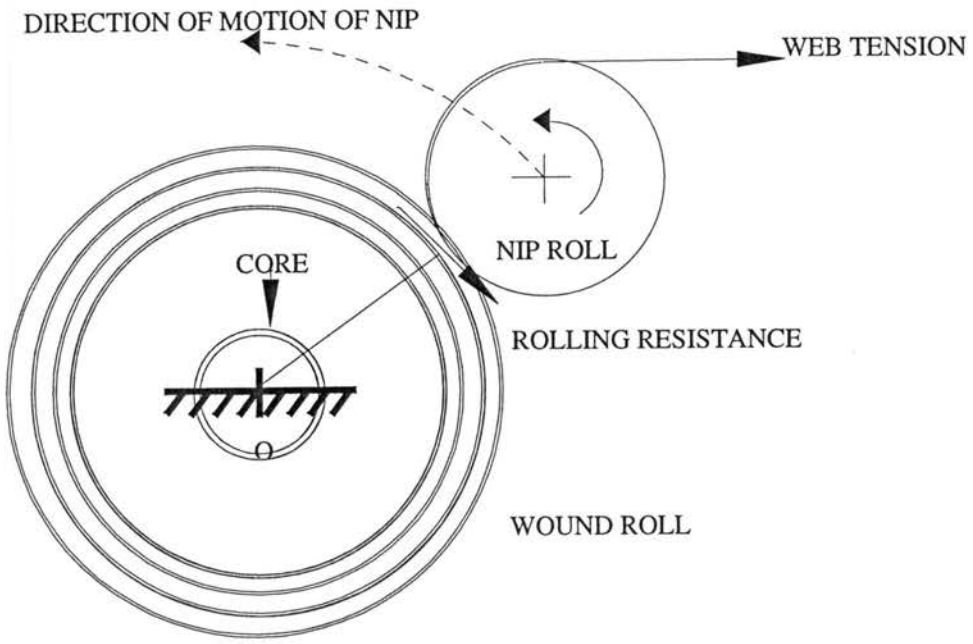

Figure 48. Rolling Resistance encountered by a Nip in the Presence of a Wound Roll.

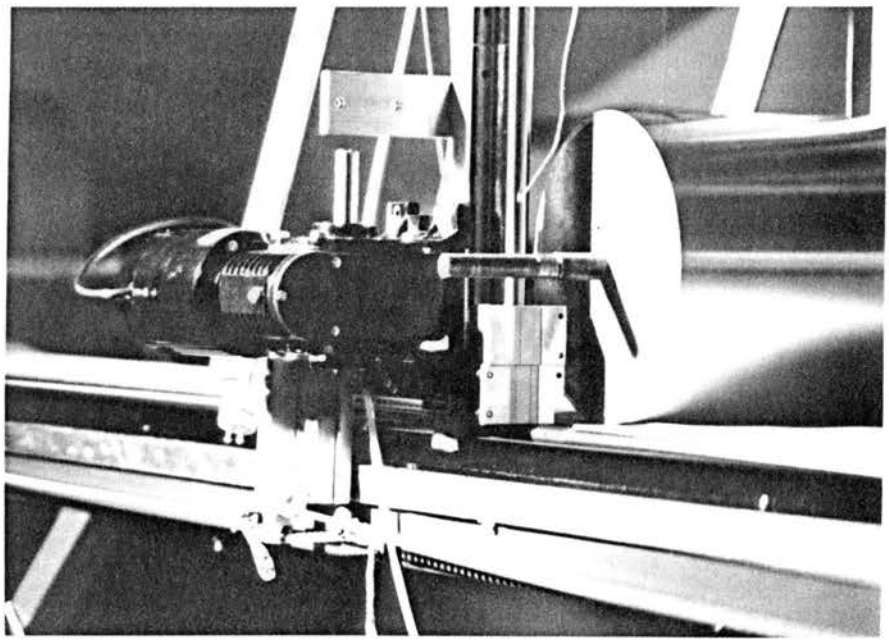

Figure 49a. The Flat Nip Mechanics Test Bed.

one end of the bed, there is a fixture which holds a bank of load cells. Individual layers of web can be wrapped around the separate load cells, and the strain induced in the individual layers can be accurately measured with this load cell bank. The other end of the test bed has provisions to individually pre-tension layers of web material placed on the bed. The purpose of this test bed is to measure the strain induced due to the passage of the nip over web materials that are laid out on the flat bed.

A nip carriage, which is a triangular frame with linear bearings (pillow blocks) at the bottom, slides on the bearing shafts such that the nip carriage can move along the entire length of the bed. The nip carriage has two vertically aligned steel bearing shafts. The vertical shafts are shorter in length in comparison to the bearing shafts aligned on the bed. A plate, which has two pillow blocks, rides on each of the vertical bearing shafts. Nip rolls of various diameters can be attached by means of bearings to these plates, making the nip rolls 'float' on the surface of the bed. A cross plate can be placed between the two plates holding the nip roll and dead weights can be placed on the cross plate to load the nips. The nip carriage can be moved along the bearing shaft by two means:

(i) By applying a horizontal force to the carriage by means of a belt attached to the frame and powered by a motor

(ii) By applying a torque to the nip by means of a flexible shaft which is connected to another motor which is attached to the nip carriage.

When layers of web material are stretched out on the flat bed and a nip rolls across the web material, the flat bed simulates a wound roll of infinite diameter over which a nip of

finite diameter rolls. Depending on the mode of locomotion, the nip carriage simulates center winding or surface winding. If the nip carriage moves by mode (i) it simulates center winding with a lay on nip roll, and if the carriage moves by mode (ii) it simulates surface winding.

The motion of the nip carriage is controlled by a computer system. The position of the carriage is sensed by a rotary potentiometer that is attached to the frame of the test bed. In the case of center winding, the belt which is attached to the frame passes over a sprocket on the motor shaft and a pulley on the rotary potentiometer. The belt completes an endless loop, by passing over another pulley positioned at the end opposite to the motor.

There is a special fixture at the point where the belt is attached to the frame, Figure 49b. This special fixture has a turn buckle, a swiveling arm, and a fixed arm. This frame was specially designed so as to be able to tighten the belt and at the same time attach a load cell such the force with which the nip carriage is moved can be measured. The pulling force on the carriage is measured by a load connected between the swiveling arm and the fixed arm of the fixture. The load cell is connected to a data acquisition system, and the force exerted on the load cell is automatically acquired into a computer.

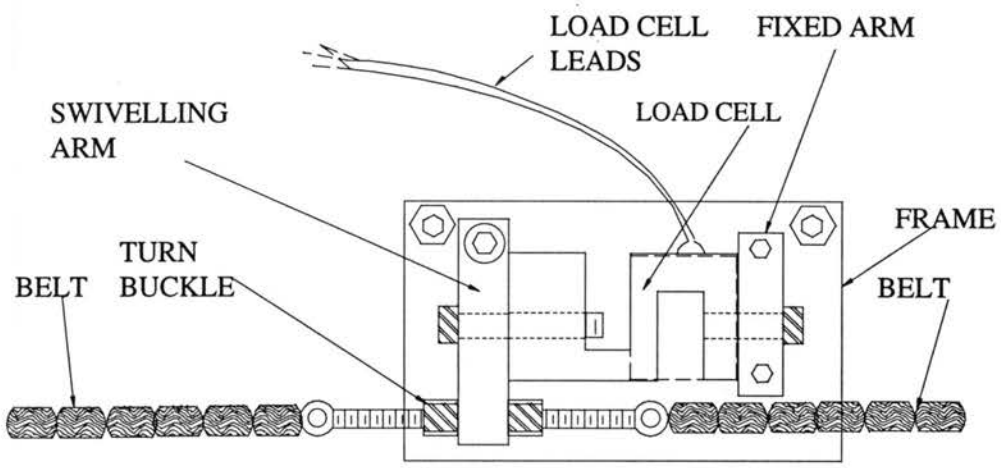

Figure 49b. Schematic Of The Load Cell Fixture.

Aluminum nip rolls were rolled over web material, stacked on the flat nip mechanics test bed. Nips were rolled with a constant velocity of 1 foot per minute across the length of the table. The force required to move the roller at a constant velocity is a measure of the rolling resistance.

All tests were done with newsprint with the characteristics outlined in TABLE 12.

TABLE 12. Conditions of the web stack used in the rolling resistance tests

Caliper	2.8 (Average) mils
Number of layers used	137
Width of Stack	6"
Length of Stack	30"
Boundary conditions on the stack	Both ends of stack are free allowing for slippage to occur

These experiments simulate the rolling resistance encountered by an undriven lay-on roll, when rolling on a wound roll of an infinite diameter. Although the geometry and torque transmission occurring in these tests are different from surface winding, this study helps develop a feel for the rolling resistance forces involved.

Three different nip rolls with diameters of 3 in, 4 in and 10 in and four different nip loads ranging from 3 pli to 25 pli were used in the experiments to elucidate the relationship between the nip loads and the radius of the nips, with respect to rolling resistance. The same stack of web was used in the rolling resistance tests for the nips with diameters of 3 inches and 4 inches. A different stack was used for the 10 inch diameter nip roll.

Results

In Figures 50 a b & c the results of the experiments are shown. The bearing resistance required to overcome the drag due to the bearings supporting the frame are also shown. These were measured for each of the three rollers tested. The rollers are simply supported on the nip carriage and the carriage was moved at the same velocity of 1 fpm, such that there was no rolling contact between the roller and the test bed. The actual rolling resistance is the difference between the bearing drag and the force measured by the load cell for each particular case of the nip roll. The bearing loads are also different for each case, as the belt tension was varied when each roller was mounted, and this is why the bearing force is at a different level for each series of nip diameters.

At this point, a measure of the rolling resistance when a nip rolls over web material is available. These results need to be quantified so that rolling resistance can be predicted. Greenwood et al's equation is a means to obtain such an end. To compare the experimental rolling resistance data, and Greenwood et al's equation (27), 'α', and 'a' for the web material, and the different nips, and nip load combinations need to be evaluated.

Using the definition of 'α', which is the fraction of energy lost when an elastic material is taken through an up-load down-load cycle, an expression can be developed for evaluating 'α' based on the areas of the upload and download curves in a stress strain plot of the web material.

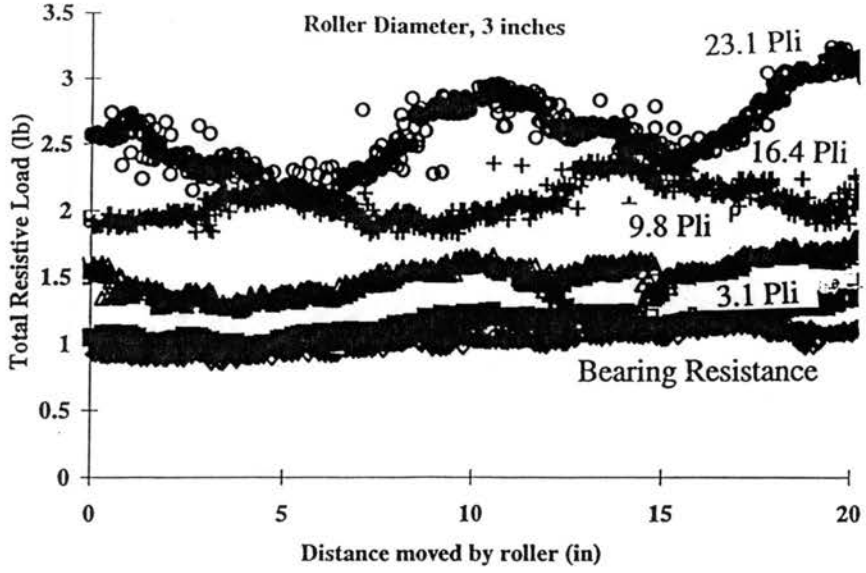

Figure 50a. Experimental Data for a Nip Diameter of 3 in. Figure shows the total resistive force encountered by the nip roll for varying nip loads. The Rolling Resistance for a particular value of nip load is the difference between the Total Resistive Load and the Bearing Resistance.

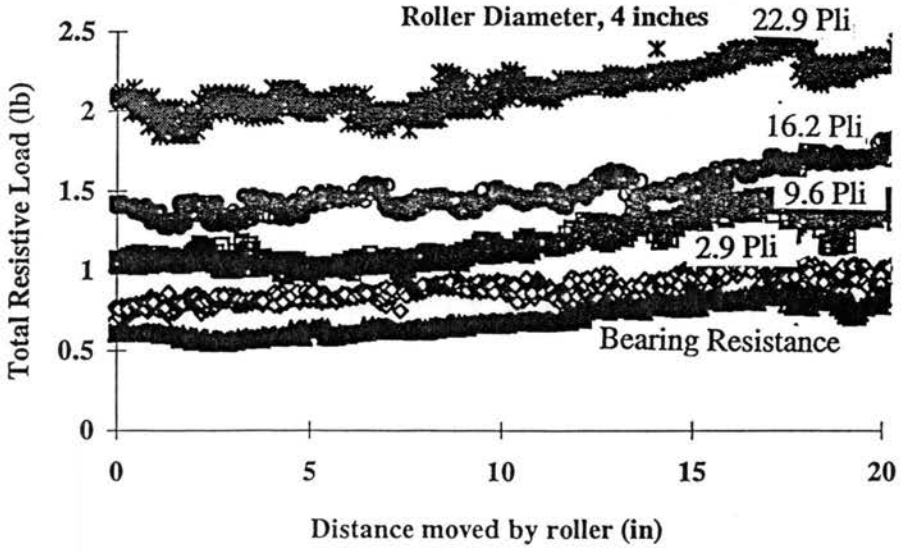

Figure 50b. Experimental Data for a Nip Diameter of 4 in. Figure shows the total resistive force encountered by the nip roll for varying nip loads. The Rolling Resistance for a particular value of nip load is the difference between the Total Resistive Load and the Bearing Resistance.

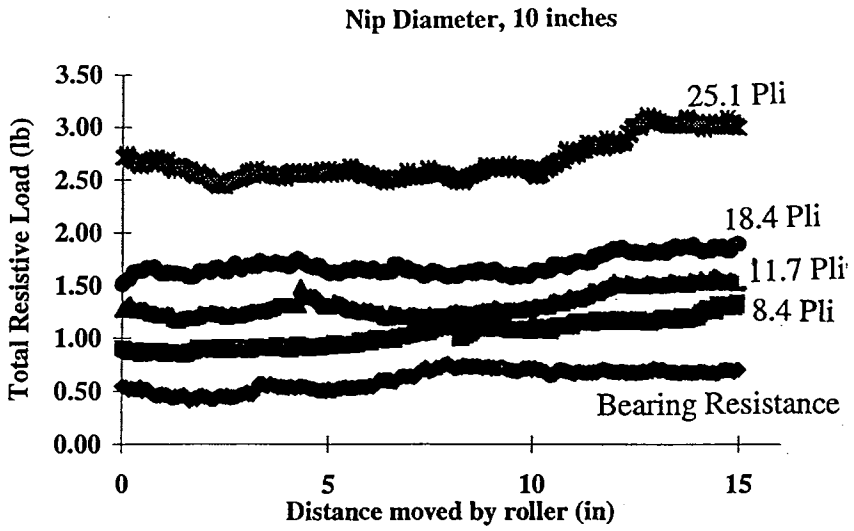

Figure 50c. Experimental Data for a Nip Diameter of 10 in. Figure shows the total resistive force encountered by the nip roll for varying nip loads. The Rolling Resistance for a particular value of nip load is the difference between the Total Resistive Load and the Bearing Resistance.

$$\alpha = \left(\frac{Area_{up-load\,curve} - Area_{down-load\,curve}}{Area_{up-load\,curve}}\right) \tag{30}$$

Using experimental values of stress and strain, obtained by performing stack tests in the laboratory, values of 'α' were computed from equation (30) for different values of pressure. A sample stress-strain curve used in evaluating α is shown in Figure 51.

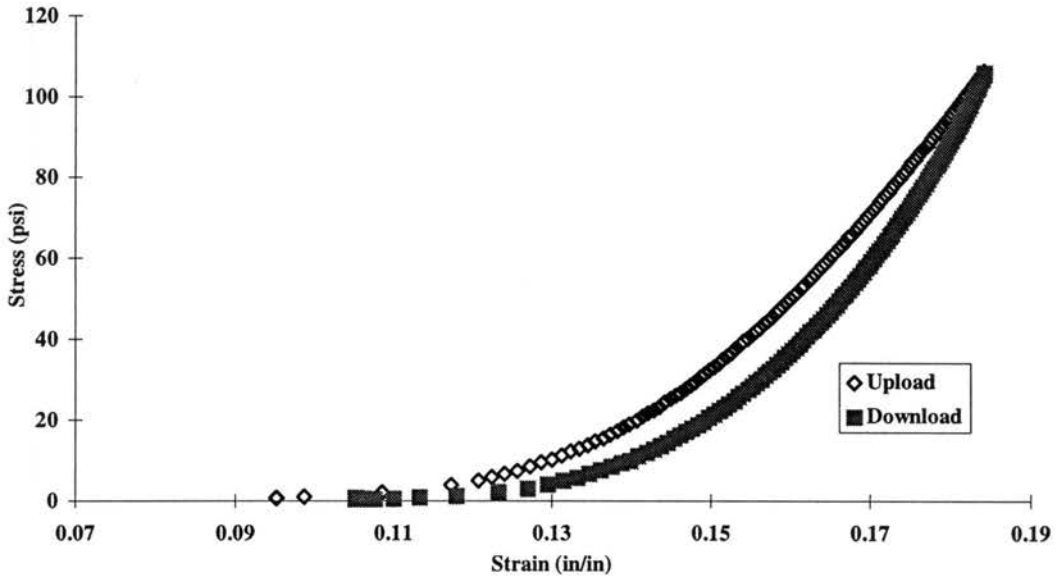

Figure 51. A sample of the stress strain value used in evaluating 'α', from a stack test. Note that the maximum value of the stress that this sample undergoes is around 110 psi.

The pressure levels considered, correspond to levels of stress that would occur directly under the nip. In addition, the variability of 'α' with respect to the pressure can be observed. Figure 52 shows the experimental values of 'α' obtained as a function of the maximum stress in each test. The results of two tests and an average value based on the two tests are, also, shown in Figure 52. These experimental values, correspond to the web stack used in the rolling resistance experiments for nip diameters of 3 and 4 inches.

A trend is that the values of 'α' appear to be centered around 0.2 (20%). This indicates that there is a 20% loss in energy during an upload download cycle and it is fairly constant independent of the maximum pressure existing in the web stack. Note that this loss factor may be different depending on different grades of web materials. The 20% is

valid only for the particular specimen of web material that was tested. The web stack used for the 10 inch diameter nip roll had a different value of 'α', equal to 0.39.

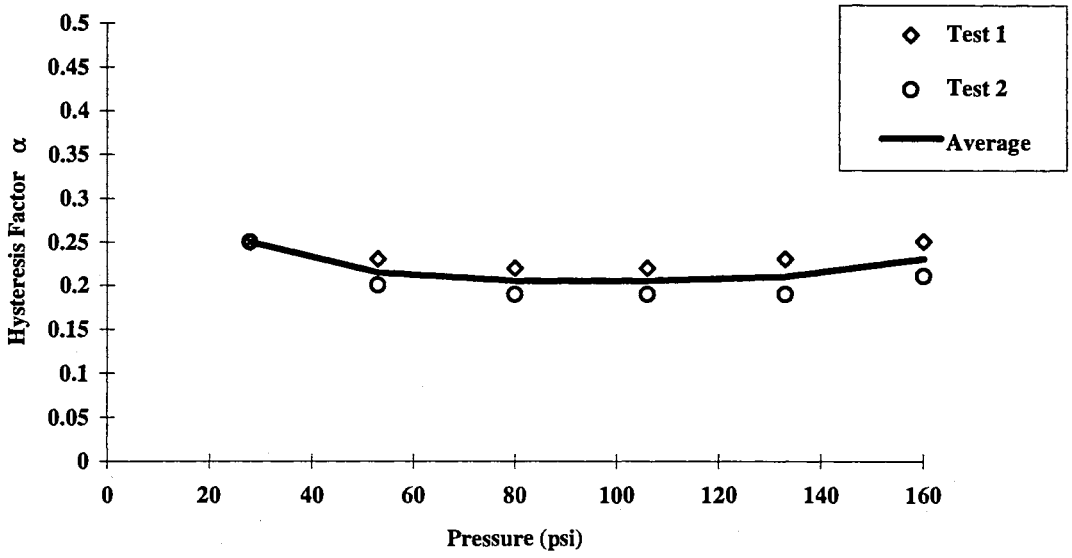

Figure 52. Variation of 'α'(the Hysteresis loss factor) with Maximum stack Pressures. Note that the values of 'α' shown in the figure correspond to web stack used with the 3 and the 4 in. Diameter Nip Rolls.

To successfully use Greenwood et al's equation (27) to predict rolling resistance 'α', 'a', 'W' and 'R' have to be known.. 'W' and 'R' need not be evaluated, but 'α' and 'a' are material properties and have to be evaluated experimentally. Using the nip rolls used in the experiments, measurement of contact widths 'a' between the nip roll and the web stack beneath was made. This was accomplished using high magnification photographs of the edge of the nip roll and the web stack. Figure 53 shows a sample of the half width measurement. A machinists rule graduated in 1/32nd's of an inch, was mounted on the

valid only for the particular specimen of web material that was tested. The web stack used for the 10 inch diameter nip roll had a different value of 'α', equal to 0.39.

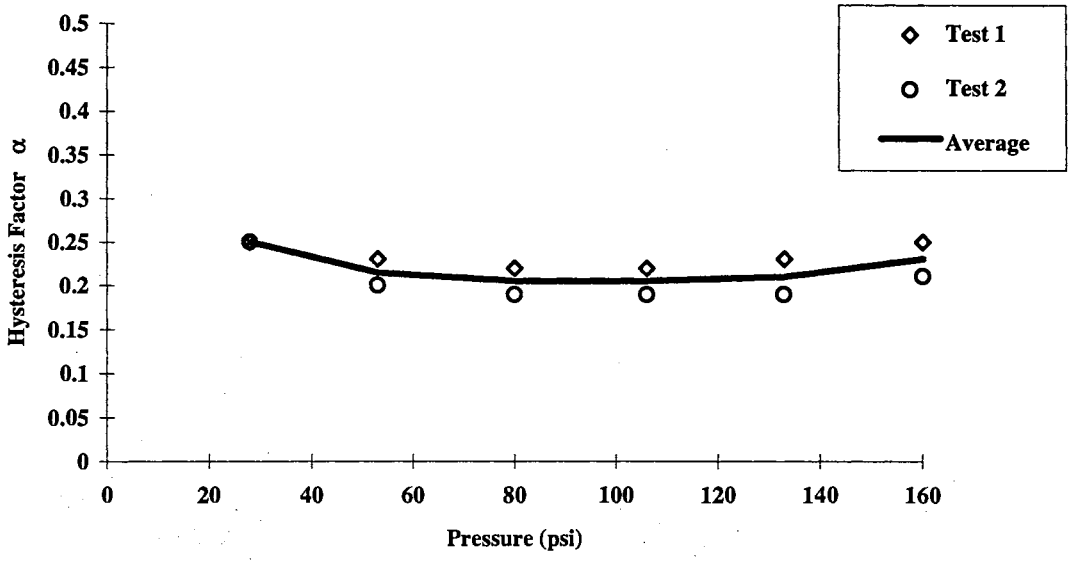

Figure 52. Variation of 'α'(the Hysteresis loss factor) with Maximum stack Pressures. Note that the values of 'α' shown in the figure correspond to web stack used with the 3 and the 4 in. Diameter Nip Rolls.

To successfully use Greenwood et al's equation (27) to predict rolling resistance 'α', 'a', 'W' and 'R' have to be known.. 'W' and 'R' need not be evaluated, but 'α' and 'a' are material properties and have to be evaluated experimentally. Using the nip rolls used in the experiments, measurement of contact widths 'a' between the nip roll and the web stack beneath was made. This was accomplished using high magnification photographs of the edge of the nip roll and the web stack. Figure 53 shows a sample of the half width measurement. A machinists rule graduated in 1/32nd's of an inch, was mounted on the

edge of the roller such that the width of contact was in focal field of the camera directly giving a measure of the width of contact from the photographs of the nip-roll, web-stack interface. The nips were loaded using dead weights corresponding to the same levels of nip load used in the experiments conducted on the flat nip mechanics test bed. TABLE 13 shows the half-width data obtained from experiments conducted in the laboratory.

TABLE 13. Experimental results of the contact width measurements.

Nip Diameter (in)	Nip Load (pli)	Half width of contact (in)
3.0	3.1	0.254
3.0	6.4	0.281
3.0	9.8	0.313
3.0	16.4	0.348
3.0	23.1	0.352
4.0	2.9	0.367
4.0	6.2	0.375
4.0	9.6	0.414
4.0	16.2	0.426
4.0	22.9	0.422
10.0	8.4	0.609
10.0	11.7	0.664
10.0	18.4	0.766
10.0	25.1	0.773

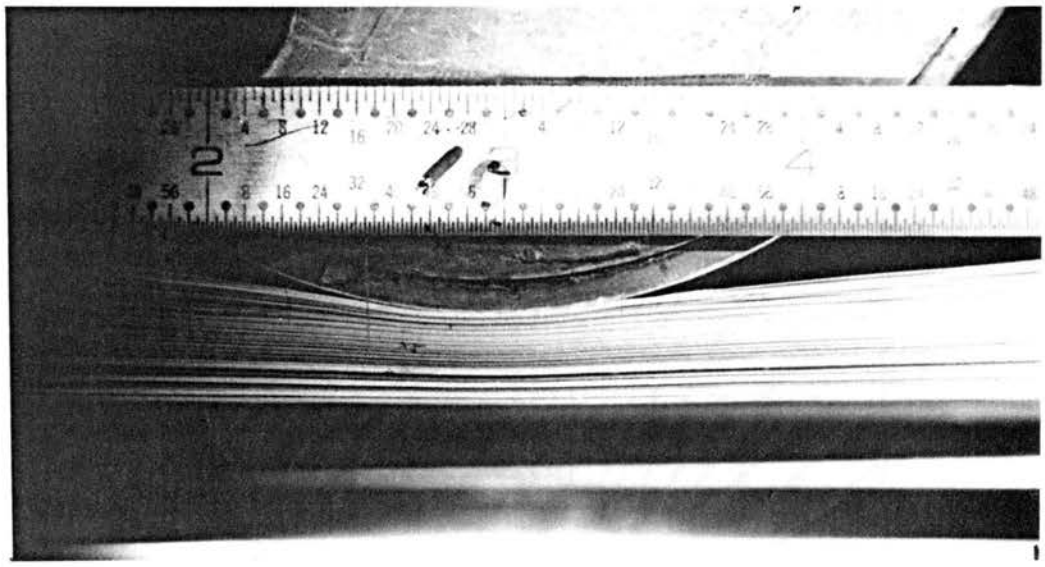

Figure 53. A Sample Photograph showing Contact width at the Nip roll - Web Stack Interface. A graduated Machinists rule is mounted on the Nip Roll to assist in making visual measurements of the half width.

Comparison of Experimental Results with Theory

As mentioned earlier, comparison of the experimental values with an equation serves the dual purpose of providing a model relating the variables and verifying the veracity of the results. This is not completely a comparison between a theoretical model and an experimental result. Greenwood et al's relationship given by equation (27) was derived on a theoretical basis. But, to use the equation to predict rolling resistance realistically, experimental inputs are needed in the form of contact widths and the hysteresis loss factor. Another point to be emphasized, is that Greenwood et al's relationship was developed for the case of a rigid cylinder rolling over an elastic medium. This is significantly different from the case of a nip rolling over a stack of web material, as the stack of web material is a layered structure with the individual layers capable of slipping.

With the values of 'a' and 'α' determined experimentally, it is possible to evaluate the rolling resistance, using equation (27) for known values of the nip load 'W' and the radius of the nip 'r'. To compare the rolling resistance data determined experimentally with the theoretical equation, an average value of the force over the distance rolled is considered as a basis for comparison. This is because Greenwood et al's equation yields a single value for rolling resistance. Furthermore, the rolling resistance predicted by Greenwood et al's equation is for a unit width of elastic material. So, the results have to be scaled by the width of the web material to compare with the experimental values.

Figures 54a, b&c show results from equation (27) (theoretical) based on experimental evaluation of 'α' and 'a' compared with the average values of rolling resistance forces from experimental results. The standard deviation values that appear along with the experimental values indicate the deviation of the average values of the experimental results. The experimental results compare well with the values of rolling resistance generated with equation (27), for nip rolls of radii 3 and 4 and 10 inches respectively. Thus, it appears that equation (27) developed by Greenwood et al may be adapted to understand rolling resistance encountered by a nip in the presence of a wound roll.

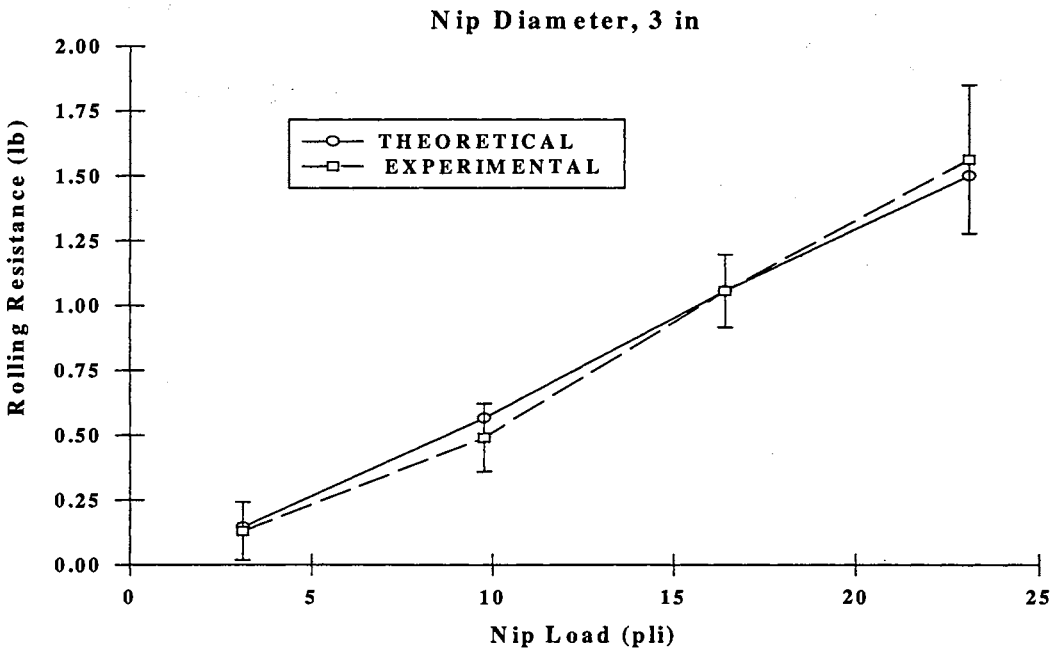

Figure 54a. Comparison of Experimental Rolling Resistance Data with the Theoretical Form of Greenwood et al's Equation. The Nip diameter is 3 inches and the hysteresis loss factor is 0.2

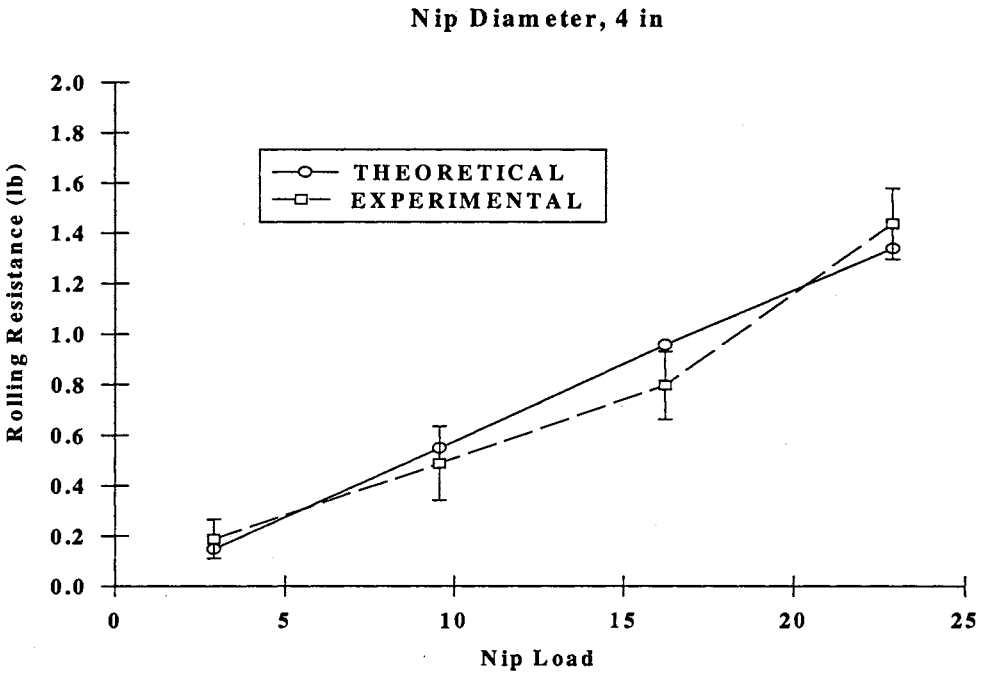

Figure 54b. Comparison of Experimental Rolling Resistance Data with the Theoretical Form of Greenwood et al's Equation. The Nip diameter is 4 inches and the hysteresis loss factor is 0.2.

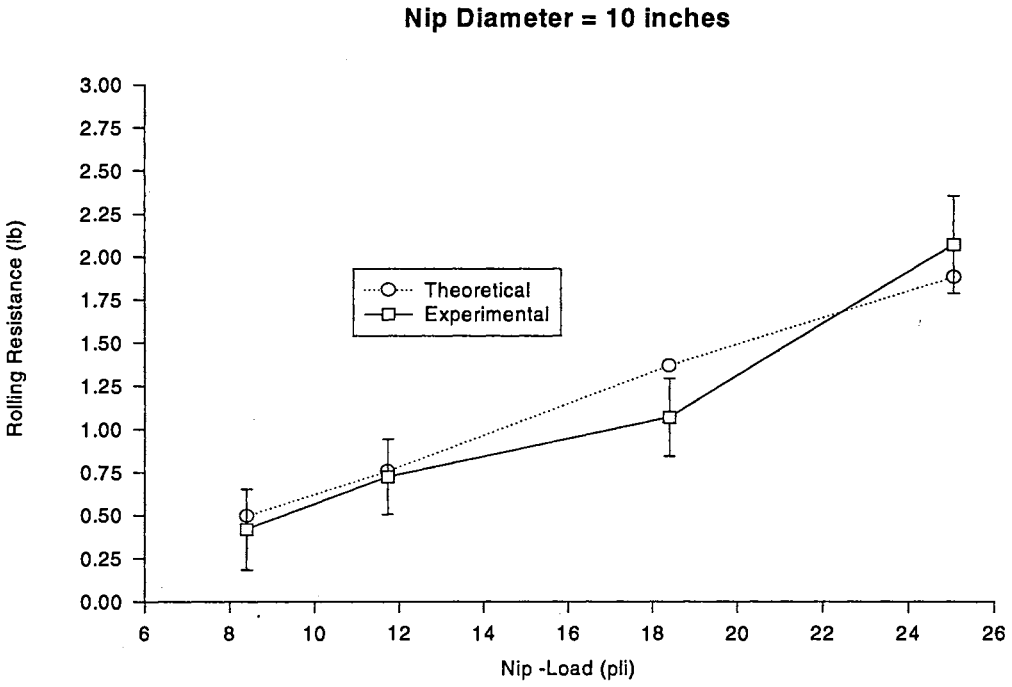

Figure 54c. Comparison of Experimental Rolling Resistance Data with the Theoretical Form of Greenwood et al's Equation. The Nip diameter is 10 inches and the hysteresis loss factor is 0.4.

Finite Element Analysis

A non linear finite element model was developed to simulate rolling resistance using MARC* in addition to a comparison of the experimental results with a theoretical equation developed by Greenwood et al. Part of the reason for this development is that the theoretical equation does not take into account different boundary conditions that a wound roll offers to a nip rolling over it. Finite element analysis helps to simulate different boundary conditions. At this time, only a pilot model to understand rolling resistance has been developed to probe the extent to which these simulations can provide useful information.

The schematics of the finite element model are simple, Figure 55. The web stack was modeled using plane strain elements. A block of plain strain elements was used in the analyses. The total length of the model was 25 in. The height of the model was 2 in. Each plane strain element was 0.25 in x 0.1 in length and width respectively. No slippage is considered at this time, as inter-layer slippage adds complexity to the model. The left end of the model is completely constrained in both the x and y directions. The bottom of the model is constrained in y direction. The nip roll is simulated as a rigid cylindrical body and the web beneath was loaded by the nip corresponding to the nip load used in the experiments. Motion is simulated by specifying a incremental linear and an angular

* MARC is a commercial Finite Element Code
Developed by MARC Analysis Inc

velocity to the center of rotation of the rigid roller. The indentation of the roller is controlled by specifying linear displacements in the vertical direction to the rigid roller.

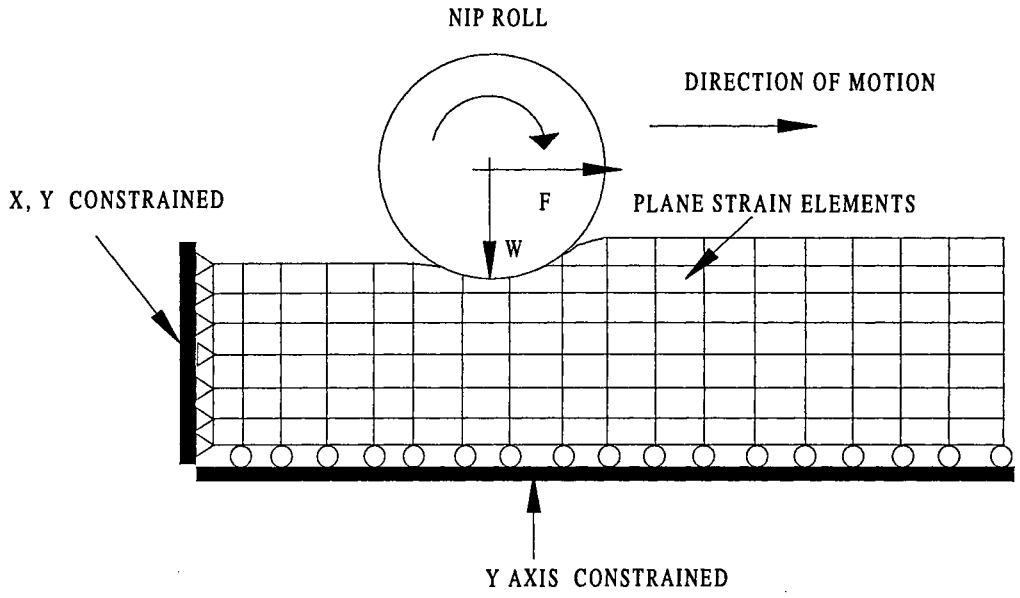

Figure 55. Schematic of the Finite Element Model with the Boundary Conditions.

Three different nip diameters and four different nip loads per roller diameter were used. The program has the capability to output the resultant forces on the rigid roller on an incremental basis.

A non linear material modulus can be input such that it simulates an actual stack of web material. The finite element model can simulate a varying material modulus depending upon the state of stress in the model. The material property of the plane strain elements is a function of whether the material is being loaded or unloaded, thus simulating hysteresis occurring in reality. To accomplish this, experimental data from a stack test were taken and an expression of the form

$$\sigma = k_1 e^{k_2 \varepsilon} \tag{31}$$

where

'σ' = stress in psi

'ε' = strain (in/in)

k_1 and k_2 are curve fit parameters

as suggested by Pfeiffer[23] was used to model the stress strain data for the up-load and download cases. With the form given by equation (31), E_r can be represented simply as the product of k_2 and σ. So:

$$E_r = \frac{d\sigma}{d\varepsilon} = k_2 \sigma \tag{32}$$

This form is a compact representation of the non-linear modulus of the material.

Using the same form of curve fit for both the up-load and down-load, two different expressions to model the up-load and the down-load data can be obtained.

$$(E_r)_{upload} = (k_2)_{upload} \sigma \tag{33}$$

$$(E_r)_{download} = (k_2)_{download} \sigma \tag{34}$$

Note that the values of k_2 are dependent on the maximum pressure on the web stack.

Figure 56 shows the variation of the k_2 factor as a function of pressure. The k_2 factors are shown for both the upload and the download cases. An interesting trend that is visible is that the k_2 factors for the up-load and the down-load differ by a constant value for all cases except for the first point.

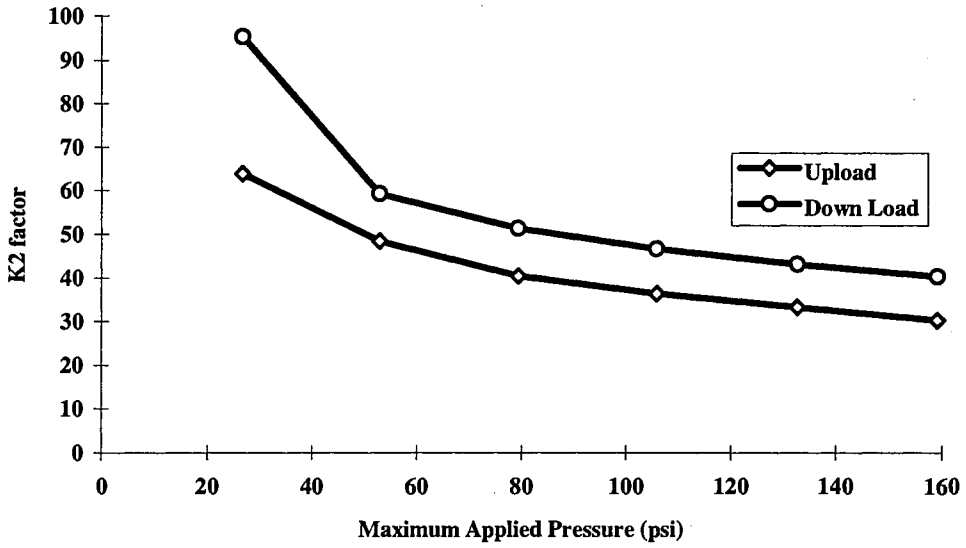

Figure 56. Variation of the k_2 factor as a function of the Maximum Stack Pressure. Note that the k_2 factors were obtained based on experimental stack test data.

Note that although k_2 is a function of the pressure, the energy loss due to hysteresis occurring in the stress strain curve at the highest pressure is the same as in a stress strain curve occurring at a lower pressure. Good[27] suggested implementing a variable k_2 as a function of pressure. However, it leads to convergence problems in the finite element model. Hence, one particular value of k_2 for up-load and down-load was chosen to generate E_r for both up-load and down-load cases. The k_2 values implemented for the analyses were 30.2 for the up-load and 40.3 for the down-load.

The results from the finite element are noisy. This is due to problems with obtaining a convergent solution for the model and problems involving slippage between the roller and the medium beneath. If the data are smoothed using running averages, interesting details start to emerge. A comparison of the results from the finite element analysis with equations (27) and (29) has been made, Figures 57a, b&c.

As was done in comparing the experimental results with Greenwood et al's relation, an average value is used from the smoothed data to make comparisons. The finite element solution is closer to equation (29) than equation (27). The boundary conditions on the model, slippage at the nip-web interface and the web-surface interface are quite possibly reasons for this trend. Studies from this analysis have generated a measure of confidence in the form of the equation developed by Greenwood et al. This model could be used as a base model for further developments if needed in future.

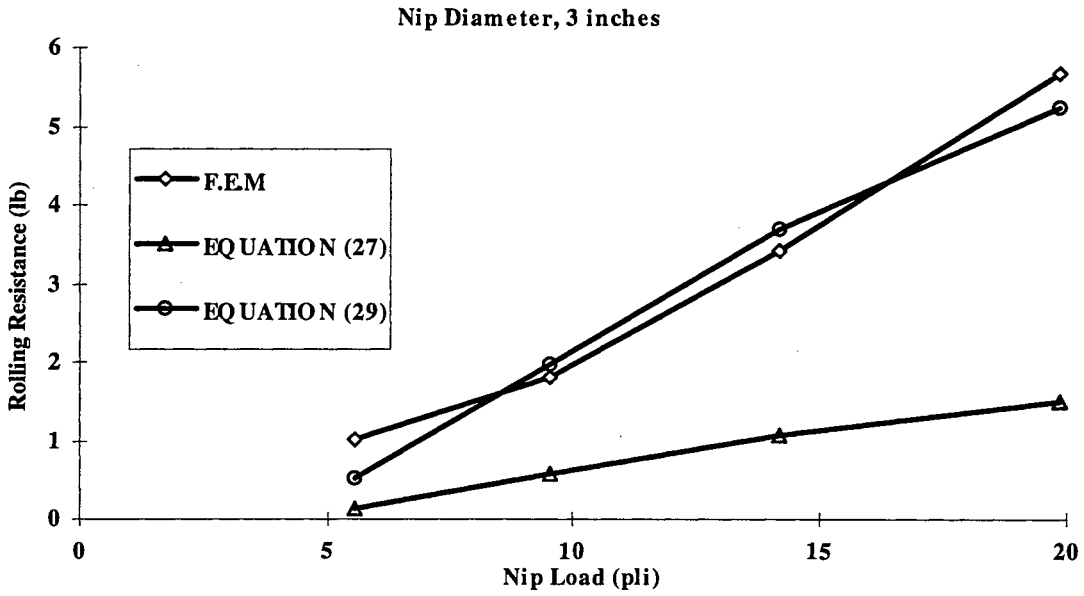

Figure 57a. Comparison of Finite Element Data with Greenwood et al's equation. The Nip Diameter is 3 inches.

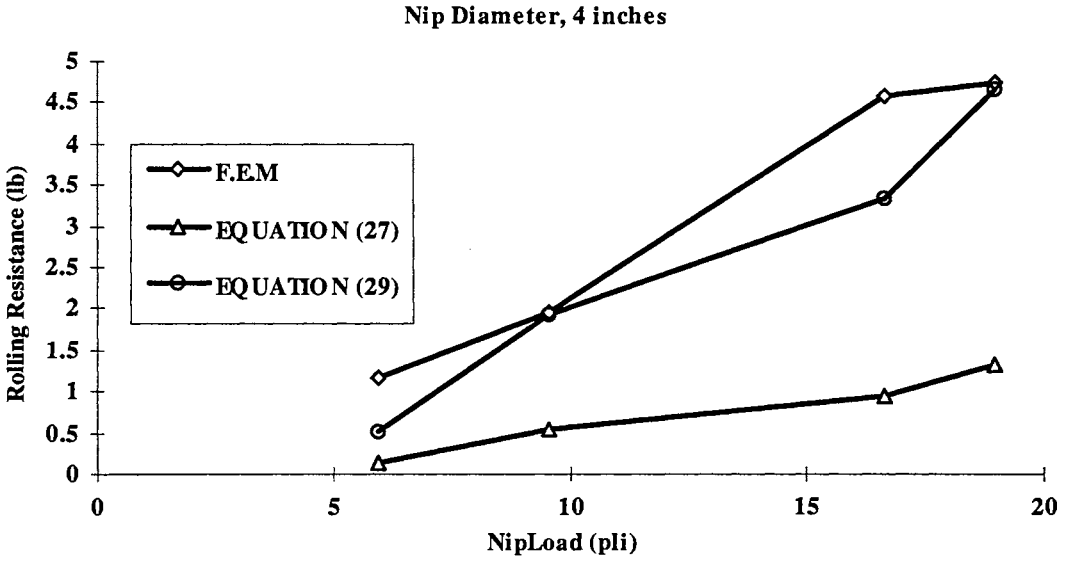

Figure 57b. Comparison of Finite Element Data with Greenwood et al's equation. The Nip Diameter is 4 inches.

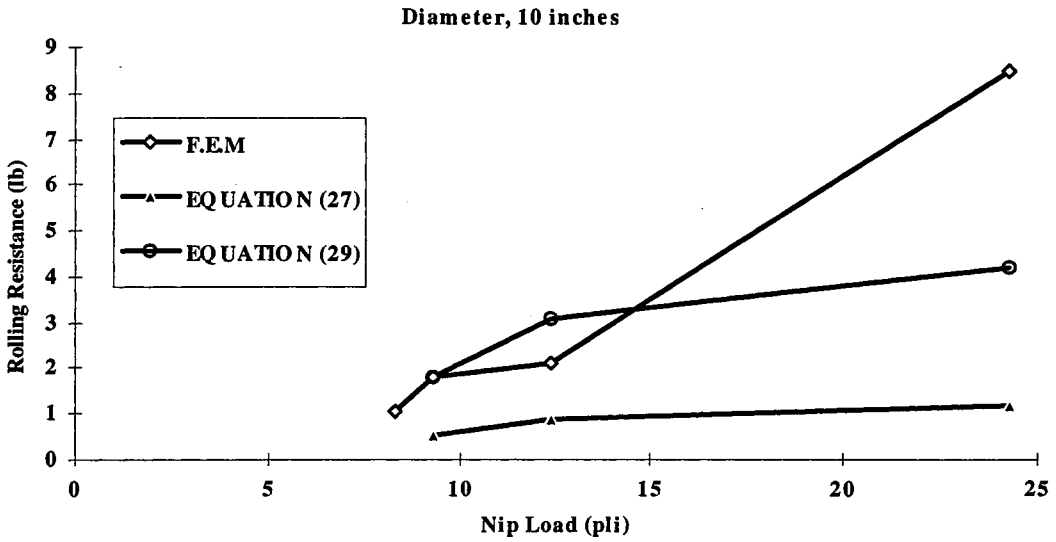

Figure 57c. Comparison of Finite Element Data with Greenwood et al's equation. The Nip Diameter is 10 inches.

So, in understanding the nip as a source producing slippage:

(a) A means has been identified to quantify the rolling resistance encountered by a nip rolling over web material, for the simple case of a roller pulled over stacks of web material. So:

$$F_{Rolling-Resistance} = \frac{2}{3\pi}\alpha\left[\frac{Wa}{r}\right]$$

(b) The rolling resistance encountered by the nip rolling over a stack of loose web been experimentally measured on the flat nip mechanics test bed.

(c) A comparison has been made of the experimental data obtained and the theoretical equation identified to quantify rolling resistance. The

experimental values of rolling resistance relate well with the equation developed above. Note that the layers of the web stack are not in tension.

d) A pilot finite element model has been developed to probe rolling resistance.

CHAPTER VII

ROLLING RESISTANCE IN SURFACE WINDING

Scope

In the previous chapter, an experimental method to determine the rolling resistance encountered by a nip roll, pulled across a stack of web material was described. This situation, is representative of center-winding with an undriven nip roll. In this chapter, experimental methods to determine the rolling resistance encountered by a torque driven nip, in contact with a wound roll, will be described. A theoretical means, based on the form of Greenwood et al's equation (27), to model the rolling resistance encountered by the surface driven nip, will be described. Comparisons between the theoretical model and the experiments will be made, to show the ability of the theoretical model to represent the rolling resistance encountered by a surface driven nip.

In this chapter and the next, two important questions pertaining to slippage will be addressed. They are:

(i) Are rolling resistance forces (torques) large enough to cause slippage in a wound roll?

(ii) Can a simple criterion to predict slippage, based on the rolling resistance, be developed for the case of slippage due to nips?

Theory

The starting point for a theoretical development of rolling resistance is Greenwood et al's equation:

$$F_{Rolling-Resistance} = \frac{2}{3\pi}\alpha\left[\frac{Wa}{r}\right] \text{ (lb/in)} \tag{35}$$

Recall that, equation (35) was developed for the case of a cylinder rolling over an elastic continuum (half-space). To adapt the equation for the case of a torque driven nip contacting a wound roll, modifications have to be made to account for the circular geometry of the wound roll. Good[27], suggested replacing 'r', with the equivalent radius of contact 'R*', of the wound roll and nip. The equivalent radius of contact depends on the radii of the nip and the wound roll, and takes into consideration the effect of the circular geometry of the nip and the wound roll.

The governing relation is:

$$\frac{1}{R^*} = \frac{1}{r_{nip-roll}} + \frac{1}{r_{wound-roll}} \tag{36}$$

which gives

$$R^* = \left(\frac{r_{nip-roll} * r_{wound-roll}}{r_{nip-roll} + r_{wound-roll}}\right) \tag{37}$$

Incorporating the geometric considerations, Greenwood et al's equation (27), now becomes:

$$F_{Rolling-Resistance} = \frac{2}{3\pi}\alpha\left(\frac{Wa}{R^*}\right) \text{ (lb/in)} \tag{38}$$

which represents the rolling resistance force, between the nip and the wound roll.

Note that the rolling resistance force is in units of force per unit length, so, to obtain the total rolling resistance force, equation (38) needs to be scaled by the width of the wound roll. This force, can then be multiplied by the nip radius to yield a torque value. So, the total rolling resistance torque is given by:

$$Torque_{Rolling-Resistance} = \frac{2}{3\pi}\alpha\left(\frac{Wa}{R^*}\right) w\, r_{nip-roll} \text{ (lb-in)} \tag{39}$$

where, 'w' is the width of the wound roll in inches and

'$r_{nip\text{-}roll}$' is the radius of the nip roll.

Recall that, Greenwood et al modified equation (27) by a scale factor of 3.5, in order to establish correlation with their experiments. Adapting this modified model for the case of the circular geometry, the modified model to represent the rolling resistance force, can be stated as:

$$F_{Rolling-Resistance} = (3.5)\frac{2}{3\pi}\alpha\left(\frac{Wa}{R^*}\right) \text{ (lb/in)} \tag{40}$$

Correspondingly, the rolling resistance torque will be scaled by a factor of 3.5. Thus, the modified model to predict the total rolling resistance torque becomes:

$$Torque_{Rolling-Resistance} = (3.5)\frac{2}{3\pi}\alpha\left(\frac{Wa}{R^*}\right) w r_{nip-roll} \text{ (lb-in)} \tag{41}$$

While using these torque models, a point to be remembered is that two of the inputs to the models, namely 'α' and 'a' are experimental. So, both the models cannot be considered to be completely theoretical. A method to compute 'a' approximately, will be outlined later.

Experimental Measurement of Rolling Resistance for a Torque Driven Nip Roll

As it is difficult to quantify the structural integrity of surface wound rolls, it becomes difficult to relate the ability of the roll to resist slippage and the rolling resistance. Center-winding, on the other hand, is better understood, as far as characterizing the radial pressure (structural integrity) of the roll via wound roll models. So, center winding was chosen for winding the rolls that were subjected to the action of a torque driven nip.

Two sets of experiments were performed for comparison with the form of equations developed by Greenwood et al. In one set of experiments, torque sensor measurements are compared to equations (27) and (29). In the second set, experimental results from static torque tests are compared with equation (29).

The dynamic torque tests and the static tests are based on different sets of rolls. The reason, for different static and dynamic torque tests, is to provide complementary sets of data, to compare with the rolling resistance models adapted from Greenwood et al. The dynamic torque test, in general, is destructive, and, in some cases, excessive slippage is induced, which loosens the roll. This leads to gradually increasing torque inputs to the roll. So, the dynamic torque tests represent the total torque input to the roll, as slippage continued to loosen the roll. The static tests, on the other hand, do not induce any slippage in the wound roll, and serves as a base case to compare with the theoretical model.

Dynamic Torque Tests

Three different values of wound on tension were chosen to center wind the rolls, which were subjected to the influence of a torque driven nip. The wound on tension values chosen were: 0.3 pli, 0.6 pli, and 1.3 pli. Nine rolls per wound on tension profile were center wound. All rolls were wound to diameters between 7 and 8.5 inches. The free edges of all the rolls were taped to the body of the roll. These rolls were then mounted on a winder, which was configured to drive the nip by a torque. Three different nip

diameters of 2.5 in, 6 in. and 8 in. were used for the rolling resistance tests. A torque sensor was mounted to measure the torque input to the nip. For any particular nip roll chosen, three different nip loads (0.83, 5, 10 and pli) were used. Three different nip rolls were used for set of rolls (9), wound with a certain value of wound on tension. A total of 27 different combinations of nip diameters, wound on tensions, and nip loads were used.

Prior to the start of each experiment, a radial line was marked on the edge of the wound roll. This was done to visually monitor slippage on the roll. The experiment consisted of mounting a roll on the windup shaft, subjecting the roll to a torque for a period of 125 seconds, simultaneously measuring the torque input via the torque sensor. A data acquisition system was set up, to continuously acquire data from the torque sensor.

Static Torque Tests

The static torque tests, were performed on different rolls. Three rolls were wound with wound on tensions of 0.3 pli, 0.6 pli, 1.3 pli. The diameters ranged from 7.5 to 7.8 inches.

The same nip rolls (diameters of 2.5 in, 6 in. and 8 in.) that were used in the dynamic tests were also used in the static tests. Three different nip loads (0.83, 5, 10 pli) per nip diameter were used. The experiment consisted of mounting each of the rolls individually on a windup shaft, loading the nip to the wound roll, and slowly rotating the loaded nip by 45 degrees, measuring the amount of torque to rotate the wound rolls. The nip was rotated by a radial arm attached to a force sensor. The force times the radial arm

represents the torque input to the wound roll. So, the roll is not subjected continuously to a loosening nip, and there is no slippage in the wound roll. Thus, the static tests provide a measure of rolling resistance without any slippage occurring in the wound roll.

For both the static and dynamic tests, the rolling resistance is measured as the difference between the bearing resistance and the total resistance offered to the nip to turn the roll. As the nip is subjected to different loads, the bearing resistance is evaluated for the changing loads. For the dynamic tests, the 6 and the 8 inch diameter nip rolls rotated with an angular velocity of 20 rpm and the 2.5 inch diameter nip rotated at angular velocity of 40 rpm.

Recall that the objectives of the torque tests was to measure the rolling resistance encountered by the nip, and, to correlate the experimental values to Greenwood et al's model for rolling resistance. To use Greenwood et al's form of the rolling resistance equation, the half width of contact between the nip and the wound roll is experimentally determined by using magnified photographs of the nip wound-roll interface, prior to subjecting the rolls to the torque tests. The hysteresis loss factor 'α' is also measured experimentally.

Discussion of the Experimental Results

Fundamentally, the models developed by Greenwood et al do not account for inter-layer slippage. In spite of this, the form of the equation developed by Greenwood et al, can be used to predict rolling resistance torques with reasonable accuracy.

The dynamic torque tests, produce higher torques than those predicted by Greenwood et al's equations (27) and (29), whenever large amounts of slippage occur. As the dynamic torque experiments progress, it is easy to visually observe a continuous re-distribution of the nip load over a smaller width of the wound roll. This leads to an increase in the nip load per unit length. There is also a continuous change in the half width of contact during this phase. This is a result of continuous change in wound roll pressure distribution due to slippage. In cases, where there is excessive slippage, induced by the nip, the experimental value from the dynamic torque test is represented by an average of gradually increasing torque values.

The 27 rolls that were used in the dynamic torque tests came from different parent rolls and the physical properties of the rolls are different. TABLE 14 lists the physical properties of the rolls.

TABLE 14. Physical properties of the parent rolls used in the Dynamic Torque tests

Parent Roll ID (Thickness)	E_r	'α'	E_t (psi) (Average)
1 (3 mils)	$297.45 + 39.39*(\sigma) - 0.206*(\sigma^2) + 0.0005*(\sigma^3)$	0.33	200000
2 (3 mils)	$229.85 + 36.74*(\sigma) - 0.219(\sigma^2) + 0.0006*(\sigma^3)$	0.38	200000
3 (3 mils)	$263.89 + 38.23*(\sigma) - 0.255*(\sigma^2) + 0.0007*(\sigma^3)$	0.37	200000
4 (3 mils)	$244.85 + 34.64*(\sigma) - 0.232*(\sigma^2) + 0.0007*(\sigma^3)$	0.36	200000
5 (3 mils)	$267.17 + 40.62*(\sigma) - 0.256*(\sigma^2) + 0.0007*(\sigma^3)$	0.35	200000
6 (3 mils)	$195.80 + 30.26*(\sigma) - 0.166*(\sigma^2) + 0.0005*(\sigma^3)$	0.39	200000
7 (3 mils)	$247.59 + 40.52*(\sigma) - 0.246*(\sigma^2) + 0.0007*(\sigma^3)$	0.35	200000
8 (2.5 mils)	$277.38 + 43.34*(\sigma) - 0.361*(\sigma^2) + 0.0013*(\sigma^3)$	0.32	380000
N1 (2 mils)	$168.02 + 31.46*(\sigma) - 0.212*(\sigma^2) + 0.0007*(\sigma^3)$	0.33	390000
N2 (2.2 mils)	$159.96 + 30.05*(\sigma) - 0.153*(\sigma^2) + 0.0004*(\sigma^3)$	0.35	390000
N3 (2.5 mils)	$195.21 + 35.39*(\sigma) - 0.264*(\sigma^2) + 0.001*(\sigma^3)$	0.33	380000
N4 (2 mils)	$179.78 + 29.59*(\sigma) - 0.181*(\sigma^2) + 0.0006*(\sigma^3)$	0.34	380000
N5 (2 mils)	$163.15 + 30.17*(\sigma) - 0.189*(\sigma^2) + 0.0006*(\sigma^3)$	0.33	380000
N6 (2.5 mils)	$213.49 + 35.64*(\sigma) - 0.276*(\sigma^2) + 0.0011*(\sigma^3)$	0.33	250000
N10 (3 mils)	$246.42 + 42.53*(\sigma) - 0.337*(\sigma^2) + 0.0011*(\sigma^3)$	0.35	250000

The results are arranged, such that the rolling resistance torques from the dynamic torque tests, are compared with two theoretical forms of Greenwood et al's equations, (39) and (41). In some cases, where excessive slippage destroyed the rolls completely, correction has been made to the theoretical form of the equation, by considering the distribution of

the final nip load profile and the final half-width of contact. In such cases, the individual points have been captioned to reflect this information. The error bars in the experimental data show the standard deviation of the experimental data over the average. The data are presented in sets of increasing order of wound on tensions, and within each set, with increasing order of nip roll diameters. The static test results are compared with the form of Greenwood et al's equation with a scale factor of 3.5, equation (41).

Nip diameter 2.5 inches, wound on tension 0.3 pli, Figures 58 a, b, c, d, e, f.

The dynamic torque tests show good correlation to Greenwood et al's equation with a scale factor of 3.5, at the 5 and 10 pli nip loads, Figure 58a. The theoretical data fall within one standard deviation of the experimental data. At the lowest nip load, it is not possible to resolve the low torque values measured. At the highest nip load, Figure 58b, the corrected theoretical value from equation (41), over-predicts the experimental value. The static torque measurements, Figure 58c, for an identical nip diameter and wound-on tension profile, show poor correlation with experimental. Figures 58d, e&f, show the slippage induced in the rolls by the nip, during the dynamic torque tests. When viewed together, the dynamic and the static torque tests show that the modified form of Greenwood et al's equation (41), provides a reasonable estimate of the rolling resistance torque.

Nip diameter 6 inches, wound on tension 0.3 pli, Figures 59 a, b, c, d, e, f.

The dynamic torque test values, Figure 59a, show reasonable correlation with equation (41) at a nip load of 5 pli. At the highest nip load of 10 pli, the correlation is poor, as excessive inter-layer slippage has occurred in the roll. When equation (41) is corrected for slippage, there is good correlation at the 5 pli nip load, Figure 59b, but, at the

maximum nip load there is poor correlation still. The static torque tests, Figure 59c, on the other hand, show a better correlation with equation (41) at both the 5 pli and the 10 pli nip load case. The static tests indicate that equation (41) gives a reasonable lower of the torque input to the roll. Figures 59d, e&f, all show slippage in the rolls in a loosening direction.

Nip diameter 8 inches, wound on tension 0.3 pli, Figures 60a, b, c, d, e, f.

The dynamic torque values at nip loads of 5 and 10 pli are higher than the values predicted by equation (41) Figure60a. But, these points seem to correlate well, when modifications are made to equation (41), to account for inter layer slippage, Figure 60b. Recall, that the modifications were based on the final half width and final nip load measurements on the wound roll. The static case, Figure 60c, has poor correlation at a nip load of 5 pli, but good correlation at the highest nip load of 10 pli. When the static and the dynamic tests are viewed together, equation (41) provides a reasonable estimate of the rolling resistance torque. Figures 60d, e&f, all show loosening slippage in the wound roll.

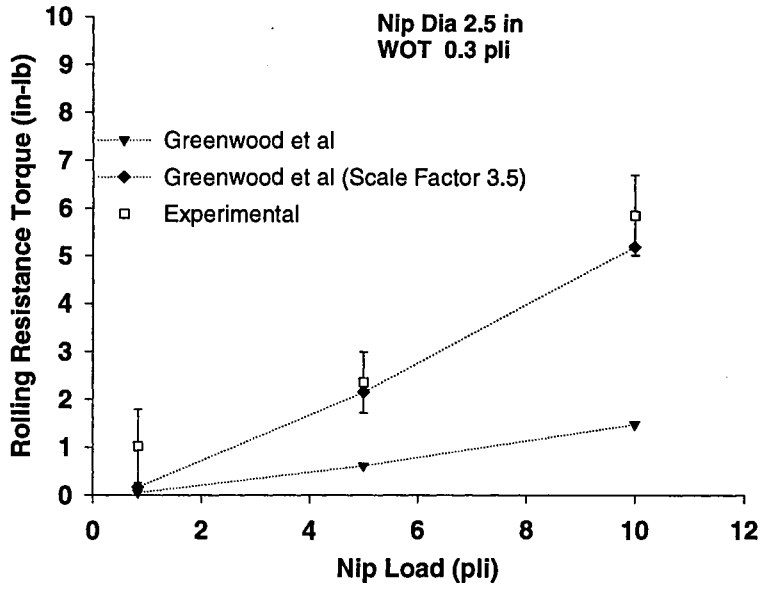

Figure 58a. Comparison between Dynamic Torque Test values and Equations (39) and (41). The Nip diameter is 2.5 inches and the W.O.T for the rolls is 0.3 pli.

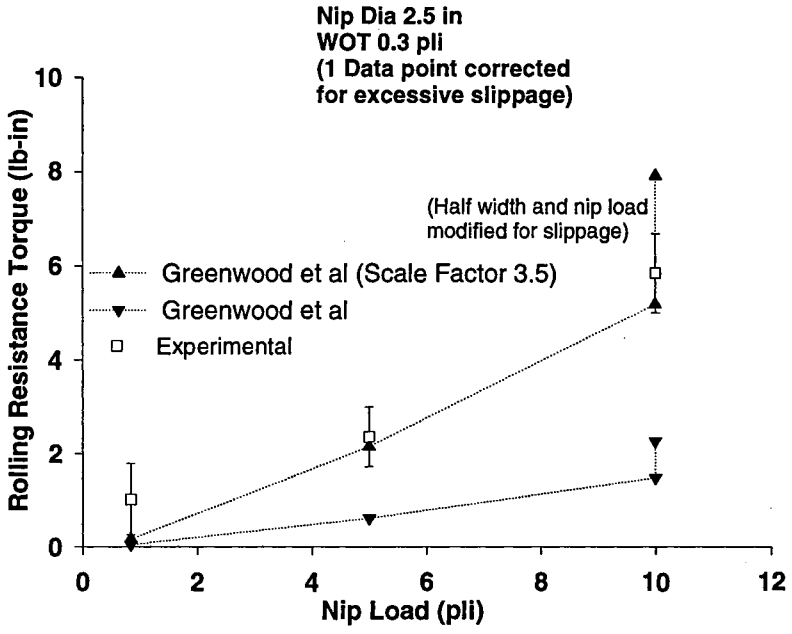

Figure 58b. Dynamic Torque test values corrected for slippage. The Nip diameter is 2.5 inches and the W.O.T for the rolls is 0.3 pli.

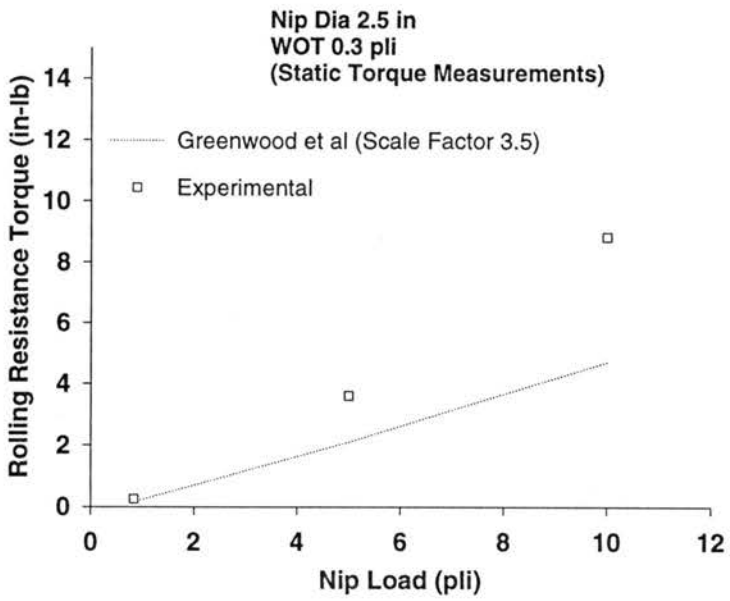

Figure 58c. Comparison between Static Torque Test values and Equation (41). The Nip diameter is 2.5 inches and the W.O.T for the rolls is 0.3 pli.

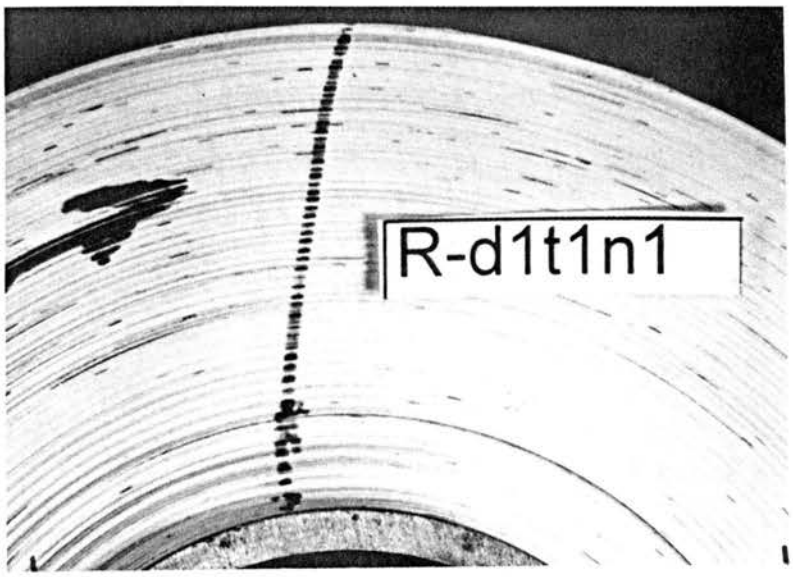

Figure 58d. Photograph of the wound roll showing slippage after the Dynamic Torque test. The Nip diameter is 2.5 inches and the W.O.T for the roll is 0.3 pli. The parent roll id. is 4, the diameter of the wound roll is 7.62 inches, the Half width of contact is 0.094 inches and the nip load is 0.83 pli.

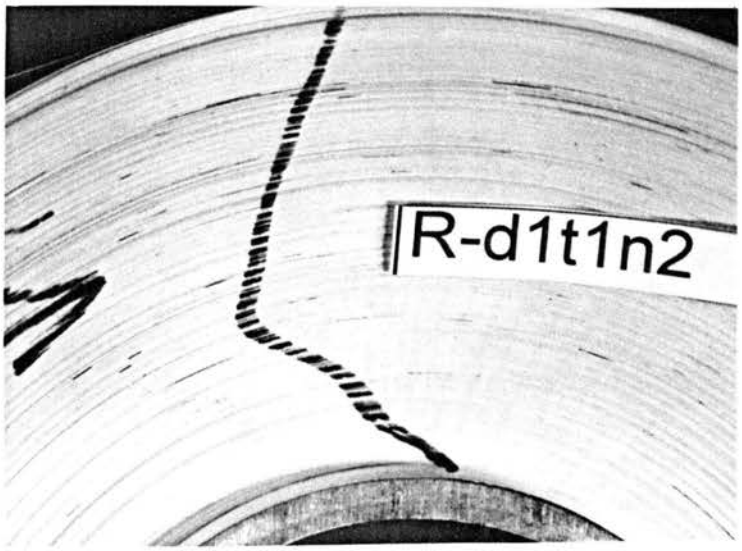

Figure 58e. Photograph of the wound roll showing slippage after the Dynamic Torque test. The Nip diameter is 2.5 inches and the W.O.T for the roll is 0.3 pli. The parent roll id. is 4, the diameter of the wound roll is 7.49 inches, the Half width of contact is 0.203 inches and the nip load is 5 pli.

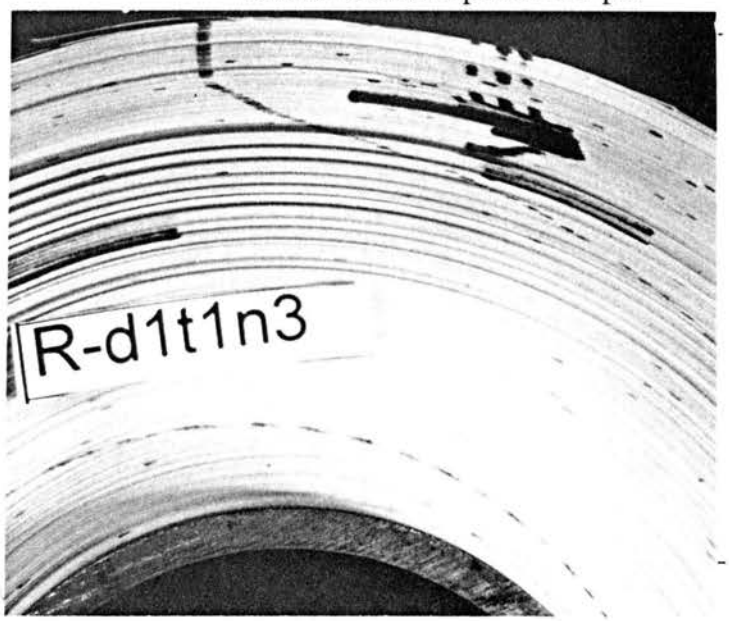

Figure 58f. Photograph of the wound roll showing slippage after the Dynamic Torque test. The Nip diameter is 2.5 inches and the W.O.T for the roll is 0.3 pli. The parent roll id. is 6, the diameter of the wound roll is 7.62 inches, the Half width of contact is 0.227 inches and the nip load is 10 pli.

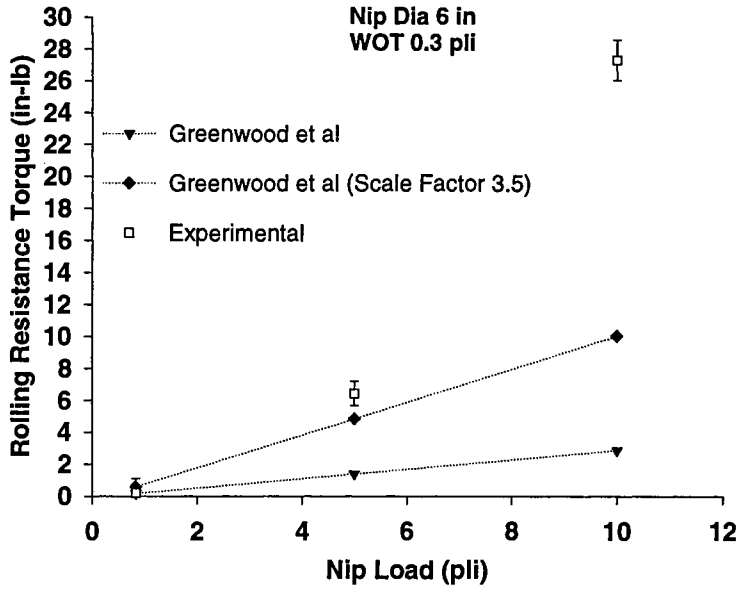

Figure 59a. Comparison between Dynamic Torque Test values and Equations (39) and (41). The Nip diameter is 6 inches and the W.O.T for the rolls is 0.3 pli.

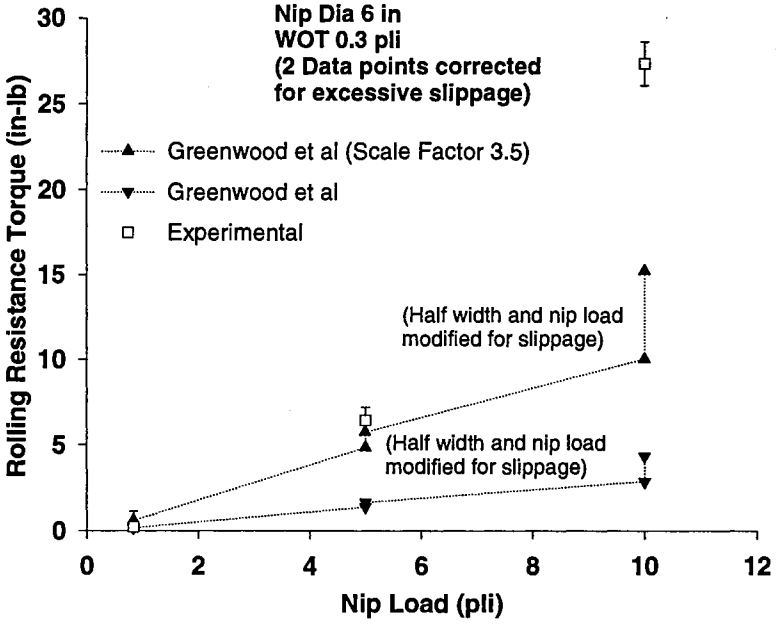

Figure 59b. Dynamic Torque test values corrected for slippage. The Nip diameter is 6 inches and the W.O.T for the rolls is 0.3 pli.

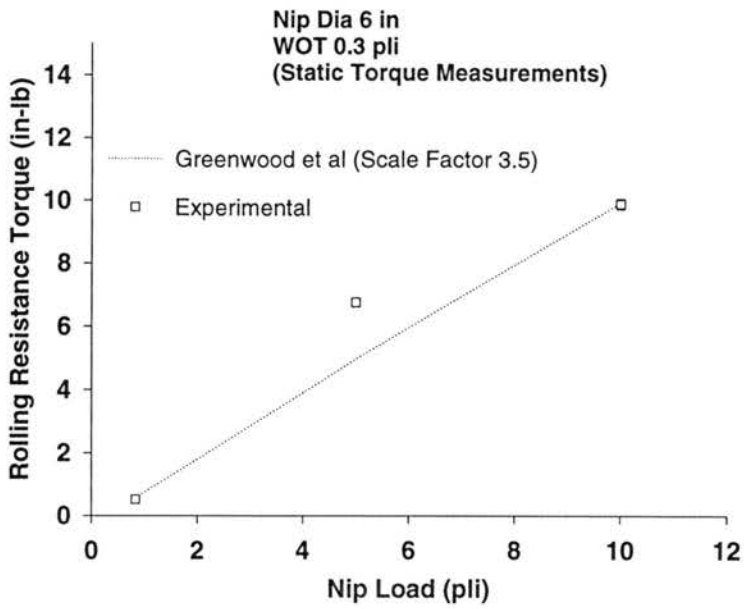

Figure 59c. Comparison between Static Torque Test values and Equation (41). The Nip diameter is 6 inches and the W.O.T for the rolls is 0.3 pli.

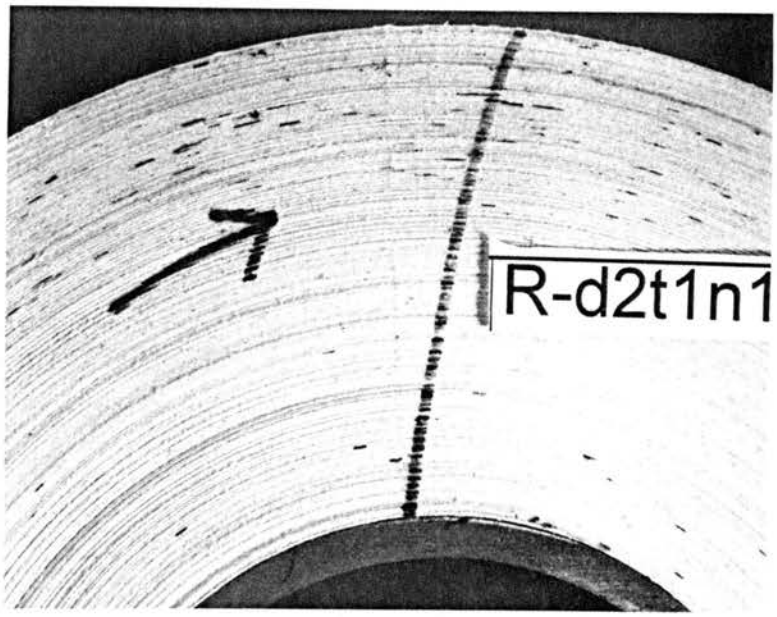

Figure 59d. Photograph of the wound roll showing slippage after the Dynamic Torque test. The Nip diameter is 6 inches and the W.O.T for the roll is 0.3 pli. The parent roll id. is 5, the diameter of the wound roll is 7.65 inches, the Half width of contact is 0.242 inches and the nip load is 0.83 pli.

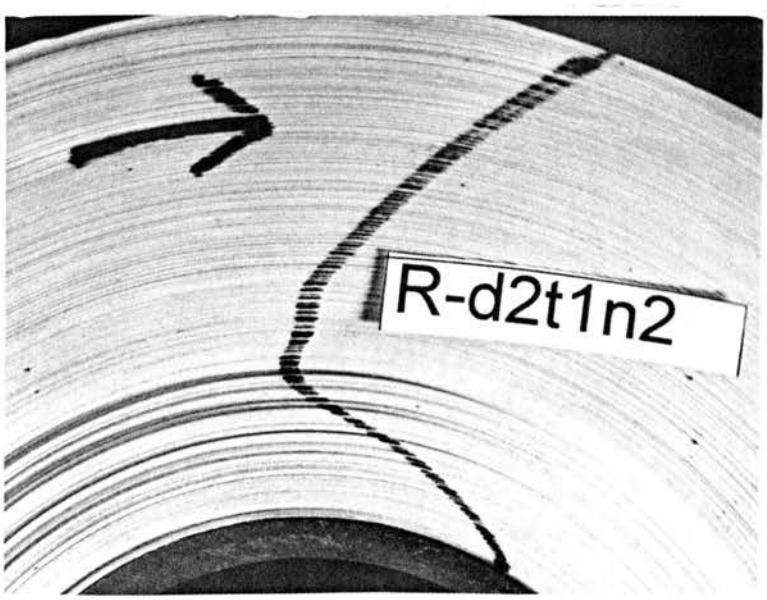

Figure 59e. Photograph of the wound roll showing slippage after the Dynamic Torque test. The Nip diameter is 6 inches and the W.O.T for the roll is 0.3 pli. The parent roll id. is 7, the diameter of the wound roll is 7.88 inches, the Half width of contact is 0.359 inches and the nip load is 5 pli.

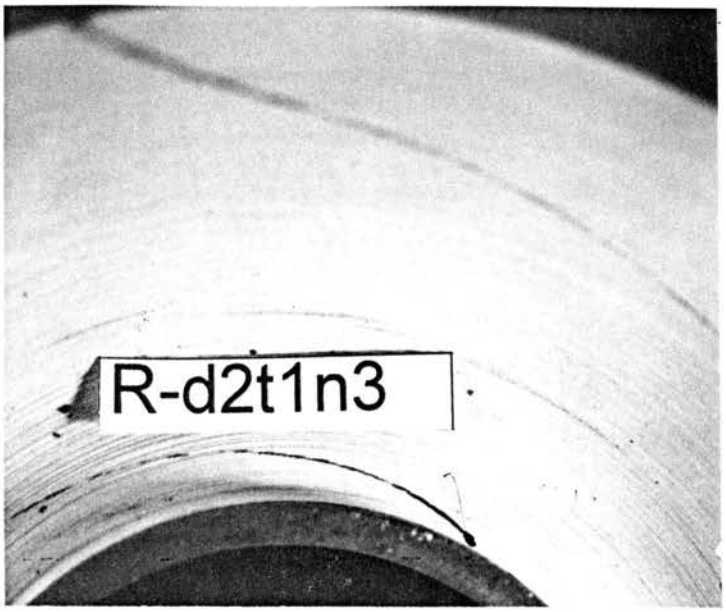

Figure59f. Photograph of the wound roll showing slippage after the Dynamic Torque test. The Nip diameter is 6 inches and the W.O.T for the roll is 0.3 pli. The parent roll id. is 6, the diameter of the wound roll is 7.48 inches, the Half width of contact is 0.359 inches and the nip load is 10 pli.

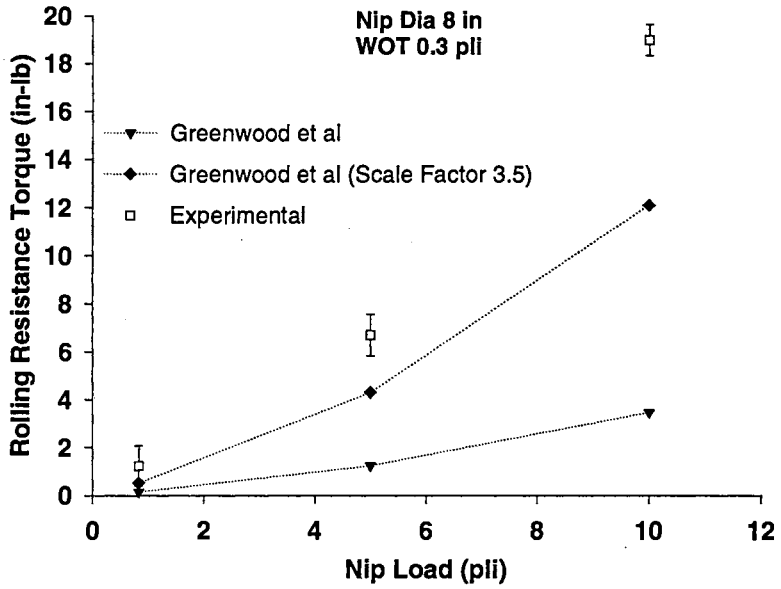

Figure 60a. Comparison between Dynamic Torque Test values and Equations (39) and (41). The Nip diameter is 8 inches and the W.O.T for the rolls is 0.3 pli.

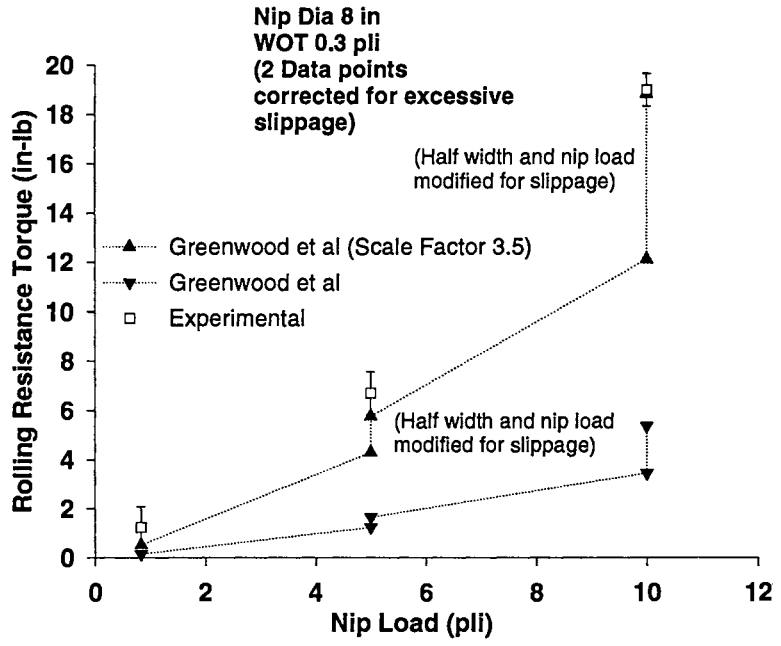

Figure 60b. Dynamic Torque test values corrected for slippage. The Nip diameter is 8 inches and the W.O.T for the rolls is 0.3 pli.

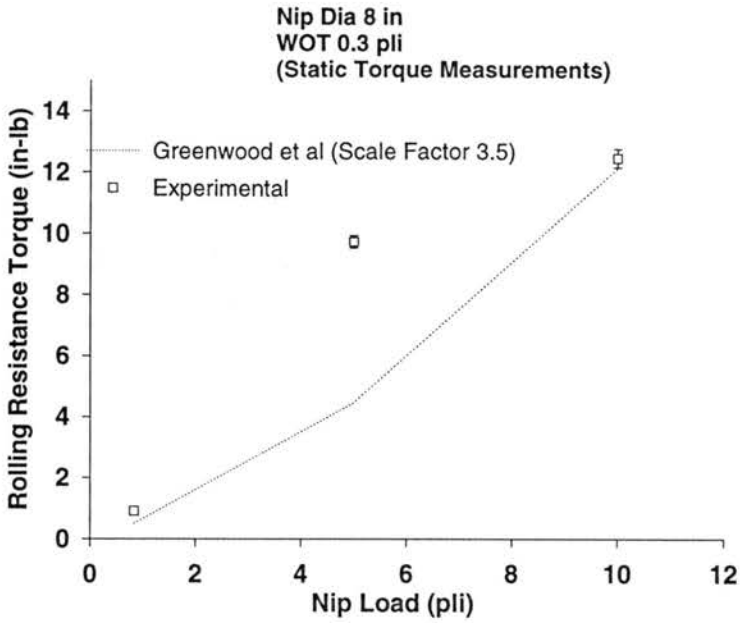

Figure 60c. Comparison between Static Torque Test values and Equation (41). The Nip diameter is 8 inches and the W.O.T for the rolls is 0.3 pli.

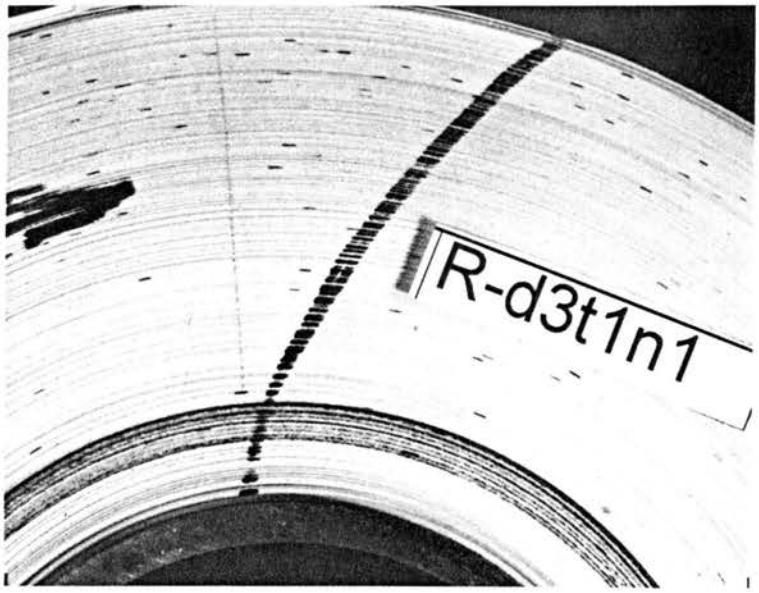

Figure 60d. Photograph of the wound roll showing slippage after the Dynamic Torque test. The Nip diameter is 8 inches and the W.O.T for the roll is 0.3 pli. The parent roll id. is 3, the diameter of the wound roll is 7.85 inches, the Half width of contact is 0.188 inches and the nip load is 0.83 pli.

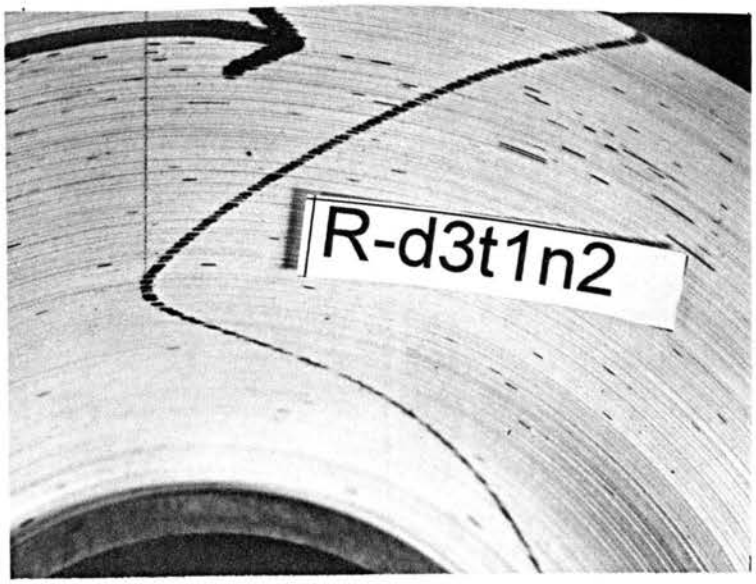

Figure 60e. Photograph of the wound roll showing slippage after the Dynamic Torque test. The Nip diameter is 8 inches and the W.O.T for the roll is 0.3 pli. The parent roll id. is 7, the diameter of the wound roll is 8.01 inches, the Half width of contact is 0.281 inches and the nip load is 5 pli.

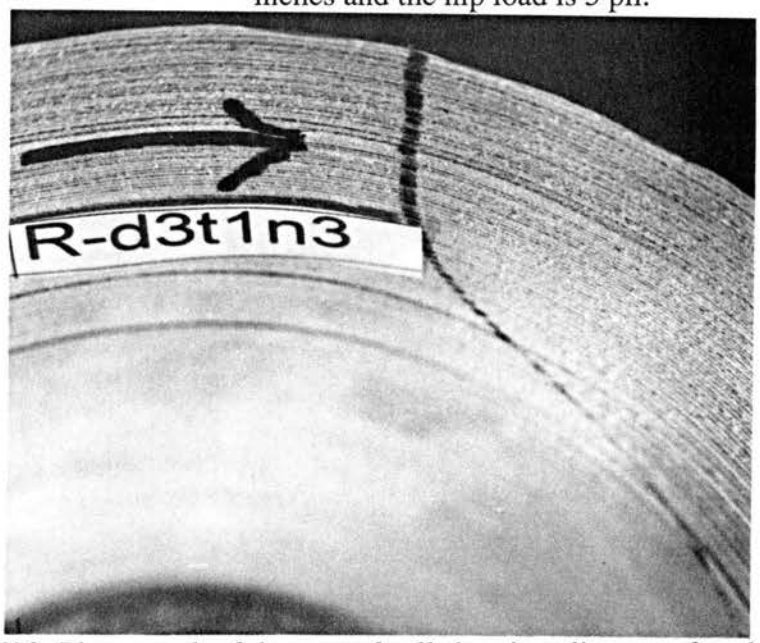

Figure 60f. Photograph of the wound roll showing slippage after the Dynamic Torque test. The Nip diameter is 8 inches and the W.O.T for the roll is 0.3 pli. The parent roll id. is 5, the diameter of the wound roll is 7.68 inches, the Half width of contact is 0.383 inches and the nip load is 10 pli.

In observing general trends for the cases presented above, the rolling resistance increases, with an increase in nip diameters for the rolls wound with the same values of wound on tensions. This appears contradictory with what would be predicted by equation (41), based on a superficial observation. But, upon closer scrutiny, as the nip diameter increases, the half width, also increases. This is responsible for the increased rolling resistance. Another trend is that the rolling resistance torques increase with increasing nip loads. This is expected, as Greenwood et al's equation would predict the same.

Nip diameter 2.5 in, wound on tension 0.67 pli, Figures 61a, b, c, d, e.

The dynamic torque test data indicate a good correlation with equation (41), at a nip load of 10 pli. The absence of an experimental value at the 5 pli nip load was due to an error in the data acquisition system. All the rolls used in this set, were wound relatively tighter than the previous cases discussed. The static test results, Figure 61b, show reasonable correlation with equation (41). Figures 61c,d&e, show interesting trends. For the case of nip diameter 2.5 in and nip load of 0.83 pli, there is no wound roll slippage. For the other two cases, there is wound roll slippage. Note that the slippage did not cause considerable damage to the rolls thus render the rolls useless.

Nip diameter 6 in, wound on tension 0.67 pli, Figures 62a, b, c, d, e.

The dynamic torque tests, Figure 62a, show good correlation at 5 pli nip load but poor correlation at 10 pli nip load. The static tests, however, indicate a reasonable correlation at 5 pli and good correlation at 10 pli nip load. When viewed together, the static and the dynamic tests show a reasonable correlation with equation (41). Figures 62c, d&e, show the rolls after being subjected to the dynamic torque tests. For the case where the nip load

was 0.83 pli, the roll did not slip. There is slippage in the other two cases, and for the case where the nip load is 10 pli, there is starring defect in the core region.

Nip diameter 8 in, wound on tension 0.67 pli, Figures 63a, b, c, d, e, f.

The dynamic torque readings correlate fairly at the 5 pli nip load and at 10 pli nip load the correlation is poor, Figure 63a. The poor correlation is due to excessive slippage at the highest nip load. When corrected for slippage, the value predicted by equation (41) correlates better with the dynamic torque value, Figure 63b. The static torque test results, Figure 63c, shows a better correlation at the highest nip load of 10 pli, (prior to slippage). At the 5 pli nip load the static torque value shows poor correlation. Viewed together, the static and dynamic torque tests, show reasonable correlation with equation (41). Figures 63d, e&f show the slippage in the rolls after being subjected to the dynamic torque tests.

For the rolls wound with the same values of the wound on tension (0.67 pli), an increase in nip diameter from 2.5 to 6 inches, shows an increase in rolling resistance torque. But an increase in diameter, from 6 to 8 inches, does not show a marked increase in rolling resistance torque. In fact, there appears to be a saturation in rolling resistance torque. Another trend that is visible, is that an increase in nip load leads to an increase in rolling resistance torque. This trend is expected, as, equation (41) would predict the same. Doubling the wound on tension from 0.3 to 0.6 pli reduced the extent of slippage and damage to the wound rolls.

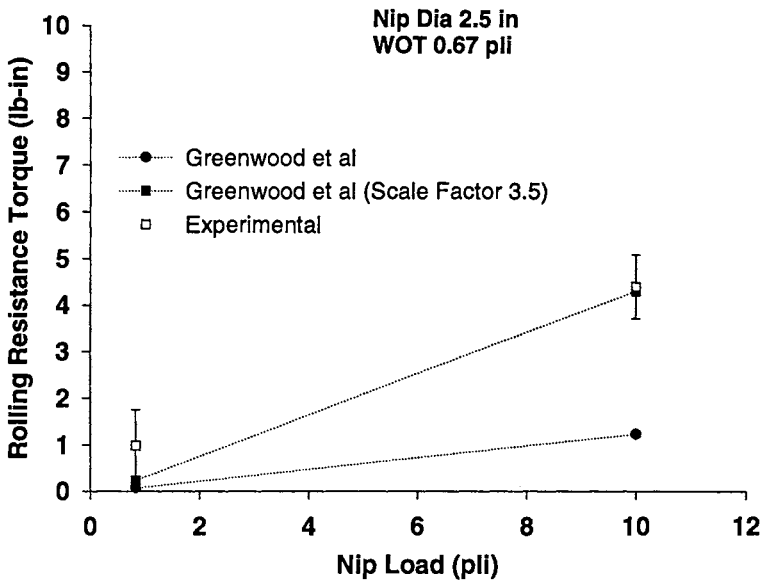

Figure 61a. Comparison between Dynamic Torque Test values and Equations (39) and (41). The Nip diameter is 2.5 inches and the W.O.T for the rolls is 0.67 pli.

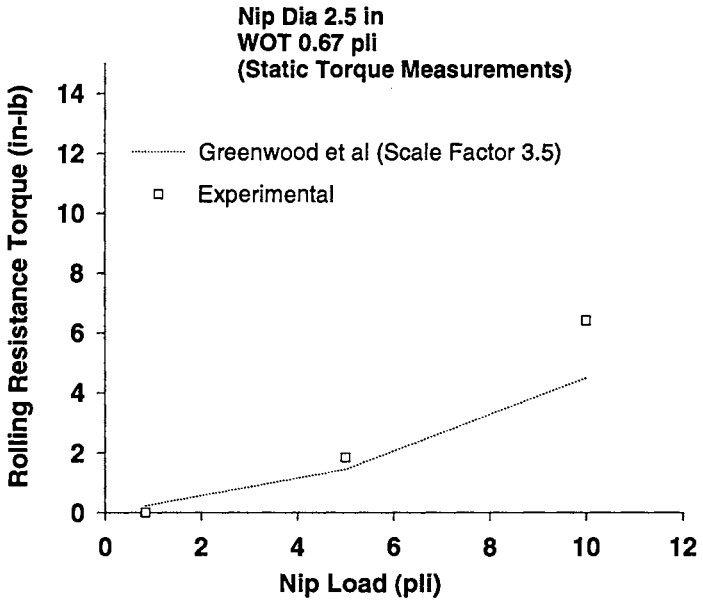

Figure 61b. Comparison between Static Torque Test values and Equation (41). The Nip diameter is 2.5 inches and the W.O.T for the rolls is 0.67 pli.

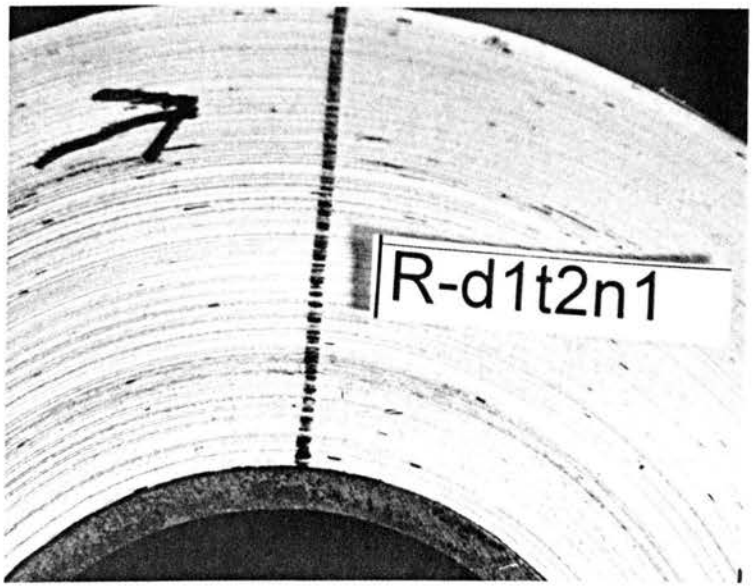

Figure 61c. Photograph of the wound roll showing slippage after the Dynamic Torque test. The Nip diameter is 2.5 inches and the W.O.T for the roll is 0.67 pli. The parent roll id. is 5, the diameter of the wound roll is 7.54 inches, the Half width of contact is 0.133 inches and the nip load is 0.83 pli.

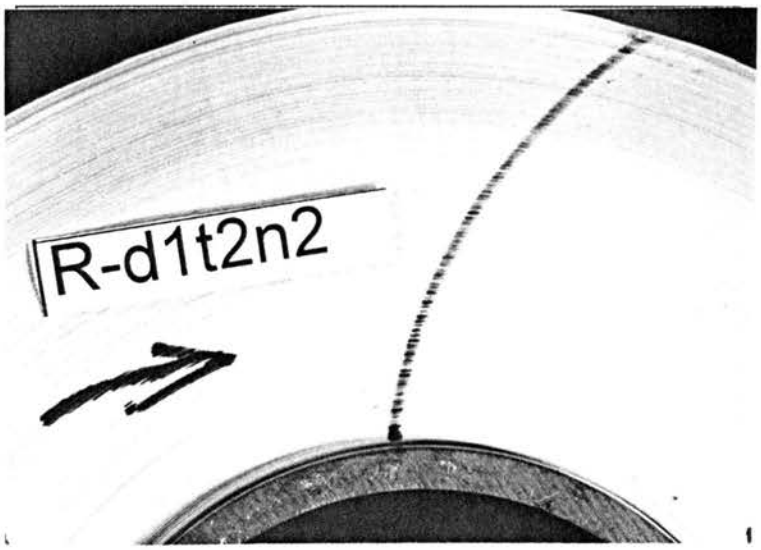

Figure 61d. Photograph of the wound roll showing slippage after the Dynamic Torque test. The Nip diameter is 2.5 inches and the W.O.T for the roll is 0.67 pli. The parent roll id. is N4, the diameter of the wound roll is 7.36 inches, the Half width of contact is 0.141 inches and the nip load is 5 pli.

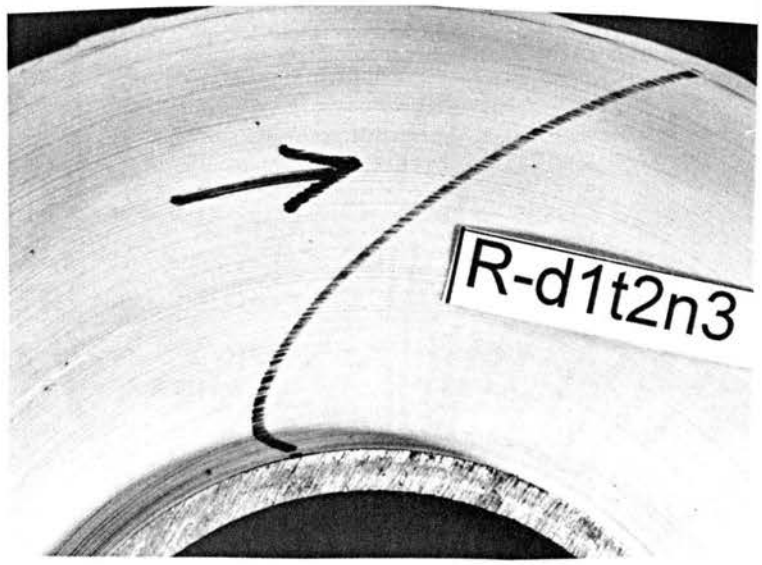

Figure 61e. Photograph of the wound roll showing slippage after the Dynamic Torque test. The Nip diameter is 2.5 inches and the W.O.T for the roll is 0.67 pli. The parent roll id. is N5, the diameter of the wound roll is 7.37 inches, the Half width of contact is 0.219 inches and the nip load is 10 pli.

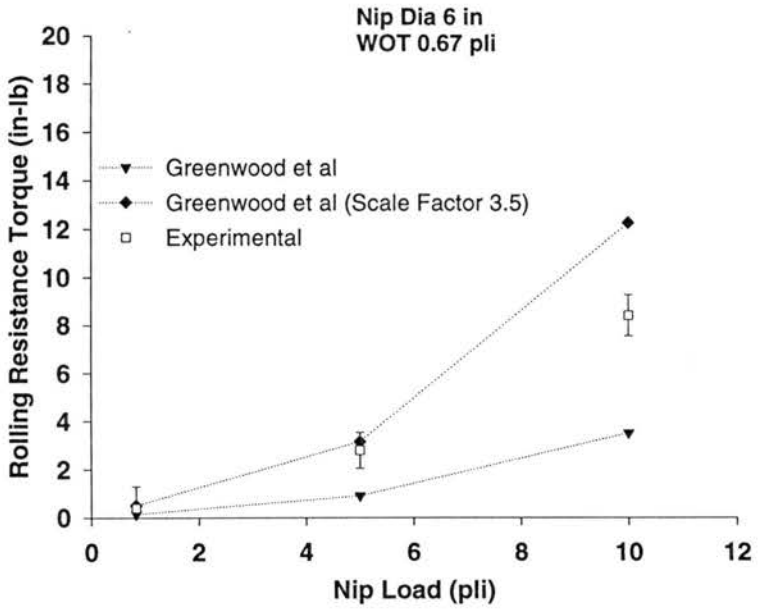

Figure 62a. Comparison between Dynamic Torque Test values and Equations (39) and (41). The Nip diameter is 6 inches and the W.O.T for the rolls is 0.67 pli.

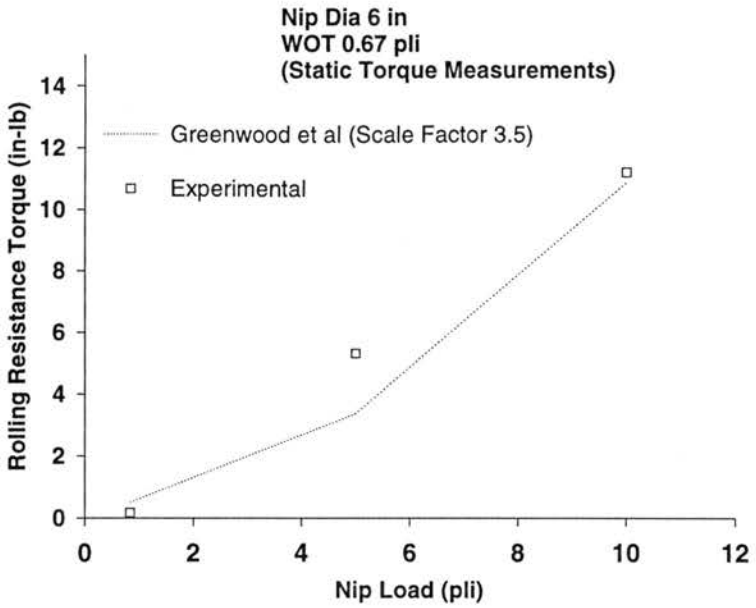

Figure 62b. Comparison between Static Torque Test values and Equation (41). The Nip diameter is 6 inches and the W.O.T for the rolls is 0.67 pli.

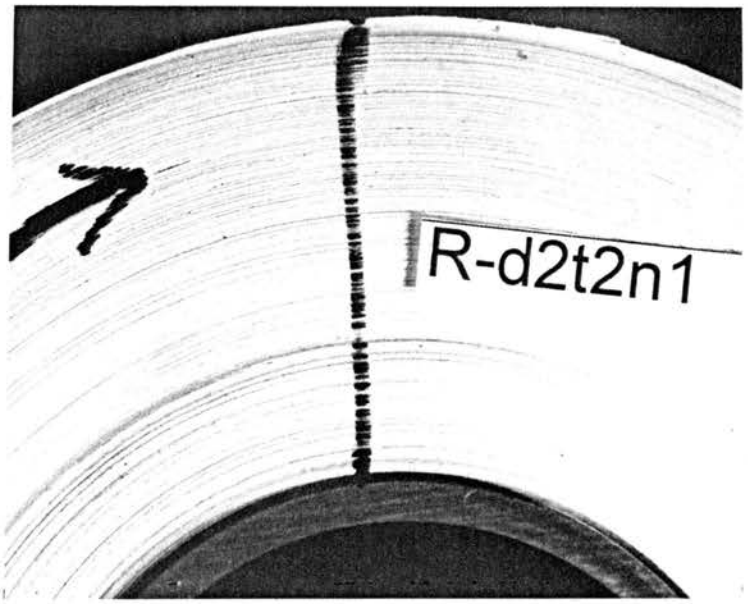

Figure 62c. Photograph of the wound roll showing slippage after the Dynamic Torque test. The Nip diameter is 6 inches and the W.O.T for the roll is 0.67 pli. The parent roll id. is 1, the diameter of the wound roll is 7.51 inches, the Half width of contact is 0.219 inches and the nip load is 0.83 pli.

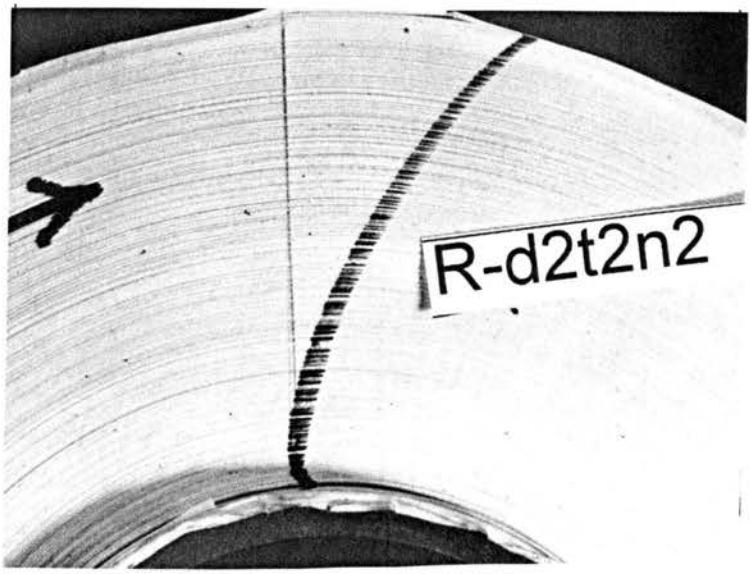

Figure 62d. Photograph of the wound roll showing slippage after the Dynamic Torque test. The Nip diameter is 6 inches and the W.O.T for the roll is 0.67 pli. The parent roll id. is 7, the diameter of the wound roll is 7.65 inches, the Half width of contact is 0.242 inches and the nip load is 5 pli.

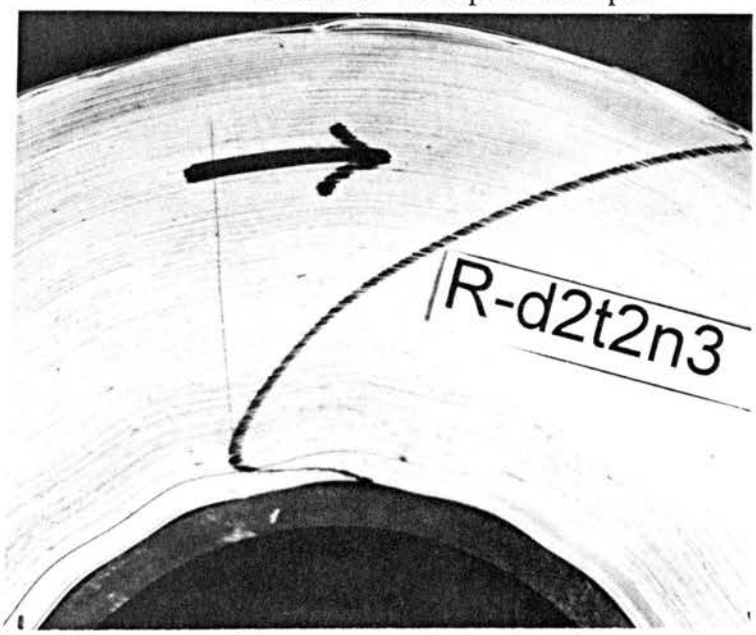

Figure 62e. Photograph of the wound roll showing slippage after the Dynamic Torque test. The Nip diameter is 6 inches and the W.O.T for the roll is 0.67 pli. The parent roll id. is N1, the diameter of the wound roll is 7.32 inches, the Half width of contact is 0.391 inches and the nip load is 10 pli.

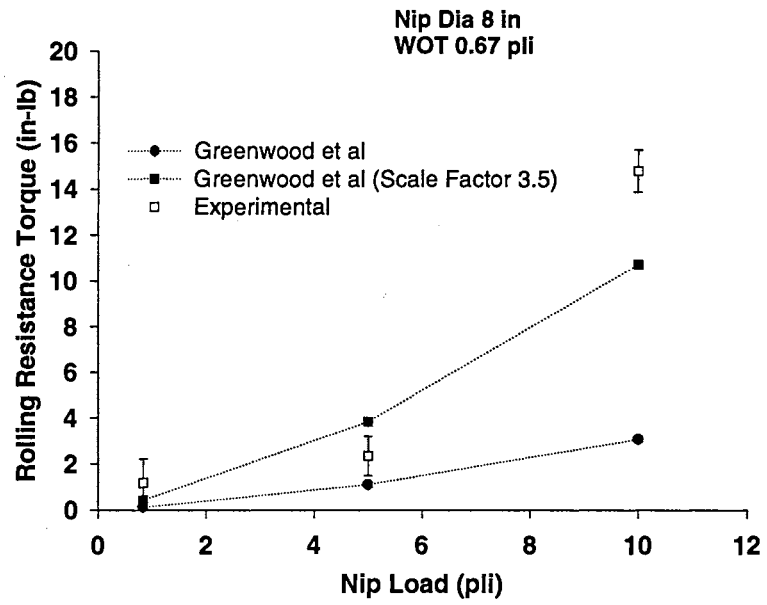

Figure 63a. Comparison between Dynamic Torque Test values and Equations (39) and (41). The Nip diameter is 8 inches and the W.O.T for the rolls is 0.67 pli.

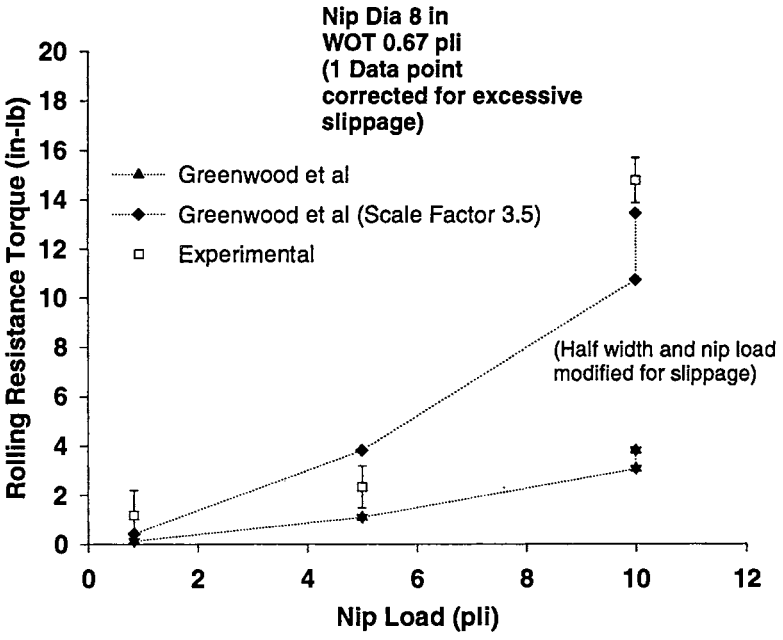

Figure 63b. Dynamic Torque test values corrected for slippage. The Nip diameter is 8 inches and the W.O.T for the rolls is 0.67 pli.

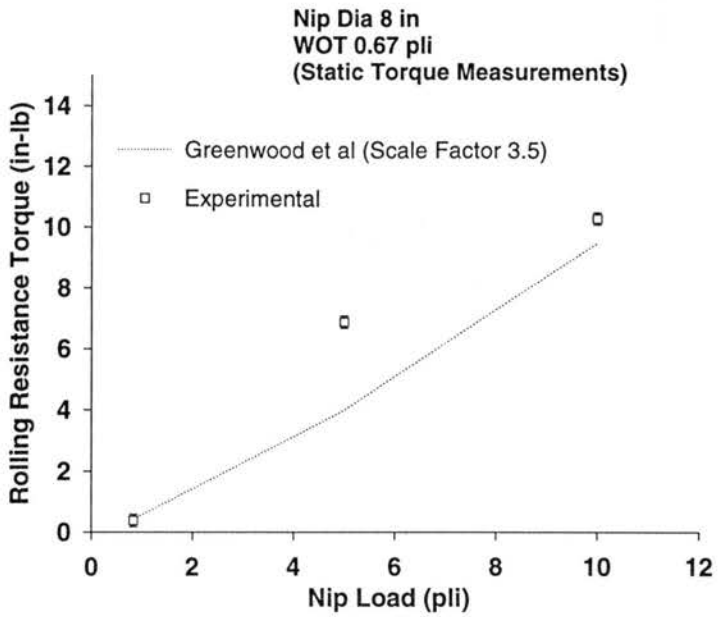

Figure 63c. Comparison between Static Torque Test values and Equation (41). The Nip diameter is 8 inches and the W.O.T for the rolls is 0.67 pli.

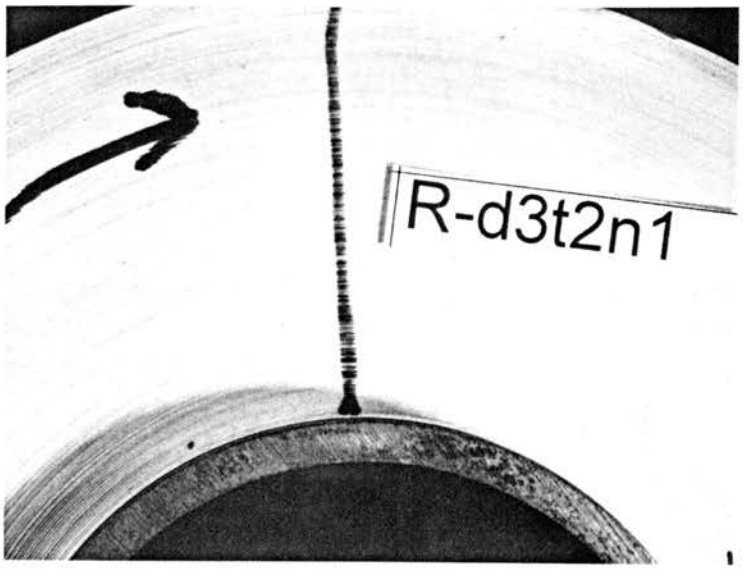

Figure 63d. Photograph of the wound roll showing slippage after the Dynamic Torque test. The Nip diameter is 8 inches and the W.O.T for the roll is 0.67 pli. The parent roll id. is N2, the diameter of the wound roll is 7.34 inches, the Half width of contact is 0.156 inches and the nip load is 0.83 pli.

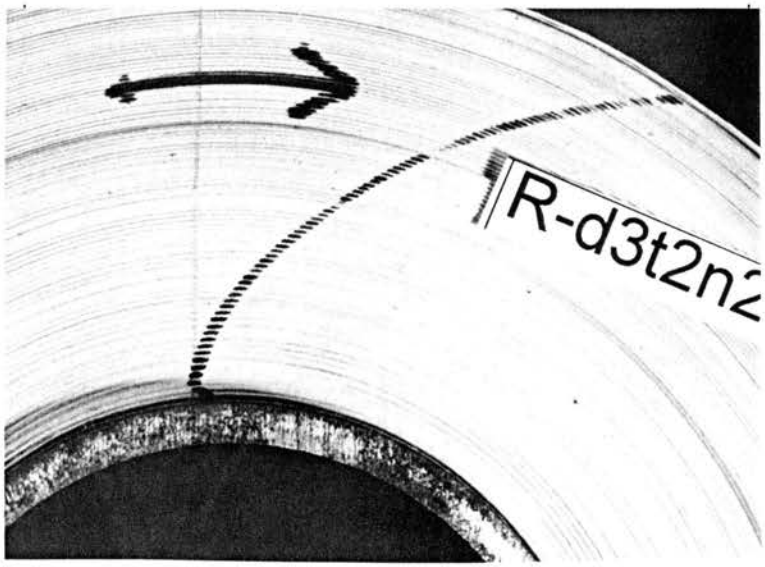

Figure 63e. Photograph of the wound roll showing slippage after the Dynamic Torque test. The Nip diameter is 8 inches and the W.O.T for the roll is 0.67 pli. The parent roll id. is N3, the diameter of the wound roll is 7.30 inches, the Half width of contact is 0.25 inches and the nip load is 5 pli.

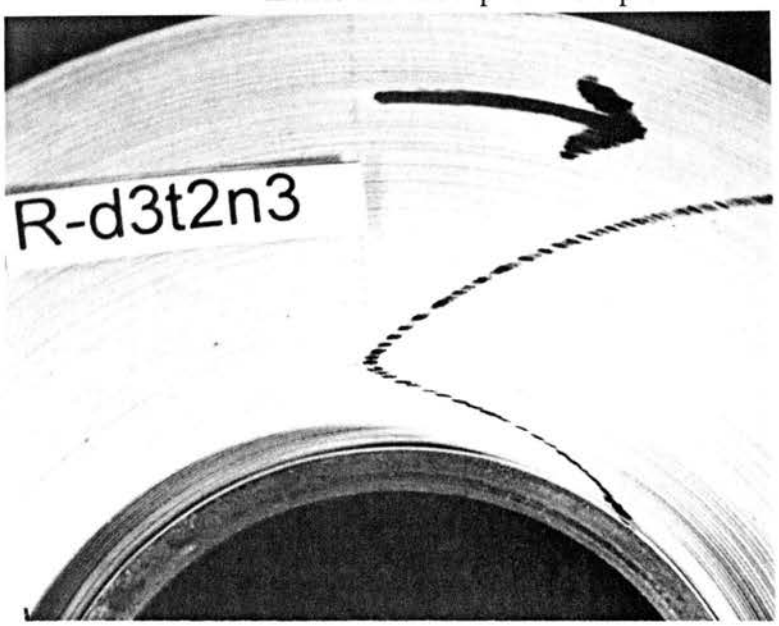

Figure 63f. Photograph of the wound roll showing slippage after the Dynamic Torque test. The Nip diameter is 8 inches and the W.O.T for the roll is 0.67 pli. The parent roll id. is N3, the diameter of the wound roll is 7.31 inches, the Half width of contact is 0.297 inches and the nip load is 10 pli.

Nip diameter 2.5 inches, wound on tension 1.3 pli, Figures 64a, b, c, d, e.

The dynamic torque test data has poor correlation at the highest nip load (10 pli). The dynamic torque test data is bounded by theoretical values generated equations (39) and (41). The static torque test data values, Figure 64b, have good correlation with equation (41). There is an increase in rolling resistance torque with increase in nip load. However, the magnitudes of the rolling resistance values, are much lower than the previous sets for the same nip diameter. In contrast with the rolls, wound at lower wound on tensions, and subjected to the same nip diameter of 2.5 inches, these rolls show a lesser amount of slippage. For the case of nip load of 0.83 pli, there is no slippage after the torque test. All the rolls maintained good structural integrity after the torque test, see Figures 64c, d&e.

Nip diameter 6 inches, wound on tension 1.3 pli, Figures 65a, b, c, d, e.

Equation (41) over predicts the rolling resistance torques, in comparison to the dynamic torque values, Figure 65a. The dynamic torque test data are bounded by theoretical values generated from equations (39) and (41). The static torque test data, Figure 65b, have good correlation with equation (41). Figures 65c, d&e show the rolls, and the associated slippage. For a nip load of 0.83 pli there is no slippage. The rolls that were subjected to nip loads of 5 and 10 pli show lesser extent of slippage. All the rolls maintained structural integrity after the torque tests.

Nip diameter 8 inches, wound on tension 1.3 pli, Figures 66a, b, c, d, e.

At a nip load of 10 pli, the dynamic torque test value, is bounded by equations (39) and (41), Figure 66a. The static test data, however, show good correlation with equation (41),

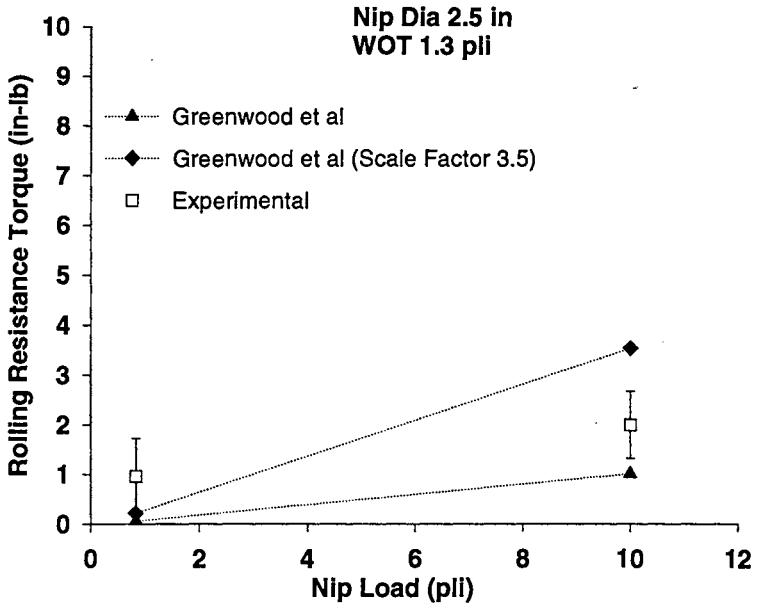

Figure 64a. Comparison between Dynamic Torque Test values and Equations (39) and (41). The Nip diameter is 2.5 inches and the W.O.T for the rolls is 1.3 pli.

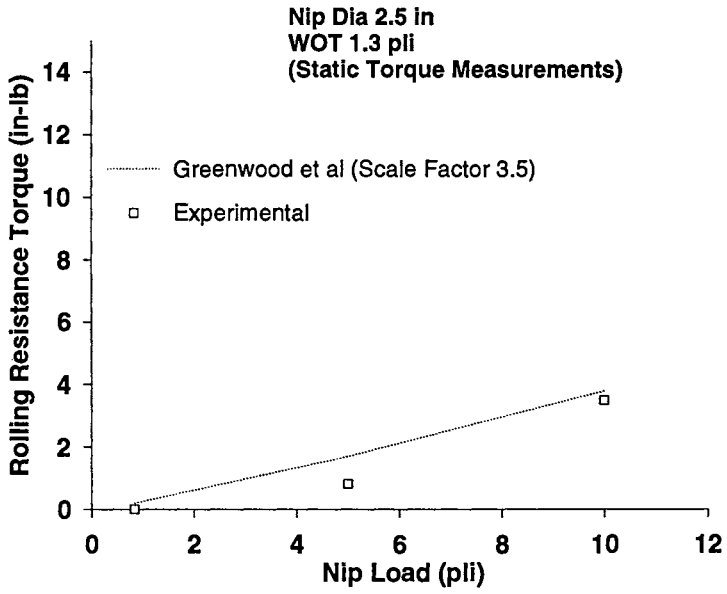

Figure 64b. Comparison between Static Torque Test values and Equation (41). The Nip diameter is 2.5 inches and the W.O.T for the rolls is 1.3 pli.

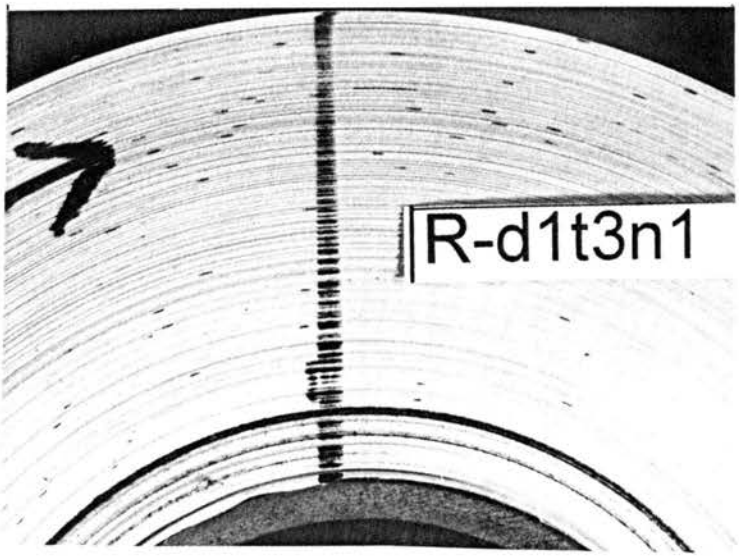

Figure 64c. Photograph of the wound roll showing slippage after the Dynamic Torque test. The Nip diameter is 2.5 inches and the W.O.T for the roll is 1.3 pli. The parent roll id. is 2, the diameter of the wound roll is 7.50 inches, the Half width of contact is 0.117 inches and the nip load is 0.83 pli.

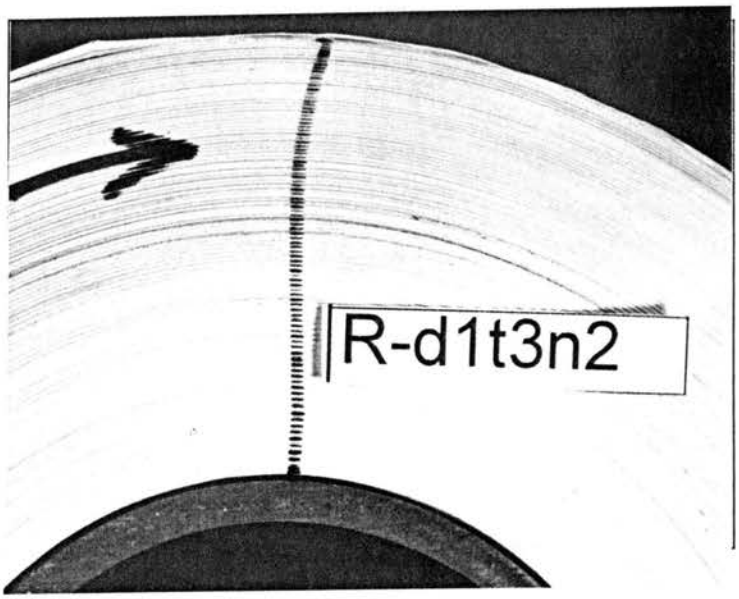

Figure 64d. Photograph of the wound roll showing slippage after the Dynamic Torque test. The Nip diameter is 2.5 inches and the W.O.T for the roll is 1.3 pli. The parent roll id. is N6, the diameter of the wound roll is 7.30 inches, the Half width of contact is 0.172 inches and the nip load is 5 pli.

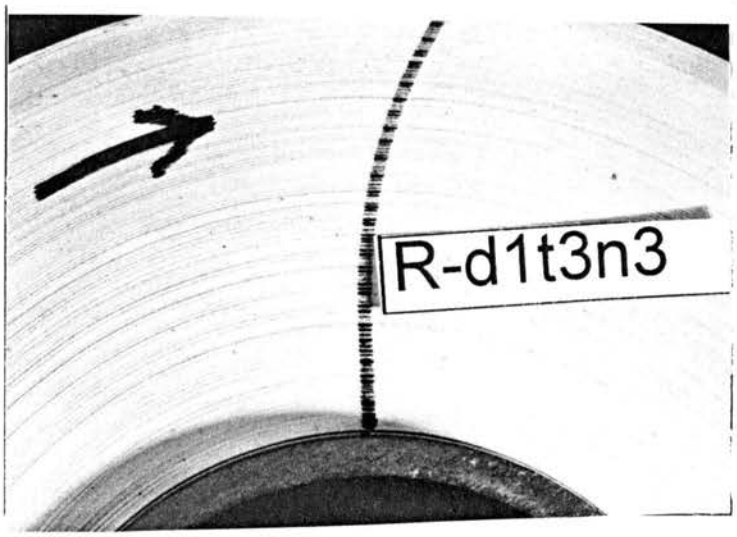

Figure 64e. Photograph of the wound roll showing slippage after the Dynamic Torque test. The Nip diameter is 2.5 inches and the W.O.T for the roll is 1.3 pli. The parent roll id. is N8, the diameter of the wound roll is 7.43 inches, the Half width of contact is 0.188 inches and the nip load is 10 pli.

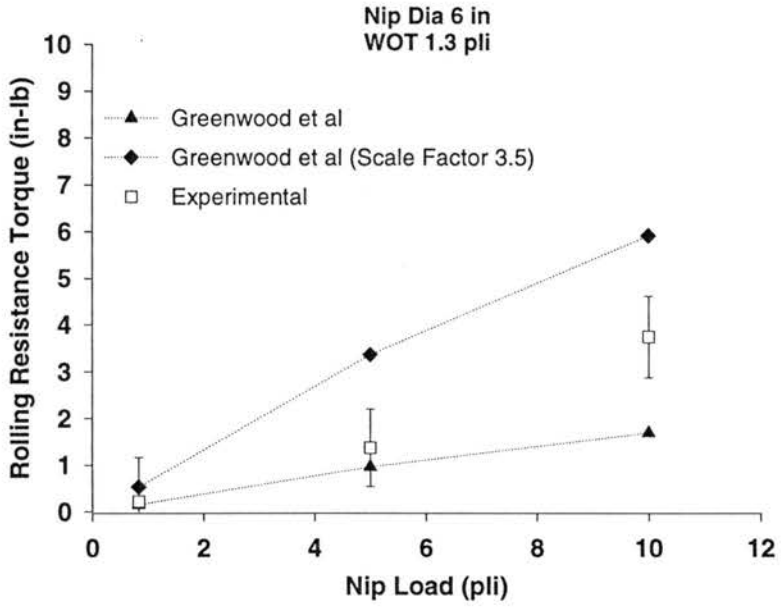

Figure 65a. Comparison between Dynamic Torque Test values and Equations (39) and (41). The Nip diameter is 6 inches and the W.O.T for the rolls is 1.3 pli.

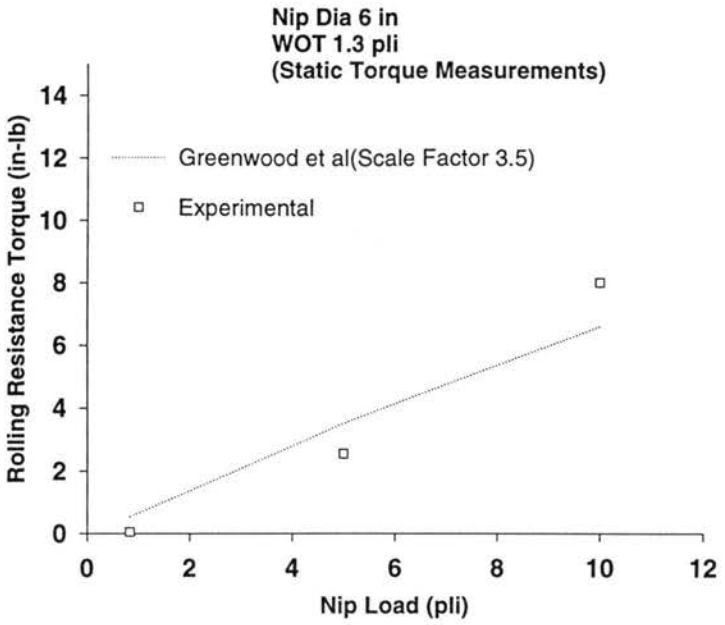

Figure 65b. Comparison between Static Torque Test values and Equation (41). The Nip diameter is 6 inches and the W.O.T for the rolls is 1.3 pli.

Figure 65c. Photograph of the wound roll showing slippage after the Dynamic Torque test. The Nip diameter is 6 inches and the W.O.T for the roll is 1.3 pli. The parent roll id. is N10, the diameter of the wound roll is 7.66 inches, the Half width of contact is 0.227 inches and the nip load is 0.83 pli.

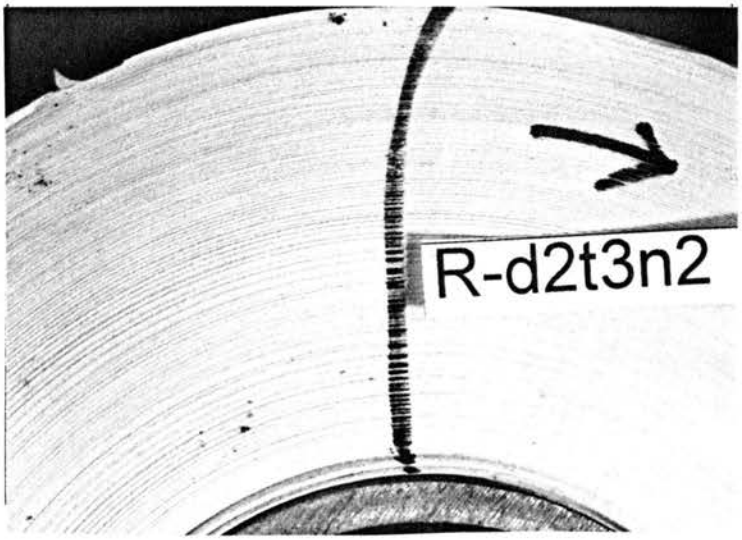

Figure 65d. Photograph of the wound roll showing slippage after the Dynamic Torque test. The Nip diameter is 6 inches and the W.O.T for the roll is 1.3 pli. The parent roll id. is N10, the diameter of the wound roll is 7.57 inches, the Half width of contact is 0.25 inches and the nip load is 5 pli.

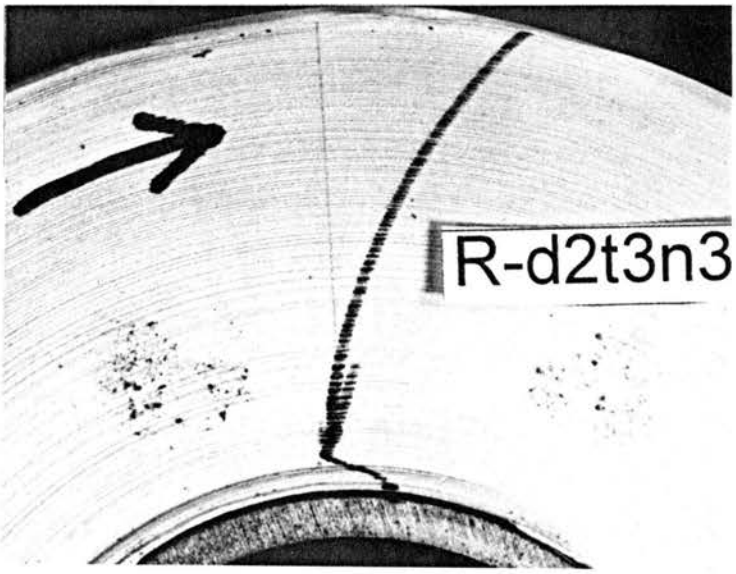

Figure 65e. Photograph of the wound roll showing slippage after the Dynamic Torque test. The Nip diameter is 6 inches and the W.O.T for the roll is 1.3 pli. The parent roll id. is N10, the diameter of the wound roll is 7.63 inches, the Half width of contact is 0.234 inches and the nip load is 10 pli.

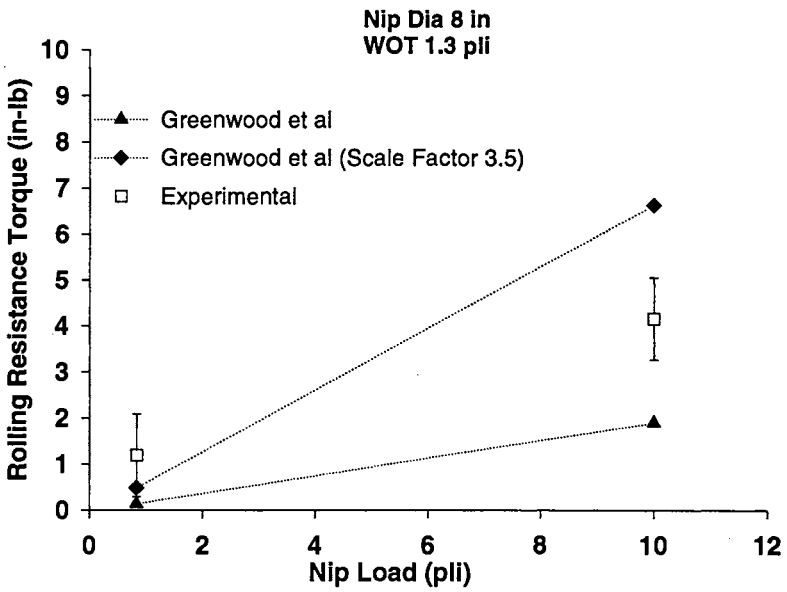

Figure 66a. Comparison between Dynamic Torque Test values and Equations (39) and (41). The Nip diameter is 8 inches and the W.O.T for the rolls is 1.3 pli.

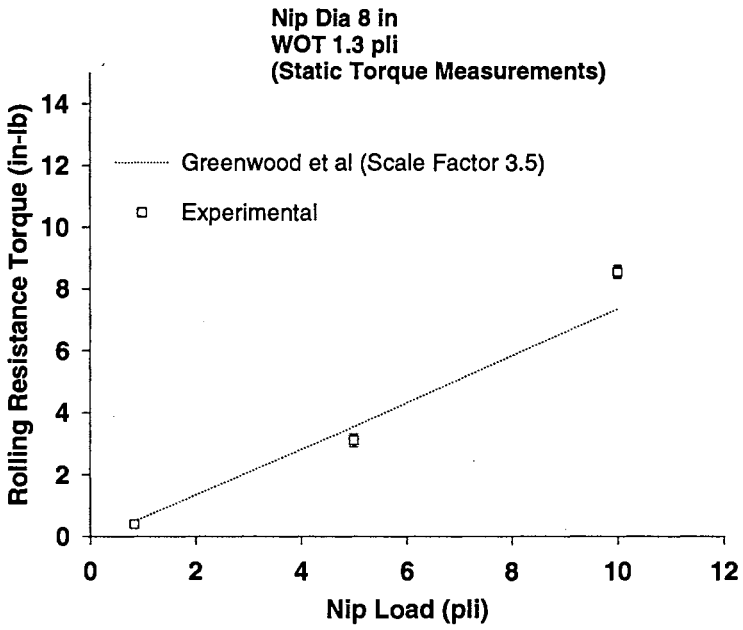

Figure 66b. Comparison between Static Torque Test values and Equation (41). The Nip diameter is 8 inches and the W.O.T for the rolls is 1.3 pli.

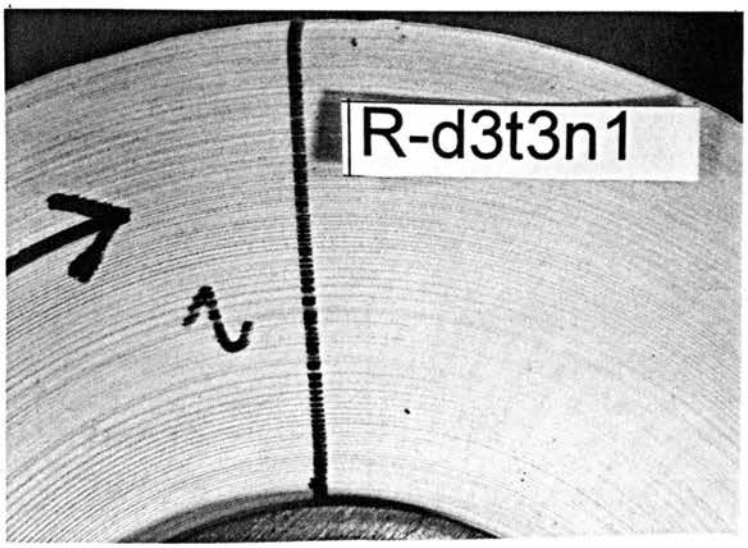

Figure 66c. Photograph of the wound roll showing slippage after the Dynamic Torque test. The Nip diameter is 8 inches and the W.O.T for the roll is 1.3 pli. The parent roll id. is N10, the diameter of the wound roll is 7.68 inches, the Half width of contact is 0.18 inches and the nip load is 0.83 pli.

Figure 66d. Photograph of the wound roll showing slippage after the Dynamic Torque test. The Nip diameter is 8 inches and the W.O.T for the roll is 1.3 pli. The parent roll id. is 4, the diameter of the wound roll is 7.54 inches, the Half width of contact is 0.219 inches and the nip load is 5 pli.

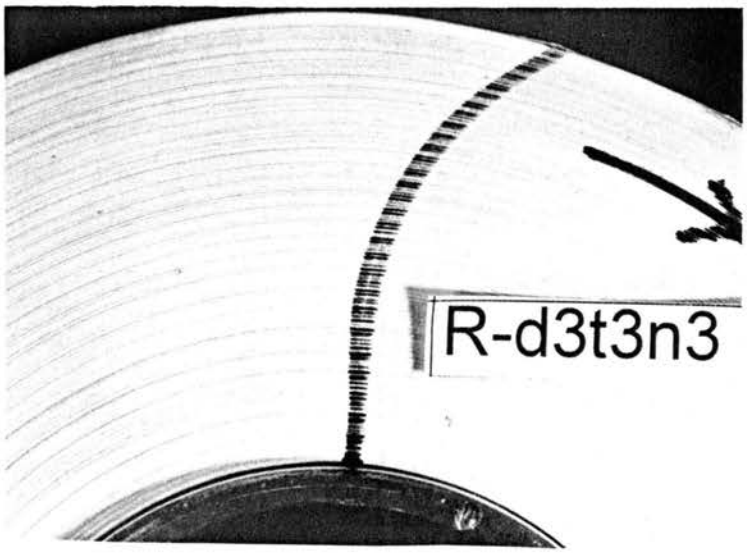

Figure 66e. Photograph of the wound roll showing slippage after the Dynamic Torque test. The Nip diameter is 8 inches and the W.O.T for the roll is 1.3 pli. The parent roll id. is 8, the diameter of the wound roll is 7.46 inches, the Half width of contact is 0.227 inches and the nip load is 10 pli.

rolls, and the rolls retained the structural integrity after the torque tests. As with the previous sets of data presented, rolling resistance torque increases with increase in diameter from 2.5 inches to 6 inches. But, an increase in diameter from 6 to 8 inches shows a saturation of rolling resistance torques. An increase in nip loads leads to an increase in rolling resistance torques.

Conclusions

The J-lines in the rolls (dynamic torque test data) provide interesting insights into the amount of slippage that occur in the rolls. The following are some of the trends that are observable:

(i) The rolls that were wound with the lowest wound on tension (0.3 pli) had the worst slippage, and, most of the rolls were rendered useless after the experiment.

(ii) With increase in the wound on tension, the amount of slippage reduced in the rolls.

(iii) For a particular value of the wound on tension, and a particular diameter chosen, the amount of slippage increased with increase in nip loading.

(iv) For the case of the lowest value of the wound on tension, the slippage increased with increase in nip diameter. At the other two values of wound on tension namely 0.67 pli and 1.3 pli, as the nip diameter increased from 2.5 inches to 6 inches there is a considerable increase in the amount of slippage, but in going from 6 inches to 8 inches, there is a saturation in the amount of slippage.

These general trends are the same as those followed by the rolling resistance values, and so the link between the rolling resistance and the slippage occurring in the rolls becomes clear.

An interesting feature, of all the static torque test data, is that as the radial stresses in the wound rolls increase, the ability to predict the rolling resistance torques with Greenwood et al's equation, increases. There is poor correlation for all the cases that were wound with a wound on tension of 0.3 pli. The correlation gets better at for the rolls wound at a

wound on tension of 0.67 pli. At the highest wound on tension of 1.3 pli, the correlation is good. Correspondingly, observing the amount of slippage, as the wound on tension increases the amount of slippage decreases. As the amount of slippage decreases, the correlation with Greenwood et al's equation with scale factor of 3.5 gets better.

Two interesting conclusions can be drawn:

(1) The rolling resistance torques are large enough to cause loosening slippage in the wound roll.

(2) The modified form of Greenwood et al's equation with scale factor of 3.5,

$$Torque_{Rolling-Resistance} = (3.5)\frac{2}{3\pi}\alpha\left(\frac{Wa}{R^*}\right)w\,r_{nip-roll}$$

can be used to estimate rolling resistance torques with reasonable accuracy.

CHAPTER VIII

SLIPPAGE PREDICTION IN SURFACE WINDING USING TORQUE CAPACITY

Scope

In the previous chapter, rolling resistance encountered by a torque driven nip roll in contact with a wound roll, was measured using experimental methods. A theoretical means of estimating the rolling resistance, for the case of the circular geometry involving the nip and the wound roll was introduced. The theoretical formula was based on Greenwood et al's equation with a scale factor of 3.5, and correlation between the theoretical formula and the experimental results was established. The rolling resistance forces were large enough to cause slippage in the wound roll. In this chapter, an attempt will be made, to predict the onset of slippage, in a wound roll in contact with a torque driven nip.

Recall that in the earlier part of this study dealing with center winding and slippage occurring during splicing and decelerations, a simple way of relating the onset of slippage to the external torque applied to the roll was introduced.

The torque capacity of the roll proved to be a valuable quantification, and in the cases discussed, slippage occurred in the rolls when:

$$T_{\text{app-external}} > T_{\text{capacity-minimum}} \tag{42}$$

In the cases where equation (42) was applied successfully to predict the onset of slippage, the torque capacity of the roll at any particular circumferential location, was not modified or disturbed until slippage occurred in the roll. Now, for the case of the experiments conducted during the rolling resistance tests, the applicabilty of the slippage algorithm becomes difficult due to contact related effects.

Slippage Model I - Torque Driven Nip

Although the rolling resistance is an external torque, for the case of the wound rolls used in the rolling resistance experiments, there is a fundamental complexity introduced due to contact at the interface between the nip and the wound roll. When the nip is loaded, the wound roll bulges outward radially, on either side of the contact zone, before it regains its original profile. In such cases, the layers separate from the wound roll for a small circumferential distance, Figure 67. Immediately beneath the nip, in the contact zone where the wound roll conforms to the nip roll's profile, there is an increase in the inter-layer pressures in the wound roll, due to the nip loading. So, the circular symmetry (axisymmetry), of the radial pressures that exist in the wound roll is disturbed, even prior to the start of motion of the nip roll. This means the torque capacity of the wound roll is

no longer axisymmetric. Further, as the nip rotates, the bulge on the incoming side of the nip is chased around the wound roll giving rise to a wave that travels in a direction opposite to the direction of rotation of the wound roll. The bulge behind nip may not completely conform to the geometry of the wound roll. This situation, makes it difficult, to use a simple slippage algorithm to predict the onset of slippage, in the case of a torque driven nip. This situation is identical, to the air entrainment mechanism outlined by Lemke et al for crepe wrinkle formation during surface winding. Pfeiffer [37] has also pointed out the existence of a wave of pressure beneath the nip, providing a loosening of the wound roll. So, the actual mechanism by which slippage is initiated during surface winding is complex, and it is beyond the scope of this study to answer the question of how slippage originates in surface winding conditions.

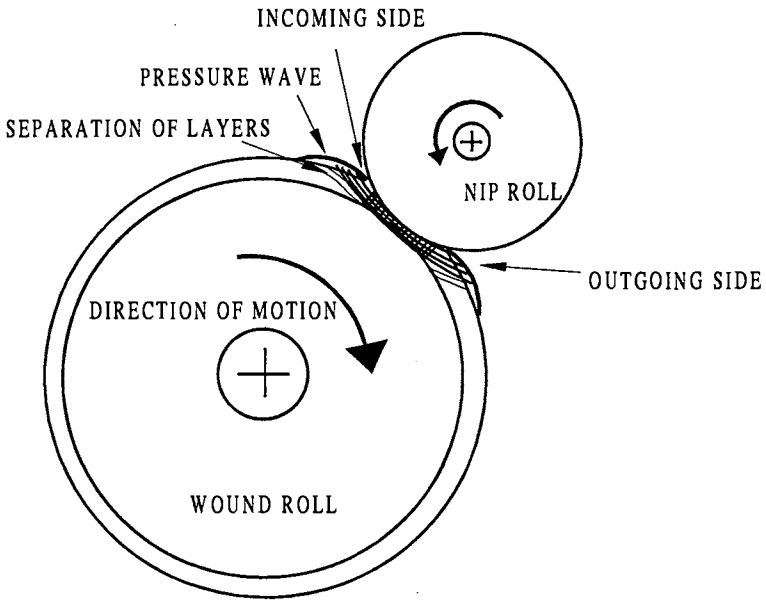

Figure 67. Schematic illustrating separation of layers in the contact zone, due to nip related effects.

Nonetheless, an attempt will be made to correlate the torque capacity of the wound roll to the rolling resistance torque due to the nip. TABLES 15a, b and c, show the results of an attempt to compare torque capacities and rolling resistance torques. The tables show the magnitudes of the forces in the outermost layer of the wound roll, resisting a force due to the rolling resistance. Column 1, in TABLES 15a, b and c, shows the pressure beneath the last lap in the wound roll, which is given by:

$$\sigma_{last-lap} = \frac{T_{wot}}{s} h \text{ (psi)} \tag{43}$$

where 'T_{wot}' is the wound on tension (psi)

'h' caliper of web (in)

's' radius of the outermost lap (in).

In the second column, the ability of the layer to resist slippage is shown as a force. This is shown as a ratio of the torque capacity of the last lap to the radius of the wound roll. In the third column, the results of the static rolling resistance torque measurements are shown as a force value. The force, is obtained by dividing the static rolling resistance torque by the radius of the wound roll. In the fourth column, the external force from the dynamic torque measurements are shown. This is shown just for comparison with the static force values.

According to the torque capacity algorithm developed for centerwinding, slippage occurs when:

$$T_{applied} > T_{capacity} \tag{44}$$

Adapting this algorithm for the situation where a torque driven nip roll is in contact with a wound roll, slippage occurs when:

$$\frac{Torque_{rolling-resistance}}{r_{nip-roll}} > \frac{T_{capacity-last-lap}}{r_{wound-roll}} \tag{45}$$

In the fifth column a prediction based on equation (45), for static torque values is shown. This prediction considers only the external force due to rolling resistance torque, and the force required to cause the last layer to slip. The sixth column shows the actual experimental outcome. TABLES 15a, b and c, are arranged in an increasing order of wound on tensions. So in every table, comparison between three different nip diameters and nip loads are shown.

TABLE 15a. Slippage Predictions for the rolls with a wound on tension of 0.3 pli.

Pressure beneath last layer (psi)	$Tcap/r_{wound\ roll}$ (lb)	Force $_{external}$ (From Static Torque Measurements) (lb)	Force $_{external}$ (From Dynamic Torque Measurements (lb)	Predicted	Observed
0.1	2.5	0.2	2.7	no-slip	slip
0.1	2.5	3.0	3.7	slip	slip
0.1	2.5	7.1	7.1	slip	slip
0.1	2.5	0.2	1.3	no-slip	slip
0.1	2.5	2.3	3.4	no-slip	slip
0.1	2.5	3.3	10.3	slip	slip
0.1	2.5	0.2	1.1	no-slip	slip
0.1	2.5	2.4	2.4	no-slip	slip
0.1	2.5	3.1	5.5	slip	slip

TABLE 15b. Slippage Predictions for the rolls with a wound on tension of 0.67 pli.

Pressure beneath last layer (psi)	$Tcap/r_{wound\ roll}$ (lb)	$Force_{external}$ (From Static Torque Measurements) (lb)	$Force_{external}$ (From Dynamic Torque Measurements (lb)	Predicted	Observed
0.2	5.0	0.0	2.7	no-slip	no-slip
0.2	5.0	1.5	1.8	no-slip	slip
0.2	5.0	5.1	5.5	slip	slip
0.2	5.0	0.1	1.1	no-slip	no-slip
0.2	5.0	1.8	1.9	no-slip	slip
0.2	5.0	3.7	3.8	no-slip	slip
0.2	5.0	0.1	1.1	no-slip	slip
0.2	5.0	1.7	1.3	no-slip	slip
0.2	5.0	2.6	4.5	no-slip	slip

TABLE 15c. Slippage Predictions for the rolls with a wound on tension of 1.3 pli

Pressure beneath last layer (psi)	$Tcap/r_{wound\ roll}$ (lb)	$Force_{external}$ (From Static Torque Measurements) (lb)	$Force_{external}$ (From Dynamic Torque Measurements (lb)	Predicted	Observed
0.4	10	0.0	2.7	no-slip	no-slip
0.4	10	0.7	no data	no-slip	slip
0.4	10	2.8	3.5	no-slip	slip
0.4	10	0.0	1.1	no-slip	no-slip
0.4	10	0.9	1.5	no-slip	slip
0.4	10	2.7	2.3	no-slip	slip
0.4	10	0.1	1.1	no-slip	no-slip
0.4	10	0.8	no-data	no-slip	slip
0.4	10	2.1	1.8	no-slip	slip

Analysis

TABLES 15a, b and c, show interesting trends. The observed outcome of the experiments, are different in a majority (14/27) of the cases, reflecting the inability of the model to predict the onset of slippage, when wound rolls are subjected to the influence of a torque driven nip. Other broad trends that appear are:

(i) With an increase in the wound on tensions,(0.67 and 1.3 pli), nip loads, and nip diameters, the extent of slippage occurring is less, and there is no permanent damage to the rolls. However, these are cases where slippage was not predicted. These are also cases where the rolling resistance torques are fairly low. Fundamentally, an increase in the wound on tension in the rolls, leads to an increase in the torque capacity of the rolls, which points to the reduced amount of slippage.

(ii) For the case of the lowest wound on tension (0.3 pli), the prediction capability of the model is better, than for the cases with 0.67 pli wound on tension and 1.3 pli wound on tension. The 0.3 pli wound on tension cases are rolls where the rolling resistance torques are higher in magnitude and the torque capacities are relatively lower.

So, the adapted model, does not perform well in predicting the onset of slippage for the case of a wound roll and a torque driven nip roll. This is because of the inherent difficulty in quantifying the torque capacity in the nip region, as the contact conditions alter the torque capacity considerably.

Slippage Model II - Torque Driven Nip

If the model is changed slightly, to incorporate the effect of gaps opening in the vicinity of the nip, by assuming zero torque capacity on either side of the nip, and an average value of the torque capacity considered, then the predictability improves. The average torque capacity now reduces to a third of the undisturbed torque capacity beneath the last layer in the vicinity of the nip. But, this method is not accurate as it does not consider the increase in torque capacity beneath the nip, due to the nip load. So, with the modified slippage criterion, slippage would occur in the presence of a surface driven nip when:

$$\frac{Torque_{rolling-resistance}}{r_{nip-roll}} > \frac{T_{capacity-last-lap}}{3\, r_{wound-roll}} \tag{46}$$

The TABLES 16a, b and c show how the adapted model behaves.

TABLE 16a. Slippage Prediction for wound on tension of 0.3 pli.

Pressure beneath last layer (psi)	$T_{cap}/r_{wound\ roll}$ (lb)	$T_{cap}/(3r_{wound\ roll})$ (lb)	Force $_{external}$ (From Static Torque Measurements) (lb)	Predicted	Observed
0.1	2.5	0.83	0.2	no-slip	slip
0.1	2.5	0.83	3.0	slip	slip
0.1	2.5	0.83	7.1	slip	slip
0.1	2.5	0.83	0.2	no-slip	slip
0.1	2.5	0.83	2.3	slip	slip
0.1	2.5	0.83	3.3	slip	slip
0.1	2.5	0.83	0.2	no-slip	slip
0.1	2.5	0.83	2.4	slip	slip
0.1	2.5	0.83	3.1	slip	slip

TABLE 16b. Slippage Prediction for wound on tension of 0.67 pli.

Pressure beneath last layer (psi)	$T_{cap}/r_{wound\ roll}$ (lb)	$T_{cap}/3r_{wound\ roll}$ (lb)	Force $_{external}$ (From Static Torque Measurements) (lb)	Predicted	Observed
0.2	5.0	1.7	0.0	no-slip	no-slip
0.2	5.0	1.7	1.5	no-slip	slip
0.2	5.0	1.7	5.1	slip	slip
0.2	5.0	1.7	0.1	no-slip	no-slip
0.2	5.0	1.7	1.8	slip	slip
0.2	5.0	1.7	3.7	slip	slip
0.2	5.0	1.7	0.1	no-slip	slip
0.2	5.0	1.7	1.7	slip	slip
0.2	5.0	1.7	2.6	slip	slip

TABLE 16c. Slippage Prediction for wound on tension of 1.3 pli.

Pressure beneath last layer (psi)	$T_{cap}/r_{wound\ roll}$ (lb)	$T_{cap}/3r_{wound\ roll}$ (lb)	External Force (From Static Torque Measurements) (lb)	Predicted	Observed
0.4	10	3.3	0.0	no-slip	no-slip
0.4	10	3.3	0.7	no-slip	slip
0.4	10	3.3	2.8	no-slip	slip
0.4	10	3.3	0.0	no-slip	no-slip
0.4	10	3.3	0.9	no-slip	slip
0.4	10	3.3	2.7	no-slip	slip
0.4	10	3.3	0.1	no-slip	no-slip
0.4	10	3.3	0.8	no-slip	slip
0.4	10	3.3	2.1	no-slip	slip

With the modified version of the slippage criterion, 16 out of 27 cases could be predicted successfully.

Summary

In summary, an attempt was made to adapt the slippage criterion that was used to predict the onset of slippage in centerwinding. The slippage criterion cannot be used as effectively, because of complexities induced by the contact phenomenon. The conditions prevailing in the contact interface, make it difficult to provide a magnitude to the torque capacity in the last lap. This should not be construed as a failure on the part of the slippage model. The model is not designed to address complexities induced due to contact phenomenon. So, to address the onset of slippage for a torque driven case, it is necessary to consider the pressure wave produced by the nip and the effect of the pressure wave on the structural integrity of the wound roll and the torque capacity.

CHAPTER IX

HALF WIDTH COMPUTATIONS

Scope

In all the cases where the rolling resistance computations were carried out using Greenwood et al's equation, experimental values of the half-width of contact were employed. Using high magnification photographs of the nip and wound roll interface, it is possible to determine the half width with an accuracy of 1/100 of an inch. For the case of the surface winder used at the WHRC, it is possible to visually observe the contact interface without any obstructions in the line of sight. However, there may be circumstances where the contact interface may not be easily visible for photography. Commercially available sensors to determine the half width of contact are expensive to use, and may be difficult to set up in an actual production machine. Hence, a theoretical means to determine the half width of contact becomes important.

The determination of the half width of contact, between a layered body such as a wound roll, and a rigid elastic roller, is a difficult problem to tackle using analytical techniques.

In addition, the radial modulus of the wound roll, is a function of inter-layer stresses. Finite element methods can be used to find reasonably accurate values of the half width of contact. But, setting up finite element models are computationally expensive and intensive.

In this chapter two methods to determine the half width of contact using Hertz's theory will be outlined. These methods yield good approximations to the half width of contact.

Theoretical Methods for Computing the Half Width

The well known Hertz theory for determining the half width of contact between two cylindrical elastic bodies will be the starting point. Adapting the equation for the half width of contact between two elastic cylinders, from Shigley[38] the half width of contact 'a' is given by:

$$a = \sqrt{\frac{2W}{\pi l}\frac{\left[\frac{\left(1-\nu_1^2\right)}{E_1}+\frac{\left(1-\nu_2^2\right)}{E_2}\right]}{\left(\frac{1}{d_1}\right)+\left(\frac{1}{d_2}\right)}} \text{ (in)} \qquad (47)$$

where

'W' is the total nip load (lb)

'l' is the length of contact (in)

'ν_1' is the Poisson's ratio of the first cylindrical body (aluminum nip roll ~ 0.3)

'ν_2' is the Poisson's ratio of the second cylindrical body (wound roll ~ 0.01)

'd_1' is the diameter of the first cylindrical body ~ nip roll (in)

'd_2' is the diameter of the second cylindrical body ~ wound roll (in)

'E_1' Young's modulus of elasticity of the first cylindrical body ~ Aluminum nip roll ($10.6*10^6$ psi)

'E_2' is the modulus of elasticity of the second cylindrical body ~ radial modulus of the wound roll (psi).

Hertz's equation for computing the half width of contact between two elastic cylinders seems easy to use, at first glance. There is one problem in that the modulus of the wound roll is not constant, but is function of the radial pressure of the wound roll. The radial pressure, in-turn, varies with the radius of the wound roll. An average value of the pressure existing in the last 100 layers can be used to generate a modulus, using the variation of E_r versus pressure for the web stack in the wound roll.

Using equation (47), computations were carried out for various combinations of nip rolls and wound rolls wound using different values of wound on tensions. The radial pressures in the last 100 layers of the wound roll were used to generate a value for the modulus E_2. An important point to be remembered is that in this method, no attempt is made to incorporate the effect of the contact stresses due to the nip load. What is considered is only the effect of the inter-layer stresses that exist in the last 100 layers of the wound roll.

'ν_1' is the Poisson's ratio of the first cylindrical body (aluminum nip roll ~ 0.3)

'ν_2' is the Poisson's ratio of the second cylindrical body (wound roll ~ 0.01)

'd_1' is the diameter of the first cylindrical body ~ nip roll (in)

'd_2' is the diameter of the second cylindrical body ~ wound roll (in)

'E_1' Young's modulus of elasticity of the first cylindrical body ~ Aluminum nip roll ($10.6*10^6$ psi)

'E_2' is the modulus of elasticity of the second cylindrical body ~ radial modulus of the wound roll (psi).

Hertz's equation for computing the half width of contact between two elastic cylinders seems easy to use, at first glance. There is one problem in that the modulus of the wound roll is not constant, but is function of the radial pressure of the wound roll. The radial pressure, in-turn, varies with the radius of the wound roll. An average value of the pressure existing in the last 100 layers can be used to generate a modulus, using the variation of E_r versus pressure for the web stack in the wound roll.

Using equation (47), computations were carried out for various combinations of nip rolls and wound rolls wound using different values of wound on tensions. The radial pressures in the last 100 layers of the wound roll were used to generate a value for the modulus E_2. An important point to be remembered is that in this method, no attempt is made to incorporate the effect of the contact stresses due to the nip load. What is considered is only the effect of the inter-layer stresses that exist in the last 100 layers of the wound roll.

TABLE 17b. Half width comparisons for wound on tension of 0.67 pli.

Nip Load (pli)	Wound Roll Diameter (in)	Nip Roll Diameter (in)	Half width using Hertzian Theory (in)	Half width from Good[39] (in)	Experimental Measurement (in)
0.83	7.54	2.5	0.051	0.17	0.13
5.0	7.36	2.5	0.149	0.24	0.14
10.0	7.37	2.5	0.223	0.27	0.22
0.83	7.51	6.0	0.058	0.15	0.22
5.0	7.65	6.0	0.153	0.24	0.24
10.0	7.32	6.0	0.25	0.35	0.39
0.83	7.34	8.0	0.065	0.23	0.16
5.0	7.30	8.0	0.148	0.26	0.25
10.0	7.31	8.0	0.204	0.30	0.30

TABLE 17c. Half width comparisons for wound on tension of 1.3 pli.

Nip Load (pli)	Wound Roll Diameter (in)	Nip Roll Diameter (in)	Half width using Hertzian Theory (in)	Half width from Good[39] (in)	Experimental Measurement (in)
0.83	7.50	2.5	0.055	0.14	0.12
5.0	7.30	2.5	0.139	0.23	0.17
10.0	7.43	2.5	0.174	0.19	0.19
0.83	7.66	6.0	0.06	0.16	0.23
5.0	7.57	6.0	0.147	0.23	0.25
10.0	7.63	6.0	0.209	0.26	0.23
0.83	7.68	8.0	0.053	0.17	0.18
5.0	7.54	8.0	0.137	0.32	0.22
10.0	7.46	8.0	0.176	0.20	0.23

Good[39], outlined a different iterative scheme for computing the half width of contact considering the effect of the deformation induced in the contact region by the nip loading. In Good's technique, the radial modulus of the wound roll, E_2, is considered as a function of the deformation produced at the contact zone.

Using Hertzian theory, Good related the contact width to the radial deformation in the contact zone. From Johnson[40], the average radial deformation in the contact zone is given by:

$$u = \frac{a^2}{2R^*} \text{ (in)} \tag{48}$$

where 'u' is the deformation at the contact zone (in.),

'a' is the half width of contact (in), and

R* is the equivalent radius of contact (in), given by equation (37) in chapter 7.

The next step in Good's algorithm, is to express the radial modulus of the wound roll, E_r as a function of the deformation. Recall, E_r is a function of the radial pressure, and can be conveniently expressed as a polynomial variation of the radial pressure. Now, using the same form of E_r, and from the original stress strain values experimentally obtained from a stack test, E_r can be easily expressed as a function of the strain. A cubic polynomial models the variation of the radial modulus as a function of the strain very well. Since the stack tests are done for a one inch stack of web material, the variation of E_r with respect to the strain is the same as the variation of E_r with respect to the deformation. Thus E_r can be conveniently expressed as a function of the deformation, 'u'. TABLE 18, shows

the E_r values, as a polynomial variation of the deformation, 'u', for the different parent roll web stacks.

The next step in the algorithm is to assume a starting value of the half width of contact 'a'. With a knowledge of 'a' and a value of R*, which is a function of the nip roll and the wound roll radii, an initial value for the deformation 'u' can be generated, using equation 48. As E_r is expressed as a function of 'u', a value can be generated for E_r. So, with values for the other material properties, namely, E_1, d_1, d_2, ν_1 and ν_2, a value can be generated for the ratio (W/l) ,by re-arranging equation (47). The ratio (W/l), represents the nip load in units of pounds per linear inch. So, with an assumed value of 'a', a value of (W/l) is generated. If this process is iterated continually until the right value of the nip load is generated, the value of 'a' which generates the right value of the nip load corresponding to a particular case, represents the half width of contact for the set of contact conditions. Using SOLVER, an optimizing routine associated with EXCEL, which is a spread-sheet program, values of 'a' can be generated, that correlate well with the experimental results.

Numerical values of the half widths, which were computed using the numerical technique outlined by Good are shown in the fifth columns in TABLES 17a, b and c. The values computed using this iterative scheme correlate well with the experimental values for the half width of contact in all the three tables. Figures 68 a to i show the static torque values recomputed using the estimated values of 'a' computed from Good's technique. The graphs show good correlation.

TABLE 18. E_r of the parent rolls expressed as a function of the deformation 'u'.

Parent Roll ID (Thickness)	$E_r(u)$ From E_r and Stress Strain Data
1 (3 mils)	$7858.1*(u) + 567864*(u^2) - 3.0E+6*(u^3)$
2 (3 mils)	$771.82*(u) + 377452*(u^2) - 2.0E+6*(u^3)$
3 (3 mils)	$-3152.3*(u) + 445113*(u^2) - 2.0E+6*(u^3)$
4 (3 mils)	$-2000.6*(u) + 278673*(u^2) - 1.0E+6*(u^3)$
5 (3 mils)	$-4605.7*(u) + 540263*(u^2) - 3.0E+6*(u^3)$
6 (3 mils)	$2693.2*(u) + 170797*(u^2) - 396757*(u^3)$
7 (3 mils)	$7787.8*(u) + 190563*(u^2) - 431107*(u^3)$
8 (N8) (2.5 mils)	$7746.6*(u) + 539815*(u^2) - 4.0E+6*(u^3)$
N1 (2 mils)	$-1899*(u) + 198006*(u^2) - 604783*(u^3)$
N2 (2.2 mils)	$260.52*(u) + 203475*(u^2) - 553053*(u^3)$
N3 (2.5 mils)	$5331.7*(u) + 259579*(u^2) - 1.0E+6*(u^3)$
N4 (2 mils)	$-1446.3*(u) + 177964*(u^2) - 466829*(u^3)$
N5 (2 mils)	$-1827.7*(u) + 182661*(u^2) - 514211*(u^3)$
N6 (2.5 mils)	$-2474.7*(u) + 267699*(u^2) - 902243*(u^3)$
N10 (3 mils)	$6886.2*(u) + 538341*(u^2) - 4.0E+6*(u^3)$

Looking at the two different ways of computing the half-widths, the first method does not consider any contribution from the nip induced contact stresses. It considers only the radial pressures in the last 100 layers. The second method yields good results, but it does not consider the effect of the stresses induced due to the wound on tension in the contact zone. Nonetheless, the scheme outlined by Good is very attractive as it provides good estimates of the half width of contact, without resorting to the more complex numerical techniques such as finite elements.

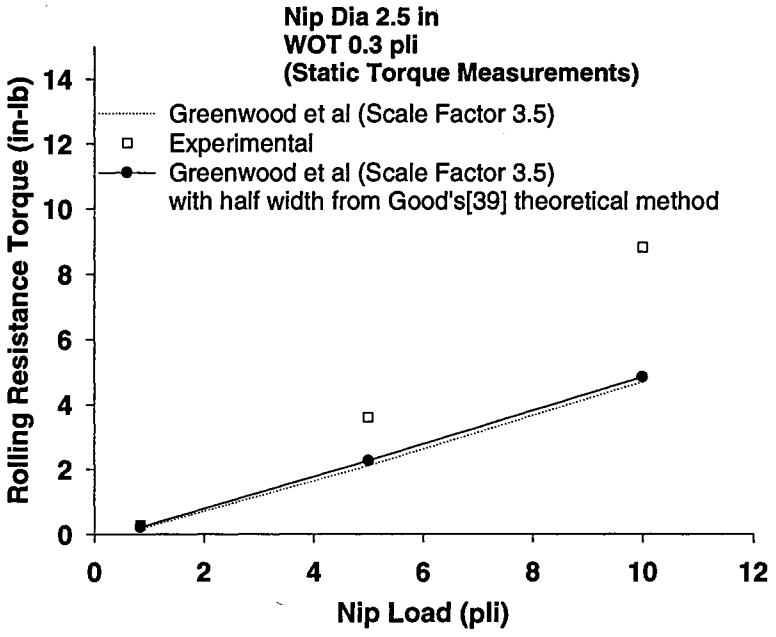

Comparison between Experimental and Theoretical Computations of Half- width. Nip Roll Diameter is 2.5 inches and the W.O.T for the Wound roll is 0.3 pli.

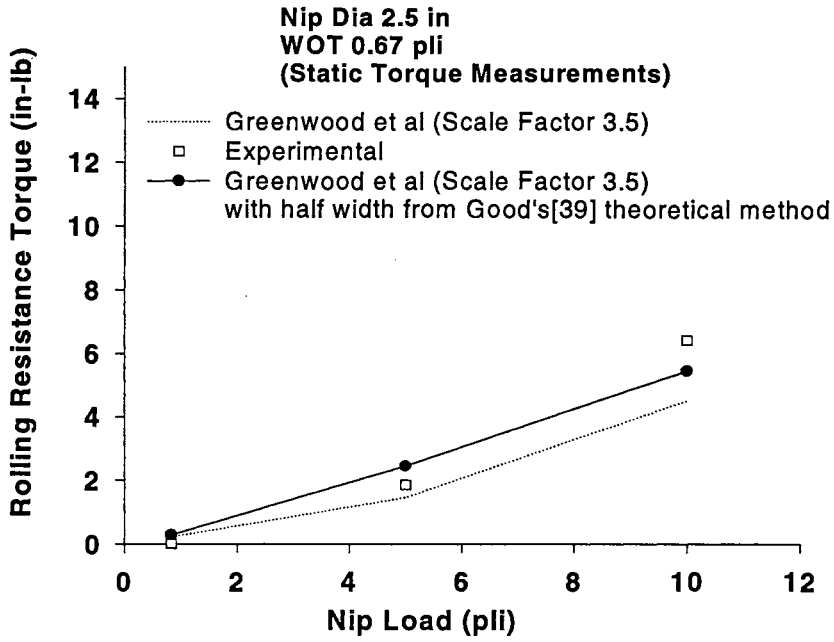

Figure 68b. Comparison between Experimental and Theoretical Computations of Half-width. Nip Roll Diameter is 2.5 inches and the W.O.T for the Wound roll is 0.67 pli.

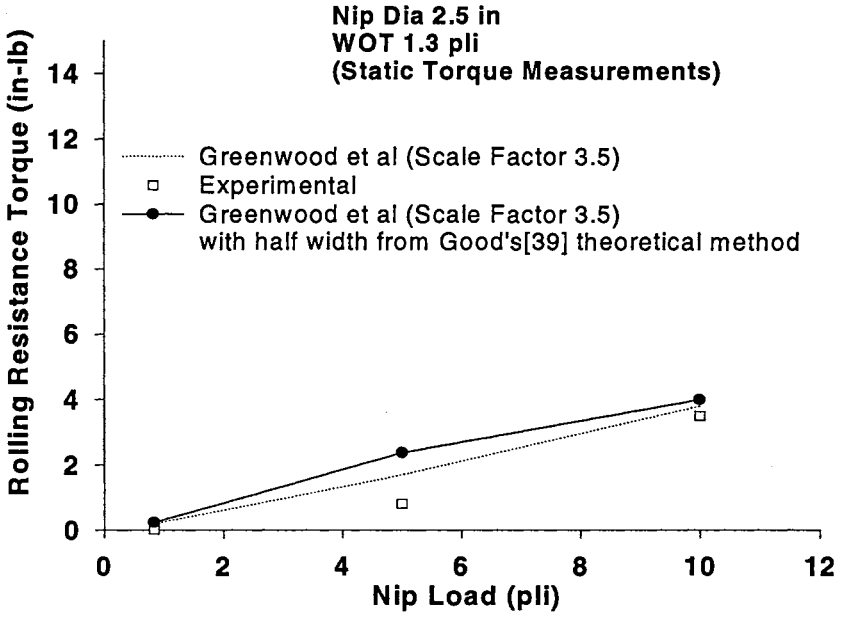

Figure 68c. Comparison between Experimental and Theoretical Computations of Half-width. Nip Roll Diameter is 2.5 inches and the W.O.T for the Wound roll is 1.3 pli.

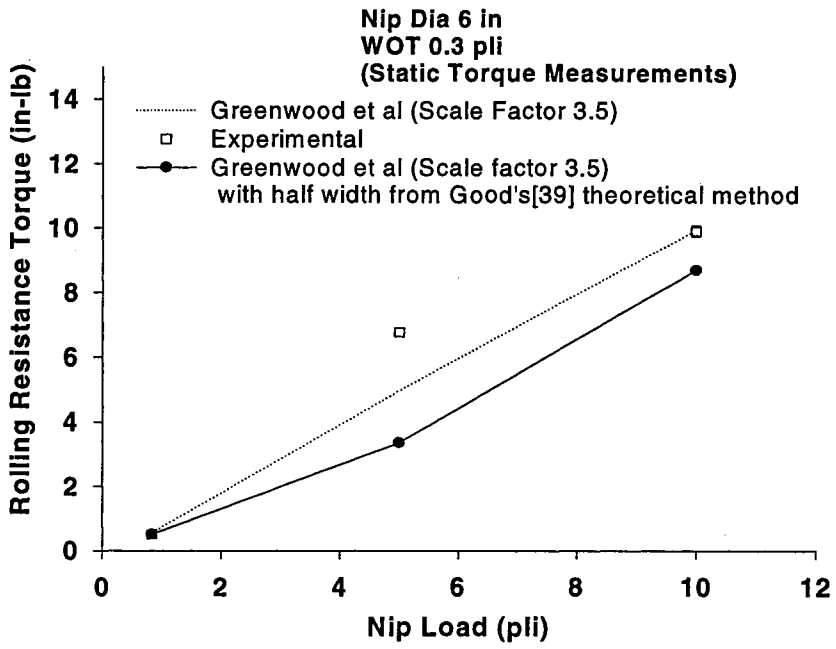

Figure 68d. Comparison between Experimental and Theoretical Computations of Half-width. Nip Roll Diameter is 6 inches and the W.O.T for the Wound roll is 0.3 pli.

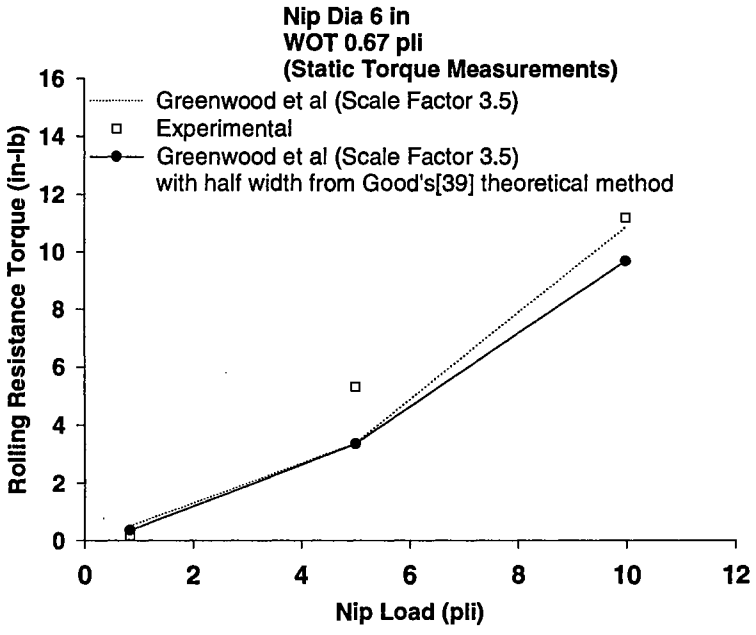

Figure 68e. Comparison between Experimental and Theoretical Computations of Half-width. Nip Roll Diameter is 6 inches and the W.O.T for the Wound roll is 0.67 pli.

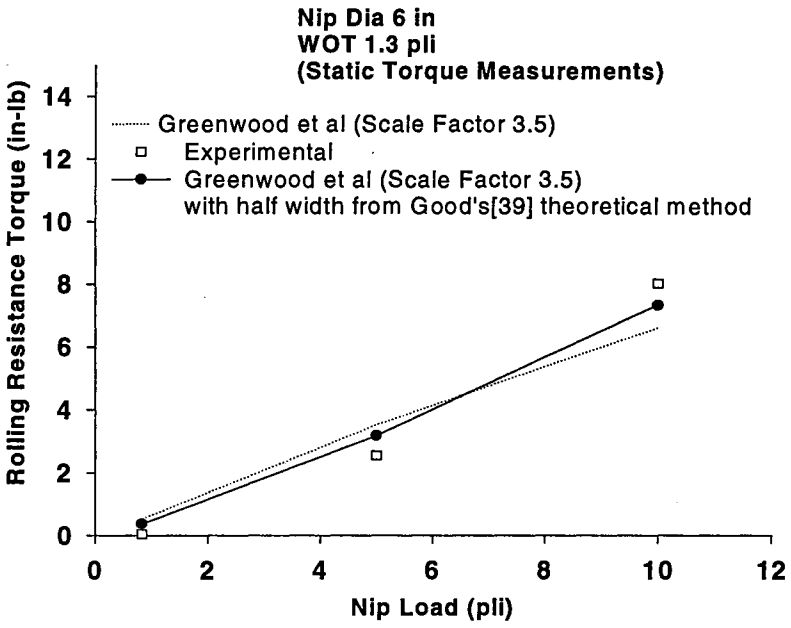

Figure 68f. Comparison between Experimental and Theoretical Computations of Half-width. Nip Roll Diameter is 6 inches and the W.O.T for the Wound roll is 1.3 pli.

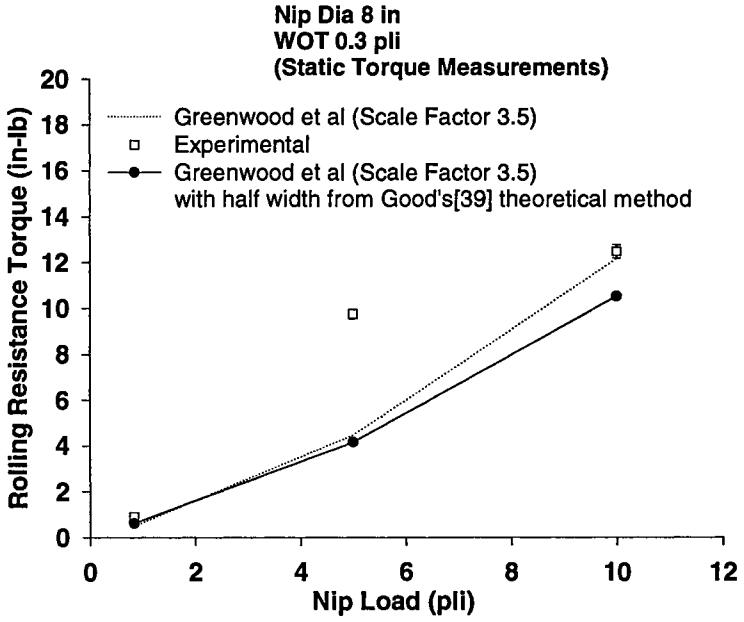

Figure 68g. Comparison between Experimental and Theoretical Computations of Half-width. Nip Roll Diameter is 8 inches and the W.O.T for the Wound roll is 0.3 pli.

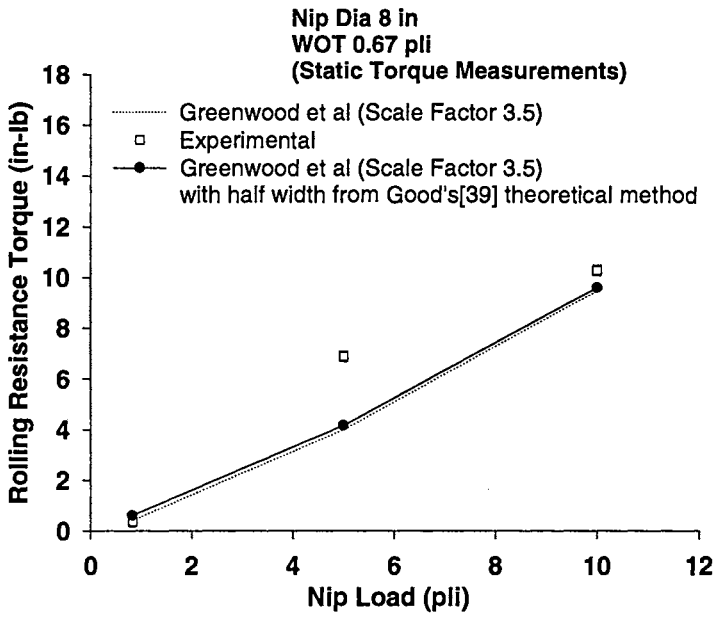

Figure 68h. Comparison between Experimental and Theoretical Computations of Half-width. Nip Roll Diameter is 8 inches and the W.O.T for the Wound roll is 0.67 pli.

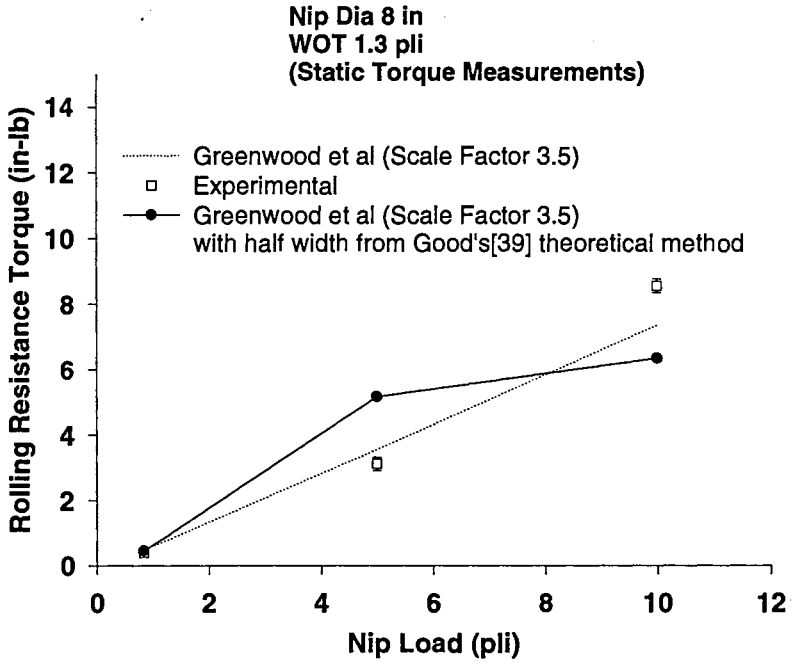

Figure 68i. Comparison between Experimental and Theoretical Computations of Half-width. Nip Roll Diameter is 8 inches and the W.O.T for the Wound roll is 0.67 pli.

CHAPTER X

PAST AND PRESENT

Scope

In the light of results from the present study, it is important to look back at the literature, to re-interpret some of the observations made. This gives an opportunity to better understand the circumstances under which the studies were made, and to provide new insights into wound roll slippage, based on the results presented in the present study. The present study fills some of the voids that were pointed out in the literature review. In particular, the present study provides quantitative data, which gives a better sense of wound roll slippage in general, and more specifically, slippage occurring during surface winding.

Re-visiting the Literature

The observations made by Laumer[5], on the nature of slippage occurring during surface winding, are correct in a general sense. The observations included comments on J-Lines, which identified them to be related to slippage induced by the nip and the extent of slippage, to the amount of compressive forces provided by the nip. Laumer also pointed out that the J-Lines curve in a loosening direction.

Based on the present study on rolling resistance in chapter 7, the comments made by Laumer are correct. The present study has shown that the extent of slippage increases in the rolls when the nip loads increase and, most of the slippage which occurs, is in a loosening direction. However, one of the points made by Laumer, pertaining to the amount of slippage and nip penetration seems to be incorrect. Laumer pointed out that a larger diameter nip roll produces smaller curving of the J-Line. But this is contradictory to the results of this study, as the extent of slippage, increases with increasing nip diameter, although saturation in the amount of slippage occurs beyond a certain point.

Laumer documented the presence of crepe wrinkles near the core region, and pointed out that the defect was related to slippage. A remedial action suggested by Laumer was to implement web tensions that are high, at the start of the wind. Within limits of wound tensions that would not cause core collapse, this observation is correct. The present study has shown that slippage occurs prior to the crepe wrinkle formation. Further, the occurrence of the defect was related quantitatively to low torque capacity zone in the core region, characteristic of constant tension winding. The remedy, is to increase the torque capacity in the core region, which is what would be achieved if Laumer's suggestion were implemented.

Daly's[6] classification of crepe wrinkles as a roll structure related defect, is correct as the present study has related slippage to the torque capacity, which in-turn is related to the radial pressures, and the radial stresses in a wound roll is a quantification of the roll structure.

The preliminary part of the present study is essentially validating a slippage model, for the case of center-winding, using the torque capacity and an applied torque. This is valid for situations when the external torque does not come into the roll through a disturbing contact interface, such as a nip. Recall, in one of the qualitative experiments discussed by Lucas[7], slippage occurred in a roll that was mounted on a core shaft, when an external torque was input to the roll by applying a tension to the outermost lap of the wound roll and a braking torque to the core. This is a classic case of wound roll slippage occurring when the torque capacity of the roll is exceeded by an applied torque resulting from tensioning the outer lap. The observation pertaining to winding rolls with tighter starts, reducing the propensity to slip, is also correct, as increasing the wound on tension at the start of the wind, leads to an increase in the torque capacity at the core region.

Lucas[4,7] identified time dependent factors which contribute to a reduction in core diameter, after the winding process, leading to slippage. This may be true, as, after the roll is wound, any reduction in pressures at the core region, leads to a reduction in torque capacity. So the chances of slippage occurring increases with a reduction in torque capacity.

Based on the present understanding of wound roll models, the observation made by Lucas, in stressing the importance of winding rolls with a good roll structure, to reduce the slippage that occurs in the rolls, is correct. The present study has shown that the roll structure can be quantified based the radial stresses that exist in the wound roll. The

radial stresses in the wound roll dictate the torque capacity of the wound roll in conjunction with the inter-layer coefficient of friction, and the width of the roll. So, a good roll structure, (large radial stresses) implies high torque capacity and greater resistance to slippage.

Another observation made by Lucas is that crepe wrinkles could occur anywhere in a wound roll. This is true, as slippage occurs wherever there is a zone of low torque capacity, and, low torque capacity zones can occur anywhere in a wound roll. Some of the low torque capacity zones in a wound roll are core regions, the periphery of the wound rolls, location of splices, and any other location wound with a low value of wound on tension. Lucas observed that increasing the nip load leads to an increase in slippage. This fact has been verified in the present study, based on the rolling resistance tests.

Lucas, identified the formation of bow-waves in a surface winding scenario, which lead to localized tension drops in the vicinity of the nip regions. In the present study, although, no bow waves were observed while surface winding, what was observed was a bulging of the web material on either side of the nip contact zone. This bulging, in-turn leads to separation of layers, for a short circumferential distance on either side of the contact zone. The loosening pressure wave, when this bulge is chased by the nip might be what was described by Lucas. But, it is also possible that the bow wave described could be an artifact of the web line configuration, and consequently the web may enter into the nip zone at a very low tension, and form a bubble at the in-going side of the nip. With regards to angular decelerations, it is clear that slippage occurs whenever the dynamic

torque due to angular decelerations exceeds the torque capacity of the wound roll. So, the observation made by Lucas, in identifying angular decelerations, as a major cause of crepe wrinkle formation is accurate.

In addressing the study by Welp[10], it appears that the radial stress profile described by Welp is one of tension loss. Tension loss is a phenomenon characteristic of soft webs such as newsprint, which has a tendency to lose most of the radial stresses, due to deformation induced by the oncoming layers of web, Giachetto[41]. The characteristic feature of a roll which has suffered tension loss, is that there is a gradual increase in the radial stress profile from the core to the periphery of the roll. Based on the information given with the discussion, it is not possible to determine if tension loss occurred in reality. The significance of tension loss is that, such a roll may have a low torque capacity and, an encounter with an external torque which is larger than the torque capacity of the roll may cause slippage in the roll. So, tension loss may be dangerous from the perspective of producing low torque capacity in the roll. Winding with a nip roll has been found as a remedy for reducing tension loss in rolls.

The need for 'high' radial stresses near the core region of a wound roll, confirms the existence of 'high' torque capacity near the core region. Based on the present study, it is not possible to validate any correlation between the amount of slippage, and the difference in speed between the nip and the wound roll.

Another interesting point that can be used to support the claims made by Welp, is that a reduction in nip load leads to a reduction in the amount of slippage. All the rolling resistance tests in the present study correlate well with this fact. So, relieving the nip load, leads to a reduction in the rolling resistance encountered by a nip. With respect to the modified winder design, and redistribution of nip load, it is possible that the rolling resistance encountered by the two slanting nip rolls (of unequal diameter), is lower than that of undistributed nip load on two nip rolls of the same diameter.

The winder process parameters that control the quality of the wound roll, as identified by Frye[11], are the same parameters that control the radial stresses that exist in a wound roll. Recall, that the radial stresses in the wound roll, help quantify the structural integrity of the roll. Frye had identified non-uniform nip loads lead to crepe wrinkle formation. Non uniform nip loads, provide a lateral force, that has a tendency to cause the incoming layer of web, or the underlying layers of web to telescope. If there is excessive slippage, then there is a possibility of crepe wrinkle formation.

The remedial action suggested by Frye to reduce crepe wrinkles while winding, is to increase the wound on tension. This is correct, as an increase in wound-on tension leads to an increase in radial stresses, which in-turn leads to an increase in the torque capacity of the wound roll. This means the roll has a greater capacity to resist slippage.

When the time taken for the wound on tension to reach a steady state value from start-up is considered, for a production winder, there is a good possibility that a zone of low radial

stress exists near the core region, because of low values of wound on tension during the start-up. This leads to a low torque capacity zone, and consequently a hot spot for slippage, or crepe wrinkle formation. This could explain the occurrence of crepe wrinkles in the vicinity of the core region for the cases documented by Frye. With regards to comments made by Frye pertaining to the roughness of the nip rolls, nothing can be directly related to the present study. With respect to misalignment of the center-line of the core in relation to the nip rolls, or drums, it is possible that a redistribution of nip load occurred, which modified the rolling resistance of the nip rolls, thereby leading to slippage in the rolls.

The study conducted by Odell et al[12] characterized process parameters such as wound on tension, nip loading and nip diameters with respect to wound roll density. The same process parameters control the radial stress profile and the capacity of the roll to resist slippage. Odell et al have emphasized on high start up wound on tensions, to achieve tight roll starts. The tight roll starts, help in generating high radial stresses near the core region. This leads to high torque capacities, and greater resistance to slippage. Considering the reduction of nip loading from the rider roll, the present studies point out to the fact that a lower nip load leads to a lower amount of rolling resistance, and hence reduced amount of slippage, and lesser propensity to form crepe wrinkles. So the results of Odell et al's study compare well with the results from the present study.

In the statistical study made by Paananen et al[14], a reduction in the coefficient of friction has been pointed out as one of the causes for the formation of crepe wrinkles.

Based on the torque capacity model, this is valid, as a reduction in the coefficient of friction leads to a reduction in torque capacity, which leads to a greater propensity to slip.

In addressing the study made by Lemke et al[3], it appears, that the pressure wave phenomenon described in the present study pertaining to rolling resistance, is what has been described on a larger scale. In this study, a bulge in the web material and separation of layers following nip indentation, has been observed occurring while large nip loads indent a wound roll. This phenomenon is pronounced in rolls wound with a low value of wound - on - tension. Based on the description given by Lemke et al, identifying a loosening torque, promoting slippage in the separated layers, it is clear that this loosening torque is the rolling resistance torque. Lemke et al point identify that the loosening torque is higher when the roll is soft, or when there is high nip deformation. The present study on rolling resistance shows identical trends. Other comments pertaining to the occurrence of slippage in the periphery of the wound roll and choice of proper diameters to reduce slippage, also point out to rolling resistance as a key player in inducing slippage in the wound roll.

Schoenmeier's[15] study identifies parameters such as the wound on tension, the radial modulus, and the inter-layer coefficient of friction as factors which are important in controlling the formation of crepe wrinkles. The first two parameters identified, play a part in determining the radial stresses. The radial stresses and the coefficient of friction determine the torque capacity of the roll, which controls the slippage in the roll. The nip

load determines the rolling resistance offered to the nip, and the amount of rolling resistance encountered by the nip determines the amount of slippage in the roll.

Schoenmeier's study identified the location of a splice in a roll as a potential crepe wrinkle location. The present study has shown that the observation made by Schoenmeier is accurate and that locations of splices are potential locations for crepe wrinkles, because of the low torque capacity in the region of the splice, which is due to a local drop in the wound on tension following the splicing operation. A remedial measure was suggested in the present study, in which the wound on tension was increased gradually as a ramp, instead of an impulse following a drop in the tension. Schoenmeier also identified the decelerations that wound rolls undergo, to be responsible for crepe wrinkle formation. This is also an accurate observation, and has been experimentally verified in the present study. Crepe wrinkles occur at locations of low torque capacity, whenever the torque capacity is exceeded by the dynamic torque due to deceleration.

The studies by Roisum[16,17,18] identified radial stresses as the key player, in dictating the structural integrity of a wound roll. The observation that high radial stresses and high coefficients of friction, lead to a higher resistance of the rolls to slippage, is accurate. This is because the torque capacity of the roll is directly related to the radial stresses and the inter-layer coefficient of friction. So, an increase in the either of the parameters, leads to a higher value of torque capacity, which leads to a greater resistance to slippage.

Roisum identified regions of negative circumferential stresses, as locations where defects such as crepe wrinkles and starring are likely to occur. This observation is true as far as starring defects are concerned. But, there is a larger picture that needs to be recognized. Starring, as observed in the present study, is due to a combination of slippage and the presence of negative circumferential stresses. Recall, in the studies pertaining to starring, it was shown that negative circumferential stresses, may exist in a wound roll but without any slippage, there is no star defect formation. Based on the results of the present study there is no correlation between locations of negative circumferential stresses and crepe wrinkles.

Observations made by Roisum, with regard to wound roll slippage, occurring whenever radial stresses are low, and low values of coefficient of friction exist, are accurate as the present study has shown that low radial stresses lead to a low torque capacity in the wound roll and an increased propensity for slippage and slippage related defects. Based on the present study, Roisum's observation on the centrifugal stresses leading to a reduction in radial stresses, and thereby a greater propensity to slip, cannot be validated. However, the present study has established that a reduction in radial stresses leads to a reduction in torque capacity.

Welp[19], identified core loading due to self-loading from the roll, and bending moments across the width of the web to be responsible for eccentricity of the core with respect to the axis of the roll. Based on the results of the present study, it is not possible correlate

the roll weight as a factor responsible for slippage unless, the roll weight contributed to nip loading. It is possible however, to validate the existence of low radial stresses in the core region due to the fact that the wound on tension might have been low due to start up effects. The resulting low radial stresses lead to the formation of a low torque capacity zone, which in turn leads to a greater propensity to slip.

In conclusion, many of the qualitative observations, made by the authors who studied the problem of wound roll defects related to slippage, have been validated using experimental evidence and theoretical models. In some cases, the observations could not be validated as the present study did not directly relate to the factors identified. In such cases, possible new interpretations have been provided and the limitations of the present study have been identified. However, most of the factors identified in the previous studies have been linked to the torque capacity of the wound rolls, and to the effects of the rolling resistance induced by a torque driven nip. The factors that control the torque capacity are the factors that control the slippage resistance characteristics of a wound roll, and consequently the quality of the wound roll.

CHAPTER XI

CONCLUSIONS AND RECOMMENDATIONS

Project Summary

Chapter 1 provided a general background of the web handling world, with particular emphasis on different kinds of winders, different winding schemes, and general trends followed in the industry. An introduction to some of the terminology, with respect to winders, was also made. Chapter 2 provided an overview of slippage related wound roll defects, with emphasis on the different tools available to monitor slippage. This chapter also provided a description of the different kinds of slippage and means to identify them. Chapter 3 provided a detailed look into the existing literature on slippage related defects, and some of the theories to understand the problem. This chapter served as the starting point for identification of parameters, considered to be responsible for slippage in wound rolls.

Chapter 4 was the starting point of this thesis. In this chapter, the torque capacity was identified as the single most important quantification of the capacity of a wound roll to resist slippage. Using wound roll models, a parametric study of the factors affecting the torque capacity was carried out. In this chapter a model for predicting slippage in a wound roll was introduced.

Chapter 5 was essentially validating the torque capacity model for wound rolls, using experimental techniques. In this chapter, a method to predict slippage in wound rolls, subjected to decelerations and splicing operations, using the torque capacity was demonstrated. Attention was focused on situations, that did not involve nip rolls, effectively isolating the action of the nip roll, from the other physical process parameters, responsible for promoting slippage in wound rolls. In chapter 5, a new mechanism by which starring occurs in wound rolls, was documented for the first time, and a method for quantitatively predicting the formation of starring was identified, based on the torque capacity model.

In Chapter 6, the thesis addressed the problem of slippage induced by a nip roll, and identified rolling resistance encountered by the nip, to be responsible for inducing slippage in wound rolls. In this chapter, a method to quantify the rolling resistance, based on Greenwood et al's theory, equation (27), was identified. Experimental validation of the applicability of the quantification, for a nip rolling over web material, was also provided.

Chapter 7 outlined the extension of the rolling resistance theory developed in chapter 6, for the case of a torque driven nip in contact with a wound roll. A modified model was provided, for estimating the rolling resistance encountered by a torque driven nip, considering the effect of the circular geometry of a nip and a wound roll. In addition, an experimental validation of the applicability of the modified model was also provided. Chapter 8, was an attempt to predict slippage for the case of the torque driven nip using

the torque capacity model. Two slippage models were [illegible], and the capacity of both the models to predict slippage, for the case of the torque driven nip in contact with a wound roll, was explored.

In chapter 9, techniques to evaluate the half width of contact between a nip and a wound roll were outlined, and a comparison with experimental results, was carried out. With this, rolling resistance could be predicted using Greenwood et al's equation if 'α' is known. Chapter 10, was a new look at the literature, that was presented in chapter 3. Based on the present study, some of the observations made in the literature were re-interpreted, and correlation was established with the present study.

Conclusions and Findings

The objective of this study was to quantify slippage that occurs in wound rolls and to identify the parameters contributing to wound roll slippage, with the focus on crepe wrinkles and starring.

The following conclusions and findings resulted from this study:

(i) Slippage was quantified in a wound roll using the torque capacity. The different parameters identified in the literature were linked via wound roll models to the radial stresses, and to the torque capacity, equations (1) and (2), chapter 4. Slippage occurs in a wound roll whenever:

$$T_{applied-external} > T_{capacity-minimum}$$

(ii) Slippage, related to deceleration was quantified, and was shown to develop crepe wrinkles and in certain cases starring defects, equations (23), (24), Table 8, chapter 5. This study also isolated the effects of the deceleration from the effects due to nip rolls. Crepe wrinkles occur during deceleration when

$$T_{dynamic} \quad >> \quad T_{capacity-minimum}$$

(iii) The occurrence of crepe wrinkles in the vicinity of splices was verified, and a means to control the defect by controlling the slippage was identified, figures 36 to 41, chapter 5.

(iv) Slippage was identified as a precursor to starring in some wound rolls, and the propensity of wound rolls to form starring defects due to slippage was quantified, figures 44 and 45, chapter 5.

(v) With respect to addressing the slippage induced by a nip:

(a) The rolling resistance that a torque driven nip encounters in the presence of a wound roll was measured experimentally, figures 58 through 66, chapter 7.

(b) The measured values correlated well with the modified form of Greenwood et al's equation with scale factor of 3.5. Thus the equation

$$Torque_{Rolling-Resistance} = (3.5)\frac{2}{3\pi}\alpha\left(\frac{Wa}{R^*}\right)wr_{nip-roll} \text{ (in-lb)}$$

can be used to model rolling resistance for torque driven nip rollers in contact with wound rolls.

It is impossible to attribute all the slippage that occurs in a surface wound roll to rolling resistance. But rolling resistance torques may be significantly large to initiate the process of slippage, and once slippage starts, rolling resistance may continually increase, figures 58b, 60b, 63b etc., and this may lead to slippage related defects such as starring. For example, figure 62e, the roll shows starring following slippage. Figures 46 b, c, d all show starring following slippage, induced by the nip during surface winding. The tests conducted in the laboratory were on a small prototype machine, so the values may not appear to be significant. But, in actual production cases, the combination of the magnitudes of the nip loads, half widths, and the equivalent radii of contact may be large, such that rolling resistance is significant. In addition, there is the existence of multiple nips, in traditional two drum winders, which may contribute to the rolling resistance.

(vi) Certain general trends were observed with respect to rolling resistance torques encountered by a torque driven nip in contact with a wound roll. These are:

(a) As the wound on tension increases, the rolling resistance torque decreases. This means, as the radial stresses in the rolls increase the rolling resistance torque decreases.

(b) As the nip load transmitted to the wound roll increases, the rolling resistance torque increases.

(c) As the nip diameter increases, the rolling resistance increases.

(vii) Certain general trends were observed with respect to the extent of slippage undergone by the wound rolls. These are:

(a) As the wound on tension increases, the extent of slippage decreases.

(b) As the nip load transmitted to the wound roll increases, the extent of slippage in the rolls increase.

(c) As the nip diameter increases, the amount of slippage increases.

(viii) The half width of contact is an important factor governing the rolling resistance torque. Two different techniques to compute the half width of contact for the case of a rigid nip contacting a layered structure were outlined.

(ix) The mechanism initiating slippage is not simple, as motion of pressure waves due to indentation at the contact interface has to be considered. So, to predict slippage using the slippage criterion outlined in (i), an accurate determination of the torque capacity in the vicinity of the nip has to be made, considering the effect of contact of the nip and the changes brought about due to nip indentation

Future Studies

(i) The actual mechanism of slippage during surface winding has to be investigated, based on the propagation of a pressure wave traveling around the circumference of the wound roll.

(ii) In order to understand surface winding better, the rolling resistance has to be evaluated continuously as the roll builds. It has become increasingly clear, that to

model surface winding, slippage induced in the roll during the winding process has to be considered.

(iii) The rolling resistance can be viewed as a loosening force. So, it is possible to incorporate this effect into a winding model, as a reduction in the value of the wound - on - tension. However, the slippage induced due to the rolling resistance, can alter the radial stresses that exist in the wound roll. So, modeling the pressure disturbance induced by slippage is a precursor to developing any surface winding models.

(iv) Finite element models can be developed to investigate the pressure waves due to the nip and wound roll interactions. In addition, models need to be developed that incorporate hysteresis, slippage at the nip web interface, the layered nature of the wound roll, and the effect of the circular geometry of the wound roll to fully understand the nature of surface winding.

(v) More accurate analytical models to predict the half width of contact between the nip and the wound roll have to be developed. These models need to consider the non - linear nature of the wound roll. Finite element analysis can also be used to verify some of the analytical models.

REFERENCES

1. Personal Communication with Dr. J. J. Shelton, WHRC, Oklahoma State University, Stillwater, Oklahoma.

2. Personal Communication with Mr. Bruce Feiertag, WHRC, Oklahoma State University, Stillwater, Oklahoma.

3. Lemke, R. J., Uotinen, J., Oinonen, H., "Factors Involved in Winding Large Diameter Newsprint Rolls on a Two-Drum Winder", Advances and Trends in Winding Technology, Proceedings of the First International Conference on Winding Technology, Stockholm, Sweden, Swedish Newsprint Research Center, (TFL) Mar. 1987.

4. Lucas, R. G., "Winder Crepe Wrinkles-Their Causes and Cures", TAPPI, Paper Finishing and Converting Conference Proceedings, Oct. 1981.

5. Laumer, E. P., "Minimizing Wound In Paper Defects Within Shipping Rolls", TAPPI Journal, Vol. 49, No. 12, Dec. 1966, pp. 127A-131 A.

6. Daly, D. A., "Study of Defects in Wound Rolls Leads to Better Winding Control", Paper Trade Journal, Dec. 1967, pp. 46-48.

7. Lucas, R. G., "Internal Gearing in a Roll of Paper", TAPPI, Finishing and Converting Conference Proceedings, October 1974.

8. Zhang, Y., M.S. Thesis, Department of Mechanical and Aerospace Engineering Oklahoma State University, 1994.

9. Tuomisto, M. V., Sorsa, K., Kyytsonen, M., "Eliminating Production Losses on a Paper Machine Reel", Vol. 78, No. 10, TAPPI Journal, October 1995.

10. Welp, E.G., Schoenmeier, H., "Improving Roll Structure - A Research Report", TAPPI Journal, Apr. 1984.

11. Frye, K. G., "Winding Variables and their effect on Roll Hardness and Roll Quality", TAPPI Journal, Vol. 50, No. 7, pp. 81A - 86A.

12. Odell, M. H., Symons, R. E., Brown, G. S., "Control of the Winding Process by Roll Density Measurement", APPITA, Vol. 38, No. 5, pp. 359-369. 13.

13. Frye, K. G., "Finishing Defects: Core Bursts and Crepe Wrinkles", TAPPI Journal, Oct. 1986, pp. 74 - 77.

14. Paananen, J., Ebeling, K., "Effect of Grammage on Formation of Crepe Wrinkles in Production of Large Diameter Rolls", Advances and Trends in Winding Technology, Proceedings of the First International Conference on Winding Technology, Stockholm, Sweden, Swedish Newsprint Research Center (TFL) Mar. 1987.

15. Schoenmeier, H., "Experience with Modern Single-Drum Winders for Newsprint", Advances and Trends in Winding Technology, Proceedings of the First International Conference on Winding Technology, Stockholm, Sweden, Swedish Newsprint Research Center (TFL) Mar. 1987.

16. Roisum, D. R., "Cores I - Crepe Wrinkles - Statistics", Beloit Corporation, Internal Report No. D87 - 003, Jan. 1987.

17. Roisum, D. R., "A History of Paper Stresses: Before, During and After Winding", TAPPI, Finishing and Converting Conference Proceedings, Oct., 1986.

18. Roisum, D. R., "The J-Line Revisited", Beloit Corporation, Internal Report No. D88 - 003, Jan. 1988.

19. Welp, E.G., "Winding Problems with Rotogravure Jumbo-Rolls", Proceedings of the First International Conference on Web Handling, Web Handling Research Center, Oklahoma State University, Stillwater, Oklahoma, U.S.A., May 1991, pp. 154-166.

20. Good, J. K., "The Science of Winding Paper Rolls," Transactions of the Tenth Fundamental Research Symposium Held at Oxford, Vol. 2, Sept. 1993.

21. Hakiel, Z., "Nonlinear Model for wound Roll Stresses," TAPPI Journal, Vol. 70, No. 5, May 1987.

22. Good, J. K., Wu, Z., Fikes, M. W. R., "Stresses within Rolls Wound in the Presence of a Nip Roller", Proceedings of the First International Conference on Web Handling, Web Handling Research Center, Oklahoma State University, Stillwater, Oklahoma, U.S.A., May 1991, pp. 123-144.

23. Pfeiffer, J. D., "Internal Pressures in a Wound Roll," TAPPI Journal, Vol. 49, No. 8, Aug. 1966.

24. Swanson, R.,P., "Er Stack Testing", Unpublished report, WHRC, Oklahoma State University, Stillwater, Oklahoma, October 1990.

25. Ducotey, K., "Tractions between Webs and Rollers in Web Handling Applications", Ph.D Thesis, Department of Mechanical and Aerospace Engineering Oklahoma State University, 1993.

26. Lee, B. E., "Buckling Analysis of Starred Roll Defects in Center Wound Rolls" Ph.D Thesis, Department of Mechanical and Aerospace Engineering, Oklahoma State University Oklahoma State University, May 1991.

27. Personal Communication with Dr. J. K. Good, WHRC, Oklahoma State University, Stillwater, Oklahoma.

28. Personal Communication with Bob Lucas, Beloit Corporation.

29. Greenwood, J. A., Minshall, H., and Tabor, D., "Hysteresis Losses in Rolling and Sliding Friction", Proceedings of the Royal Society of London, Series A, Vol 259, pp. 480- 507, January 1961.

30. May, W., D., Morris, E., L., and Atack, D., "Rolling Friction of a Hard Cylinder over a Viscoelastic Material", Journal of Applied Physics, Vol.30, No. 11, pp. 1713 - 1724, November 1959.

31. Hunter, S., C., "The Rolling Contact of a Rigid Cylinder With a Viscoelastic Half Space", Journal of Applied Mechanics, pp. 611 - 617, December 1961.

32. Morland, L., W., "A Plane Problem of Rolling Contact in Linear Viscoelastic Theory", Journal of Applied Mechanics, pp.345 - 352, June 1962.

33. Lynch, F., S., "A Finite Element Method of Viscoelastic Stress Analysis with Application to Rolling Contact Problems", International Journal for Numerical Methods in Engineering, Vol. 1, pp. 379 - 394, 1969.

34. Schuring, J., D., Rubber Division Symposia, Vol. 1, Tire Rolling Resistance, Papers given at the Symposium on Tire Rolling Resistance at the 122nd Meeting of the Rubber Division, Chemical Society at Chicago, Illinois, October 5- 7, 1982.

35. Snyder, R., H., "Tire Rolling Losses and Fuel Economy - An R&D Planning Workshop P- 74", October, 18 - 20, 1977.

36. Wannop, G., L., Archard, J., F., "Elastic Hysteresis and a Catastrophic Wear Mechanism for Polymers", Proceedings of the Institution of Mechanical Engineers, Vol. 187 52/73, 1973.

37. Pfeiffer, J. D., "Instrumenting Rolling Nips for Video Recording and Strain Recording", Proceedings of the Second International Conference on Web Handling, Web Handling Research Center, Oklahoma State University, Stillwater, Oklahoma, U.S.A., June 6 - 9 1993.

38. Shigley, J. E., and Mitchell, L. D., "Mechanical Engineering Design", 4th edition, Mcgraw Hill, New York, pp. 87 - 88, 1983.

39. Personal Communication with Dr. J. K. Good, WHRC, Oklahoma State University, Stillwater, Oklahoma.

40. Johnson, K. L., "Contact Mechanics", Cambridge University Press, pp. 92 - 93, 1989.

41. Giachetto, R. M., "Tension Losses Encountered in CenterWound Rolls", M. S. Thesis, Department of Mechanical and Aerospace Engineering, Oklahoma State University Oklahoma State University, May 1992.

2

VITA

Nandakumar Vaidyanathan

Candidate for the Degree of

Doctor of Philosophy

Thesis: A STUDY ON WOUND ROLL SLIPPAGE

Major Field: Mechanical Engineering

Biographical:

Personal Data: Born in Guntakal, India, January 18, 1968, the son of Vaidyanathan Venkataraman and Jayalakshmi Vaidyanathan.

Education: Graduated from T.V.S. Lakshmi Higher Secondary School, Madurai, 1985; received Bachelor of Engineering (Honors) degree from Birla Institute of Technology and Science, Pilani, Rajasthan, India, with a Major in Mechanical Engineering in June 1989; received the Master of Science degree from Oklahoma State University with a Major in Mechanical Engineering in May 1991; completed requirements for the Doctor of Philosophy degree, with a major in Mechanical Engineering, in July, 1996.

Professional Experience: Worked as a research assistant at Oklahoma State University from January, 1990, through January, 1991, principally on Nip induced Tension mechanisms in wound rolls; worked for VITec in Plano, Texas as a software engineer from May 1991, through December 1991 on developing microcode for image processing systems; worked as a research assistant and a teaching assistant at Oklahoma State University from January 1992 to the present, investigating slippage related wound roll defects.